

Ecological Studies 251

Valentí Rull · Teresa Vegas-Vilarrúbia

Vegetation and Landscape Dynamics of the Iberian Pyrenees During the Last 3000 Years

The Montcortès Palynological Record

 Springer

Ecological Studies

Analysis and Synthesis

Volume 251

Series Editors

David A. Wardle, Department of Ecology and Environmental Science, Umeå University, Umeå, Sweden

Josep G. Canadell, CSIRO Oceans and Atmosphere, Canberra, ACT, Australia

Sandra Díaz, National University of Córdoba, Córdoba, Argentina

Gerhard Heldmaier, University of Marburg, Marburg, Germany

Robert B. Jackson, Stanford University, Stanford, CA, USA

Delphis F. Levia, University of Delaware, Newark, DE, USA

Ernst-Detlef Schulze, Max Planck Institute for Biogeochemistry, Jena, Germany

Ulrich Sommer, GEOMAR | Helmholtz Centre for Ocean Research Kiel, Kiel, Germany

Ecological Studies is Springer's premier book series treating all aspects of ecology. These volumes, either authored or edited collections, appear several times each year. They are intended to analyze and synthesize our understanding of natural and managed ecosystems and their constituent organisms and resources at different scales from the biosphere to communities, populations, individual organisms and molecular interactions. Many volumes constitute case studies illustrating and synthesizing ecological principles for an intended audience of scientists, students, environmental managers and policy experts. Recent volumes address biodiversity, global change, landscape ecology, air pollution, ecosystem analysis, microbial ecology, ecophysiology and molecular ecology.

Valentí Rull • Teresa Vegas-Vilarrúbia

Vegetation and Landscape Dynamics of the Iberian Pyrenees During the Last 3000 Years

The Montcortès Palynological Record

 Springer

Valentí Rull 
Botanic Institute of Barcelona
Spanish National Research Council (CSIC)
Barcelona, Spain

Institut Català de Paleontologia Miquel
Crusafont (ICP-CERCA)
Universitat Autònoma de Barcelona
Barcelona, Spain

Teresa Vegas-Vilarrúbia 
Department of Evolutionary Biology,
Ecology and Environmental Sciences
Universitat de Barcelona
Barcelona, Spain

ISSN 0070-8356

Ecological Studies

ISBN 978-3-031-57440-5

<https://doi.org/10.1007/978-3-031-57441-2>

ISSN 2196-971X (electronic)

ISBN 978-3-031-57441-2 (eBook)

© The Editor(s) (if applicable) and The Author(s), under exclusive license to Springer Nature Switzerland AG 2024

This work is subject to copyright. All rights are solely and exclusively licensed by the Publisher, whether the whole or part of the material is concerned, specifically the rights of translation, reprinting, reuse of illustrations, recitation, broadcasting, reproduction on microfilms or in any other physical way, and transmission or information storage and retrieval, electronic adaptation, computer software, or by similar or dissimilar methodology now known or hereafter developed.

The use of general descriptive names, registered names, trademarks, service marks, etc. in this publication does not imply, even in the absence of a specific statement, that such names are exempt from the relevant protective laws and regulations and therefore free for general use.

The publisher, the authors, and the editors are safe to assume that the advice and information in this book are believed to be true and accurate at the date of publication. Neither the publisher nor the authors or the editors give a warranty, expressed or implied, with respect to the material contained herein or for any errors or omissions that may have been made. The publisher remains neutral with regard to jurisdictional claims in published maps and institutional affiliations.

This Springer imprint is published by the registered company Springer Nature Switzerland AG
The registered company address is: Gewerbestrasse 11, 6330 Cham, Switzerland

If disposing of this product, please recycle the paper.

Introduction

Annually laminated (varved) lake sediments are especially well suited for high-resolution paleoecological studies, as they are able to provide seasonal to annual records that can be merged with modern ecological records to develop long-term past–present ecological time series (Rull 2014). These time series are useful not only to understand ecological dynamics but also to feed predictive models on ecological responses to changing environmental conditions, which may be helpful to inform biodiversity and ecosystem conservation in the face of ongoing global change.

More than 140 lakes with varved sediments have been studied around the world, mainly in northern temperate and boreal areas, where these lakes are more frequent due to the special conditions needed for varve formation and preservation (Fig. 1). In the Mediterranean region, only a tenth of varved sediments have been documented in the latest review by Zolitschka et al. (2015), with no African representatives (Fig. 1). These authors have classified the varved sequences into three main groups: (i) continuous sequences with more than 100 years, (ii) continuous sequences with less than 100 years, and (iii) discontinuous and/or floating sequences. Floating sequences lack a chronological anchor point and thus provide relative, yet precise, chronologies. In the Iberian Peninsula, where the target lake of this study (Lake Montcortès) is located, six lakes with varved sediments have been documented, including a Pliocene paleolake (Muñoz et al. 2002) and five extant karstic lakes: La Cruz (Romero-Viana et al. 2008), Zóñar (Martín-Puertas et al. 2009), Banyoles (Morellón et al. 2015), Arreo (Corella et al. 2011a), and Montcortès (Corella et al. 2012).

Varves represent annual sedimentary cycles and are composed of two or more seasonal laminae with differential properties such as color, composition, texture, structure, and/or thickness. Therefore, climatic seasonality and its sedimentary manifestations are major drivers of varve formation. A number of reviews on varve formation and preservation are available (e.g., Saarnisto 1979; O’Sullivan 1983; Anderson et al. 1985; Boygle 1993; Brauer 2004; Saarnisto and Ojala 2009; Zolitschka et al. 2015), which are summarized below.

Three main types of varves exist: clastic, biogenic, and endogenic varves. Clastic varves predominate in glacial lakes from polar and alpine regions, where the lack of vegetation facilitates the erosion and sedimentation of large quantities of minerogenic (clastic) matter (Fig. 2). Runoff seasonality is the most relevant driver of clastic varves, which are formed by couplets of coarse-grained and fine-grained

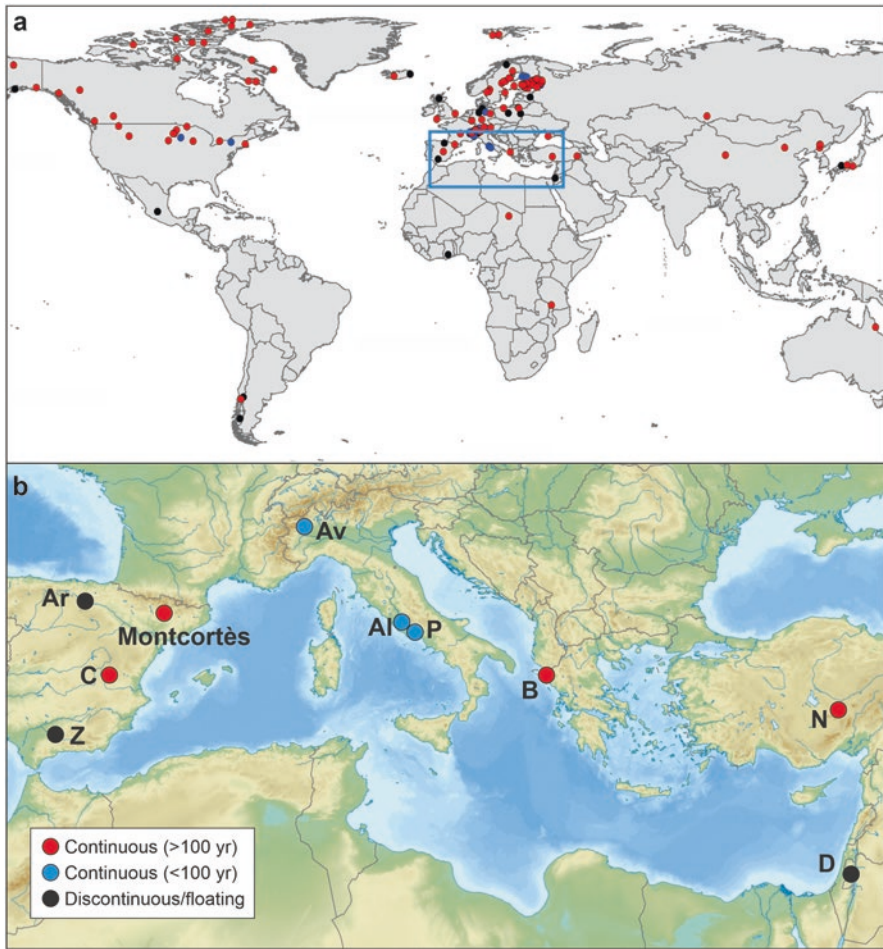


Fig. 1 Geographical distribution of varved Pleistocene and Holocene lake records from peer-reviewed publications. **(a)** Worldwide distribution. The Mediterranean region is highlighted by a blue box. Redrawn from Zolitzschka et al. (2015). **(b)** Mediterranean region. Lake Montcortès, the target of this book, is spelled in full. Other lake abbreviations: Al, Albano (Italy); Ar, Areo (Spain); Av, Aigliana (Italy); B, Butrint (Albania); C, La Cruz (Spain); D, Dead Sea (Jordan/Israel); N, Nar (Turkey); P, San Puoto (Italy); Z, Zóñar (Spain). Redrawn from Rull et al. (2021c)

laminae, representing the seasons of maximum runoff (summer) and of nonturbulent deposition under winter ice cover, respectively. Biogenic varves are more characteristic of temperate regions where the catchment area is vegetated and the availability of clastic particles to be transported into the lake is lower. These varves reflect the cycle of annual productivity of the lake. During spring/summer, rising temperatures and the leaching of nutrients into the lake increase the productivity of aquatic ecosystems, which leads to algal blooms—diatoms in early spring and green/blue algae in summer—which form a sedimentary lamina of diatom frustules



Fig. 2 Clastic varves of a former glacial lake from the coasts of Hudson Bay (Canada). Photo: V. Rull

and other algal microfossils. In contrast, the fall/winter lamina is darker and rich in amorphous organic matter and plant detritus, as well as clastic materials, as a result of lower lake productivity and increased catchment runoff. Lakes with biogenic varves use to develop an oxygen-depleted hypolimnion by microbial oxidation of organic matter. Endogenic varves are the result of biologically or physically precipitated minerals originating in the water column. The most frequent of these minerals is calcite (CaCO_3), which forms a pale sedimentary lamina during dry summers with elevated productivity and high evaporation rates, alternating with a dark lamina of minerogenic grains and organic detritus formed during colder and moister winters.

These types of varves are often mixed, showing intermediate types. Clastic varves are the only type that can occur in a more or less pure form, but clastic-organic and clastic-biogenic varves are not infrequent. In calcareous terrains, biogenic varves may contain endogenic minerals, mostly calcite, which precipitates when its concentration exceeds the solubility product of this compound. The most frequent process is the temperature-related increase in photosynthetic activity in the water column, which consumes CO_2 from the water and increases the pH up to 9, thus reducing calcite solubility. This spring–summer combination of higher temperatures and increased biological activity forms a well-defined whitish carbonate layer typical of carbonaceous-biogenic varves (Dean and Megard 1993).

Not only varve formation but also the preservation of these sedimentary structures is essential for the existence of varved sediments. Varve preservation is favored by the absence of postdepositional erosion, resuspension, and redeposition, which may be due to seismic liquefaction, gravity-induced sediment reworking, or wave- and current-induced sediment movements.

The action of wind is especially important in shallow lakes and the littoral zone of deeper lakes, where it can create currents and waves that can resuspend

superficial sediments and promote their further downslope transport and deposition. In addition, deep lakes are more prone to develop a suboxic/anoxic hypolimnion, which contributes to the preservation of biogenic varves by preventing the growth of sediment dwellers such as fishes, mollusks, crustaceans, and worms. Sediment bioturbation by this type of organisms is the most important process of sediment mixing in lakes. The development of a suboxic/anoxic hypolimnion is especially frequent in deep temperate lakes with pronounced seasonality in climatic and productivity conditions. During the warmest season, deep lakes tend to be stratified into a warm superficial epilimnion and a deep colder hypolimnion, separated by a thermocline, which is a thin layer of strong temperature gradient in between (Fig. 3). This thermal stratification is also a density stratification (chemocline) that maintains the epilimnion and the hypolimnion relatively isolated from physical and chemical (chemocline) points of view.

Chemical stratification is especially significant in the case of dissolved oxygen, which is consumed in the hypolimnion by oxidation of organic matter and is not replenished due to physical isolation from the epilimnion. This can cause suboxic to anoxic conditions in the hypolimnion, which may persist until the coldest season, when low temperatures, lower biological activity, and enhanced wind intensity can break the thermocline and restart vertical water circulation, leading to the homogenization of the water column and the renewal and oxygenation of deep waters. Lakes with this type of seasonal behavior are called monomictic if there is a single mixing season or dimictic if there are two mixing seasons. Examples of dimictic lakes are those with two stratification seasons, usually summer (by temperature increase) and winter (by the development of an ice cap), with spring and autumn as mixing seasons. However, in very deep and very productive lakes, the anoxic hypolimnion may persist throughout the year, thus excluding it from seasonal water circulation. These lakes with a permanent hypolimnion are called meromictic and are especially well suited for the development and preservation of biogenic and endogenic varves due to the lack of sediment disturbance from both mechanical and biological origins. In other lakes with seasonal mixing, varves would also be formed and well preserved if hypolimnetic conditions prevail long enough over the year.

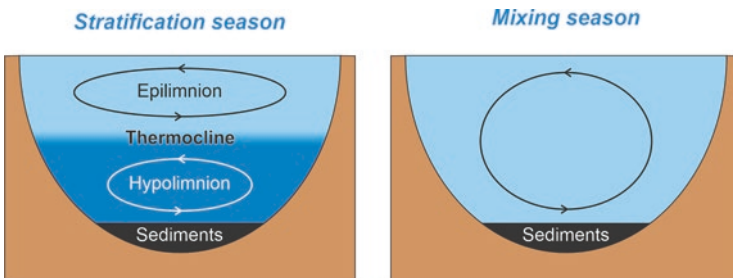


Fig. 3 Schematic view of the two main seasonal states of a lake regarding annual stratification and vertical circulation regimes

This book is focused on the varved sediments of Lake Montcortès, located on the Iberian side of the Pyrenees (Fig. 1), which are unique and exceptional in many senses, as will be seen throughout the book. The discovery of Lake Montcortès varved sediments was not casual but was based on the above considerations about the mixing regime. The first limnological studies carried out in this lake in the 1970s concluded that the lake was meromictic with some anomalous years in which full mixing of the water column was observed (Camps et al. 1976; Modamio et al. 1988). See Sect. 5 of Chap. 1 for more details. This suggested to the authors of this book—who returned to Spain after a long ~20-year stay in the Neotropics—that Lake Montcortès could contain varved sediments, but to their surprise, this lake had never been cored. The same occurred with Lake Sant Maurici, situated ~25 km north of Lake Montcortès on the Pyrenean highlands, which remained uncored despite its emblematic nature in the National Park of “Aigüestortes i Estany de Sant Maurici” (PNAESM). Both lakes were easily accessible by road, which enabled the transportation of heavy coring equipment to the lakeshores, and made it even more surprising that they remained uncored until then (Rull 2023).

In 2003, the authors contacted the research group on Quaternary Paleoenvironments and Global Change from the Pyrenean Institute of Ecology (Zaragoza, Spain), who had access to suitable equipment to core the lake. This group manifested great interest and included lakes Montcortès and Sant Maurici in a large campaign aimed at coring a set of representative lakes over the whole Iberian Peninsula, with the collaboration of the Limnological Research Center (LRC) of the University of Minnesota (Minneapolis, USA). Within this campaign, the lake was cored in April 2004, and >6 m of varved sediments came to light, thus initiating the high-resolution multiproxy study of the longest continuous record of the last 3000 years for the circum-Mediterranean region (Fig. 4). This coring campaign, known as MON04, was followed by others specifically designed for the study of Lake Montcortès sediments, but MON04 was the one that inaugurated the study of this emblematic paleoarchive. The case was different for Lake Sant Maurici, which was not cored during the 2004 coring campaign due to weather constraints but was finally cored in 2013 (Rull 2023).

Since its coring in 2004, Lake Montcortès has become a crucial paleoarchive and a benchmark location for paleoenvironmental research in the western Mediterranean region. A great variety of paleoenvironmental studies have been carried out encompassing a wide range of topics, such as the formation and dating of varves, the history of sediment yield, reconstructions of past temperature and precipitation (including significant rainfall events), occurrences of hypoxia and oxygenation events, paleolimnological reconstructions (diatoms, pigments, and other algae remnants), changes in vegetation and landscape, the timing and patterns of human impact (burning, deforestation, cultivation, grazing), the deposition of heavy metals (Hg and Pb) from the atmosphere over the past millennium, comparisons between paleoecological and historical records, and modern-analog studies for reconstructing paleoclimatic and paleoecological conditions using various physical, chemical, and biological indicators, including biomolecular markers (Cao et al. 2020; Corella et al. 2011b, 2012, 2014, 2016, 2017, 2019; Montoya et al. 2018; Rull and



Fig. 4 First coring campaign of Lake Montcortès sediments (April 2004). (a) General view of the LRC coring platform. (b) Dropping the Kullenberg corer until the surface of lake sediments. (c) Loading the cap of the Kullenberg corer (400 g). (d) Full sediment core. (e) Extracting the plastic (polycarbonate) core sediment from its metallic casing. (f) Cut core ready to be transported to the laboratory for analysis. Photos: V. Rull

Vegas-Vilarrúbia, 2014, 2015, 2021b; Rull et al. 2011, 2017, 2021b, c; Scussolini et al. 2011; Trapote et al. 2018a, b; Vegas-Vilarrúbia et al. 2018, 2020, 2022). The study continues and is expected to increase information on the Late-Holocene environmental and ecological history of the Iberian Pyrenees, not only as a source of background knowledge but also of long-term ecological data to be incorporated into predictive models aimed at informing conservation actions in the face of ongoing global change.

In this book, the focus is on long-term vegetation and landscape dynamics in relation to climatic changes and anthropogenic activities. The ecological history of the region is reconstructed using pollen analysis, and the cultural history is based on archaeological evidence and historical documents. Paleoclimatic trends are taken from studies using climatic proxies independent from pollen, such as tree-ring and speleothem reconstructions, as well as physicochemical characteristics of sediments from Lake Montcortès and other nearby lakes. The paleoecological reconstruction encompasses the last ~3000 years, beginning in the Late Bronze Age and ending in 2013, which is the last date recorded in the sediment cores retrieved to date.

The first chapter provides the geographical, geological, climatic, and vegetational context, along with a brief explanation of the limnological cycle of the lake, which is useful for understanding the formation and preservation of varves. The second chapter synthesizes the cultural history of the historical Pallars region, where the lake is located, to provide the political and socioeconomic background

needed to place the reconstructed ecological and landscape shifts in the appropriate context of human impact. The third chapter aims to provide some methodological hints on paleoclimatic and paleoecological reconstruction needed to understand further interpretations and comparisons of past ecological trends. This chapter does not fully explain the paleoecological methods used but emphasizes some aspects that facilitate the reader to follow paleoecological reconstruction with a minimum background. The following chapters explain in detail the history of vegetation and landscape of the region from the first anthropization event recorded to date to the present, using a chronological sequence—Late Bronze to Roman Empire (Chap. 4), Middle Ages (Chap. 5), and Modern-Contemporary times (Chap. 6). The account goes beyond a description of facts, as it attempts to establish causal relationships with natural (mostly climatic) and anthropogenic (fire, cultivation, grazing, etc.) drivers of landscape change, with the aid of independent paleoclimatic reconstructions and historical documentation. Chapter 7 compares the three major historical deforestation–recovery cycles (Roman, Medieval, and Modern) and analyzes forest change in terms of resilience, in the face of anthropogenic pressure. Chapter 8 summarizes the results and main conclusions obtained in Lake Montcortès, situates this paleoecological sequence within the Iberian and Mediterranean contexts, and suggests some future research lines that could be useful to enhance and improve the available knowledge in this particular subject.

References

- Anderson RY, Dean WE, Bradbury JP, Love D (1985) Meromictic lakes and varved lake sediments in North America. *US Geol Surv Bull* 1607:1–19
- Boyle J (1993) The Swedish varve chronology – a review. *Prog Phys Geogr* 17:1–19
- Brauer A (2004) Annually laminated lake sediments and their paleoclimatic relevance. In: Fischer H (ed) *Climate in historical time: towards a synthesis of holocene proxy data and climate models*. Springer, Heidelberg, pp 108–128
- Camps J, Gonzalvo I, Güell J, López P, Tejero A, Toldrà X et al (1976) El lago de Montcortès, descripción de un ciclo annual. *Oecol Aquat* 2:99–110
- Cao M, Rivas-Ruiz P, Trapote MC, Vegas-Vilarrúbia T, Rull V, Rosell-Melé A (2020) Seasonal effects of water temperature and dissolved oxygen on the isoGDGT proxy (TEX86) in a Mediterranean oligotrophic lake. *Chem Geol* 551:119759
- Corella JP, Amran A, Sigró J, Morellón M, Rico E, Valero-Garcés B (2011a) Recent evolution of Lake Arreo, northern Spain: influences of land use change and climate. *J Paleolimnol* 46:469–485
- Corella JP, Moreno A, Morellón M, Rull V, Giralt S, Rico MT et al (2011b) Climate and human impact on a meromictic lake during the last 6,000 years (Montcortès Lake, Central Pyrenees, Spain). *J Paleolimnol* 46:351–367
- Corella JP, Brauer A, Mangili C, Rull V, Vegas-Vilarrúbia T, Morellón M et al (2012) The 1.5-ka varved record of Lake Montcortès (southern Pyrenees, NE Spain). *Quat Res* 78:323–332

- Corella JP, Benito C, Rodriguez-Lloveras X, Brauer A, Valero-Garcés BL (2014) Annually-resolved lake record of extreme hydro-meteorological events since AD 1347 in NE Iberian Peninsula. *Quat Sci Rev* 93:77–90
- Corella JP, Valero-Garcés B, Vicente-Serrano SM, Brauer A, Benito C (2016) Three millennia of heavy rainfalls in Western Mediterranean: frequency, seasonality and atmospheric drivers. *Sci Rep* 6:38206
- Corella JP, Valero-Garcés BL, Wang F, Martínez-Cortizas A, Cuevas CA, Saiz-López A (2017) 700 years reconstruction of mercury and lead atmospheric deposition in the Pyrenees (NE Spain). *Atmos Environ* 155:97–107
- Corella JP, Benito G, Wilhelm B, Montoya E, Rull V, Vegas-Vilarrúbia T et al (2019) A millennium-long perspective of flood-related seasonal sediment yield in Mediterranean watersheds. *Glob Planet Change* 177:127–140
- Dean WE, Megard RO (1993) Environment of deposition of CaCO₃ in Elk Lake, Minnesota. In: Bradbury JP, Dean WE (eds) *El Lake, Minnesota: evidence for rapid climate change in the North-Central United States*. *Geol Soc Am Spec Pap* 276:97–114
- Martín-Puertas C, Valero-Garcés BL, Brauer A, Mata MP, Delgado-Huertas A, Dulski P (2009) The Iberian-Roman Humid Period (2600–1600 cal yr BP) in the Zóñar Lake varved record (Andalucía, southern Spain). *Quat Res* 71:108–120
- Modamio X, Pérez V, Samarra F (1988) Limnología del lago de Montcortès (ciclo 1978–79) (Pallars Jussà, Lleida). *Oecol Aquat* 9:9–17
- Montoya E, Rull V, Vegas-Vilarrúbia T, Corella JP, Giral S, Valero-Garcés B (2018) Grazing activities in the southern Pyrenees during the last millennium as deduced from the non-pollen palynomorphs (NPP) record of Lake Montcortès. *Rev Palaeobot Palynol* 254:8–19
- Morellón M, Anselmetti FS, Valero-Garcés B, Barreiro-Lostres F, Aziztegui D, Giral S et al (2015) Local formation of varved sediments in a karstic collapse depression of Lake Banyoles (NE Spain). *Geogaceta* 57:119–122
- Muñoz A, Ojeda J, Sánchez-Valverde B (2002) Sunspot-like and ENSO/NAO-like periodicities in lacustrine laminated sediments of the Pliocene Villarroya Basin (La Rioja, Spain). *J Paleolimnol* 27:453–463
- O’Sullivan PE (1983) Annually laminated lake sediments and the study of Quaternary environmental changes – a review. *Quat Sci Rev* 1:245–313
- Romero-Viana L, Julià R, Camacho A, Vicente E, Miracle MP (2008) Climate signal in varve thickness: La Cruz (Spain), a case study. *J Paleolimnol* 40:703–714
- Rull V (2014) Time continuum and true long-term ecology: from theory to practice. *Front Ecol Evol* 2:75
- Rull V (2023) Anticipation, discovery and serendipity in Quaternary paleoecology: personal insights from the Iberian Pyrenees. *Quaternary* 6:42
- Rull V, Vegas-Vilarrúbia T (2014) Preliminary report on a mid-19th century Cannabis pollen peak in NE Spain: historical context and potential chronological significance. *The Holocene* 24:1378–1383
- Rull V, Vegas-Vilarrúbia T (2015) Crops and weeds from the Estany de Montcortès catchment, central Pyrenees, during the last millennium: a comparison of palynological and historical records. *Veget Hist Archaeobot* 24:699–710

- Rull V, Vegas-Vilarrúbia T (2021) Conifer forest dynamics in the Iberian Pyrenees during the Middle Ages. *Forests* 12:1685
- Rull V, González-Sampériz P, Corella JP, Morellón M, Giralt S (2011) Vegetation changes in the southern Pyrenean flank during the last millennium in relation to climate and human activities: the Montcortès lacustrine record. *J Paleolimnol* 46:387–404
- Rull V, Trapote MC, Safont E, Cañellas-Boltà N, Pérez-Zanón N, Sigró J et al (2017) Seasonal patterns of pollen sedimentation in Lake Montcortès (Central Pyrenees) and potential applications to high-resolution paleoecology: a 2-year pilot study. *J Paleolimnol* 57:95–108
- Rull V, Vegas-Vilarrúbia T, Corella JP, Valero-Garcés B (2021a) Bronze Age to Medieval vegetation dynamics and landscape anthropization in the south-central Pyrenees. *Palaeogeogr Palaeoclimatol Palaeoecol* 571:110392
- Rull V, Vegas-Vilarrúbia T, Corella JP, Trapote MC, Montoya E, Valero-Garcés B (2021b) A unique Pyrenean varved record provides a detailed reconstruction of Mediterranean vegetation and land-use dynamics over the last three millennia. *Quat Sci Rev* 268:107128
- Saarnisto M (1979) Application of annually-laminated lake sediments: a review. In: Vasari Y, Saarnisto M, Seppälä M (eds) *Palaeohydrology of the temperate Zone: Proceedings of the Working Session of Commission on Holocene – INQUA*, pp 97–108
- Saarnisto M, Ojala AEK (2009) Varved sediments. In: Gornitz V (ed) *Encyclopedia of paleoclimatology and ancient environments, encyclopedia of earth sciences series*. Springer, pp 973–975
- Scussolini P, Vegas-Vilarrúbia T, Rull V, Corella JP, Valero-Garcés B, Gomà J (2011) Middle and late Holocene climate change and human impact inferred from diatoms, algae and aquatic macrophyte pollen in sediments from Lake Montcortès (NE Iberian Peninsula). *J Paleolimnol* 46:369–385
- Trapote MC, Vegas-Vilarrúbia T, López P, Puche E, Gomà J, Buchaca T et al (2018a) Modern sedimentary analogues and integrated monitoring to understand varve formation in the Mediterranean Lake Montcortès (Central Pyrenees, Spain). *Palaeogeogr Palaeoclimatol Palaeoecol* 496:292–304
- Trapote MC, Rull V, Giralt S, Montoya E, Corella JP, Vegas-Vilarrúbia T (2018b) High-resolution (subdecadal) pollen analysis of varved sediments from Lake Montcortès (southern Pyrenean flank): a fine-tuned record of landscape dynamics and human impact during the last 500 years. *Rev Palaeobot Palynol* 259:207–222
- Vegas-Vilarrúbia T, Corella JP, Pérez-Zanón N, Buchaca T, Trapote MC, López P et al (2018) Historical shifts in oxygenation regime as recorded in the laminated sediments of lake Montcortès (Central Pyrenees) support hypoxia as a continental-scale phenomenon. *Sci Total Environ* 612:1577–1592
- Vegas-Vilarrúbia T, Rull V, Trapote MC, Cao M, Rosell-Melé A, Buchaca T et al (2020) Modern analogue approach applied to high-resolution varved sediments – a synthesis for Lake Montcortès (Central Pyrenees). *Quaternary* 3:1

- Vegas-Vilarrúbia T, Corella JP, Sigró J, Rull V, Dorado-Liñán I, Valero-Garcés B et al (2022) Regional precipitation trends since 1500 CE reconstructed from calcite sublayers of a varved Mediterranean lake record (Central Pyrenees). *Sci Total Environ* 826:153773
- Zolitschka B, Francus P, Ojala AEK, Schimmelmann A (2015) Varves in lake sediments – a review. *Quat Sci Rev* 117:1–41

Acknowledgments

The research on Lake Montocortès was funded by the Spanish Ministry of Science and Technology, projects RyC2003, LIMNOCLIBER (REN 2003-09130-C02-02), and MEDLANT (CGL 2016-7215-R), and the Spanish Ministry of Economy and Competitiveness, project MONT-500 (CGL 2012-3665 and CGL 2017-85682-R). Fieldwork permits were granted by the Territorial Service of the Department of Agriculture, Livestock, Fishing and Natural Environment of Catalonia (Barcelona). The collaboration of local entities and persons, notably the Council of Baix Pallars (Gerri de la Sal), was crucial for fieldwork development. Historical documentation was provided by the Pallars Sobirà District Archive (Sort).

Contents

1	Lake Montcortès and Its Surroundings	1
1.1	Geographical Setting	1
1.2	Geology	5
1.3	Climate	7
1.4	Vegetation	11
1.5	The Varves	18
	References	22
2	Cultural History of the Pallars Region	25
2.1	Bronze Age (2700–800/750 BCE)	28
2.1.1	Early Bronze (2700–2100 BCE)	28
2.1.2	Middle Bronze (2100–1650 BCE)	28
2.1.3	Late Bronze (1650–800/750 BCE)	30
2.2	Iron Age (800/750–72 BCE)	30
2.2.1	First Iron Age (800/750–450 BCE)	30
2.2.2	Second Iron Age (450–72 BCE)	31
2.3	Roman Epoch (72 BCE–418 CE)	31
2.3.1	Commercial Activities	32
2.3.2	Farming and Forest Exploitation	32
2.3.3	Mining	33
2.4	Middle Ages (418–1488 CE)	33
2.4.1	Chronology	34
2.4.2	Territory and Society	37
2.4.3	The Feudal Landscapes	40
2.4.4	The Late Medieval Crisis	42
2.5	Modern Age (1488–1789 CE)	42
2.5.1	Territory	42
2.5.2	Population	45
2.5.3	Institutions	46
2.5.4	The Economy	47
2.6	Contemporary Times (1789–2005)	49
2.6.1	Traditional Precapitalist Society (Late Eighteenth Century to 1870 CE)	52
2.6.2	The Crisis of the Subsistence Economy (1870–1910 CE)	53

2.6.3	The Transition to Modern Society (1910–1960 CE)	54
2.6.4	The Second Crisis (1960–1980 CE)	55
2.6.5	The Modern Capitalist Society (1980–2005 CE)	55
2.7	Summary	56
	References	58
3	Methodological Hints	61
3.1	Coring and Core Sampling	62
3.1.1	Coring	62
3.1.2	Chronology and Sedimentation Rates	63
3.1.3	Core Sampling	64
3.2	Pollen Analysis and Interpretation	66
3.2.1	Sample Processing, Analysis, and Interpretation Insights	66
3.2.2	Modern-Analog Survey	68
3.3	Comparison with External Drivers of Ecological Change	78
	References	79
4	From Prehistory to the Roman Empire	85
4.1	The Pollen Diagram	85
4.1.1	General Description	85
4.1.2	Zonation	87
4.2	Vegetation and Landscape Dynamics	89
4.2.1	Late Bronze Age	89
4.2.2	Iron Age	92
4.2.3	Roman Epoch	94
	References	97
5	Middle Ages	99
5.1	The Pollen Diagram	99
5.1.1	General Description	99
5.1.2	Zonation	101
5.2	Vegetation and Landscape Dynamics	103
5.2.1	Visigothic Period	103
5.2.2	Muslim Period	106
5.2.3	Frank Period	107
5.2.4	County of Pallars	107
5.3	A Closer Look to Medieval Deforestation	109
5.4	Highland Forests	112
5.4.1	Lake Liebreta	114
5.4.2	Sant Maurici	115
5.4.3	Subalpine Deforestation and Microrefugia	120
5.5	Comparison of Montcortès and Sant Maurici Medieval Forests	123
	References	125

6	Modern and Contemporary Times	129
6.1	The Pollen Diagram	129
6.1.1	General Description	129
6.1.2	Zonation	131
6.2	Vegetation and Landscape Dynamics	132
6.2.1	Modern Age	132
6.2.2	Precapitalism	135
6.2.3	Demographic Crises and the Transition to Capitalism	136
6.2.4	Capitalism	137
6.3	Hemp Industry in Lake Montcortès and Surrounding Areas	137
6.3.1	The Montcortès Record	137
6.3.2	Direct Evidence for Hemp Retting	142
6.3.3	The Estanya Record	146
6.3.4	The Iberian Peninsula	147
6.4	Modern Age Deforestation.	148
6.5	High-Resolution Statistical Analysis of Forest Succession	150
6.5.1	Paleoenvironmental Records	150
6.5.2	Statistical Analyses	152
6.5.3	Individual Responses	154
6.5.4	Assemblage and Succession Analysis	158
6.5.5	The Role of External Factors in Regional Forest Succession.	161
	References.	162
7	Historical Deforestations and Forest Resilience	167
7.1	Resilience and Associated Concepts	168
7.2	Resilience of Montcortès Forests.	169
7.2.1	Bulk Resilience	170
7.2.2	Mosaic Resilience	171
7.2.3	Community Resilience.	175
7.3	Comparisons and Conservation Insights	175
7.3.1	Comparisons with Other Pyrenean Records	180
7.3.2	Applications to Conservation.	181
	References.	182
8	Synthesis, Comparisons, and Future Studies	185
8.1	Chronological Synthesis	186
8.2	Statistical Synthesis	192
8.3	The Iberian and Mediterranean Contexts.	196
8.3.1	The Iberian Peninsula: Anthropization Patterns	196
8.3.2	The Mediterranean Region: The Uniqueness of the Montcortès Record.	198
8.4	Potential Future Developments	201
	References.	204



Lake Montcortès and Its Surroundings

1

Abstract

Lake Montcortès is one of the few lakes with annually laminated (varved) sediments documented in the Mediterranean region. This small (400–500 m diameter) and deep (32 m) kidney-shaped carstic lake is situated on the Iberian side of the central Pyrenees at 1027 m elevation under a seasonal temperate montane climate with Mediterranean influence. The annual average temperature is 9.7 °C, with winter minima of 2.0 °C and summer maxima of 19.0 °C. The total annual precipitation averages 1031 mm, with maxima in spring (110 mm) and autumn (90 mm) and minima in summer (70 mm) and winter (58 mm). The regional vegetation is a mosaic of three main forest types—evergreen Mediterranean sclerophyll forests dominated by *Quercus rotundifolia*, and deciduous submontane forests dominated by *Q. pubescens/Q. subpyrenaica*, and conifer montane forests dominated by *Pinus nigra*—intermingled with shrublands, meadows, grasslands, herbaceous crops, and badlands. A fringe of well-developed and diverse aquatic vegetation dominated by grasses and sedges grows on the lake shores. Limnologically, Lake Montcortès shows meromictic/monomictic behavior, which favors the formation and preservation of seasonal laminations of the biogenic/endogenic type, with alternating light (calcite) and dark (organic) layers. The Montcortès laminated sequence is unique across the Mediterranean region, as it is continuous and absolutely dated, encompassing at least the last 3000 years.

1.1 Geographical Setting

Lake Montcortès (Fig. 1.1) is located in the northwestern Iberian Peninsula, which is situated in the westernmost part of the circum-Mediterranean region (Fig. 1 of the Introduction). Topographically, the lake lies on the southern-central flank of the



Fig. 1.1 Lake Montcortès in different seasons. (a) View of the lake from the SW in summer (July 2017). (b) View of the lake from the NE in autumn (November 2018). The lake surroundings are dominated by deciduous oak forests, and the background evergreen forests are dominated by pines (see Sect. 4 for more information). Photos: V. Rull

Pyrenean range, which is a natural barrier that coincides with the political boundary between Spain and France (Fig. 1.2). Physiographically, the lake lies in the headwaters of the Noguera Pallaresa River, a tributary of the Segre River draining to the south as part of the Ebro River basin, which flows into the Mediterranean Sea. Politically, the lake belongs to the Pallars Sobirà district (*comarca*) of the Spanish autonomous community of Catalonia (see Chap. 3; Cultural History).

The area considered in this book is located between approximately $42^{\circ}15'–42^{\circ}30'N$ and $0^{\circ}50'–1^{\circ}10'E$ and comprises the upper valleys of the Noguera Pallaresa River and one of its tributaries, the Flamisell River, which converges in the largest town of the area, La Pobla de Segur, with almost 3000 inhabitants (Fig. 1.3). The other comparable town is Sort (~2200 inhabitants), the capital of the Pallars Sobirà, whereas other urban centers are significantly smaller, with ~750 (La Torre de Capdella), ~660

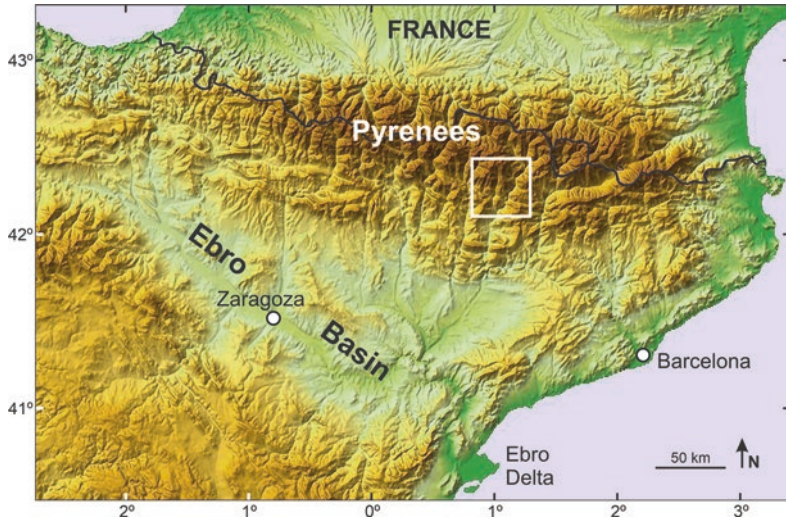


Fig. 1.2 Topographic map of northwest Spain with emphasis on the Pyrenees and the Ebro Basin. The study area is represented as a white box (see Fig. 1.3 for more details)

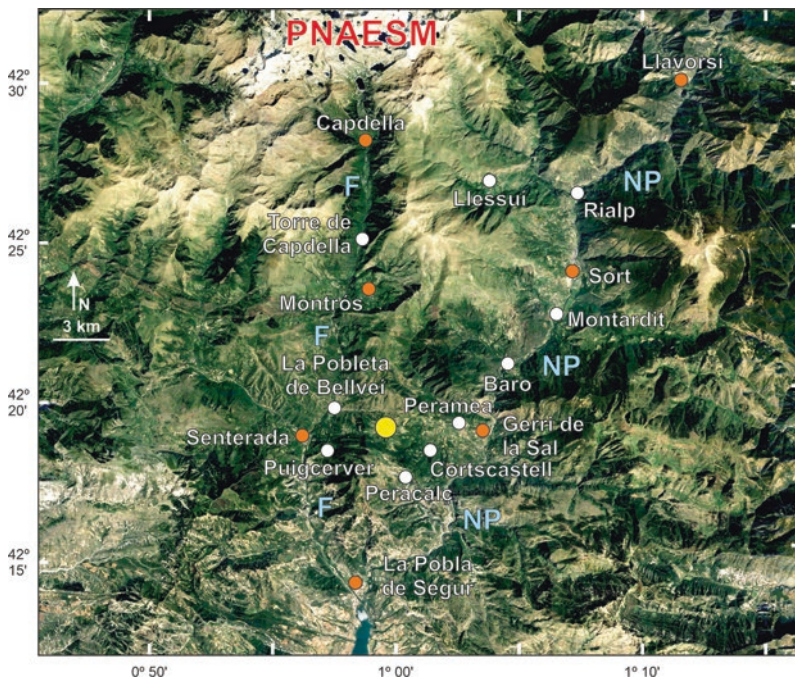


Fig. 1.3 Google Earth image of the study area (see Fig. 1.2 for location) indicating the main towns and villages (those having weather stations are highlighted by orange dots; see Sect. 3) along the Noguera Pallaresa (NP) and Flamisell (F) valleys. PNAESM, National Park of Aiguestortes i Estany de Sant Maurici (glacial highland landscape). The location of Lake Montcortès is indicated by a yellow dot. Base image: Google Earth



Fig. 1.4 (a) View of the erosional depression (highlighted by a white solid line) where Lake Montcortès (central black patch) is situated between the Flamisell (F) and Noguera Pallaresa (NP) valleys. Base image: Google Earth. (b) Summit of the Peracalç Range (up to 1315 m elevation), which is known as the “sleeping giant,” with the “head” on the left side and the “feet” on the right side. Photo: V. Rull

(Rialp), ~350 (Llavorsí), ~200 (La Pobleta de Bellvei), or barely 100 inhabitants (Gerri de la Sal, Montardit, Peramea, Senterada). Others are hamlets inhabited by one or a few-tenths of people. Lake Montcortès lies on an erosional depression situated between Gerri de la Sal (east) and Senterada (west) and flanked by the Ruixou and Culroi ranges to the north and the Peracalç Range to the south (Fig. 1.4).

In this area, Lake Montcortès is situated at $42^{\circ}19'50''\text{N}$ – $0^{\circ}59'41''\text{E}$ and has an elevation of 1027 m a.s.l. This lake has a kidney-like shape and is relatively tiny, measuring approximately 400–500 m in diameter. Its total surface area spans 0.14 km^2 , and it reaches a maximum depth of 32 m. The lake’s watershed is also modest, covering 1.4 km^2 , and it is mainly nourished by underground water sources, while it is occasionally supplemented by a few intermittent small creeks and scattered springs (Bayarri 2005). No detailed information is available on the hydrology of superficial or underground waters. There is a permanent outlet in the north (Fig. 1.5).

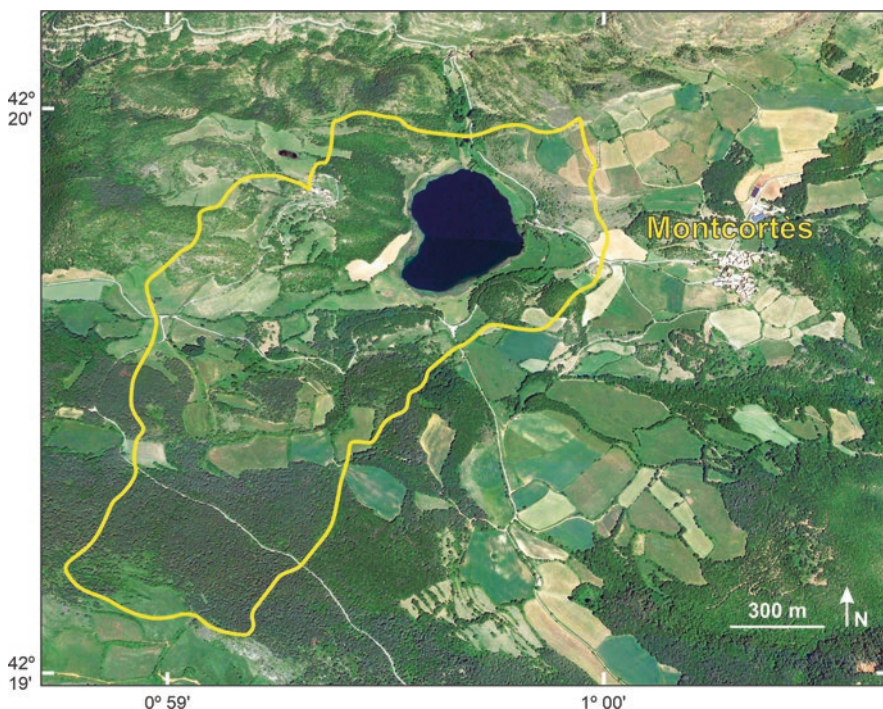


Fig. 1.5 Lake Montcortès (black patch) and its surroundings. The yellow contour is the approximate extent of the lake watershed. The hamlet of Montcortès (~20 inhabitants) is at right. Base image: Google Earth

1.2 Geology

The erosional depression on which Lake Montcortès lies is characterized by Triassic evaporitic (halites) and nonevaporitic (limestones) rocks, together with Quaternary sediments, which are especially abundant around the lake (Fig. 1.6). The northern and southern mountain ranges are formed by Silurian slates (Culroi), Cretaceous carbonates (Peracalç), or Eocene-Oligocene conglomerates (Ruixou). See Fig. 1.4 for the locations of these ranges. The depression originated from the lateral spreading of the Peracalç Range after the Puigcerver-Senterada and Gerri de la Sal-Peramea landslides. This was combined with subsidence due to the interstratal dissolution of halite-bearing Triassic evaporites (Fig. 1.6). The Puigcerver-Senterada landslide is located on the eastern margin of the Flamisell valley and covers ~3 km², involving Cretaceous and Triassic rocks. The Gerri de la Sal-Peramea landslide is located on the western margin of the Noguera Pallaresa valley and covers ~7 km², affecting Triassic limestones, as well as the underlying clays and evaporites. Evaporite dissolution is difficult and plays a significant role in this gravitational deformation, which is supported by the occurrence of numerous saline springs situated at the foot of the landslide. Some radiocarbon ages provide evidence for Late

Holocene (~1300–1200 yr BP) landslide activity in the area. On the other hand, the carbonate sequence of the Peracalç Range has spread in an NNE to NE direction toward the Montcortès depression covering ~4.5 km². Differential subsidence of fault blocks in the carbonate sequence due to the interstratal karstification of the underlying evaporites has been considered an important process to explain the lateral spread of the Peracalç Range. Minimum ages for the lateral spread of the Peracalç range correspond to the Late Pleistocene (~45 kyr BP). The Montcortès depression, where the lake is situated, is an east–west syncline with Triassic evaporitic sediments (Facies Keuper) overlain by limestones (Facies Muscheskalk). An ellipsoidal evaporitic collapse area is present around the lake (Fig. 1.6), forming a karstic depression resulting from the coalescence of several collapse sinkholes

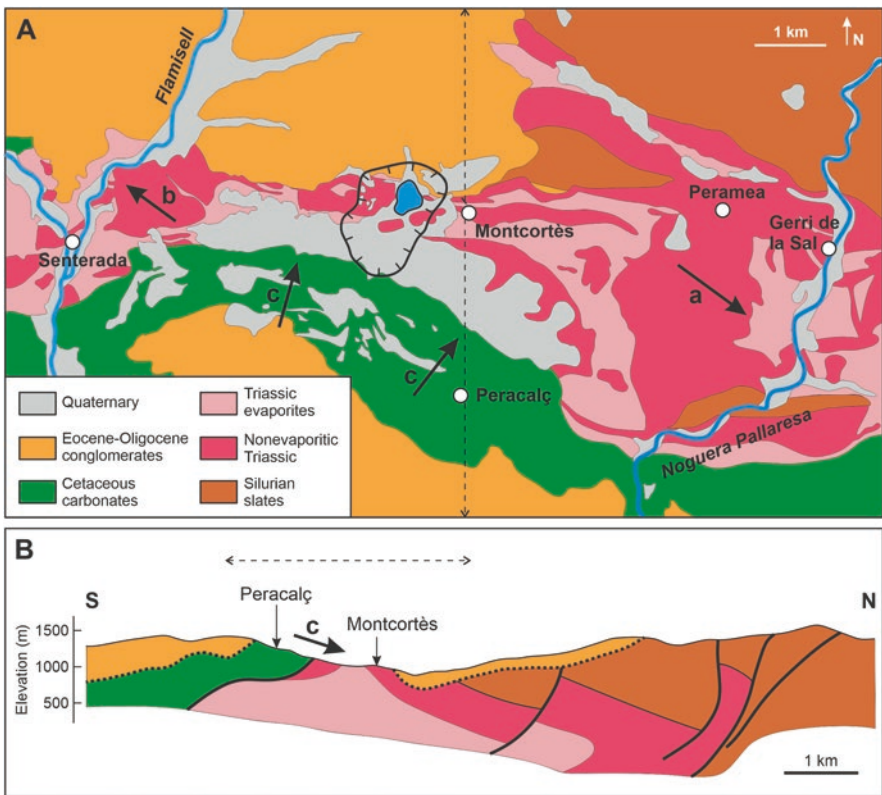


Fig. 1.6 Geology of the Senterada-Gerri de la Sal erosional depression (Fig. 1.4). (a) Geological map. Lake Montcortès is represented as a blue patch, and the area affected by evaporite dissolution collapse is highlighted by a black solid line. White dots are towns, and blue lines are rivers. The vertical dotted line indicates the direction of the cross section represented in the lower panel. a, Gerri de la Sal-Peramea landslide; b, Puigcerver-Senterada landslide; c, Peracalç Range lateral spread. (b) North–South cross section across the dotted line of the upper panel. Faults are represented as thick solid lines, and unconformities are depicted as dotted lines. Redrawn and modified from Gutiérrez et al. (2012)

(Gutiérrez et al. 2012). This process is common in the formation of most Pyrenean and Iberian karstic lakes (Corella et al. 2011; Valero-Garcés et al. 2014). It has been proposed that groundwaters feeding Lake Montcortès circulate mostly by Triassic limestones (Bayarri 2005).

1.3 Climate

The absence of a local weather station in Lake Montcortès has hindered the climatic characterization of the site. However, a recent study using data from a network of nearby stations has enabled us to define the main climatic patterns of the area and to estimate the climatic patterns based on seven weather stations situated along the Noguera Pallaresa and Flamisell valleys between approximately 530 and 1280 m elevation (Fig. 1.3). These stations have variable measurement intervals, encompassing the period 1955–2020 (66 years). The climatic characterization of these stations in terms of temperature and precipitation using climatic diagrams (climographs) for representative time periods (WMO 2017) is shown in Fig. 1.7. Overall, the highest temperatures are observed during the summer months of July and August, while the lowest temperatures occur in the winter, specifically in January and December. Elevation plays a significant role in temperature variation. Precipitation patterns are less consistent, but the greatest amounts typically fall during the spring and autumn seasons. Summers tend to be drier, suggesting some Mediterranean influence. However, unlike typical Mediterranean climates, the period of summer dryness is shorter and less severe than the dry spells experienced in winter, particularly from January to March and in December. February stands out as the driest month, while May is the wettest month.

Using these data, it was possible to derive statistically significant elevational gradients in temperature and precipitation for the Montcortès area (Rull et al. 2022). The annual average temperature decreased at an average rate of $-0.59\text{ }^{\circ}\text{C}/100\text{ m}$ elevation ($r = -0.899$; $p = 0.006$), and the total annual precipitation increased at an average rate of $82\text{ mm}/100\text{ m}$ ($r = 0.996$; $p = 0.0004$). These lapse rates are comparable to those measured in other areas from the Pyrenees and other Iberian mountains, as well as in the Alps (Rolland 2003; Navarro-Serrano et al. 2018). The corresponding regression equations allowed the estimation of annual average temperature ($9.70\text{ }^{\circ}\text{C}$) and precipitation (1031 mm) for the elevation of Lake Montcortès (1027 m). Statistically significant gradients in these parameters were also obtained for monthly averages, which allowed estimation of monthly temperature and precipitation values, which were used to assemble a climogram for the lake site (Fig. 1.8).

According to this climogram, the highest average temperatures, $\sim 19\text{ }^{\circ}\text{C}$, are seen in July and August, while the lowest temperatures, ranging from 2 to $2.5\text{ }^{\circ}\text{C}$, occur in January and February. The peak in precipitation, approximately 110 mm , occurs in May and June. After a drop in July to $\sim 70\text{ mm}$, it increases to values exceeding 90 mm from August to November. The lowest precipitation levels are observed from January to March, with February being the driest

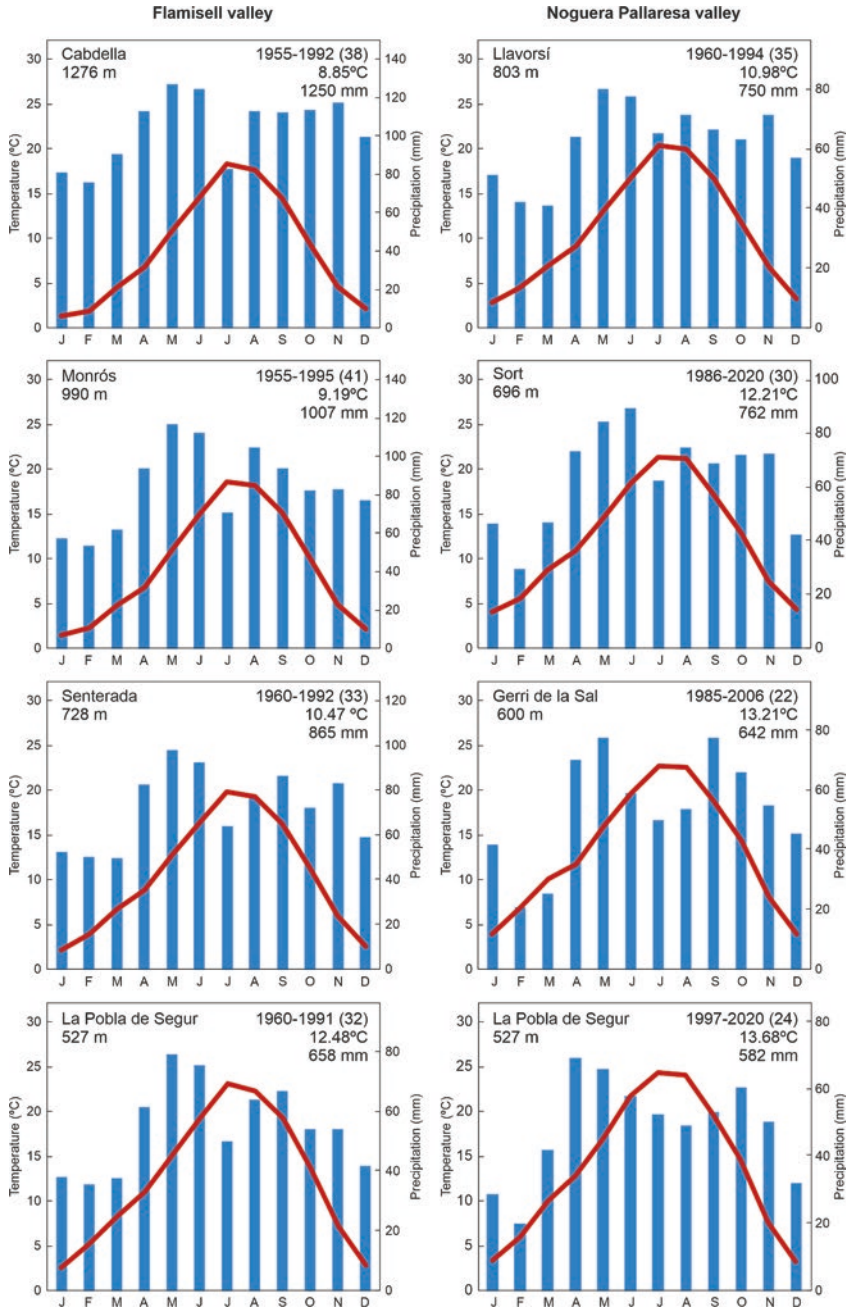


Fig. 1.7 Climographs for seven weather stations analyzed. There are two separate diagrams for the La Poble station, each representing distinct measurement periods. The climographs are sorted based on elevation and their respective valleys, with the Flamisell valley displayed on the left side and the Noguera Pallaresa valley on the right side (Fig. 1.7). Redrawn from Rull et al. (2022)

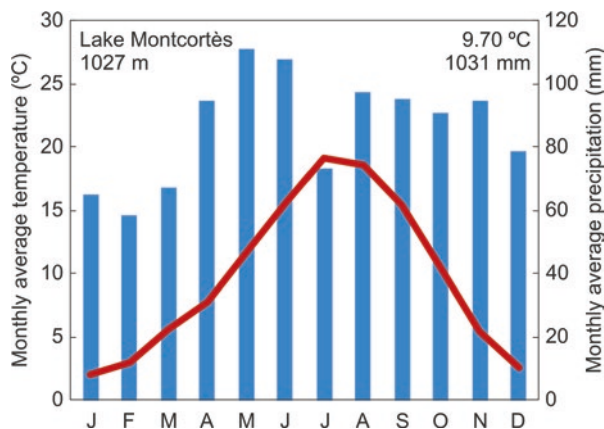


Fig. 1.8 Estimated climograph for Lake Montcortès obtained by linear interpolation using statistically significant elevational gradients. Redrawn from Rull et al. (2022)

month (58 mm). When considering the annual average temperature and precipitation, the Montcortès climogram falls between Montrós and Capdella but is more similar to Montrós (Fig. 1.7). The temperature follows the same seasonal pattern as other diagrams, while the precipitation trends are similar to those of the Capdella station, albeit with slightly higher temperatures and lower precipitation levels due to the difference in elevation. Overall, this suggests that the climate of Lake Montcortès, despite its intermediate location between the Flamisell and Noguera Pallaresa valleys, is more akin to the stations in the first, especially in terms of seasonality. This implies that the Mediterranean influence on the Montcortès climate is weaker compared to the stations in the Noguera Pallaresa valley, which are at lower elevations and have a stronger orientation toward the Mediterranean.

Composite temperature and precipitation series using these data in the form of anomalies with respect to the average values have provided the trends of these climatic parameters for the last 66 years in the study area (Fig. 1.9). During the 1960s, there was a noticeable drop in temperatures, leading to a period of cooler weather in the 1970s, with temperatures reaching as much as approximately 1 °C below the usual average. In 1980, there was a sudden increase in temperature, marking the start of an ongoing overall warming trend. By the end of the observation period in 2020, temperatures had risen to ~2 °C above the cooler phase observed from 1965 to 1980. In terms of precipitation, it was at its highest in 1960 but quickly began a prolonged decline, which continued throughout the cold phase from 1965 to 1980, reaching its lowest levels, ~200 mm below the average, coinciding with the warming trend in 1980. This dry period extended until 1990, and after a decade of gradual increases in precipitation, a new dry period started in 2004, lasting until 2017. A brief recovery was observed from 2017 to 2020. Interestingly, throughout the 1980–2020 warming period, precipitation levels mostly remained below or around the average.

These climatic data series can also be valuable for modern analog studies and proxy calibration, particularly in the context of the lake and its vicinity. Indeed, the temperature and precipitation anomalies depicted in Fig. 1.9 can be employed to develop transfer functions able to estimate past temperature and precipitation patterns using a variety of physicochemical and biological proxies from the Montcortès varved record. If necessary, the climatic data series can be broken down into seasonal data series or supplemented with maximum and minimum values to assess whether correlations between climate and proxies improve, ultimately enhancing the reliability of reconstructions. For example, in a study by Vegas-Vilarrúbia et al. (2022), a regional climatic training set was used to establish a significant correlation between the thickness of calcite layers in varves and autumn precipitation. This correlation allowed the development of a transfer function for reconstructing autumn

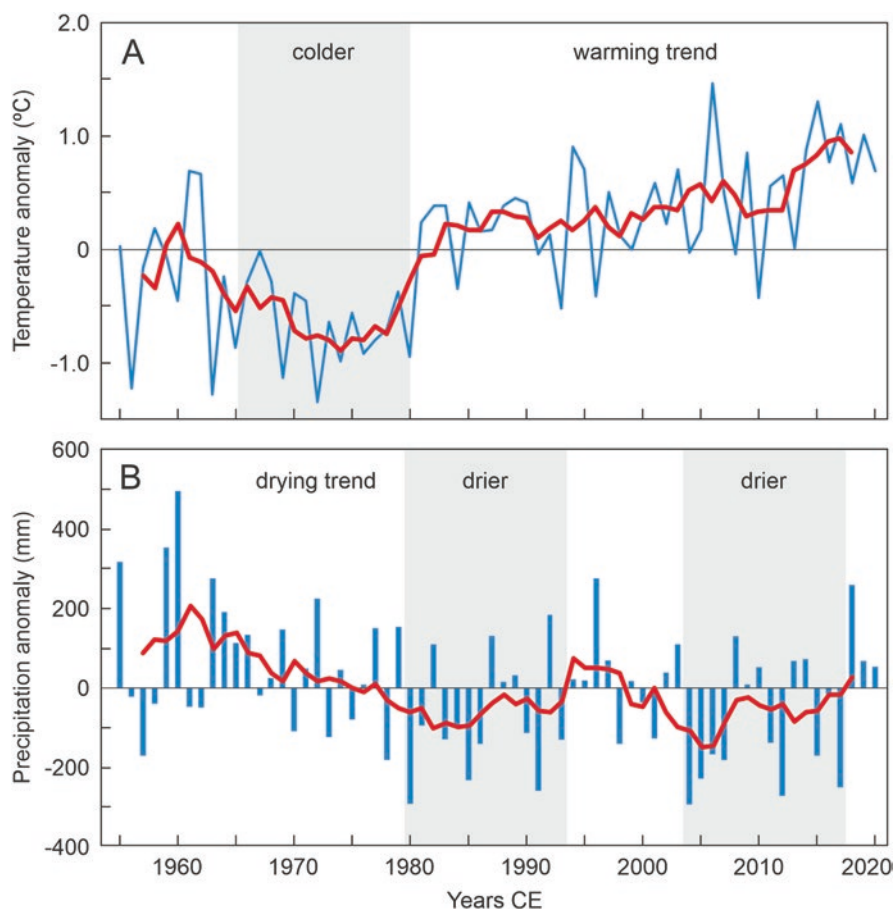


Fig. 1.9 Temperature (a) and precipitation (b) trends of the last seven decades based on the average anomalies of the seven weather stations referenced in Fig. 1.3. Blue lines/bars are actual measures, and red lines are 5-yr moving averages. Redrawn from Rull et al. (2022)

paleoprecipitation from calcite thickness over the past 500 years. It would be interesting to replicate this analysis using the dataset provided here to determine whether this relationship remains consistent or if different patterns emerge at a more local scale.

1.4 Vegetation

Lake Montcortès is situated close to the altitudinal boundary between the submontane and montane belts, typically found at elevations of approximately 800–1000 m in the Pyrenees, varying based on local conditions, as noted in Vigo and Ninot (1987) (Fig. 1.10). This location exhibits four distinct forest formations that mirror this particular elevation boundary (Fig. 1.11): (1) Mediterranean sclerophyllous forests, represented by *Quercus rotundifolia* woodlands; (2) submontane deciduous oak forests, which experience higher precipitation and are primarily dominated by *Quercus pubescens* and *Q. subpyrenaica*; (3) conifer forests primarily composed of *Pinus nigra* subsp. *salzmannii*, often replacing deciduous oak forests, as observed by Folch (1981) and Bolòs et al. (2004); (4) forests at higher elevations dominated by *Pinus sylvestris*, serving as the transition zone between the submontane and montane belts. It is worth noting that some of these conifer forests might have been intentionally planted. The primary vegetation types in the Montcortès erosional depression are represented in Fig. 1.12 using the CORINE system specifically applied to Catalonia (Carreras et al. 2005–2006).

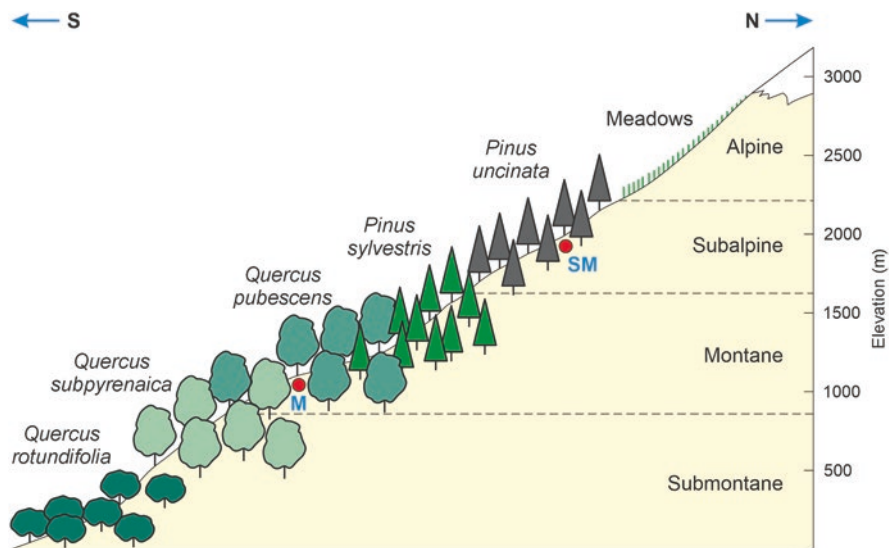


Fig. 1.10 Elevational arrangement of the dominant forest types in the southern-central Pyrenees. M, Lake Montcortès; SM, Lake Sant Maurici. Modified from Vigo (2008) and Ninot et al. (2017)



Fig. 1.11 General aspect of the Montcortès landscape during fall, showing the transition between the submontane and montane forest belts. Submontane forests dominated by *Quercus subpyrenaea* (deciduous) are light-brown, while evergreen *Q. rotundifolia*-*Pinus nigra* subsp. *salzmannii* forests appear as dark green. In the background, at higher elevations, montane forests are dominated by *Q. pubescens* (deciduous) and *P. sylvestris* (evergreen). Photo: V. Rull

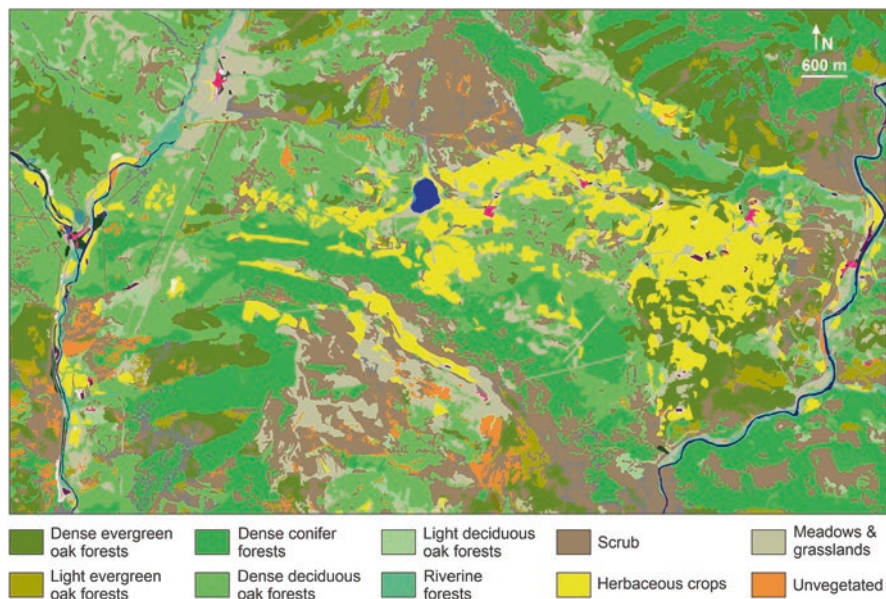


Fig. 1.12 Vegetation map of the Montcortès erosional depression and adjacent mountain ranges. The lake is the central blue patch. Base map downloaded from the Institut Cartogràfic i Geològic de Catalunya (ICGC) (<https://www.icgc.cat/>, accessed 18 March 2022). Urban areas are represented as red patches. Vegetation units according to Carreras et al. (2005–2006)

There are two primary categories of regional shrubland, one characterized by the prevalence of *Amelanchier ovalis*, *Buxus sempervirens* and *Rhamnus saxatilis*, while the other is dominated by *Arctostaphylos uva-ursi* alongside *Buxus sempervirens*. Herbaceous ecosystems predominantly include meadows and pastures featuring *Aphyllanthes monspelliensis* and *Arrhenaterum elatius*, herbaceous cereal crops such as *Hordeum* sp., *Avena sativa*, *Triticum* sp., *Secale cereale*, and certain forage plants, such as *Medicago sativa*. These areas also exhibit the presence of various weeds, such as *Lolium rigidum*, *Papaver rhoeas*, *Polygonum aiiculare* and *Bromus* sp. Additionally, there are abandoned croplands that have been colonized by shrubs and ruderal species, as well as barren badlands with sparse vegetation or scattered shrubs and herbs from different communities (Carreras et al. 2005–2006). Figure 1.12 shows the distribution of these vegetation types, and Table 1.1 provides information on their composition and key environmental characteristics.

Table 1.1 Main components and environmental features of the vegetation types defined for the region around Lake Montcortès (Fig. 1.12)

Vegetation types	Main components	Environmental observations
Conifer forests	<i>Pinus sylvestris</i> or <i>Pinus nigra</i> subsp. <i>salzmanii</i> , poorly developed understory	Diverse substrates
Evergreen oak forests	<i>Quercus rotundifolia</i> , well-developed understory with abundant sclerophyllous shrubs (<i>Quercus coccifera</i> , <i>Rhamnus alaternus</i> , <i>Rhamnus saxatilis</i> , <i>Prunus spinosa</i> , <i>Buxus sempervirens</i> , <i>Lonicera etrusca</i>). Herbaceous stratum with nemoral (shadow-adapted) species: <i>Rubia peregrina</i> , <i>Teucrium chamaedrys</i> , <i>Asparagus acutifolius</i> , and <i>Brachypodium retusum</i>	Well-exposed sites of lowland plains, hills, and slopes
Deciduous oak forests	<i>Quercus pubescens</i> , sometimes with <i>Pinus sylvestris</i> or, less frequently, <i>Fagus sylvatica</i> or <i>Tilia cordata</i> . Other trees: <i>Quercus cerrioides</i> , <i>Quercus subpyrenaica</i> , <i>Acer monspessulanum</i> , <i>Acer opalus</i> subsp. <i>opalus</i> ; Shrubs: <i>Buxus sempervirens</i> , <i>Coronilla emerus</i> , <i>Amelanchier ovalis</i> , <i>Colutea arborescens</i> , <i>Cytisophyllum sessilifolium</i> , <i>Viburnum lantana</i> ; Herbs: <i>Primula veris</i> subsp. <i>columnae</i> , <i>Hepatica nobilis</i> , <i>Brachypodium phoenicoides</i> , <i>Campanula persicifolia</i>	Well-exposed warm slopes, submontane stage, up to 1500 m a.s.l., calcareous substrates
Scrub 1	<i>Amelanchier ovalis</i> , <i>Buxus sempervirens</i> and <i>Rhamnus saxatilis</i> . Up to 2 m high, with an irregular herbaceous stratum of heliophyllous plants. Other shrubs: <i>Coronilla emerus</i> , <i>Ligustrum vulgare</i> , <i>Cytisophyllum sessilifolium</i> ; Herbs: <i>Tanacetum corymbosum</i> , <i>Viola alba</i> , <i>Teucrium chamaedrys</i> , <i>Carex halleriana</i>	Well-exposed rocky slopes, on calcareous terrains. Secondary colonizer where the forest has been removed
Scrub 2	<i>Arctostaphylos uva-ursi</i> , with some emergent shrubs (<i>Buxus</i>) or trees (<i>Pinus</i> , <i>Quercus</i>). Other shrubs: <i>Juniperus communis</i> , <i>Amelanchier ovalis</i> ; Herbs: <i>Primula veris</i> subsp. <i>columnae</i> , <i>Lavandula angustifolia</i> subsp. <i>pyrenaica</i> , <i>Hepatica nobilis</i> , <i>Cruciata glabra</i> , <i>Carex humilis</i> , <i>Avenula pratensis</i> subsp. <i>iberica</i>	Deforested areas and forest clearings on calcareous soils

(continued)

Table 1.1 (continued)

Vegetation types	Main components	Environmental observations
Meadows	<i>Aphyllanthes monspelliensis</i> . Shrubs: <i>Salvia lavandulifolia</i> , <i>Santolina chamaecyparissus</i> , <i>Ononis natrix</i> , <i>Teurcium polium</i> , <i>Genista scorpius</i> , <i>Helianthemum italicum</i> , <i>Euphorbia nicaeensis</i> , <i>Thymus vulgaris</i> ; Herbs: <i>Avenula pratensis</i> subsp. <i>iberica</i> , <i>Koeleria vallesiana</i> , <i>Brachypodium phoenicoides</i> , <i>Leuzea conifera</i> , <i>Linum narbonense</i> , <i>Carduncellus monspeliensium</i> , <i>Catananchoe caerulea</i> , <i>Asperula cerasiferus</i> , <i>Asperula cynanchica</i>	Light pastures from 1000 to 1400 m a.s.l., on calcareous, generally unstable terrains
Mowing meadows	<i>Arrhenaterum elatius</i> . Other herbs: <i>Trisetum flavescens</i> , <i>Trifolium pretense</i> , <i>Dactylis glomerata</i> , <i>Rhinanthus mediterraneus</i> , <i>Gentiana lutea</i> , <i>Plantago lanceolata</i> , <i>Lotus corniculatus</i> , <i>Daucus carota</i> , <i>Rumex acetosa</i>	Plains and gentle slopes with deep and eutrophic soils
Herbaceous crops	Cereals, rarely forages, with abundant weeds. Herbs: <i>Hordeum sp.</i> , <i>Avena sativa</i> , <i>Triticum sp.</i> , <i>Secale cereale</i> , <i>Medicago sativa</i> ; Weeds: <i>Lolium rigidum</i> , <i>Papaver rhoeas</i> , <i>Bromus sp.</i> , <i>Polygonum aviculare</i>	Open valleys and gentle slopes, on clayey deep soils
Unvegetated	Devoid of vegetation or with few scattered plants like <i>Achnatherum calamagrostis</i> , <i>Brachypodium phoenicoides</i> , <i>Erucastrum nasturtifolium</i> , <i>Tussilago farfara</i> , <i>Genista scorpius</i> , <i>Thymus vulgaris</i> or <i>Lithospermum fruticosum</i>	Highly eroded terrains, generally on steep slopes
Urban areas	Diverse ruderal and cultivated flora	

Littoral vegetation is depicted in more detail in Fig. 1.13. Simplified from Rull et al. (2011), after Carreras et al. (2005–2006)

Mercadé et al. (2013) conducted a detailed survey of the flora and vegetation in and around the lake. They documented a total of 534 plant species, representing 291 genera and 76 families. The most prominent family was Asteraceae, accounting for 15.7% of the species, followed by Poaceae (10.4%), Papilionaceae (9.0%), and Cyperaceae (3.9%). Among the five pteridophytes they found (constituting 0.9% of the plant life), only the horsetail *Equisetum arvense* was associated with aquatic environments. In general, the flora in Montcortès is similar to other pre-Pyrenean areas (Vigo and Ninot 1987). However, the unique micro-environments created by the lake contribute to a higher level of plant diversity. From a phytogeographical perspective, the Montcortès flora is primarily a mixture of Eurosiberian and Mediterranean elements, with variations depending on the type of vegetation. Eurosiberian species are more prominent in forests, meadows, and pastures, especially those with meridional and sub-Mediterranean characteristics, while strictly Mediterranean elements are dominant in drier environments.

Forest species with a broad Eurosiberian distribution, including *Betula pendula*, *Cornus sanguinea*, *Hepatica nobilis*, *Hieracium lachenalii*, and *Lonicera*

xylosteum, can be contrasted with species, such as *Buxus sempervirens*, *Coronilla emerus*, *Cytisophyllum sessilifolium*, *Cotoneaster tomentosus*, and *Primula veris* subsp. *columnae*, which tend to be more sub-Mediterranean in their distribution. In regard to hay meadows, Eurosiberian elements like *Arrhenatherum elatius*, *Avenula pubescens*, *Holcus lanatus*, and *Trisetum flavescens* from the Poaceae family are noteworthy, along with various species from other families. In mesophilic pastures, Eurosiberian elements such as *Briza media*, *Carex caryophyllea*, *Cirsium acaule*, *Plantago media*, and *Trifolium montanum* are commonly found. It is also worth noting the presence of Atlantic distribution species, such as *Centaurea nigra* in hay meadows, mesophilic pastures, and forest edges, and *Pulmonaria longifolia* in forests.

In *Aphyllanthes* grasslands, Mediterranean elements are represented by dominant species such as *Catananche coerulea*, *Lavandula latifolia*, *Leuzea conifera*, and *Thymelaea pubescens*. Dry slopes and low scrubs are characterized by *Brachypodium retusum*, *Dorycnium pentaphyllum*, *Helichrysum stoechas*, and *Santolina chamaecyparissus*, among others. High Mediterranean mountain regions are home to species such as *Merendera montana* and *Rosa sicula*.

A significant portion of the Montcortès flora consists of calcicolous species, primarily because of the prevalence of calcareous substrates. Nevertheless, the presence of acidic ophytes contributes to the presence of silicicolous or acid-loving plants such as *Chamaespartium sagittale*, *Danthonia decumbens*, *Dianthus armeria*, *Hieracium sabaudum*, *Trifolium arvense*, and *Trifolium glomeratum*. Some arvense species that are currently rare, such as *Camelina sativa* subsp. *microcarpa*, *Caucalis platycarpos*, *Centaurea cyanus*, *Delphinium peregrinum* subsp. *verdunense*, and *Galium tricornutum*, continue to thrive in cultivated fields. This suggests that herbicides and pesticides are either used sparingly or not at all.

In general, the vegetation is primarily of a Submediterranean nature, although there are some Mediterranean elements present, along with azonal communities associated with the lake and other wet regions. Aquatic vegetation is quite diverse, especially when considering vascular plants alone. It comprises a noticeable strip of plants adapted to wet conditions, which can be divided into four clearly distinguishable zones from the water's edge to the land: (1) areas with *Typha domingensis* or *Cladium mariscus*, (2) reedbeds of *Phragmites australis*, (3) communities of *Carex riparia*, and (4) patches of rushes and grasslands found on periodically flooded soils. These zones are not evenly distributed along the lake's shoreline, with only the second zone forming a continuous strip. More information on the specific types of aquatic and semiaquatic vegetation is provided in Table 1.2, and their spatial distribution around the lake is illustrated in Fig. 1.13.

Table 1.2 Habitat and vegetation units defined by Mercadé et al. (2013) for Lake Montcortès margins using the CORINE system (CEC 191)

Habitats	Vegetation types	Vegetation units
A Aquatic/ semiaquatic	1 Submerged vegetation, sometimes with floating leaves	1a Smaller pondweeds (<i>Potamogeton crispus</i> , <i>P. pectinatus</i>) and other submerged rooted plants (<i>Myriophyllum spicatum</i>)
		1b <i>Chara</i> spp., <i>Nitellopsis obtusa</i> submerged carpets
		1c <i>Utricularia australis</i> and <i>Ranunculus trichophyllus</i> with both submerged and floating leaves on shallow waters with fluctuating water levels
		1d Rooted pondweeds with large floating leaves (<i>Potamogeton coloratus</i>)
		1e <i>Polygobum amphibium</i> , often rooted and with floating leaves
	2 Water-fringe vegetation	2a <i>Cladium mariscus</i> beds
		2b Reedmace (<i>Typha dominguensis</i>) beds
		2c <i>Iris pseudocarus</i> formations
		2d Flooded <i>Phragmites</i> beds
	B Hygrophyle vegetation on wet or inundated soils	3 Vegetation of inundated soils
3b Common spikerush (<i>Eleocharis palustris</i>) beds		
3c Formations occupying the banks of small rivers or springs		
4 Vegetation of wet or temporarily flooded soils		4a Beds of <i>Scirpus lacustris</i> , <i>Juncus subnodulosus</i> , and other rushes
		4b Brown sedge (<i>Carex distincta</i>) beds
		4c Subnitrophilous rushes and sedges (<i>Juncus inflexus</i> , <i>Carex hirta</i>)
		4d Meadows and grasslands of <i>Molinia coerulea</i> , <i>Cirsium monspessulanum</i> , and <i>Carex lepidocarpa</i>
		4e Hygrophyle rugh and tall grass formations with <i>Scirpus holoschoenus</i>
		4f Red beds dry for a large part of the year
C Temporarily wet or flooded soils		5 Vegetation of temporarily wet or flooded soils
	5b <i>Cyperus fuscus</i> (temporarily flooded)	
	5c Grasslands on compact impermeable soils with <i>Plantago serpentina</i>	

(continued)

Table 1.2 (continued)

Habitats	Vegetation types	Vegetation units
D Meadows and pastures	6 Meadows, pastures, and dwarf grasslands	6a Hay meadows with false oat grass (<i>Arrhenatherun eliiatus</i>)
		6b Calcicolous mesophile (usually mowed) grasslands with <i>Trifolium incarnatum</i> subsp. <i>molineri</i>
		6c Mesophile grasslands with <i>Filipendula vulgaris</i>
		6d Xerophilous calcareous grasslands with <i>Festuca gr. ovina</i> , <i>Koeleria vallesiana</i> , and abundant therophytes
		6e Calcicolous <i>Aphyllanthes</i> grasslands rich in camaephytes
		6f Dwarf annual siliceous grasslands often on sandy soils
		6g Dwarf annual grasslands with <i>Poa bulbosa</i> on compact soils
E Shrubby vegetation	7 Shrubby vegetation	7a Sub-Mediterranean blackthorn (<i>Prunus spinosa</i>) and bramble thickets
		7b Box formations with scattered trees intermingled with <i>Aphyllanthes</i> grasslands and low scrubs
		7c <i>Genista Scorpius</i> formations
		7d Calcicolous open low scrubs with <i>Thymus vulgaris</i> , <i>Satureja montana</i> , and <i>Onobrychis hispanica</i>
F Forests and forest fringes	8 Forests and forest fringes	8a Ash (<i>Fraxinus excelsior</i>) forests
		8b Calcicolous white oak (<i>Quercus oubescens</i> , <i>Q. pyrenaica</i>) woods
		8c Silicicolous white oak (<i>Quercus oubescens</i> , <i>Q. pyrenaica</i>) woods
		8d Mesophile aspen (<i>Populus tremula</i>) stands
		8e Willow (<i>Salix atrocinerea</i>) shrubby formations
		8f Mixed forests with <i>Quercus rotundifolia</i> , <i>Q. pubescens</i> , and <i>Q. subpyrenaica</i>
		8x Hems or semidry oak woods, often with <i>Coronilla varia</i>
		8y Hems or mesophile woods with <i>Trifolium medium</i> and <i>Valeriana officinalis</i>
		8z Subnitrophilous shady woodland edges
G Anthropic habitats	G Anthropic vegetation	9a Dry or mesophile intensive pastures
		9b Dry extensive crop fields
		9c Deciduous tree spots
		9d Kitchen gardens
		9e Ruderal communities
		10 Country houses

See Fig. 1.12 for the spatial arrangement of these vegetation units around the lake. Redrawn and modified from Mercadé et al. (2013)

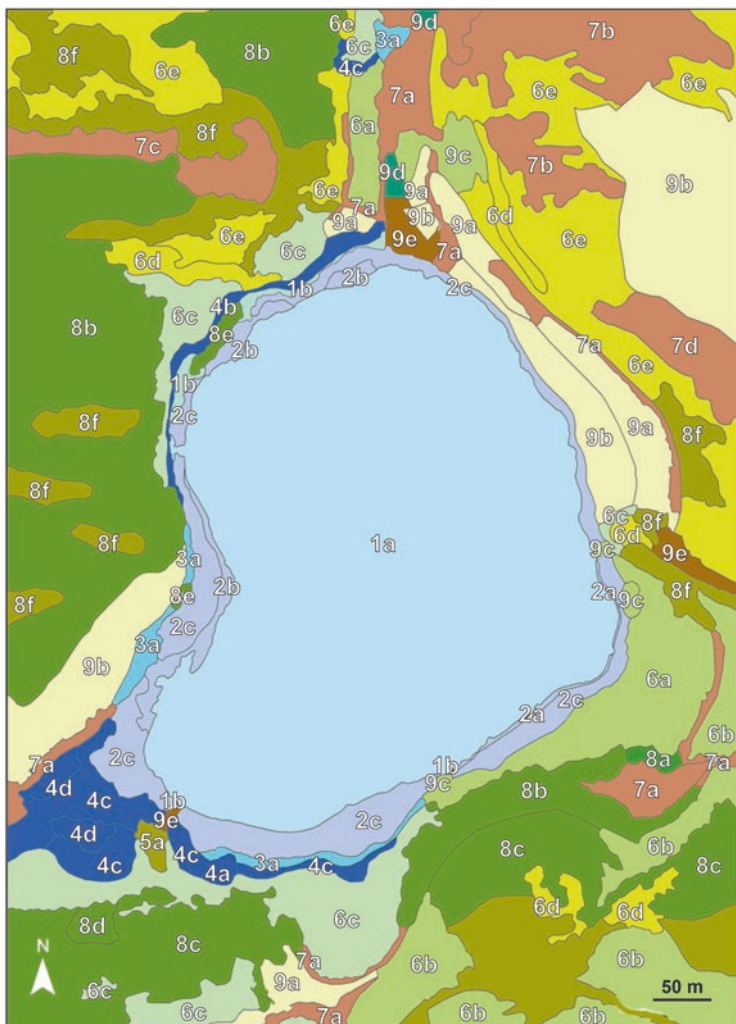


Fig. 1.13 Vegetation map of Lake Montcortès margins using the CORINE units (CEC 1991) defined in Table 1.2

1.5 The Varves

Lake Montcortès holds the necessary conditions for varve formation and preservation, including strong seasonal contrast, multiple autochthonous and allochthonous sources of sedimentary material, and lack of postdepositional reworking and sediment mixing. As explained in the introductory chapter, deep lakes such as Montcortès are especially well suited for the formation and preservation of varved sediments because they are stratified and favor oxygen depletion in bottom waters (hypolimnion), a situation that can persist throughout the year (meromixis) or can be

disrupted by one or two periods of vertical mixing and oxygenation of deep waters (monomixis/dimixis). The occurrence of a prolonged period of anoxic/hypoxic conditions in the hypolimnion is essential for the formation and preservation of varves by preventing bioturbation. The reader is referred to the introductory chapter for more information on this subject.

Lake Montcortès is a deep karstic structure (Sect. 2) with a total depth of ~40 m or more, including >30 m of water and a minimum sedimentary thickness of 6 m. The bathymetry shows that maximum water depths are attained close to the shore due to their steep internal slopes, which makes a large part of the lake >20 m deep (Fig. 1.14). Under these conditions, thermal stratification and the development of a relatively isolated and persistent anoxic/hypoxic hypolimnion is favored, as demonstrated by the available limnological studies.

The first limnological studies of Lake Montcortès showed a meromictic regime characterized by the existence of a permanent anoxic hypolimnion throughout the year (Camps et al. 1976). Some years later, the total mixing of the water column was recorded during fall and winter, and the anoxic hypolimnion disappeared, which was attributed to a strong rainfall increase that homogenized the water column (Modamio et al. 1988). The conclusion was that the lake was meromictic, but external meteorological disturbances, in this case heavy rainfall episodes, may eventually break the meromictic regime, thus fostering monomictic dynamics (Modamio et al. 1988). Further studies developed during two consecutive years (Trapote et al. 2018) reported thermal homogenization of the water column and well-oxygenated hypolimnetic conditions during winter (January–February). Thermal stratification and the development of a hypoxic hypolimnion (<2 mg O₂ L⁻¹) began in spring

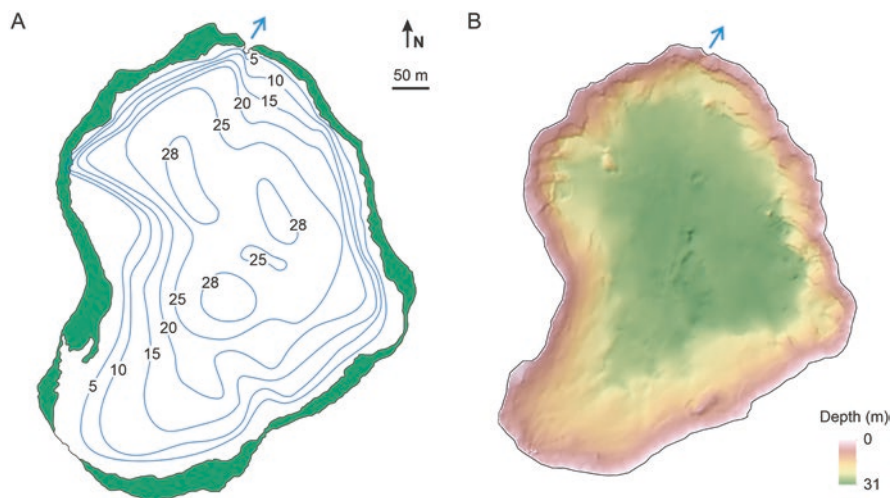


Fig. 1.14 Bathymetry of Lake Montcortès. (a) Bathymetric map (isobaths in m) of Modamio et al. (1988) using manual depth measures. The green fringe represents the aquatic and semiaquatic vegetation (see Sect. 4 for more information). (b) Bathymetric map of Corella et al. (2019) based on a detailed seismic survey. Blue arrows indicate the lake outlet

(March–April) and intensified in summer (June) with the formation of an anoxic hypolimnion (0 mg O₂ L⁻¹) that remained until December. The maximum development of this anoxic hypolimnion occurred at the summer/fall transition (September–October), reaching 15–17 m depth, which is approximately half of the total water depth (Fig. 1.15). This supported that the lake was not strictly meromictic, and the thermal homogenization and oxygenation of the water column observed by Modamio et al. (1988) in winter (monomixis) could be considered a usual feature rather than an anomaly. Nevertheless, the persistence of hypoxic/anoxic hypolimnetic conditions for most of the year (10 months) creates suitable conditions for varve formation and preservation (Trapote et al. 2018).

In addition, there is evidence for significant interannual variability in mixing and oxygenation conditions leading to complex meromictic/monomictic dynamics over time. Indeed, a study based on physicochemical sedimentary proxies for oxic/anoxic conditions revealed four types of four main scenarios during the last 500 years: (A) years with abrupt sediment inputs; (B) years with outstanding mixing and oxygenation of the water column; (C) years with strong stratification, anoxia, and increased biomass production; and (D) years with stratification and anoxia but relatively less biomass production. Overall, ~45% of the last 500 years were mixing years, while ~55% were meromictic, showing a remarkable clustering into groups of consecutive years. The period 1500–1820, when human impact was stronger, was D-years, whereas the period 1850–1899 was a typical A-year. B-years were more irregularly distributed but were best represented in the period 1820–1849. The twentieth century was dominated by C-years, which has suggested that global warming is favoring the development of hypoxic/anoxic conditions, a situation that seems to be of global reach (Vegas-Vilarrúbia et al. 2018).

Lake Montcortès sedimentary varves are of the biogenic/endogenic type (Zolitschka et al. 2015), specifically of the carbonaceous-biogenic type (Dean

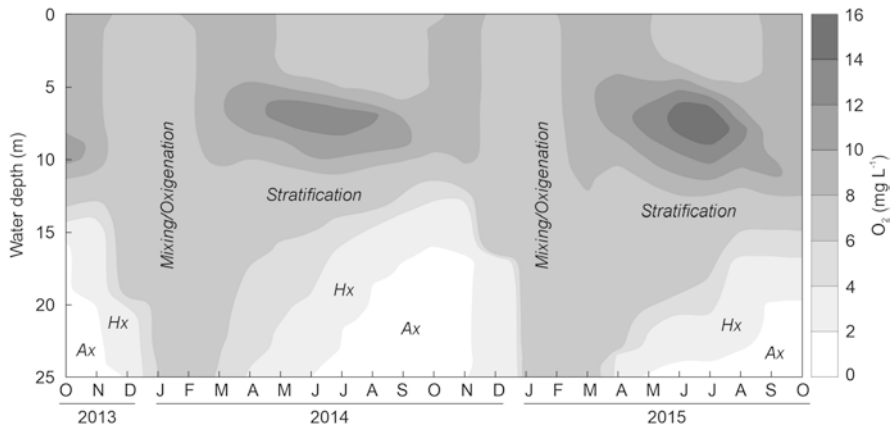


Fig. 1.15 Yearly evolution of dissolved oxygen in relation to water depth showing the monomictic character of Lake Montcortès during two consecutive annual cycles. Simplified from Trapote et al. (2018). Ax, anoxia; Hx, hypoxia

and Megard 1993). These varves consist of couplets of light calcite and brownish organic layers (microfacies M1) that are believed to have been deposited in spring/summer and fall/winter, respectively, as occurs in biogenic varves typical of karstic lakes (Brauer 2004). A variant of these couplets is triplets, formed by the inclusion of a grayish detrital layer between the calcite and the organic layers (microfacies M2) (Corella et al. 2012). The calcite layer is composed of calcite crystals with diatoms and has been interpreted as the result of biogenic calcite precipitation during the seasons of maximum productivity of limnetic communities. The organic layer is composed of amorphous organic matter, diatoms, detrital carbonate, and quartz and is thought to reflect seasonal changes in sediment delivery to the lake controlled by rainfall and runoff. The detrital layers are composed of detrital calcite, quartz and feldspar grains, plant remains, and clay minerals, which were deposited during periods of increased runoff in the catchment (Corella et al. 2012). However, a further study using permanent traps to capture the sediments deposited throughout the year (see Chap. 3, Sect. 4.2.1 for methodological details) showed slightly different seasonal patterns, as the calcite layer was formed mostly in summer/fall and the organic layer was deposited during winter/spring (Trapote et al. 2018). According to the same study, the organic layer would represent the background lake productivity throughout the year, whereas the calcite layer would represent the summer/fall increases in temperature and primary production. The uncompacted varves that form today are a few cm thick, but the compacted varves formed in the past are of millimetric scale, ranging from 0.28 mm (fourth–fifth centuries CE) to 2.62 mm (eleventh–fourteenth centuries CE) of total thickness (Fig. 1.16) (Corella et al. 2012).

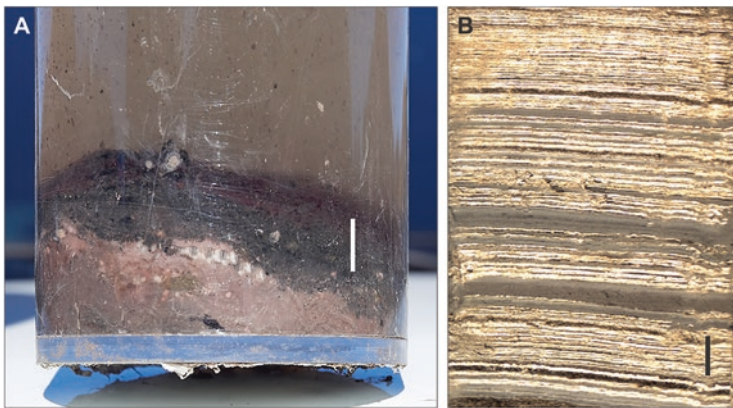


Fig. 1.16 Present and past sedimentary varves from Lake Montcortès. (a) Uncompacted varve formed by a light-dark couplet sedimented during a 2016–2017 annual cycle in a transparent tubular pollen trap submerged near the lake bottom (see Chap. 3 for methodological details). Photo: V. Rull. (b) Compacted varves corresponding to a section of core MON04-4A-1K (drive 4), accumulated during the Roman epoch, between approximately 240 CE and 400 CE (see Fig. 3.3). Vertical bars represent 1 cm

References

- Bayarri J (2005) Origen de les Aigües del Llac de Montcortès (Baix Pallars, Lleida). Treball de Fi de Carrera, Univ Barcelona, Barcelona
- Bolòs O, Vigo J, Carreras J (2004) Mapa de la Vegetació Potencial de Catalunya 1:250.000. Inst Estudis Catalans, Barcelona
- Brauer A (2004) Annually laminated lake sediments and their paleoclimatic relevance. In: Fischer H (ed) *Climate in historical time: towards a synthesis of holocene proxy data and climate models*. Springer, Heidelberg, pp 108–128
- Camps J, Gonzalvo I, Güell J, López P, Tejero A, Toldrà X et al (1976) El lago de Montcortès, descripció de un ciclo anual. *Oecol Aquat* 2:99–110
- Carreras J, Vigo J, Ferré A (2005–2006) Manual dels hàbitats de Catalunya, vols I–VIII. Departament de Medi Ambient i Habitatge, Generalitat de Catalunya, Barcelona
- Corella JP, Moreno A, Morellón M, Rull V, Giralt S, Rico MT et al (2011) Climate and human impact on a meromictic lake during the last 6,000 years (Montcortès Lake, Central Pyrenees, Spain). *J Paleolimnol* 46:351–367
- Corella JP, Brauer A, Mangili C, Rull V, Vegas-Vilarrúbia T, Morellón M et al (2012) The 1.5-ka varved record of Lake Montcortès (southern Pyrenees, NE Spain). *Quat Res* 78:323–332
- Corella JP, Benito G, Wilhelm B, Montoya E, Rull V, Vegas-Vilarrúbia T et al (2019) A millennium-long perspective of flood-related seasonal sediment yield in Mediterranean watersheds. *Glob Planet Change* 177:127–140
- Dean WE, Megard RO (1993) Environment of deposition of CaCO₃ in Elk Lake, Minnesota. In: Bradbury JP, Dean WE (eds) *El Lake, Minnesota: evidence for rapid climate change in the North-Central United States*. *Geol Soc Am Spec Pap* 276:97–114
- Folch R (1981) *La Vegetació dels Països Catalans*. Ketres, Barcelona
- Gutiérrez F, Linares R, Roquè C, Zarroca M, Rosell J, Galve JP et al (2012) Investigating gravitational grabens related to lateral spreading and evaporite dissolution subsidence by means of detailed mapping, trenching, and electrical resistivity tomography (Spanish Pyrenees). *Lithosphere* 4:331–353
- Mercadé A, Vigo J, Rull V, Vegas-Vilarrúbia T, Garcés S, Lara A et al (2013) Vegetation and landscape around Lake Montcortès (Catalan pre-Pyrenees) as a tool for palaeoecological studies of Lake sediments. *Collect Bot* 32:87–101
- Modamio X, Pérez V, Samarra F (1988) *Limnología del lago de Montcortès (ciclo 1978–79) (Pallars Jussà, Lleida)*. *Oecol Aquat* 9:9–17
- Navarro-Serrano F, López-Moreno JJ, Azorin-Molina C, Alonso-González E, Tomás-Bruguera M, Sanmiguel-Valladolid A et al (2018) Estimation of near-surface air temperature lapse rates over continental Spain and its mountain areas. *Int J Climatol* 38:3233–3249
- Ninot JM, Carrillo E, Ferré A (2017) The Pyrenees. In: Loidi J (ed) *Vegetation of the Iberian Peninsula*. Springer, Cham, pp 323–366
- Rolland C (2003) Spatial and seasonal variations of air temperature lapse rates in Alpine regions. *J Clim* 16:1032–1046
- Rull V, González-Sampéris P, Corella JP, Morellón M, Giralt S (2011) Vegetation changes in the southern Pyrenean flank during the last millennium in relation to climate and human activities: the Montcortès lacustrine record. *J Paleolimnol* 46:387–404
- Rull V, Sigró J, Vegas-Vilarrúbia T (2022) Present climate of Lake Montcortès (central Pyrenees): paleoclimatic relevance and insights on future warming. *Geogr Res Lett*. <https://doi.org/10.18172/cig.5412>
- Trapote MC, Vegas-Vilarrúbia T, López P, Puche E, Gomà J, Buchaca T et al (2018) Modern sedimentary analogues and integrated monitoring to understand varve formation in the Mediterranean Lake Montcortès (Central Pyrenees, Spain). *Palaeogeogr Palaeoclimatol Palaeoecol* 496:292–304
- Valero-Garcés B, Morellón M, Moreno A, Corella JP, Martín-Puertas C, Barreiro F et al (2014) Lacustrine carbonates of Iberian karst lakes: sources, processes and depositional environments. *Sed Geol* 299:1–29

- Vegas-Vilarrúbia T, Corella JP, Pérez-Zanón N, Buchaca T, Trapote MC, López P et al (2018) Historical shifts in oxygenation regime as recorded in the laminated sediments of lake Montcortès (Central Pyrenees) support hypoxia as a continental-scale phenomenon. *Sci Total Environ* 612:1577–1592
- Vegas-Vilarrúbia T, Corella JP, Sigró J, Rull V, Dorado-Liñán I, Valero-Garcés B et al (2022) Regional precipitation trends since 1500 CE reconstructed from calcite sublayers of a varved Mediterranean lake record (Central Pyrenees). *Sci Total Environ* 826:153773
- Vigo J (2008) *Flora i Vegetació de l'Alta Muntanya Catalana*. Inst Estudis Catalans, Barcelona
- Vigo J, Ninot JM (1987) Los Pirineos. In: Peinado M, Rivas-Martínez F (eds) *La Vegetación de España*. Univ Alcalá de Henares, Madrid, pp 349–389
- WMO (2017) *WMO Guidelines on the calculation of climate normals*. World Meteorological Organization, Geneva
- Zolitschka B, Francus P, Ojala AEK, Schimmelmann A (2015) Varves in lake sediments – a review. *Quat Sci Rev* 117:1–41



Abstract

Lake Montcortès is situated in the Pallars geopolitical and historical region. In the chronological context of this book, six main prehistoric/historical phases can be distinguished: Late Bronze Age (1100–800 BCE), Iron Age (800–72 BCE), Roman Epoch (72 BCE–418 CE), Middle Ages (418–1488 CE), Modern Age (1488–1789 CE), and Contemporary times (1789 CE–present). Prehistoric cultures were essentially autochthonous and characterized by small scattered nomadic groups evolving toward more organized Neolithic societies living in fortified cities. The Roman occupation of the Pallars was mostly marginal, and autochthonous cultures persisted. After short phases of Visigoth, Muslim, and Carolingian domination, the Middle Ages witnessed the development of the independent County of Pallars (872–1488 CE)—characterized by a feudal regime, the abandonment of slash-and-burn practices, and the development of long-distance horizontal transhumance—which ended with the conquest of the region by the Castilla-Aragon Crown. In the Modern Age, the feudal organization was replaced by a precapitalist society, characterized by the development of extraregional communications and the ensuing commercial intensification. Contemporary times began with the French occupation (1808 CE) and ended with the establishment of modern democracy (and the Bourbons again) after the Franco dictatorship (1939–1975 CE). This was paralleled by the progressive development of capitalism and industrial society, initiated by the second half of the nineteenth century.

Having a comprehensive understanding of cultural (i.e., political, economical, migratory, etc.) history is crucial for enhancing our interpretation of paleoecological records, particularly in regard to distinguishing between the influences of natural and human factors on changes in vegetation and landscape dynamics over time.

While the cultural history of the Pallars region, where Lake Montcortès is situated, is relatively well documented, it is primarily available in the Catalan language, which poses a barrier for international readers. In this context, we present an English summary based on the book edited by Marugan and Rapalino (2005), which is focused specifically on the Pallars region, as a whole. In the last decade, some archeological studies have been conducted on the central Pyrenean highlands including part of the PNAESM, which falls within the Pallars region (Fig. 1.3). These studies enriched the knowledge on pastoralist activities and will be mentioned when necessary.

The Pallars region, located in the Spanish autonomous region of Catalonia, has undergone various transformations over the centuries. However, it has consistently maintained a geographical unity centered around the Medieval County of Pallars (872–1488 CE), which roughly corresponds to the present-day administrative divisions known as Pallars Jussà, Pallars Sobirà, and Alta Ribagorça (Fig. 2.1). Geographically, the Pallars region spans from the highest peaks of the Catalan Pyrenees (exceeding 3000 m) in the north to lower elevations (approximately 500 m) in the south (Fig. 2.2). This elevation gradient is locally interrupted at the southernmost edge of the Pallars region by the Montsec Range, a relatively small and narrow mountain range that extends for approximately 40 km and reaches heights of nearly 1700 m. The Montsec Range serves as a natural barrier separating the Pallars region from the lowlands in the south (elevations ranging from 100 to 300 m), and it has played a significant role in the region's history. To provide a comprehensive overview, our account begins in the Bronze Age, aligning with the chronological framework of available vegetation reconstructions, which encompass the period from the Late Bronze Age (~3050 BP or ~1100 BCE) up to the present day (2013 CE) (refer to Rull et al. 2011, 2021a, c; Trapote et al. 2018a, b for more



Fig. 2.1 The Pallars region. (a) Political subdivision of Spain with the location of Catalonia (red area) and the adjacent regions (Aragon, Valencia) that have played a significant historical role. (b) Political subdivision of Catalonia. The three *comarques* that make up the historical Pallars region are highlighted by the red outline. Other *comarques* and cities that have been important historically are also indicated: VA, Val d'Aran; AU, Alt Urgell; C, Cardona; L, Lleida

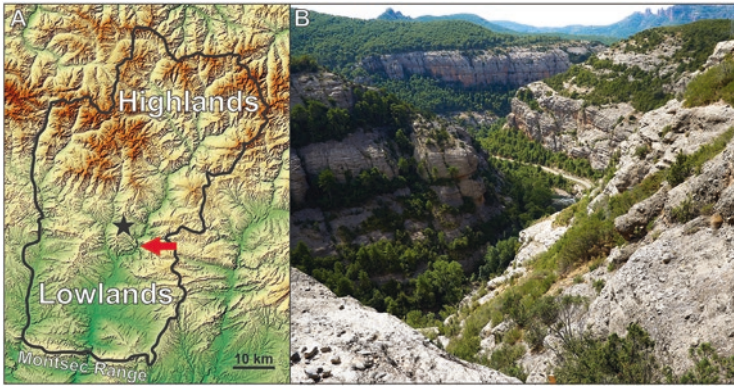


Fig. 2.2 (a) Topographic map of the Pallars region. Highlands in orange and lowlands in green. Lake Montcortès is represented by a black star and the Collegats gorge is indicated by a red arrow. (b) View of the Collegats gorge and the old pathway (now an abandoned route) built in the late seventeenth century (Sect. 5.4.6). Photo: V. Rull

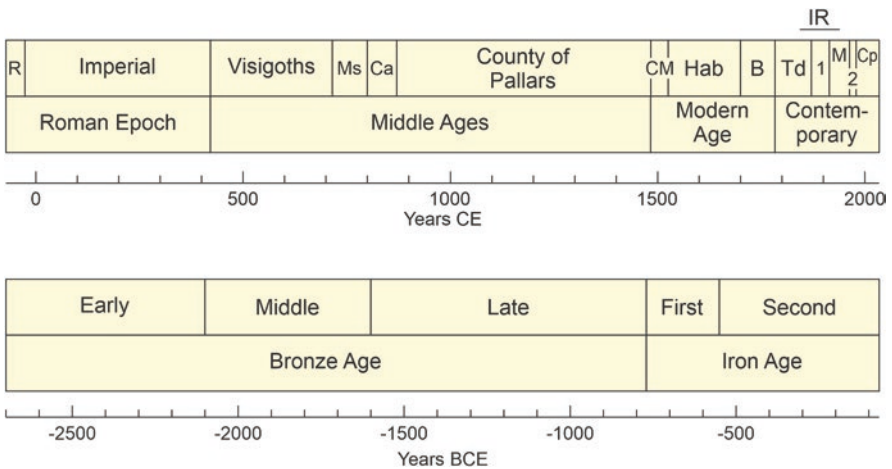


Fig. 2.3 Prehistoric/protohistoric (below) and historical (above) chronology of the Pallars region according to Cots (2005), Marugan and Rapalino (2005), Bringué (2005), and Farràs (2005). R, Republican period; Ms., Muslims; Ca, Carolingians; CM, Catholic monarchy; Hab, Habsburg; B, Bourbon; Td, traditional precapitalist society; 1, crisis of the subsistence economy; M, modernization; 2, second crisis as a consequence of the Catalan Industrial Revolution (IR); Cp, capitalism

details). A summary of the chronology of the Pallars region, spanning from prehistory to the present, is presented in Fig. 2.3.

In general, much more abundant and detailed information is available for the historical period, since the Middle Ages onward, due to the existence of written documents. Prehistoric information, based primarily on archaeological evidence, is comparatively scarcer. Archaeological evidence for human occupation before the

Bronze Age, especially for high-mountain environments, is available at Esteban (2003), Rodríguez et al. (2016), Gassiot et al. (2017), Obea et al. (2021), and literature therein.

2.1 Bronze Age (2700–800/750 BCE)

The Bronze Age was defined by the advancement of farming methods and the use of refined stone tools. It commenced with the introduction of metallurgical practices involving the copper-tin alloy, commonly known as bronze. In the Pallars region, the Bronze Age started approximately 2700 BCE (or 4650 years BP) and boasts significant archaeological evidence (Fig. 2.4). This age can be further categorized into three primary phases: Early Bronze (*Bronze Antic*), Middle Bronze (*Bronze Ple*), and Late Bronze (*Bronze Final*), as described by Cots (2005).

2.1.1 Early Bronze (2700–2100 BCE)

This phase, known as the Chalcolithic or Copper Age, was characterized by the emergence of copper and bronze metallurgy, along with commercial activities. However, materials such as stone (quartz and flint), bone, and wood remained prevalent for crafting tools, weapons, and various objects. Ceramics, particularly notable for their innovative decorative elements, were also common. Human communities were small and dispersed, residing in caves and open settlements, and organized into family clans with early signs of social distinctions. The primary economic activity was nomadic pastoralism in specific geographical regions, while agriculture was still in its early stages. Hunting, focusing on animals such as deer and wild boar, as well as fishing for trout and eel, played vital roles. Burial was the primary funerary practice, and there is evidence of megalithic customs, including dolmens and other collective burial structures scattered throughout the area (see Fig. 2.4).

2.1.2 Middle Bronze (2100–1650 BCE)

The phase was marked by significant changes resulting from the interaction between the indigenous Neolithic population and small groups arriving from the north, particularly from what is now France. These groups crossed the Pyrenees by using river routes. This encounter not only brought about a shift in material culture, particularly evident in changes to ceramic styles, but also led to a transformation in the ethnic makeup of human populations. This transformation is evident in the blending of different cranial morphologies, with a mixture of brachycephalic and dolichocephalic characteristics. While bronze became the primary raw material during this period, stone tools did not disappear entirely. Instead, they saw a significant decrease in use and were mainly employed to support metallurgical activities, such as sharpening, melting pots, and mold making. The most common bronze tools produced

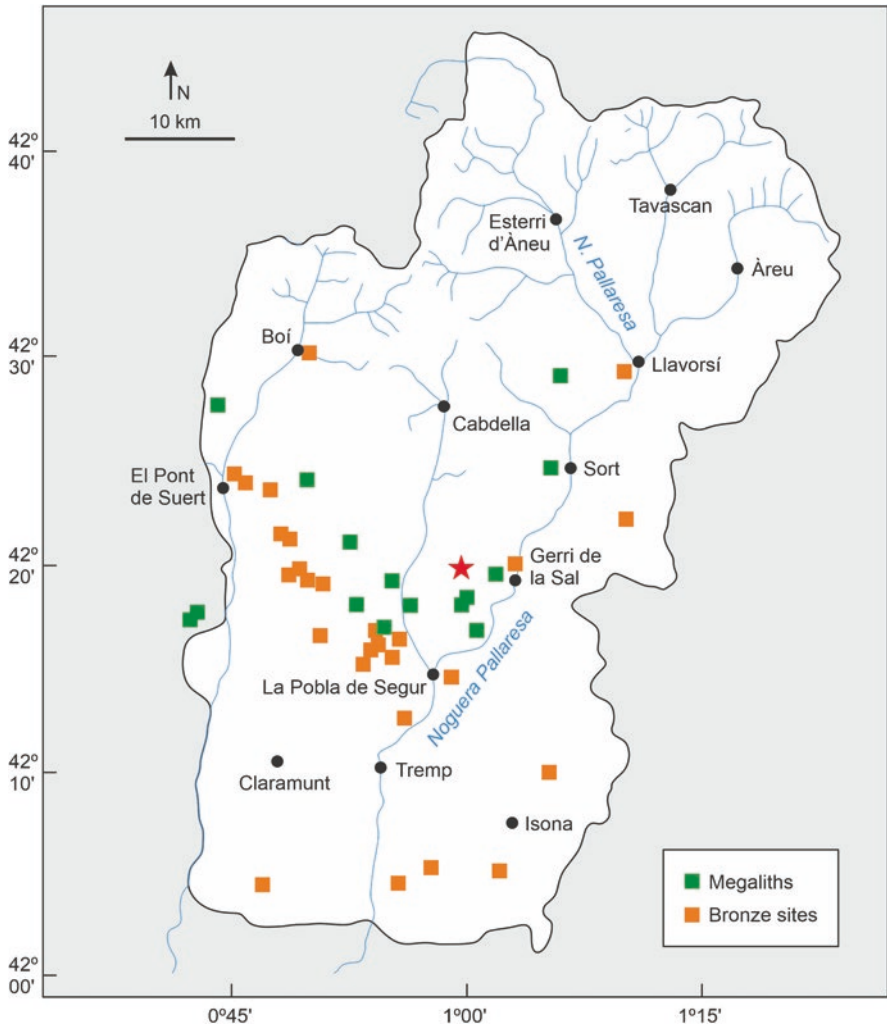


Fig. 2.4 Medieval Pallars County (see Fig. 2.1 for location), indicating the Bronze megaliths and archaeological sites, with the main present towns and rivers for reference (Cots 2005). Lake Montcortès is indicated by a red star

included axes, daggers, arrowheads, spear points, a variety of ornaments, and fishing hooks. The development of the bronze industry needed trade practices on both sides of the Pyrenees to secure the necessary products and raw materials. This increased contact across the Pyrenees, potentially involving other items such as flint, salt, pearls, shells, and livestock herds. The nomadic way of life continued during this phase, and caves and outdoor settlements may have been occupied seasonally. Funerary practices, particularly collective burials, persisted, but individual burials in the form of stone cists also emerged during this period.

2.1.3 Late Bronze (1650–800/750 BCE)

During this phase, there was a peak in the production and distribution of bronze items, while megalithic constructions started to decline. Significant changes in burial practices were observed, with a shift from traditional burials to cremation or incineration, followed by placing the remains in individual pots or urns. These cemeteries were characterized by collections of vessels containing ashes, leading to the civilization adopting this ritual by 1200 BCE being referred to as the Urn Fields (*Camps d'Urnes*). Some scholars have drawn parallels between the *Camps d'Urnes* in the Pallars region and those in the southern lowland meadows, suggesting the presence of a single cultural group with nomadic pastoral practices between lowlands in winter and mountainous regions in summer. During this phase, there was a significant improvement in the quality and refinement of the ceramic, particularly black pottery. Bronze metallurgy remained similar to the Middle Bronze Age, but there was a notable increase in the quantity and variety of ornamental objects. It was a common practice to conceal metallic objects in hidden deposits, presumably as a strategy to safeguard one's wealth from potential traders or individuals engaged in melting and reusing metals, which was common during that era. Human settlements remained reminiscent of the preceding Bronze phases, with many caves and outdoor sites located along the main river courses. Although population groups were small and had limited contact with one another, it appears that there were ongoing interactions between the northern trans-Pyrenean regions during this phase, as evidenced by some Indo-European characteristics such as the *Camps d'Urnes*. Some researchers posit the existence of a relatively unified ethnic population on both sides of the central Pyrenees during the Late Bronze Age. The primary subsistence activities during this time included pastoralism, farming, hunting, and gathering, with pastoralism possibly becoming more extensive and possibly involving transhumance for the first time, in a vertical (elevational) sense.

2.2 Iron Age (800/750–72 BCE)

It is challenging to pinpoint specific chronological divisions in the Pallars region and the Pyrenees overall for this time period. As a result, researchers have adopted the central European Alpine chronology, which distinguishes between two primary phases: the First Iron Age, corresponding to the Hallstatt culture, and the Second Iron Age, linked to the La Tène culture (Cots 2005). This is a merely chronological framework with no cultural implications.

2.2.1 First Iron Age (800/750–450 BCE)

This phase marked the progression of the Late Bronze culture, albeit with a gradually growing significance of iron. Nevertheless, iron metallurgy remained significant throughout this period. The *Camps d'Urnes* culture, a Late Bronze characteristic,

attained its peak development. The earliest written records indicate a noticeable disconnect between the Pallars region and the southern lowlands, possibly indicating the decline of the vertical transhumance that had evolved during the Late Bronze Age.

2.2.2 Second Iron Age (450–72 BCE)

This phase marked the peak of development in the iron industry, which demanded more intricate methods compared to bronze production. To smelt iron, the ore had to be subjected to high temperatures, requiring substantial quantities of charcoal and proper ventilation to support combustion. This manufacturing process led to a wide range of specialized jobs, resulting in increased social diversification and the emergence of a hierarchical societal structure. This hierarchical structure was evident in burial practices, where the most prominent individuals were interred or cremated in monumental mounds, while the rest of the population was buried in extensive necropolises. Horses, typically used for labor, transitioned into riding animals, marking the appearance of the first knights. However, in regions with challenging geography, external influences had limited penetration, and Late Bronze Age cultures still predominated. As a result, certain characteristic developments of Iberian culture, such as population growth and the construction of fortified cities, did not occur in the Pallars region, except in the more accessible southern lowlands. It has been proposed that pastoral activities remained a significant economic pursuit, with pastures managed collectively, although the evidence for this assertion remains limited. Our understanding of the protohistoric culture in Pallars comes in part from documents written by Roman conquerors. According to these records, the ethnic groups in the region just before the Roman conquest were diverse, including *arenosins* and *andosins* in the northern highlands and *ilergetes* in the southern lowlands. Consequently, the population appeared more diverse than it was during the Bronze Age.

2.3 Roman Epoch (72 BCE–418 CE)

The Roman incursion into the Pallars region primarily advanced from the southern direction. The initial significant event in Roman colonization in Pallars was the establishment of *Aeso*, which is modern-day Isona (Fig. 2.4), by 72 BCE. There are indications of another early Roman settlement to the west called Orretum, which was close to the current town of El Pont de Suert. Ongoing conflicts between the northern (Gallia) and southern (Hispania) Roman factions led to the founding of *Lugdunum Conventarum* (72–69 BCE), which is the present-day French town of Saint Bertrand de Comminges, located just 20 km north of the current Spain–France border. This event may have contributed to the idea of the Pyrenees serving as a political boundary. Interestingly, Roman culture had a more significant impact on the Aran region, the present-day Catalan comarca of Val d’Aran (Fig. 2.1),

compared to the Pallars region. This difference is attributed to the Pallars region's geographical isolation and its preservation of Iberian cultural and socioeconomic characteristics. Generally, the Roman presence in the Pallars region was considered somewhat peripheral. However, recent discoveries of potential Roman villa remains near Isona, Sort, and El Pont de Suert (Fig. 2.4) indicate the need for further archaeological investigations to develop a more comprehensive understanding. Numismatic evidence suggests that the marginal status of the Pallars region was more pronounced during the Roman Republic era, up to 27 BCE, than in the Imperial Period (Fig. 2.3). Three significant aspects of Roman culture have been emphasized in the Pallars region, as pointed out by Cots (2005):

2.3.1 Commercial Activities

In the Roman era, the primary trade items consisted of salt, wine, oil, timber, minerals, and marble. Salt is essential for human consumption and food preservation and, even more crucially, for livestock farming. Presently, the more famous salt flats in the area are located in Gerri de la Sal (Fig. 2.4), but there is no evidence of their use during Roman times. This also applies to wine and oil, which were likely imported from the southern lowlands. Exported goods included wood, minerals, marble, and other products from livestock farming. Typically, these goods were transported by mules, capable of crossing mountainous terrain, or by carriages in flatter areas. Rivers were also important transportation routes, possibly used to carry materials such as wood and marble on rafts, especially in the northern Pyrenean region. During the Pax Romana, a period of approximately 200 years (27 BCE to 180 CE) marked by stability, order, and prosperity in the Roman Empire, the Aran region possibly served as the key link in the Pyrenees, connecting the Pallars region with northern territories. This facilitated trade between the Gallic city of *Lugdunum Conventarum* and the Hispanian *Aeso*.

2.3.2 Farming and Forest Exploitation

The historical record of these activities remains vague due to the relative obscurity of the Pallars region during the Roman period. It is suggested that most of their efforts were focused on local subsistence, employing a biannual crop rotation system, with one year for planting and one year for fallow, similar to practices in other areas. The cultivation of fruits, particularly chestnuts and walnut trees introduced by the Romans, thrived in the valley bottoms. Orchards and gardens were likely a minor component, producing items such as onions, garlic, leeks, and possibly flax and hemp. It is probable that agricultural work was carried out with the assistance of domestic animals, similar to earlier times. Forests were primarily exploited for wood, charcoal production, hunting, and foraging. Wood served various purposes, including construction and the crafting of tools, as well as for cooking and heating homes. Charcoal was predominantly used in public and private baths. In addition to

wood and fruit collection, forests were valuable for bark harvesting, especially from oak, chestnut, and pine trees (used in leather tanning), and for obtaining forage for livestock. Pastoralist practices were mostly intensive and localized with herds rarely exceeding 1000 heads (Gassiot and Pèlachs 2017). Honey and wax were gathered from wild beehives. The establishment of hunting reserves served both as entertainment for the Roman elite and as a source of meat and leather. Common preys included bears, wolves, deer, wild cats, sables, and otters. Spears, arrows, and nets were the primary hunting tools.

2.3.3 Mining

During Roman rule, there was a strong emphasis on the exploration of mineral resources, with a particular focus on iron, copper, lead, gold, and silver. Mining operations were typically carried out by local or community groups, but the ownership of these mines was vested in the Empire. Those engaged in ore extraction reaped the rewards necessary to offset leasing, extraction, and processing expenses. The ore deposits were typically modest in size and situated near residential areas, and the processing industry was also a localized endeavor. However, the overall economy and the distribution of these products were subject to stringent oversight by the central Roman administration.

2.4 Middle Ages (418–1488 CE)

In a broad sense, the Middle Ages encompasses a span of over a millennium, beginning with the decline of the Western Roman Empire in 476 CE and concluding with the Turkish conquest of Constantinople in 1453 CE, marking the end of the Eastern Roman Empire. On a continental scale, the transition from the Roman Empire to the Middle Ages is commonly referred to as the Migration Period (376–568 CE; Halsall 2008). This phase was defined by the invasion of the Western Roman Empire by various barbarian groups, including the Huns, Vandals, Visigoths, Ostrogoths, Franks, Angles, and Saxons (Fig. 2.5). While the Migration Period, also known as the Dark Ages or the Early Middle Ages, is not explicitly outlined for the Pallars region, the onset of the Middle Ages in this area is traditionally traced back to 418 CE when the Visigoths established themselves in the nearby French city of Toulouse (then known as Tolosa) (Fig. 2.5). The conclusion of the Middle Ages in the Pallars region is marked at 1488 CE, coinciding with the conclusion of the County of Pallars. Chronologically, the Middle Ages in the Pallars region are divided into four primary phases: Visigothic rule, the Muslim period, Carolingian occupation, and the County of Pallars (Marugan and Oliver 2005). These phases will be briefly elucidated below, followed by a discussion of the principal social and land-use characteristics of Medieval Pallars, culminating in the extended crisis that affected the Pallars region until the advent of the Modern Age.

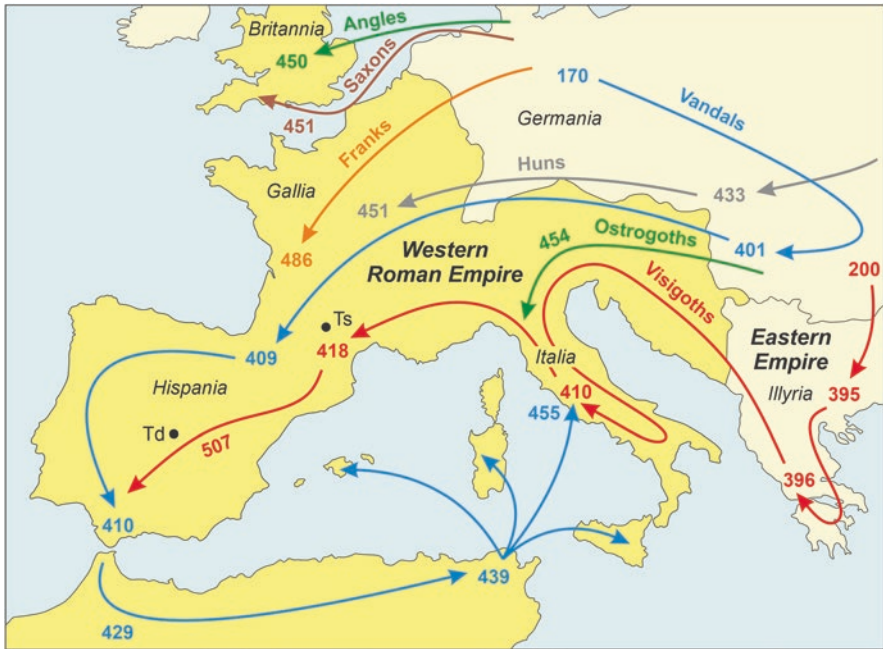


Fig. 2.5 Sketch map representing the barbarian invasions of the Western Roman Empire (as defined in 395 CE) during the Migration Period (376–568 CE; Halsall 2008). Numbers are dates in years CE. Ts, Tolosa/Toulouse; Td, Toledo. Simplified from Encyclopaedia Britannica (1994); dates of Visigothic incursion in southern Gallia and Hispania after Marugan and Oliver (2005)

2.4.1 Chronology

2.4.1.1 The Visigothic Epoch (418–711 CE)

In the southern part of Gallia, the Visigoths solidified their control when they established the reign of Toulouse in the Septimania region in 418 CE. However, Toulouse was later captured by the Franks in 507 CE, compelling the Visigoths to migrate toward the Iberian Peninsula. There, they established the Kingdom of Toledo, which endured until the Muslim invasion in 711 CE. The historical records of the Visigoths' presence in the Pallars region are scant, often considered a period of limited information prior to the feudal system's emergence. Nevertheless, insights into this era have been gleaned from archaeological and paleobotanical findings. The decline of the Roman Empire triggered significant transformations in the way natural resources were exploited, especially in mountainous areas where Roman influence had been less pronounced compared to the lowlands. As the Roman world disintegrated, local indigenous societies gained strength, and new strategies for agriculture, mining, and livestock management emerged.

2.4.1.2 The Muslim Phase (711–800 CE)

The Muslim Empire exerted control over a substantial portion of the Iberian Peninsula, known as *Al-Andalus*, extending northward to the Pyrenees. Limited historical records exist regarding the impact of Muslim influence on the Pallars region and the broader Pyrenees, but it is generally thought that there were no substantial socioeconomic alterations in comparison to previous eras. The Pallars region, situated at the northern border of *Al-Andalus*, was inhabited by a diverse range of cultures during this relatively brief period, lasting less than a century, until it was conquered by the Carolingians.

2.4.1.3 The Carolingian Occupation (Frank Empire) (800–872)

On behalf of the Carolingian Empire and with funding from Charlemagne, the counts of Toulouse successfully captured the Pallars in 800 CE with the aim of integrating this region into what was known as the *Marca Hispanica*, a defensive zone established to guard against potential Muslim incursions from the south (Fig. 2.6). Consequently, the Pallars became a part of the Frank Empire, and the Counts of Toulouse gained authority over a substantial territory that extended across both sides of the Pyrenees. Following a tumultuous period marked by frequent changes in the political administration of the Pallars, Count Ramon II eventually concluded the process of breaking away from Toulouse and establishing the independent County of Pallars.



Fig. 2.6 The ninth-century boundary zone between the Frank and Muslim empires, represented by the Carolingian *Marca Hispanica*. Redrawn and modified from Marín (1995)

2.4.1.4 The County of Pallars (872–1488)

This marked the lengthiest era, spanning over six centuries, within the context of Medieval Pallars. It extended from the time when the county gained its independence from the Frank Empire to its eventual subjugation by the Catalan-Aragonese crown, which was a result of the dynastic union between the Kingdom of Aragon and the Principality of Catalonia in the fifteenth century. Initially, the Frank counts of Toulouse retained certain political privileges in the County of Pallars, which also endured violent attacks from the southern Muslim Empire, particularly those factions based in Zaragoza (Fig. 2.6). The full independence of Pallars was not achieved until the death of Count Ramon II in 920. However, this independence was accompanied by a division of territory among the descendants of Ramon II, a practice that continued for several generations until the early eleventh century. During that period, Pallars County was split into two counties, Jussà and Sobirà (Fig. 2.7), and this division laid the foundation for the modern concept of the Pallars region. Subsequently, succession disputes and armed conflicts became commonplace between Jussà and Sobirà counties, with the involvement of the County of Urgell, which roughly corresponds to the present-day comarca known as Alt Urgell, situated to the east of the Pallars region (Fig. 2.1). It is worth noting that most of these struggles for political power and territorial expansion occurred within the feudal system (as explained below) and were largely motivated by the desire to maximize income. By the end of the eleventh century, an internal agreement was reached, and certain disputed territories were placed under shared jurisdiction between the Jussà and Sobirà counts, although disputes still persisted in the southeastern region with the County of Urgell (Fig. 2.7).

The County of Pallars did not vanish but underwent a significant reduction when, due to a lack of heirs, the Jussà territory was sold to the Catalan-Aragonese crown and integrated into their realm. This occurred during the reign of Jaume I (1208–1276 CE), when the Catalan-Aragonese crown held sway over a substantial portion of the eastern Iberian Peninsula, encompassing what is now Catalonia, Aragon, and Valencia, along with the Balearic Islands (Fig. 2.1). This expansion followed the expulsion of Muslims, who were confined to the Granada region in the southeastern part of the Iberian Peninsula (Fig. 2.8).

From this moment onward, only Pallars Sobirà County remained in the picture. Nevertheless, this county faced economic troubles and was transferred to the House of Comenge from the northern side of the Pyrenees in 1236 CE, a situation that persisted until 1294 CE. However, Pallars Sobirà managed to maintain its political independence as a county, even as the Catalan-Aragonese crown's involvement grew. From 1295 to 1488 CE, the Catalan House of Mataplana took control of Pallars, and it endured repeated attacks from the Gascons, who also hailed from the north of the Pyrenees. This led to the invasion of Pallars by Aragonese King Jaume II. The relationship between this kingdom and the aristocrats of Pallars, who staunchly defended their independence, was fraught with difficulties. It resulted in more wars and conflicts, culminating in a rebellion against Aragonese King Fernando I in 1462 CE. The final count of Pallars, Hug Roger III, continued to resist the crown, but he was defeated and sentenced to life imprisonment. In 1488 CE, the



Fig. 2.7 The Pallars County in the eleventh century. Lake Montcortès is indicated by a red star. Redrawn and modified from Marugan and Rapalino (2005)

County of Pallars was conquered by Aragonese King Fernando II on behalf of the newly formed Castilla-Aragon crown. The county was elevated to a marquisate under the leadership of the dukes of Cardona (Fig. 2.1), who also became the Marquises of Pallars.

2.4.2 Territory and Society

The feudal system began to take shape in the ninth century under Carolingian rule and reached its full establishment in the eleventh century under the leadership of the Pallars counts. It revolved around dividing the land based on natural valleys and organizing it into political units, initially counties, and later, it centered around the nobility's castles and the parishes of the Catholic church. This passage encapsulates these key aspects and offers a brief overview of the social structure in the Pallars region during the feudal epoch.



Fig. 2.8 Political subdivisions of the Iberian Peninsula by the final Middle Ages. P = Medieval Pallars region, NC = Northern Catalonia. Redrawn and modified from Marín (1995)

2.4.2.1 The Pyrenean Valleys

The earliest records of Pallars County can be traced back to the mid-ninth century. Initially, the term “Pallars” denoted a particular region, which might have been an ancient Roman or Visigothic city (*civitas*) located in the central part of the Noguera Pallaresa River, to the south of Llavorsí (Fig. 2.4). Similar regions with distinct geographical boundaries existed and were grouped into valleys. Over time, these initial regions were gradually absorbed into a unified county jurisdiction as more castles and parishes emerged, each with its own territory. Within this context, it is believed that Pallars County evolved from the expansion of the initial Pallars district.

2.4.2.2 The Feudal Castles

During the era of feudalism, the castles and the lands under their authority served as essential components of governance. These fortresses were governed and managed by nobles, who received their delegated responsibilities from the counts of Pallars. In line with the typical structure of feudal systems, these nobles held civil authority over the inhabitants of their domains, providing protection in exchange for tribute, maintenance, and labor on the land. The initial strongholds, which were heavily fortified, emerged in the tenth century. They were primarily located to the south, near the border between Pallars and the Muslim Empire, and to the west, where Roman and Visigothic influences had historically been more prominent. In the northern highland valleys, where local organizational structures were more robust, the church played a significant role in exerting feudal control. The frequent succession and territorial disputes in the eleventh century further led to a proliferation of castles in the Pallars region. Another wave of castle construction occurred during



Fig. 2.9 The Romanesque temple (twelfth century) of Santa Maria de Gerri, as the only remnant of the ancient monastery founded in 809 CE. Photo: V. Rull

the thirteenth and fourteenth centuries, particularly in response to frequent invasions by the northern Gascons into Pallars Sobirà.

2.4.2.3 The Ecclesiastic Organization

Before Visigothic rule, the Pallars churches fell under the jurisdiction of the Catholic diocese of Lleida (Fig. 2.1). However, this connection was disrupted when Muslims conquered the city. In the year 800 CE, when the Counts of Toulouse took control of the Pallars, this region became part of the diocese of Urgell, and this arrangement persisted throughout the Medieval period. In the ninth and tenth centuries, the Pallars region witnessed the establishment of numerous monasteries, earning recognition as a significant hub for the development of monastic life in Catalonia. Many of these monasteries eventually declined, vanished, or were absorbed into other monastic communities. Only the Santa Maria de Gerri monastery (Fig. 2.9), located near the present village of Gerri de la Sal (Fig. 2.4), less than 6 km east of Lake Montcortès, survived and played a prominent role in the evolution of Medieval Pallars. The heritage of this monastery expanded rapidly, thanks to contributions from counts and influential nobles, as well as the assimilation of smaller nearby monasteries and their assets. Collaboration between religious and political authorities was a common feature of the Middle Ages, leading to the creation of parishes (*parròquies*) with ecclesiastical, administrative, and military duties. This cooperation also involved an increased influence of the diocese of Urgell in county affairs.

2.4.2.4 The Social Composition

In the feudal system, the feudal lord held ownership over both the land within his dominium and the laborers (*rustici*) who toiled on it. These laborers paid rent for their residence and work, and this payment necessitated the generation of surplus agricultural products. This surplus not only ensured the sustenance of the *rustici* but

also supported the upkeep of the feudal lords, covering expenses such as transportation, storage, and the sale of the final goods. The nobility, a select minority, primarily dedicated themselves to either military pursuits or a career in the church. The upper echelon of the nobility comprised the magnates, who possessed substantial estates and had closer ties to the counts. The second class included the *castlans*, who owned a single castle, while the third class, the minor nobles, typically served as knights under the counts or the church. The majority of the population consisted of farming families who owned their own lands (*alous*) and lived in small villages, often with shared resources that were collectively managed. Starting in the tenth century, the *alous* gradually succumbed to feudal pressures and became part of the extensive properties owned by secular and ecclesiastical nobility. Nevertheless, some peasant properties resisted this feudal shift and continued to exist locally.

2.4.3 The Feudal Landscapes

2.4.3.1 Settlement and Land Use

The Medieval Pallars was essentially a rural region with no significant cities. It had two distinct areas: residential zones and working areas, each with their respective communication networks. Villages often developed near churches, and there were numerous isolated houses with associated lands (known as *masos*). Additionally, cave dwellings were common in the southern Pallars, where the climate was more suitable for such habitation. The primary working lands consisted of crop fields, meadows, and pastures, as they were easier to control under the feudal system for rent collection compared to less stable terrains such as wetlands, riverbanks, or forests. Slash-and-burn agriculture was mainly practiced in mountainous regions, offering diverse land use in a compact area, suited to the seasonal changes in these environments. However, these practices disappeared with the establishment of the feudal system between the ninth and eleventh centuries, which necessitated strict control over land and its production to collect rent payments. This marked the transition from the earlier subsistence economy to a more stable and extensive land use system.

The primary crops cultivated were cereals, olives, and vines, which are considered the three most traditional Mediterranean crops. The first cereal mills, powered by hydraulics, emerged in the ninth and tenth centuries and were also controlled by feudal lords who received rents for their use. To counter the nutrient depletion caused by intensive cereal farming, crop rotation with legumes was practiced. The use of animal manure for crops was not documented until the twelfth century, likely limited to barley cultivation due to its high nutrient demands. Olive tree cultivation became extensive in the Pallars from the eleventh century, particularly in the southern lowlands where the climate was more favorable for olive trees. This initiative was also feudal in nature, given the time, facilities, and commercialization demands of olive cultivation. The introduction of vine cultivation in the Pallars region was seen as an extension of a Roman tradition, possibly favored by a warmer climate during the Middle Ages. The first vineyards were recorded in the ninth century, near

churches and monasteries, for local consumption. After feudal consolidation in the eleventh century, vineyards expanded, and viticulture became a planned crop subject to rent payments, even reaching mountainous areas at altitudes above 1000 meters.

2.4.3.2 Pastures

One of the key advancements during the Middle Ages was the development of herding practices that involved the seasonal movement of livestock over long distances (horizontal transhumance). As previously mentioned, vertical transhumance had been in practice since ancient times, possibly as far back as the Bronze Age, and it remained the primary method of livestock migration in the Pallars region until the ninth century. Vertical transhumance entailed the seasonal short-distance migration of livestock herds, mainly composed of sheep, and the people responsible for them, between summer pastures in the highlands and winter pastures in the lower valleys. This practice was predominantly carried out in mountainous regions by small landowners. In contrast, horizontal transhumance entailed the long-distance movement of livestock across expansive regions, necessitating a distinct social organization and a more specialized herding system (Garcia and Gassiot 2023). Monasteries were the first to adopt long-distance transhumance, with other secular feudal landowners embracing this practice in the tenth century. However, smaller individual landowners (*masos*) continued to exist, contributing to a diversity of pastoralism and transhumant practices. Horizontal transhumance involved large herds, which were partially obtained from individual landowners in the form of living animals. Ongoing conflicts between and within ecclesiastic and secular landowners over the use of pastures were extensively documented from the eleventh century onward throughout the Medieval period. However, there is a notable absence of documentation regarding the location and extent of pastures and other related facilities for this activity, such as water sources, salt deposits, temporary enclosures, and shepherd huts. This lack of information hampers our ability to draw conclusions about important economic aspects, including whether overgrazing was a concern.

2.4.3.3 Mineral Resources

Salt plays a crucial role in animal diets, providing essential sodium and chlorine. It was particularly vital for the growth of large sheep herds and horizontal transhumance. Much like other essential resources, the extraction and trade of salt were monopolized by feudal lords between the ninth and fifteenth centuries. In the context of metal, the Visigoths inherited Roman mining techniques and expanded mining activities into previously economically insignificant areas. Precious metal production was curtailed in favor of iron production, catering to local demands for weaponry and farming tools. This arrangement persisted until the ninth century when secular and ecclesiastical feudal landowners took charge of iron production and trade. This shift fostered agricultural expansion, the growth of the weapon industry, and the rise of professions such as blacksmithing, tanning, and shoemaking. To facilitate these industries, the first smithies and forges were strategically placed near watercourses, utilizing hydraulic power, often in proximity to castles and monasteries.

2.4.4 The Late Medieval Crisis

During the waning years of the Medieval period, specifically between 1350 and 1487 CE, the Pallars region experienced a significant decrease in its population due to mass emigration to major urban centers. This resulted in widespread impoverishment and a fundamental transformation of the region's landscape, marked by a constant struggle for control over abandoned fields, pastures, and forests. This depopulation unfolded in two distinct phases. The initial phase commenced in the late thirteenth century, prompted by Gascon invasions and the devastating outbreak of the Black Plague in 1348 CE. The second phase of depopulation was closely tied to the escalating conflicts between the Pallars counts and the Catalan-Aragonese crown, known as the Pallars War. These conflicts reached their zenith in the late fourteenth century and culminated in the incorporation of the Pallars region into the kingdom. Additionally, the arrival of the Little Ice Age, a period characterized by colder climates in contrast to the warmer Medieval era, might have contributed to the Medieval crisis. However, it is important to note that wars and climate changes alone do not fully account for the late Medieval crisis, which was also the consequence of a more comprehensive breakdown of the feudal social order. For a long time, the conventional explanation for the Medieval crisis centered on a supposed overpopulation and diminishing agricultural yields. However, this interpretation neglects the potential impact of a substantial number of nonproductive individuals, including both secular and ecclesiastical feudal lords. These individuals devoted their efforts to obliging others to toil for their own benefit, thereby increasing their own economic prosperity. This factor should be regarded as crucial in explaining the self-induced collapse of the feudal system.

2.5 Modern Age (1488–1789 CE)

In the Pallars region, the Modern Age spanned from the conclusion of the Pallars War in 1488 CE to the onset of the French Revolution in 1789 CE. From an economic and social perspective, this age marked the shift from the feudal system of the Middle Ages to the precapitalist society that emerged in the late eighteenth century. Moreover, it is important to note that the Pallars region experienced significant political transformations during this period, which are crucial to comprehending its socioeconomic evolution (Box 2.1).

In this political-chronological context, Bringué (2005) identifies thematic categories for the Modern Age in the Pallars region, which include territory, population, institutions, and economy.

2.5.1 Territory

As previously mentioned, the conclusion of the Pallars War marked the transformation of the County of Pallars Sobirà into a marquissate governed by the Cardona

Box 2.1 Political chronology of the Modern Age in Spain

The Catholic Monarchs (1469–1516 CE). The marriage of Fernando II of Aragon and Isabel I of Castilla, famously known as the Catholic Monarchs, in 1469 CE, marked a significant event at the close of the Medieval era, leading to the union of these kingdoms (Fig. 2.8). Nevertheless, the Aragonese realm, which encompassed the Principality of Catalonia, saw relatively few alterations in its domestic policies, with the nobility retaining their privileges well into the early eighteenth century. The political consolidation of what are now the Spanish territories did not take place until Castilla and Aragon jointly achieved the conquest of the Kingdoms of Granada in 1492 CE and Navarra in 1512 CE, ushering in the Modern Age. The capture of Granada occurred concurrently with Christopher Columbus's voyage to the Americas, a venture financed by Catholic Monarchs. Following the passing of Isabel I in 1504 CE, her husband, Fernando II, governed until 1516 CE and, as noted earlier, was responsible for the conquest of the County of Pallars in 1488, subsequently annexing it to the Kingdom of Aragon as a marquisate.

The Habsburg dynasty (1517–1700 CE). For nearly two centuries, the Habsburgs, also known as the *Austrias*, ruled over the united Spanish kingdoms through a series of dynastic successions. The first Habsburg monarch, Charles I, had a familial connection to the Catholic Monarchs, who were his grandparents. Charles I inherited a vast realm that included Castilla, Aragon, the recently acquired American territories, as well as Austria, the Netherlands, and their adjacent lands from his various grandparents, including Maximilian I of Austria and Mary of Burgundy. This made Charles I one of the most significant European rulers in the sixteenth century. Following the death of his grandfather Maximilian I in 1519 CE, he assumed the title of Holy Roman Emperor as Charles V. However, he later abdicated in 1556 CE. A pivotal moment during the Habsburg era for the Principality of Catalonia was the Treaty of the Pyrenees, inked in 1659 CE. This treaty was signed by the Spanish King Felipe IV, who reigned from 1621 to 1665 CE, and the French King Louis XIV. The treaty marked the end of a conflict between Castilla-Aragon and an Anglo-French coalition over various European territories. It had a profound impact on Catalonia, leading to the loss of its northernmost region, known as Northern Catalonia (Fig. 2.8), which was incorporated into France.

War of the Spanish succession (1700–1714 CE). The final Habsburg monarch of Spain was Carlos II, who passed away in 1700 CE, leaving no heirs. This event sparked the War of Succession between two opposing factions: the French Bourbons, led by Felipe d'Anjou (the grandson of Louis XIV), and the Austrian side of the empire, represented by Leopold I. This division reflected the longstanding fragility of the unity between Castilla and Aragon. Castilla threw its support behind the Bourbons, while Aragon sided with the Austrians. The conflict escalated into an international war with the involvement of England, Portugal, and the Netherlands, which supported the

Austrians to thwart French expansionism. The war ultimately concluded with the Treaties of Utrecht and Rastatt in 1713–1714 CE, which officially recognized Felipe d'Anjou as the king of Castilla-Aragon (known as Felipe V), on the condition that he renounced his claim to the French throne. As part of the settlement, the Austrian side also acquired certain European territories under Spanish dominion, significantly diminishing French dominance and balancing the power among European nations. The proclamation of Felipe V marked the end of the Aragon kingdom, with its final stronghold being the Catalan city of Barcelona, which was conquered in 1714 CE by the Castilian army with assistance from France. Throughout the War of Succession, a significant portion of the Pallars region was occupied by the French army, which advanced as far as Tremp in 1712 CE.

The Bourbon dynasty (1714–1808 CE). The establishment of the Bourbon dynasty marked the end of Catalonia's distinct institutional features and civil rights, which had been preserved under the rule of the Aragon crown until the conclusion of the Habsburg dynasty. The culmination of the emerging absolutist regime was the *Nueva Planta* decree of 1716 CE, which established Spanish citizenship without differentiation between Castilian and Aragonese identities, as had been the case before. Internal borders and customs were eliminated, except in the Basque territory, thereby granting all Spaniards the right to engage in trade with the American colonies, not just Castilians as previously. Most regional institutions were abolished, and key government officials were appointed from the king's court in Madrid. Castilian was declared the exclusive language of administration, displacing Latin, Catalan, and other languages. These decrees laid the groundwork for the Spanish absolutist monarchy centered on Castilla, which prevailed until the final Bourbon monarch of the Modern Age, Carlos IV, who ruled from 1788 to 1808 CE when the French occupation began.

family under the rule of the Aragonese kingdom. It is estimated that this marquisate encompassed approximately 53% of the current Pallars Sobirà region and 27% of the present-day Pallars Jussà (Fig. 2.1). This marquisate was not a continuous territory and shared the medieval Pallars region with various other royal and noble domains, such as viscounts, baronies, abbeys, lordships, and smaller manors (Fig. 2.10). The northern mountainous regions of the marquisate were historically known as Pallars Sobirà until the seventeenth century, while the southern lowlands were referred to as Pallars Jussà. Nevertheless, the Pallars region preserved its identity as a unified historical area.

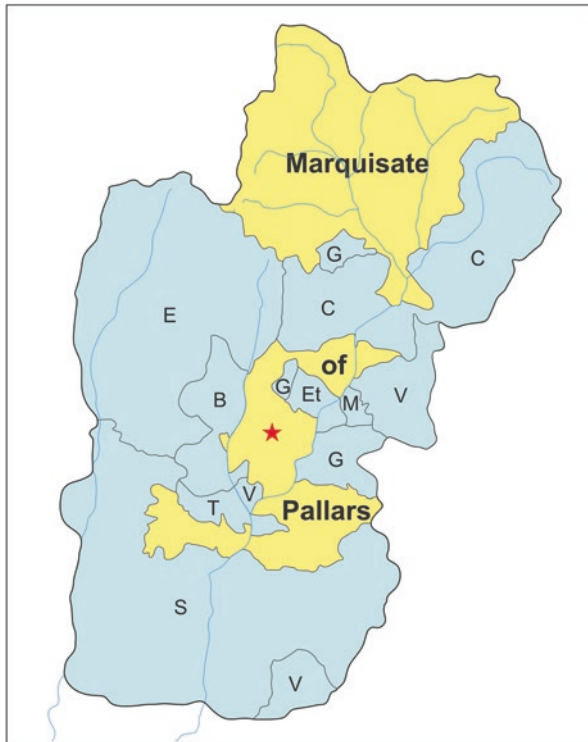


Fig. 2.10 The Pallars region in the early Modern Age (late fifteenth century). The Marquisate of Pallars is marked in yellow and the territories owned by other manors in blue. B = Bellera, C = Viscounty of Castellbò, E = Barony of Eril, Et = Barony of Estac, G = Abbey of Gerri, M = Barony of Copons de Malmercat, S = Smaller manors, T = Viscounty of Torella, and V = Viscounty of Vilamur. The red star indicates the location of Lake Montcortès. Redrawn and modified from Bringué (2005)

2.5.2 Population

The late Medieval crisis led to the disappearance of one-third of the villages, with the remaining villages suffering significant declines. The recovery during the Modern Age was quite swift, with the number of houses increasing by 2.5 times during the sixteenth century (Fig. 2.11). This growth was attributed to new houses being built by the descendants of more powerful landowners and a substantial influx of migrants from Gascony, north of the Pyrenees. The establishment of these new houses and the resulting population growth heightened competition for natural resources and accentuated the legal and social distinctions between the stronger and less fortunate households. Weaker households, lacking tax obligations and with fewer rights, held a less prominent role in community affairs. A second crisis emerged in the seventeenth century, evident in the declining number of houses, particularly those belonging to the stronger households.

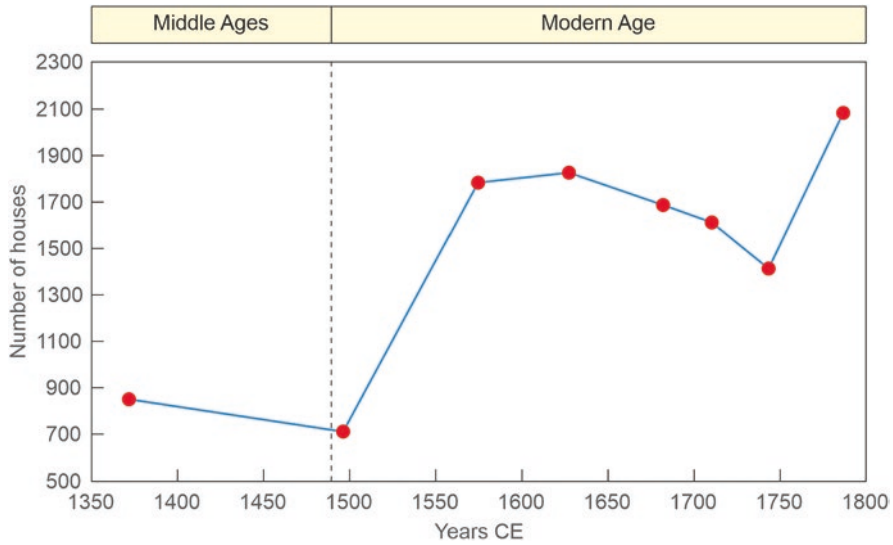


Fig. 2.11 Modern Age population trends in the Pallars region following the late Medieval crisis. Raw data from Bringué (2005)

In the eighteenth century, the tensions between the duke and the king exacerbated the crisis, reaching its peak in 1744 CE. The situation began to improve in 1750 CE when efforts to rebuild the houses lost in the seventeenth century and construct new ones led to an increase, surpassing the number of houses from the sixteenth century. Nevertheless, the population figures of the eleventh to thirteenth centuries, prior to the late Medieval crisis, were never once again attained.

2.5.3 Institutions

During the fifteenth and sixteenth centuries, the Pallars region experienced significant territorial fragmentation, as shown in Fig. 2.10. This led to a complex jurisdictional situation. The Duke of Cardona and the Marquis of Pallars did not reside in the Pallars region but governed it through a governor, who was also known as the General Procurator. This governor held the highest political, legal, and administrative authority within the marquisate. Other parts of the region were under the authority of local secular or religious leaders, but they were politically integrated into a larger royal structure known as the *sotsvegueria* of Pallars. What set the Pallars region apart from the rest of Catalonia were two key factors: the *franc alou* land-property system and the persistence of a communal exploitation system. Under the *franc alou* system, local landowners had complete ownership of the land, and they only paid taxes to the marquisate or the crown, depending on their specific location and the economic strength of their households. These local landowners formed communities and divided the land into *termes*, which were governed by these

communities. They managed activities such as land sales or rentals, cultivation, grazing practices, and forest exploitation while also safeguarding the community's collective rights. This communal system faced challenges and pressures, particularly during the sixteenth and eighteenth centuries, but it endured until the nineteenth century when liberalism gained prominence. In contrast to the previously extinct feudal system, these communities served as genuine administrative, political, and legal institutions that controlled the land and its utilization throughout most of the Modern Age.

Upon the advent of the Bourbon dynasty and the issuance of the *Nueva Planta* decree in 1716 CE, which eliminated the traditional structures of the Aragonese realm, including Catalonia, the distinctive features of the Pallars institutions, particularly their political and legal powers, were annulled. Nevertheless, the *franc alou* property system and the communal utilization of shared resources persisted. These local privileges received stronger protection in the marquisate of Pallars, thanks to the steadfast defense of marquises against royal interests. Nonetheless, the landscape underwent significant transformation in the 1770s, when the *franc alou* system came under scrutiny, heralding a new socioeconomic order that ultimately led to the emergence of a precapitalist system.

2.5.4 The Economy

2.5.4.1 Crops

Cereals, with wheat as the predominant variety, followed by barley and oats, constituted the primary crop in this region, as was common in most Catalan areas, serving as the main source of sustenance. The primary distinction between the northern valleys and the southern watersheds lies in the cultivation of olives and grapes. Olive cultivation was primarily found in the southern lowlands, with its northern boundary typically around Gerri de la Sal (Fig. 2.1). While grape cultivation extended to valleys such as Llavorsí, it was more prevalent south of Sort (Fig. 2.1). Livestock distribution, particularly sheep and pigs, exhibited contrasting patterns, with pastures being more prevalent in the northern valleys. During the seventeenth and eighteenth centuries, there was a shift toward diversifying productive activities. This shift was evident in the conversion of crop fields into pastures, a gradual substitution of cereals with legumes, a progressive replacement of wheat with rye, a decrease in grape cultivation in the northern valleys, and a significant increase in livestock farming. This transformation in economic activities was closely connected to the crisis that began in the seventeenth century.

2.5.4.2 Livestock

Raising livestock on shared lands played a crucial role in generating economic prosperity. Horizontal transhumance continued to be a common practice (Garcia and Gassiot 2023), with sheep herds ranging from 20,000 to 40,000 animals covering extensive distances, which was not uncommon. Sheep farming primarily aimed at producing and selling various products such as meat, wool, and dairy items, while

cattle were primarily used for agricultural work and transportation. Horses were a privilege reserved for the nobility, and their trade was subject to strict regulation. The community that owned the pastures was responsible for determining which lands were designated for grazing and transhumance, as well as managing the grazing intensity and schedule. Disputes regarding ownership and use of pastures and livestock were typically resolved within the communities involved. However, in the eighteenth century, there were attempts to alter this exploitation model. Some influential households circumvented the communal organization and directly petitioned the king to gain additional privileges for pasture usage. These powerful households, which often included the nobility, were the primary owners of livestock, while poorer households had limited or no livestock of their own. As a result, long-distance transhumance, an expensive and complex practice essential for securing winter grazing, was primarily undertaken by powerful households or associations of middle-class households, often in collaboration with major pasture owners.

2.5.4.3 Forests

Unlike pastoralism, where herding was a collective endeavor, the extraction of wood from forests was an individual task carried out by each household. It was crucial for these households to have access to woodlands to meet their subsistence needs. The forests served as a source of wood for constructing and repairing both individual structures such as houses, corrals, and cabins, as well as communal projects such as bridges, churches, and other public buildings. Additionally, the wood harvested from the forests could be sold in distant regions. These activities were unrestricted but governed by community regulations. Forests were also utilized for obtaining wood for heating and lighting, as well as for producing charcoal and providing food for livestock. In certain cases, forests were partially cleared or intentionally burned to enable temporary cultivation or the expansion of pastures.

2.5.4.4 Land Renting

Pastures and forests were also utilized for business purposes, allowing foreign operators to obtain exploitation licenses and rent or buy land. External livestock owners often leased summer mountain pastures for their seasonal grazing needs. Wood extraction was a common commercial practice involving the leasing or sale of a specified amount of timber from a particular forest for a set period. All of these activities, including the transportation of timber downstream along rivers, were under strict community control until the eighteenth century, when the *Nueva Planta* Decree transferred these privileges to the crown. However, by the end of the same century, the communities regained their former rights to exploit, transport, and trade wood. Forest regeneration was typically encouraged, and the threat of deforestation primarily stemmed from land clearance for agriculture and, to a lesser extent, charcoal production for the metallurgical industry.

2.5.4.5 Other Natural Resources

Apart from forests and meadows, the communities also managed various natural resources such as salt, iron, lime, hydraulic power, hunting, and fishing. The salt and

iron industries held particular significance, playing a crucial role in promoting collective interests over individual interests. Regarding salt, communal rights were upheld during the sixteenth and seventeenth centuries but were extinguished at the start of the eighteenth century when the crown took control of the salt flats and integrated them into the royal holdings. Conversely, the iron industry, closely linked to charcoal production and forge development, contributed to the revival of some communal institutions that had been abolished by the *Nueva Planta* decree in 1716 CE. In the Pallars region, iron mining is believed to have been active in the sixteenth and seventeenth centuries, although historical documentation is limited. By the late seventeenth century, the number of documented forges increased, and ore extraction techniques saw significant advancements, primarily driven by private owners. In the mid-eighteenth century, communities reached an agreement with these private owners, establishing a mixed production system. This marked the beginning of a prosperous period for the iron industry, leading to the construction of numerous forges. This growth heightened the demand for charcoal and raised concerns about deforestation, a pressing issue for the communities. To strengthen their industrial capabilities, they constructed new forges and, in 1800 CE, formed a union comprising a substantial number of villages and public societies in the region.

2.5.4.6 Commerce

A significant turning point in the advancement of trade in the Pallars region occurred in 1687 CE when a new route was opened through the Collegats gorge (Fig. 2.2). This pathway greatly eased the exchange of goods with the southern lowlands and the broader extra Pyrenean regions. To the north, fresh commercial endeavors emerged with towns in France located across the Pyrenees. Key commodities included iron, wine, oil, and various groceries. Timber and other goods were transported downstream via rivers to larger southern lowland towns such as Lleida and major coastal cities such as Barcelona (Fig. 2.1).

2.6 Contemporary Times (1789–2005)

Farràs (2005) categorized the socioeconomic history of Pallars over the last two centuries into five primary periods: (1) the traditional precapitalist society (late eighteenth century to 1870 CE); (2) the crisis in the subsistence economy (1870–1910 CE); (3) the shift between traditional society and modernity (1910–1960 CE); (4) the second crisis stemming from the Industrial Revolution (1960–1980 CE); and (5) the modern capitalist society (1980–2005 CE). Similar to the previous section, we also offer a summary of the key political developments to provide a historical context for these socioeconomic phases (see Box 2.2).

Prior to delving into the socioeconomic stages of modern Pallars as outlined by Farràs (2005), a chronological comparison between these stages and the political history of Spain presented in Box 2.2 is offered for context (Fig. 2.12).

Box 2.2 Political chronology of Contemporary Spain

The French occupation and the independence war (1808–1813 CE). In 1807 CE, the French Emperor Napoleon Bonaparte took control of Spain, citing the invasion of Portugal as the justification. This move was made in accordance with an earlier agreement with the Spanish government. In 1808 CE, he appointed his brother Joseph as the King of Spain. This action triggered a widespread uprising and marked the commencement of the Spanish Independence War. The war ultimately concluded in 1813 CE when a Spanish-Anglo-Portuguese alliance defeated the French army.

Return to the Bourbon monarchy (1813–1868 CE). The brief period of French occupation, lasting only six years, marked a fleeting chapter in the Bourbon monarchy's history. This era was followed by the reign of Fernando VII, the son of Carlos IV, who ruled from 1813 to 1833 CE until his passing. After Fernando VII, his daughter Isabel II ascended to the throne, holding power until 1868 CE. However, two regents temporarily managed the crown until 1844, when Isabel reached adulthood and assumed personal governance of the nation. The initial financial crisis of Spanish capitalism emerged in 1866 CE, and it was succeeded by a subsistence crisis between 1867 and 1868 CE, brought about by unfavorable crop yields during those years. The combination of these two crises had a significant impact on business figures, politicians, and the general population, culminating in a widespread socio-economic crisis. This crisis eventually led to a revolution, marking the start of the so-called *Sexenio Democrático*.

The Six-Year Democracy and the First Republic (1868–1874 CE). In 1868 CE, a military uprising occurred, resulting in the removal and exile of Isabel II from the throne. A provisional government was established, advocating for inaugural democratic elections to establish constituent assemblies tasked with crafting a fresh constitution. Although the democratic parliament was primarily composed of monarchists, the outcome was a constitution favoring a monarchy that necessitated the selection of a new king. Following a vote, Amadeo I of the Italian Savoy dynasty was chosen by the parliament, and he ruled from 1871 to 1873 CE. However, he later abdicated due to the challenges of maintaining a stable government. Immediately thereafter, the parliament abolished the monarchy and declared the First Spanish Republic, which lasted for a brief period until 1874 CE, when the Bourbon monarchy was reinstated.

The Bourbon restoration (1875–1931 CE). Following the collapse of the First Republic, the Bourbon dynasty returned with Alfonso XII, the son of Isabel II, who ruled until his passing in 1885 CE. During this period, there was a six-month gap before the birth of his son and heir, Alfonso XIII. Consequently, Alfonso XII's wife, María Cristina of Habsburg, served as a regent until Alfonso XIII reached adulthood in 1902 CE. The political system remained a parliamentary monarchy. By 1898 CE, Spain had lost its

remaining colonies in the Americas and the Pacific, retaining only a few African territories. During the First World War (1914–1918 CE), Spain maintained a neutral stance. However, this, combined with the challenging postwar conditions, had significant social, economic, and political repercussions, ultimately leading to the crisis of the restoration period. This crisis culminated in the dictatorship of Primo de Rivera, which lasted from 1923 to 1930 CE. Between 1927 and 1929 CE, another economic downturn occurred, aggravated by the repressive actions of the government. These factors led to the unification of the parliamentary opposition and the establishment of the Second Republic.

The Second Republic (1931–1936 CE). In 1931 CE, the Republican Party emerged victorious in urban elections in major cities, leading to the establishment of the Second Spanish Republic. During this time, Francesc Massià declared the Catalan Republic, and the Autonomy Statute of Catalonia received approval. In 1936 CE, the Popular Front, a coalition of left-leaning parties comprising republicans, socialists, and communists, won elections, triggering a violent response from totalitarian fascists and nationalists, ultimately sparking the Spanish Civil War.

The civil war (1936–1939 CE). The conflict began with Francisco Franco's rise to power in Africa, where he led the National Movement, with the intention of swiftly taking control. However, the effective resistance of the republicans in key urban centers such as Madrid, Barcelona, and Valencia marked the start of an extended civil war throughout the nation. The war's turning point occurred in 1939 CE when Barcelona and Madrid fell to the National Front, marking the onset of Franco's dictatorship.

The Franco dictatorship (1936–1975 CE). Francisco Franco, who declared himself as the Head of State, governed Spain from the conclusion of the civil war in 1936 CE until his passing in 1975 CE. The political system, referred to as *franquismo* (Francoism), was a dictatorial military regime rooted in Spanish nationalism, Catholicism, fascism, and opposition to communism. Francoism vehemently opposed any form of social or political freedom, including democracy and the division of political, executive, and legislative powers. The once-democratic parliament was transformed into a pseudodemocratic institution dominated by a single party, the Movimiento Nacional, which adhered to the dictator's directives. Fundamental civil rights were also curtailed or eliminated, and independence and regionalist movements, particularly those in Catalonia, were proscribed and subjected to persecution.

The modern democracy (1975 CE–present). Franco's death paved the way for the restoration of democracy in Spain, but well in advance of his passing, he had already named his successor as the Head of State six years prior. The chosen individual was Juan Carlos of Bourbon, who subsequently became King Juan Carlos I. In 1976 CE, a provisional government was appointed with the task of revamping political laws, organizing democratic elections in

1977 CE, and crafting a new constitution in 1978 CE. The establishment of the new Spanish democracy was solidified in 1982 CE. The parliamentary monarchy was reinstated, with the same Bourbon dynasty occupying the throne. This continuity persists today, with Juan Carlos I's son and successor, Felipe VI, reigning as the current king. Consequently, the Bourbon dynasty, which began its rule in Spain three centuries ago, has continuously held the crown.

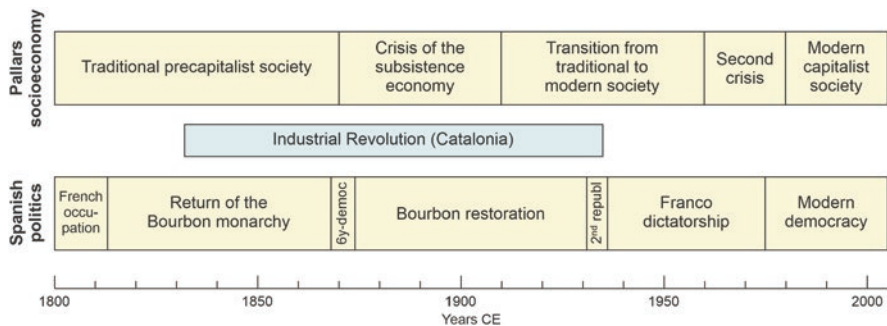


Fig. 2.12 The socioeconomic developments of the Pallars region during the last two centuries, in the chronological framework of Spanish political history (data from Farràs 2005). Catalan Industrial Revolution according to Maluquer de Motes (2019)

2.6.1 Traditional Precapitalist Society (Late Eighteenth Century to 1870 CE)

During this period, the Pallars region was characterized by its physical isolation, reliance on subsistence economy, and adherence to traditional values. Until the mid-nineteenth century, the primary routes in the region were used for livestock migration and the transportation of goods and people on horseback. These routes played a vital role in local circulation, contributing to the Pallars' relative separation from the outside world. This isolation encouraged diversified production to enhance self-sufficiency and reduce dependence on neighboring regions.

Within the Pallars, there were two distinct regions: the southern basin and the northern mountains (Fig. 2.3). The basin had an excess of commercial products such as wine and olive oil, which had replaced cereals, forests, and fallow land since the late eighteenth century. As a result, cereals, particularly wheat, could not meet local demands and had to be imported from nearby areas. Other products, such as legumes, vegetables, potatoes, hemp, and fruit trees, were grown for local consumption. Livestock, including sheep herds, draft animals, pigs, and poultry, also served local needs. In contrast, the mountains had surpluses of sheep, draft animals, and wood, which were exported to other regions, including the Catalan coast and France,

often using rafts to navigate major rivers such as the Garona and Noguera Pallaresa. Like the basin, the mountains also produced some goods exclusively for local use.

Among the traditional preindustrial activities, only iron production and salt extraction were suitable for external trade. These industries were concentrated in the northern High Pallars (iron) and Gerri de la Sal (salt). Food processing, textile fiber production, and construction materials were primarily for internal consumption. The main food-related activities involved transforming raw materials into flour, olive oil, and wine, while textiles were made from wool, flax, hemp, and leather. Extractive industries revolved around forests (wood and charcoal) and mineral deposits, including metallic resources like iron and copper, and nonmetallic resources such as lime, gypsum, and lignite.

Commercial activities were structured around three main spatial domains: local, intraregional (basin-mountain), and supraregional (external) markets. The local market was limited to individual valleys or small areas, mainly dealing with the few surpluses produced by the local subsistence economy. In the intraregional market, the basin and the mountain regions exchanged their surpluses, such as olive oil and wine from the basin and wood, wool, iron, leather, and livestock from the mountains. In the supraregional market, the Pallars region exported various products to Catalonia and Aragon, including wool, iron, wood, charcoal, leather, and draft animals, while importing items such as fish, rice, and goods from overseas colonies. The neighboring French territories were also part of the supraregional market.

The traditional values of the region were organized around three key social structures: the family (house), the town (neighborhood community), and the supramunicipal sphere. The family and house represented a combination of architectural, residential, and economic elements working as a single unit. Typically, each house was inhabited by three or four generations of the same family, ensuring the preservation of traditional family functions, including the passing down of family names, the continuity of the house, and the inheritance of property. Economically, the house served as the basic unit for production and consumption, featuring a fixed social and gender-based division of labor. The town was the heart of traditional society, where most individuals spent their entire lives, from birth to death. Towns organized economic activities around a small commercial network, various trades, and liberal professions, providing essential services. Street life was vibrant, and religious events were significant, breaking the monotony of daily work. Supramunicipal activities included weekly markets, popular meetings known as *aplecs*, and annual fairs.

2.6.2 The Crisis of the Subsistence Economy (1870–1910 CE)

In the late nineteenth century, the traditional foundations of Pallars society started to erode, and by the early twentieth century, Pallars had experienced a 33% decline in its population. Several factors contributed to this population crisis. First, the Pallars crisis mirrored the broader Spanish and European crises at the end of the nineteenth century, primarily due to the inherent flaws in the subsistence economic

system. In Pallars, this crisis was worsened by the appropriation of communal assets and properties, which were sold to private individuals. Second, adverse climatic conditions led to a series of poor harvests between 1893 and 1896 CE, resulting in higher prices for essential goods. Third, the grape phylloxera infestation in 1900 CE devastated the vineyards in the southern basin, causing a significant loss of wealth in the region and disrupting commercial ties with the mountains and the basin.

This crisis disproportionately affected the poorer and more isolated segments of the population, leading to a sharp decline in demographics. Nevertheless, the primary reason for depopulation was the migration of Pallars residents to other regions within Catalonia and southern France. Initially, these migration patterns were seasonal, driven by the pursuit of temporary employment, but over time, the destinations became more permanent. Barcelona became a significant settlement area, providing jobs in industry, domestic service, and small businesses. However, the primary destination for Pallars emigrants was South America, particularly Argentina.

In response to the population crisis, various local and external initiatives aimed to modernize the region. Modernization efforts encompassed three main aspects: infrastructure, social activities, and politics. A crucial milestone in this transformation was the construction of a road connecting Gerri de la Sal to the southern lowlands through the Montsec Range in the late nineteenth century, ending Pallars' traditional isolation. This road allowed for the establishment of a regular bus service between 1908 and 1912 CE, greatly improving external communication. Major towns in the region underwent significant urban development, and domestic and collective services such as water, electricity, telegraph, and sewer systems were introduced in the final decade of the nineteenth century. Social initiatives included the creation of various publications and a range of cultural, economic, and political associations, as well as initiatives aimed at advocating for and mobilizing citizens. On the political front, the Pallars region had historically been represented by outsiders imposed by the central Spanish government with the support of local leaders. This changed in 1907 CE when Pallars deputies became local politicians.

2.6.3 The Transition to Modern Society (1910–1960 CE)

A new economic model emerged when the first hydroelectric power stations were built between 1911 and 1916 CE. These stations were introduced and managed by companies and capital from outside the Pallars region, leading to a loss of control over one of its crucial natural resources. The electric sector's development brought about various changes, including a reduction in migratory movements, enhancements in communication and transportation networks, an infusion of external capital, the creation of new job opportunities, a revival of the commercial and service sectors, and the modernization of social practices. This transition to capitalism happened more swiftly in the Pallars Jussà. In Pallars Sobirà, the modernization of agriculture was an additional factor, marked by the abandonment of the traditional subsistence economy and the integration of mountain areas into the market economy. The most significant aspect of this transformation was the gradual shift from the beef industry to the sheep industry, which led to the growth of the dairy sector

by cooperative and private companies. While wood exploitation remained important, its transportation method changed from using rafts to trucks due to the construction of a system of river reservoirs.

The process of modernization reached its peak during the Second Republic (1931–1936 CE), but during the Civil War (1936–1939 CE) and the subsequent postwar period under the Franco dictatorship, there was a significant regression in the path toward a modern society. During this time, the Pallars region experienced considerable economic hardship, but signs of recovery started to emerge in the 1950s with the revitalization of mining activities, the construction of new hydroelectric stations, and the introduction of railways to the most important towns, which improved the transportation of goods.

2.6.4 The Second Crisis (1960–1980 CE)

During the 1960s, the urbanization of Catalonia's major cities and the mechanization of farming had a significant impact on the migration of people from rural to urban areas. This had particularly devastating effects in the Pallars region. If we compare the population peak in 1860 CE, which was approximately 46 thousand people, to the current population of approximately 19 thousand people, it becomes evident that ~60% of the Pallars population has been lost. This resulted in the disappearance of many towns and villages, with only medieval demographic crises matching the scale of this situation. Despite these changes, socioeconomic modernization continued, and local and regional agricultural structures became more dependent on the central Spanish state and even international interests. This economic transformation led to the replacement of traditional crops such as vineyards and olive groves with crops such as almonds, as well as the growth of intensive livestock farming, including pigs, cows, and chickens. Additionally, industrial activities, particularly in textiles, and tourism began to thrive during this period. Other signs of modernization included the widespread adoption of mass media such as radio, TV, and newspapers, the proliferation of personal cars, and increased exposure to foreign countries and cultures due to migrations and the growth of the tourism industry. As a result of these changes, the traditional family and house concept mentioned earlier was abandoned for architectural, organizational, and productive reasons. Toward the end of this crisis, the Franco dictatorship came to an end, and a gradual return to political and civil rights began (Box 2.2).

2.6.5 The Modern Capitalist Society (1980–2005 CE)

Currently, the disparity highlighted earlier between Pallars Sobirà, which is experiencing a swifter economic rebound due to tourism, and Pallars Jussà persists. Some have contended that Pallars is increasingly focusing on providing entertainment for city dwellers, and as a result, the region's environment and natural resources may gradually take precedence over its traditional economic pursuits such as farming and forestry, with tourism becoming the primary focus. This shift is already

underway, and it remains uncertain whether this is the sole course of action or if there are alternative models to explore for a more sustainable, diverse, and equitable approach to development.

2.7 Summary

The information presented in the preceding sections has been condensed into three primary periods: pre-Medieval, Medieval, and post-Medieval, as depicted in Figs. 2.13, 2.14, and 2.15. This categorization aligns with the divisions employed in the paleoecological reconstruction chapters (Chaps. 4, 5 and 6, respectively). These figures will offer a concise overview of significant historical and political events, as well as cultural advancements, for the purpose of comparing them to paleoecological reconstructions. This comparison will help us uncover the impact of human activities on the Montcortès vegetation and landscape throughout different time periods.

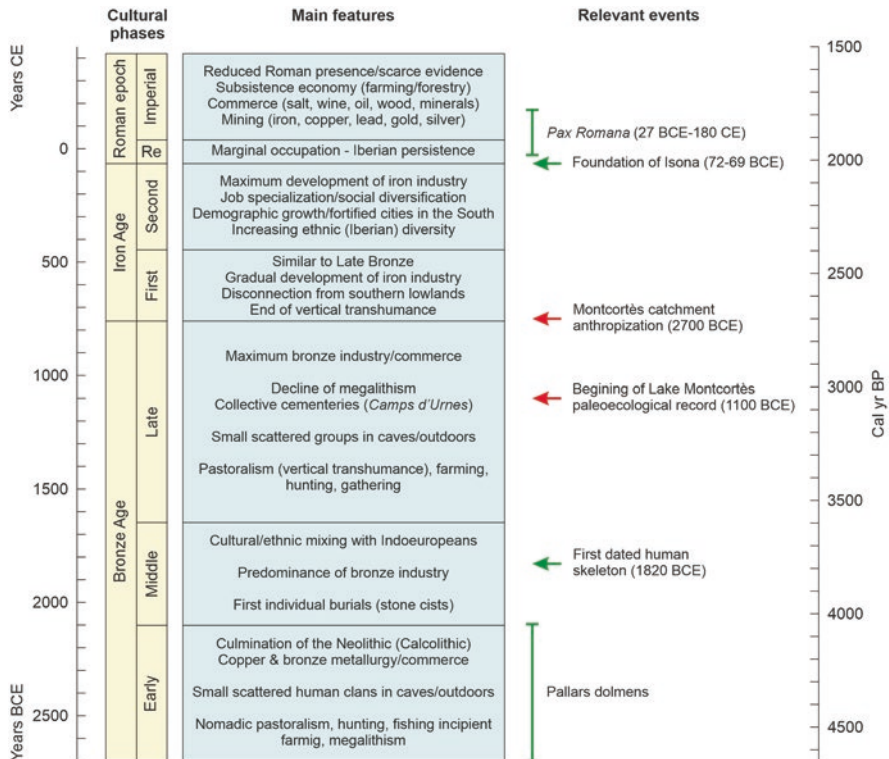


Fig. 2.13 Pre-Medieval cultural phases and the main developments and events of the Pallars region during these time periods, based on Cots (2005). Red arrows indicate the oldest estimated date of the palynological analysis and the date of anthropization of Lake Montcortès catchment, according to Rull et al. (2021a)

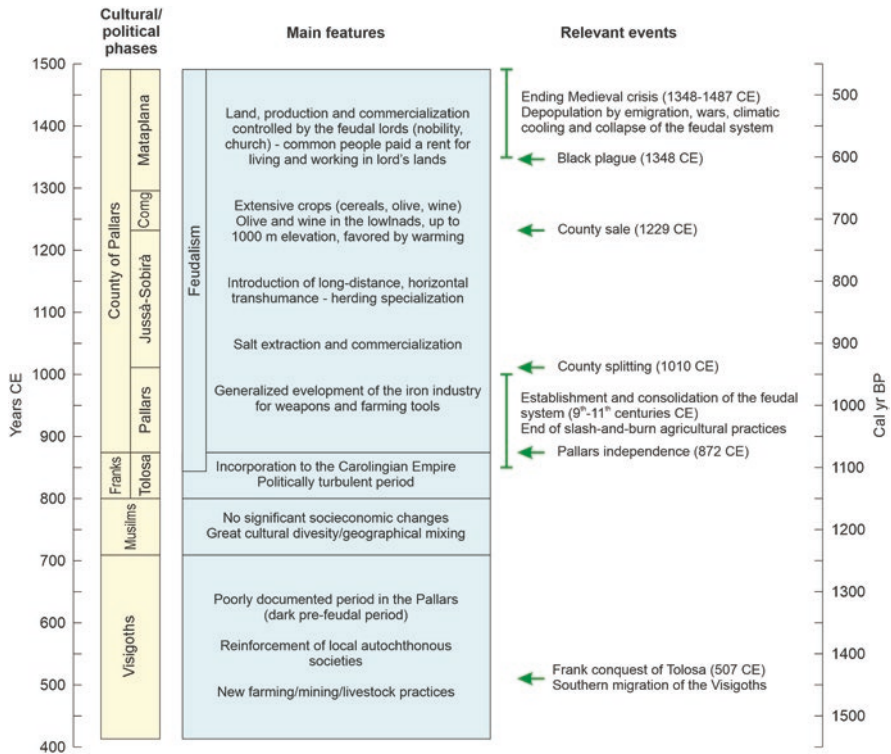


Fig. 2.14 Medieval cultural and political chronology of the Pallars region, with the main socioeconomic features and the most relevant historical events. The subdivisions of the County of Pallars period correspond to the houses that governed this county (Comg = Comenge)

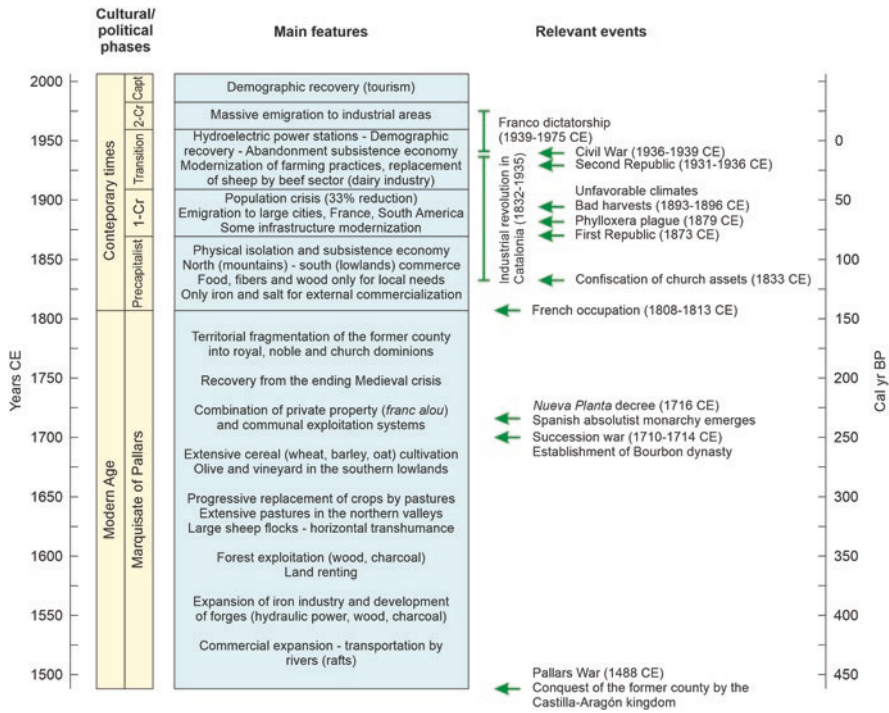


Fig. 2.15 Post-Medieval cultural and political chronology with the main socioeconomic features and the most relevant historical events. Precapitalist, traditional precapitalist society; 1-Cr, crisis of subsistence economy; Transition, transition to the modern society; 2-Cr, second demographic crisis; Capt, modern capitalist society

References

Bringué JM (2005) L'edat moderna. In: Marugan CM, Rapalino V (eds) *Història del Pallars. Dels Orígens als Nostres Dies*. Pagés Ed, Lleida, pp 87–119

Cots P (2005) Els pobles de la prehistòria i l'antiguitat. In: Marugan CM, Rapalino V (eds) *Història del Pallars. Dels Orígens als Nostres Dies*. Pagés Ed, Lleida, pp 13–43

Encyclopaedia Britannica (1994) *The New Encyclopaedia Britannica* (15th ed), Macropedia, Vol 18, European History and Culture, pp 590–727

Esteban A (2003) *La Humanización de las Altas Cuencas de la Garona y las Nogueras (4500 a.C.–1995 d.C.)*. Org Aut Parques Nacionales, Madrid

Farràs F (2005) El Pallars contemporani. In: Marugan CM, Rapalino V (eds) *Història del Pallars. Dels Orígens als Nostres Dies*. Pagés Ed, Lleida, pp 121–144

Garcia D, Gassiot E (2023) The mobility of sheperds in the Upper Pyrenees: a spatial analysis of pathways and site-location differences from medieval times to the 20th century. *Quat Int*, <https://doi.org/10.1016/j.quaint.2023.07.007>

Gassiot E, Pèlachs A (2017) La ocupación ganadera de los Pirineos occidentales de Catalunya en época romana e inicios de la Edad Media. *Treb Arqueol* 21:287–306

- Gassiot E, Mazzucco N, Clemente I, Rodríguez D, Obea L, Quesada M et al (2017) The beginning of high mountain occupations in the Pyrenees. Human settlements and mobility from 18,000 cal BC to 2000 cal BC. In: Catalan J, Ninot JM, Aniz MM (eds) High mountain conservation in a changing world. Springer, Cham, pp 75–105
- Halsall G (2008) *Barbarian Migrations and the Roman West (376–568)*. Cambridge University Press, Cambridge
- Maluquer de Motes J (2019) La Revolució Industrial a Catalunya (1832–1935). *Butll Soc Cat Est Hist* 30:125–179
- Marín M (1995) *Atlas Histórico*. Marín, Barcelona
- Marugan CM, Oliver J (2005) El Pallars medieval. In: Marugan CM, Rapalino V (eds) *Història del Pallars. Dels Orígens als Nostres Dies*. Pagés Ed, Lleida, pp 45–86
- Marugan CM, Rapalino V (2005) *Història del Pallars. Dels Orígens als Nostres Dies*. Pagés Ed, Lleida
- Obea L, Celma M, Piqué R, Gassiot E, Martín M, Salvador G et al (2021) Firewood-gathering strategies in high mountain areas of the Parc Nacional d'Aigüestortes i Estany de Sant Maurici (Central Pyrenees) during prehistory. *Quat Int* 593-594:129–143
- Rodríguez D, Gassiot E, Mazzucco N, Clemente I, Obea L, García D (2016) Del medio natural a los paisajes pastorales. Ocupación de las zonas de alta montaña en los Pirineos centrales de Cataluña desde el Mesolítico a la Edad del Bronce (c. 9000-1000 cal ANE). *Munibe* 67:325–337
- Rull V, González-Sampéris P, Corella JP, Morellón M, Giralt S (2011) Vegetation changes in the southern Pyrenean flank during the last millennium in relation to climate and human activities: the Montcortès lacustrine record. *J Paleolimnol* 46:387–404
- Rull V, Vegas-Vilarrúbia T, Corella JP, Valero-Garcés B (2021a) Bronze Age to Medieval vegetation dynamics and landscape anthropization in the south-central Pyrenees. *Palaeogeogr Palaeoclimatol Palaeoecol* 571:110392
- Rull V, Vegas-Vilarrúbia T, Corella JP, Trapote MC, Montoya E, Valero-Garcés B (2021b) A unique Pyrenean varved record provides a detailed reconstruction of Mediterranean vegetation and land-use dynamics over the last three millennia. *Quat Sci Rev* 268:107128
- Trapote MC, Vegas-Vilarrúbia T, López P, Puche E, Gomà J, Buchaca T et al (2018a) Modern sedimentary analogues and integrated monitoring to understand varve formation in the Mediterranean Lake Montcortès (Central Pyrenees, Spain). *Palaeogeogr Palaeoclimatol Palaeoecol* 496:292–304
- Trapote MC, Rull V, Giralt S, Montoya E, Corella JP, Vegas-Vilarrúbia T (2018b) High-resolution (subdecadal) pollen analysis of varved sediments from Lake Montcortès (southern Pyrenean flank): a fine-tuned record of landscape dynamics and human impact during the last 500 years. *Rev Palaeobot Palynol* 259:207–222



Abstract

The paleoecological study of Lake Montcortès began in 2004 with the first coring campaign of its varved sediments. In the first instance, these sediments were ^{14}C dated and analyzed palynologically at low resolution (centennial). Further studies based on varve counting provided a detailed yearly chronology that allowed the development of high-resolution reconstructions of a diversity of proxies, including pollen and spores, covering the last 3000 years. The palynological reconstruction disclosed in this book is based on a composite sequence using cores from 2004 and further coring campaigns, with an average resolution of ~ 16 years (decadal to bidecadal). Core sampling, sample processing, and pollen analysis were conducted using standard methods, and the interpretation was based on a two-year modern-analog study of pollen sedimentation using sediment traps. These studies provided information useful for paleoecological and paleoclimatic reconstruction, such as bulk annual pollen sedimentation, seasonal patterns, and the relationship between sedimentary pollen and the main meteorological variables. Overall, pine and oak pollen were dominant ($>75\%$ of pollen assemblage), followed by *Cannabis*, grasses, and other herbs. These pollen types varied seasonally, defining two well-differentiated assemblages corresponding to spring/summer and fall/winter. Significant correlations were found among these pollen assemblages and meteorological parameters such as temperature, precipitation, relative humidity, and wind intensity/direction.

This chapter provides a brief account of the methods used to produce the Lake Montcortès palynological record since the initial coring campaign (April 2004). The methods are not explained in detail, as they are common paleoecological procedures that have been abundantly described in the literature. The most relevant references are provided when necessary. The chapter concentrates on the specific

case of Lake Montcortès and is focused on the construction of the continuous composite section encompassing the last 3000 years and its detailed chronology, as well as on the main hints regarding the interpretation of palynological results in terms of vegetation and environmental change. Special emphasis is placed on the modern-analog study conducted in the lake, aimed at obtaining relevant information on the seasonality of pollen sedimentation and its internal (lake dynamics) and external (meteorological parameters) drivers, along with the usefulness of this information for paleoecological reconstruction.

3.1 Coring and Core Sampling

3.1.1 Coring

The palynological record presented in this book was obtained after the assemblage of four cores retrieved in the deepest part of the lake (Table 3.1). The deep cores of the MON04 coring campaign were recovered with a Kullenberg corer (Introduction; Fig. 4), and the most superficial core was recovered during the MONT-0713 coring campaign with a gravity corer. Details on these coring devices are provided by Leroy and Colman (2001) and Glew et al. (2001). The locations of the cores and the most recent varves are shown in Fig. 3.1. The cores retrieved during the first campaign (MON04) were preserved at 4 °C in the Pyrenean Institute of Ecology (Zaragoza, Spain), and those recovered in the MONT-0713 campaign were preserved under the same conditions in the Institute of Earth Sciences Jaume Almera (Barcelona, Spain), both belonging to the Spanish National Research Council (CSIC).

Table 3.1 Cores/drives used to assemble the composite section presented in this study, indicating the time interval covered, the number of samples analyzed, and the average resolution (Rull et al. 2021b)

Core/drives	Type	Date	Time interval (yr)	Samples	Y/S	Resolution
MON-0713-G05	G	Jul 2013	1423 CE–2013 CE (590)	95	6.21	Subdecadal
MON04-1A-1 K/2-4	K	Apr 2004	828 CE–1881 CE (1053)	36	29.25	Multidecadal
MON04-3A-1 K/4	K	Apr 2004	669 CE–821 CE (152)	20	7.60	Subdecadal
MON04-4A-1 K/4	K	Apr 2004	8 BCE–659 CE (667)	19	35.11	Multidecadal
MON04-4A-1 K/5	K	Apr 2004	(1100 BCE)–148 BCE (952)	22	43.27	Multidecadal
Total			(1100 BCE)–2013 CE (3113)	192	16.21	Bidecadal

Extrapolated ages are in brackets. G, gravity; K, Kullenberg; Y/S, years per sampling interval (average). See Fig. 3.1 for the locations of these cores

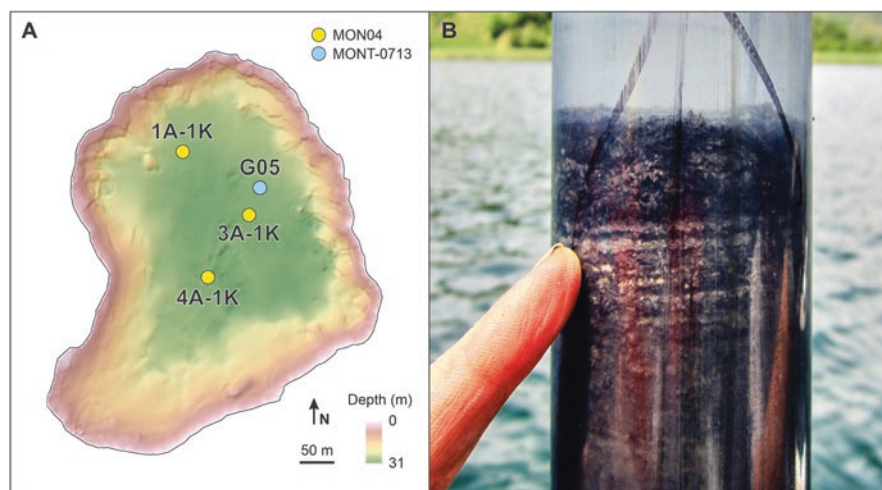


Fig. 3.1 Core location and recent varves. (a) Location of cores used to assemble the composite section presented in this study. Based on Corella et al. (2011a, b) and Vegas-Vilarrúbia et al. (2018). See Table 3.1 for details on these cores. (b) Top of a gravity core from the MON-0713 campaign showing the most recent varves. The uppermost uncompressed varve above the finger corresponds to the year 2013, when the core was taken (Rull et al. 2017)

3.1.2 Chronology and Sedimentation Rates

The age-depth model for the Montcortès composite section was based on microscopic varve counting in thin slides combined with ^{14}C and ^{210}Pb dating (Fig. 3.2). The resulting varve chronology was independent and absolute, as it was anchored in the coring year (2013), whose varve was clearly recognizable (Fig. 3.1). According to this model, the upper 543.5 cm of the section were deposited between 763 BCE (2713 cal yr BP) and the present (Corella et al. 2016), whereas the basal interval (543.5–573 cm)—where laminations were not of biogenic/endogenic origin and, therefore, their annual character was not guaranteed—was established assuming linear accumulation rates similar to the overlying samples (see below), which provided an estimated basal age of 1100 BCE (3050 cal yr BP) for the whole section (Rull et al. 2021a). Some intervals were interpolated due to poor varve preservation. Varves were very well preserved between 118 CE (1832 cal yr BP) and the present, and only 1.2% of this interval needed interpolation. Varve preservation was poorer between 117 CE and 763 BCE (2713 cal yr BP), and interpolation using the mean varve thickness of the upper and lower centimeters was required in 37% of the cases. Overall, the varved model showed very good agreement with other independent dating methods based on radiometric techniques (Fig. 3.2), which confirms the annual nature of the laminations (Corella et al. 2012, 2014, 2016).

Varves may be intercalated with turbiditic intervals originating from events of enhanced sediment delivery from the basin due to increased runoff episodes. Sedimentation rate (SR) changes largely depend on these runoff events, which are

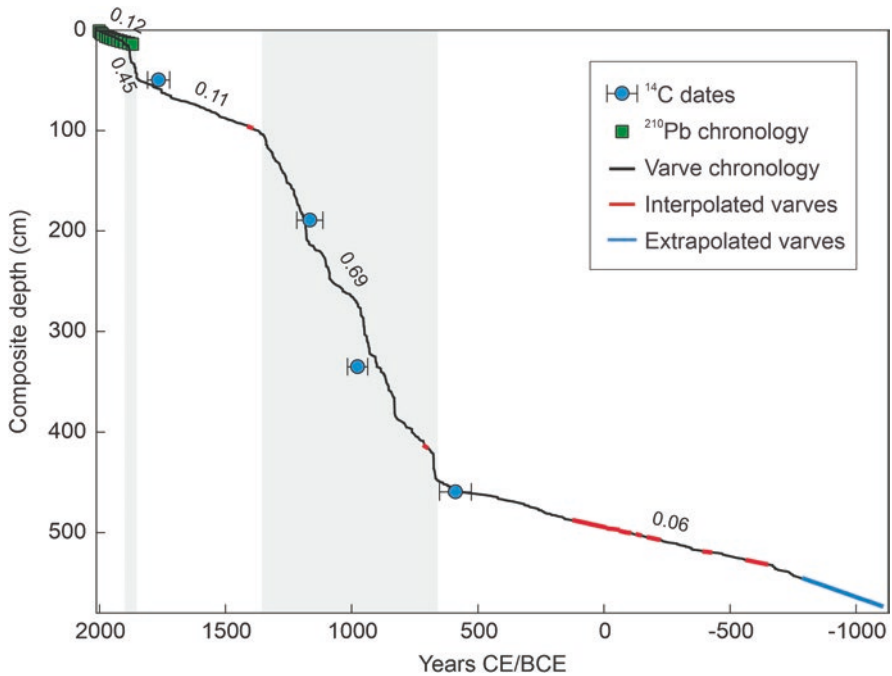


Fig. 3.2 Age-depth model for the Lake Montcortès composite section based on varve counting and radiometric dating (^{14}C and ^{210}Pb). Sedimentation rates (cm yr^{-1}) are indicated near the age-depth curve, and the intervals with higher values are highlighted by gray bands. Modified from Rull et al. (2021b) after raw data from Corella et al. (2014, 2016)

particularly significant in the intervals 1852–1901 CE (0.45 cm yr^{-1}) and 563–1362 CE (0.69 cm yr^{-1}) (Fig. 3.2). Turbidites are thinner and less frequent in the intervals 1902–2012 CE and 1363–1651 CE, which show lower SRs of 0.12 and 0.11 cm yr^{-1} , respectively. The lowest and most constant SD (0.06 cm yr^{-1}) occurs between 762 BCE and 562 CE, due to the lack of thick turbidites. The basal age of the studied sedimentary sequence was extrapolated using the latter SD value (Rull et al. 2021a).

3.1.3 Core Sampling

Samples for pollen analysis were taken in varved intervals, avoiding turbidites except in core MON04-1A-1K, which had been sampled systematically for several proxies shortly after the initial coring campaign (before detailed varve dating), and no material was left for further resampling (Fig. 3.3). A total of 192 samples were taken for pollen analysis, which were dated according to the age-depth model explained above (Fig. 3.2). The sampling resolution was variable due to the changing varve thickness, the presence of turbiditic intervals, and the occurrence of minor

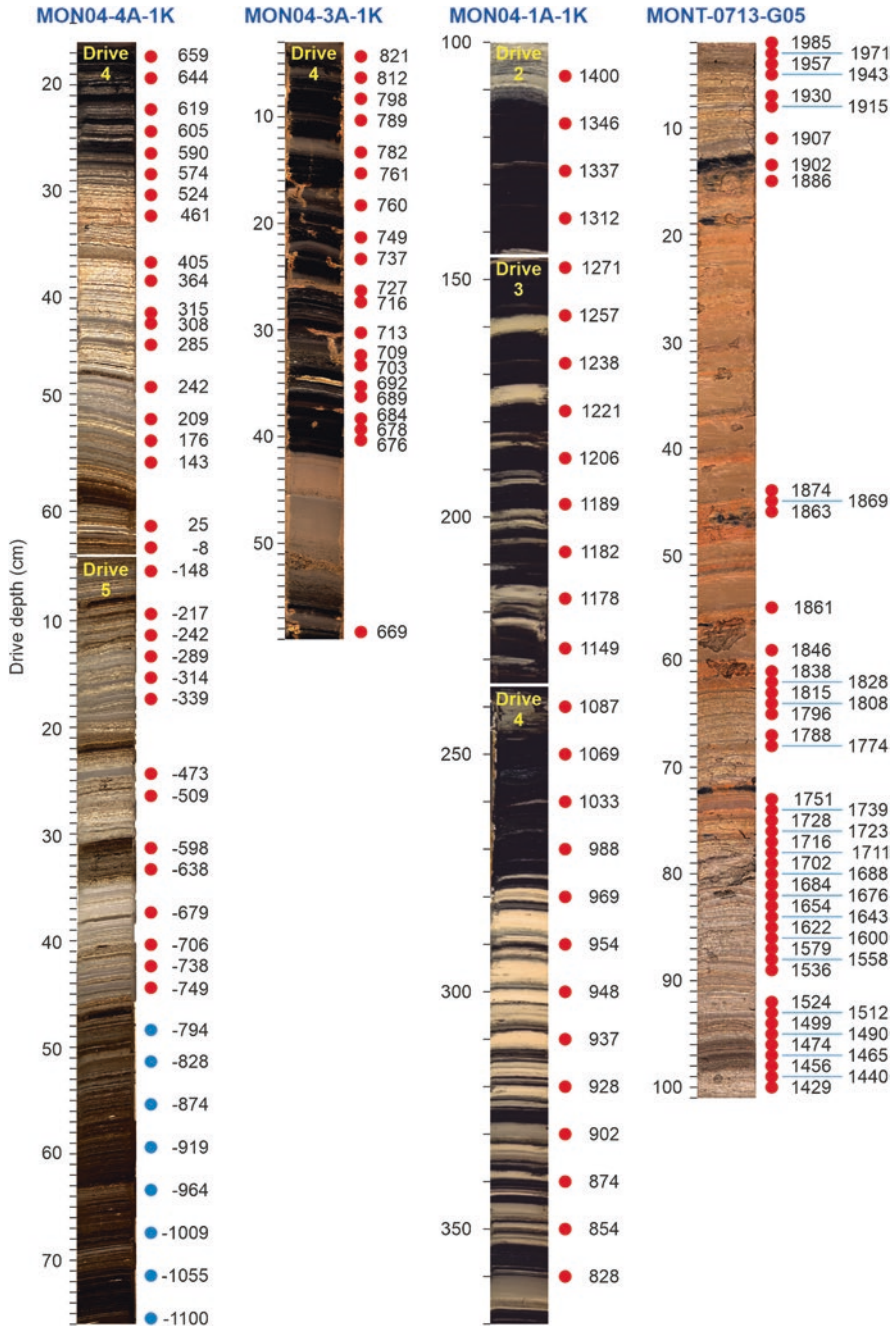


Fig. 3.3 Samples taken for pollen analysis (red dots) and their respective top ages (BCE for negative numbers and CE for positive numbers), according to the age-depth model of Fig. 3.2. Red dots are pollen samples with extrapolated ages taken at the interval on nonbiogenic/endogenic varves (see Sect. 1.2). Not all samples of core MONT-0713-G05 have been represented due to the high resolution of sampling (every 5 mm). Note that core MON04-1A-1K is represented on a different depth scale

coring gaps between adjacent cores. The average resolution per core ranged from subdecadal to multidecadal, and the overall resolution of the composite section was bidecadal (Table 3.1). The maximum resolution (subdecadal) was attained in the early Middle Ages (669–821 CE; drive MON04-3A-1K/4) and the last ~1400 years (core MONT-0713-G05). Considering the millimetric to submillimetric thickness of varves (Introduction; Sect. 5) and the minimum required material for pollen analysis (1 cm³), this is the maximum resolution that could be attained. Samples were taken with a 0.5-mm-diameter syringe to maximize sampling resolution. The upper two cores, MON-0713-G05 and MON04-1A-1K, have an overlap spanning almost 460 years, from 1423 CE to 1881 CE (as shown in Table 3.1). When combining the composite section, we excluded the uppermost part of core MON04-1 A-1K since core MON-0713-G05 had a more detailed analysis. Nevertheless, we carefully verified that the chronological consistency of these results matched previous lower-resolution analyses of the upper half of core MON04-1 A-1K conducted by Rull et al. (2011). Additionally, it is worth noting that there are no sediments corresponding to the period from 8 BCE to 148 BCE, which represents the transition between cores 4 and 5 in core MON04-4 A-1K.

3.2 Pollen Analysis and Interpretation

3.2.1 Sample Processing, Analysis, and Interpretation Insights

The core samples were processed for palynological analysis by N. Cañellas-Boltà at the Laboratory of Paleocology (PALAB) of the Institute of Earth Sciences Jaume Almera (Barcelona, Spain) using HCl, KOH, and HF digestions and acetolysis, with previous spiking with *Lycopodium* tablets. The samples were mounted in glycerin jelly for microscopic observation. Details on these methods can be found in Faegri et al. (1989), Moore et al. (1991), and Bennett and Willis (2001). Taxonomic identification was based on the existing pollen/spore atlases and catalogs for the region (e.g., Reille 1992–98; Moore et al. 1991) and the PALAB pollen reference collection, which was prepared by N. Solé de Porta. Counting followed the criteria of Rull (1987), namely, a minimum pollen sum of 200 grains and the saturation of diversity. In this book, only the most relevant pollen and spore taxa have been considered, and detailed analyses can be found in Rull and Vegas-Vilarrúbia (2014, 2015, 2021, 2022; Rull et al. 2011, 2021a, c), Montoya et al. (2018), and Trapote et al. (2018a, b). The pollen sum included only the pollen of terrestrial angiosperms, and ferns and aquatic/semiaquatic plants (Cyperaceae, *Typha*, *Cladium*) were excluded.

The case of *Cannabis*—a cultivated plant with multiple human uses, including the production of hemp fiber (Clarke and Merlin 2016; Rull 2022)—is worth mentioning as, in the first studies, its pollen was actually included in the pollen sum (e.g., Rull et al. 2011). However, it was later realized that the high abundances (60–80%) of *Cannabis* pollen in certain time intervals could only be explained by retting (i.e., the process of separating the hemp fiber from the stalk by immersion in water), rather than by local or regional cultivation (Rull and Vegas-Vilarrúbia 2014).

Therefore, the inclusion of this pollen type in the pollen sum could cause distortions in the reconstruction of past vegetation by affecting the percentages of wild and cultivated plants. At present, the pollen of *Cannabis* is excluded from the pollen sum (Rull and Vegas-Vilarrúbia 2022; Rull et al. 2021b), a rule that is also followed in this book. Another relevant issue is the differentiation between the pollen of *Cannabis* and *Humulus* (hop), a sister genus of the same family (Cannabaceae) bearing similar pollen morphology but contrasting ecological requirements and cultural connotations. Several morphological characteristics, especially the combination of size and pore features, have been proposed to differentiate the pollen of these genera (Fleming and Clarke 1998; Mercuri et al. 2002). McPartland et al. (2018) proposed an indirect and complementary approach, also called the assemblage approach (Rull 2022), based on the fact that wild *Cannabis* occurs mostly in open temperate steppes with grasses, chenopods and *Artemisia*, whereas *Humulus* is typical of temperate deciduous forests dominated by alder (*Alnus*), willow (*Salix*), and poplar (*Populus*). *Cannabis* also occurs as a cultivated plant associated with cereals such as oats (*Avena*), barley (*Hordeum*), rye (*Secale*), and wheat (*Triticum*). Using these morphological and assemblage approaches together, the Cannabaceae pollen found in Lake Montcortès sediments was identified as *Cannabis* pollen (Rull and Vegas-Vilarrúbia 2014).

Some nonpollen palynomorphs (NPPs), such as algae remains (*Botryococcus*, *Pediastrum*), spores of coprophilous (*Sporormiella*, *Sordaria*) and mycorrhizal (*Glomus*) fungi, and microcharcoal particles, were also identified and counted. Algae remains have been used as indicators of limnological conditions such as water chemistry or trophic state, among others (Jankovská and Komárek 2000; i 2001). The spores of coprophilous fungi (*Sporormiella*, *Sordaria*) have been considered indicative of grazing (van Geel et al. 2003; Lee et al. 2022), whereas *Glomus* has been related to increased erosion rates (Anderson et al. 1984). Charcoal particles are commonly considered the best palynological proxies for fire incidence, usually associated with human practices (Whitlock and Larsen 2001).

All cores were analyzed by V Rull except core MONT-0713-G05, which was part of a PhD dissertation by MC Trapote under the supervision of the authors of this book (Trapote 2019). E Montoya analyzed the NPP from core MON04-1A-1K. Pollen diagrams were plotted and zoned using *Psimpoll 4.27* and the method of optimum splitting by information content (OSIC) (Bennett 1996), considering only the taxa inside the pollen sum. Statistical analyses were performed with *MVSP 3.22* (Kovach 1989, 1993) and *Past 4.09* (Hammer and Harper 2006; Hammer et al. 2001).

The interpretation of palynological results in terms of vegetation and landscape shifts has been based on present-day ecological requirements of the involved taxa and the communities they form, as well as on the sedimentary patterns of their pollen/spores and other remains. The amount of these particles that finally reach lake sediments is a function of a number of parameters, such as pollen production, dispersal, water-surface sedimentation, and internal lake dynamics. In addition, other postdepositional processes, notably reworking and diagenesis, may affect the final composition of the sedimentary pollen assemblage (Birks and Birks 1980). An

eventual analytical approach would consider all these factors to try to deduce past vegetation patterns from sedimentary pollen assemblages. However, such a task is unfeasible in a reasonable amount of time, and a synthetic approach known as the modern-analog approach has been developed.

This method compares the pollen spectra deposited in modern sediments with the source vegetation and establishes qualitative and quantitative relationships between them useful to infer past vegetation patterns and human impact from fossil pollen spectra (e.g., Overpeck et al. 1985; MacDonald and Ritchie 1986; Anderson et al. 1989; Rässänen 2001; Yang et al. 2012; Zanon et al. 2018). It is also possible to establish straightforward relationships between modern pollen assemblages and present-day climatic parameters and use them to infer paleoclimatic trends from past pollen records (e.g., Markgraf et al. 2002; Zheng et al. 2014; Court-Picon et al. 2006; Williams and Schuman 2008; Tarasov et al. 2011; Herbert and Harrison 2016). In this case, quantitative estimates are derived from transfer functions calibrated in climatic terms by using modern pollen datasets and a variety of statistical techniques (Birks 1998; Birks et al. 2012). In the Iberian Pyrenees, a few studies of this type exist that are based mainly on modern pollen, vegetation, and climate datasets along elevational gradients (Pla and Catalan 2005; Cañellas-Boltà et al. 2009; Ejarque et al., 2011; López-Vila et al. 2014).

Identifying the source vegetation area for the pollen deposited in lake sediments is a crucial step in the modern-analog approach. According to Jacobson and Bradshaw (1981) and Prentice (1985), even small- to moderate-sized lakes (~1 ha or 0.01 km²) have relatively large source areas and reflect regional vegetation. This is the case for Lake Montcortès (0.14 km²), whose modern sedimentary pollen spectra can be considered representative of the regional vegetation, as depicted in Fig. 1.12, which is useful for inferring Late-Holocene regional vegetation patterns from the composite sedimentary sequence analyzed in this study. The same is true for regional climatic patterns (Chap. 2; Sect. 3). With this in mind, a modern-analog survey was carried out, which is described in more detail in the following section.

3.2.2 Modern-Analog Survey

The main aims of the Montcortès modern-analog study were (i) to document the annual cycle of pollen sedimentation, (ii) to compare pollen seasonality with varve formation and composition, (iii) to unravel the most relevant meteorological parameters influencing the annual pollen cycle, and (iv) to obtain clues for the interpretation of downcore pollen records in terms of vegetation dynamics. The main features of Lake Montcortès varves and local/regional vegetation are provided in Chap. 1 (Sects. 4 and 5). Meteorological data were from the nearby station of La Pobla de Segur (Fig. 1.3) and included average temperature (T_m) in °C, average relative humidity (H_m) in %, average pressure (P_m) in hPa, total precipitation (PPT) in mm, wind velocity (W) in m s⁻¹, and wind direction (W_d) in degrees, with 0° representing northern winds. The sampling period was from fall 2013 to fall 2015, and the study was carried out using sediment traps, which is a widely used method in the study of

lakes with varved sediments (Bloesch and Burns 1980; Mieszcankin 1997; Mieszcankin and Noryskiewicz 2000; Punning et al. 2003; Giesecke and Fontana 2008; St Jacques et al. 2008; Huguet et al. 2012; Zolitschka et al. 2015).

3.2.2.1 Sediment Traps

A battery of sediment traps was installed in fall 2013 to follow the annual cycle of sedimentation for a variety of proxies, including (i) calcite and organic matter for varve formation; (ii) Fe and Mn for the annual oxygenation cycle; (iii) pollen and nonpollen palynomorphs (algae remains, fungi spores, charcoal), diatoms and photosynthetic pigments for paleoecological and paleolimnological reconstruction; and (iv) glycerol dialkyl tetraethers (GDGTs) as paleotemperature proxies. Sediment traps were suspended from a floating platform situated above the deepest part of the lake, from where the sediment cores of MONT-0713 were obtained for paleoecological study (Fig. 3.1). Each trap was composed of a nontransparent cylindrical plastic tube measuring 8.5 cm in diameter and 80 cm in length. It had an open top and a sealed bottom, and it was suspended in the water at a depth of 20 meters (Fig. 3.4). The pollen trap contents were collected seasonally: March (winter), June (spring), September (summer), and December (fall). The sediments were allowed to settle in the laboratory for at least 48 hours. The results obtained for proxies other than pollen, including varve formation and composition, are reported in Trapote et al. (2018a) and Vegas-Vilarrúbia et al. (2020). The results of pollen analysis are described here in more detail following Rull et al. (2017). The sediment recovered

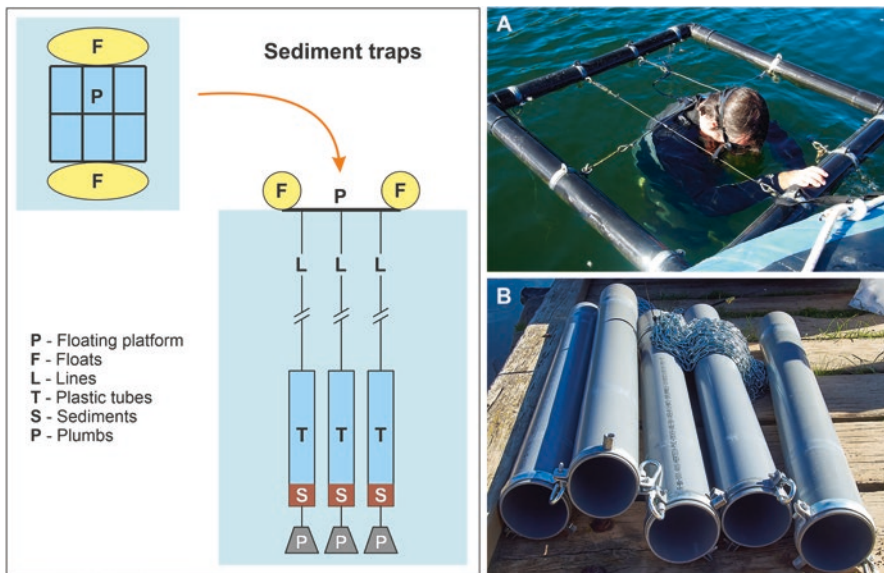


Fig. 3.4 Schematic view of the sediment-trap battery installed in September 2013 (left). (a) Floating platform. (b) Plastic tubes that collected the sediment for the different proxies. Photos: V. Rull

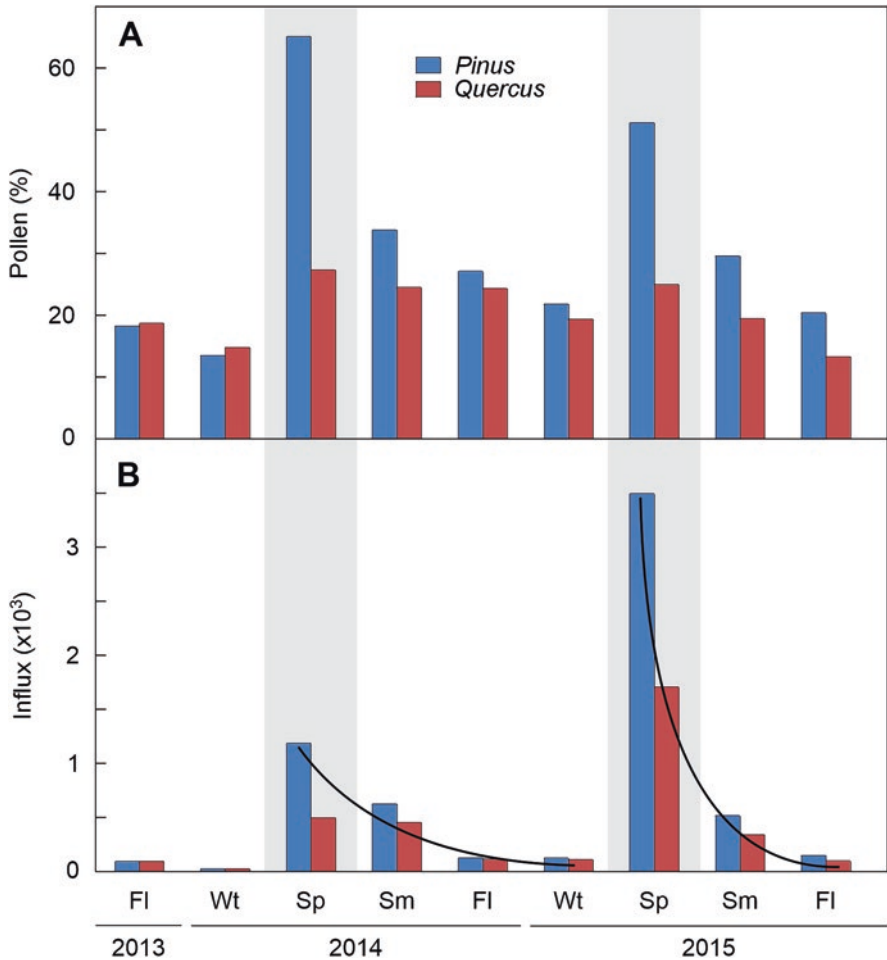


Fig. 3.5 Pollen percentage (a) and influx (b) of *Pinus* and *Quercus*, the major components of modern pollen assemblages (influx in grains cm^{-2} season $^{-1}$). Sp, spring; Sm, summer; FI, fall; Wt, winter. Modified from Rull et al. 2017)

after decanting and filtering the seasonal samples was processed and analyzed for pollen analysis using the same methods as in the core samples (Sect. 4.1).

3.2.2.2 Pollen Seasonality and Varves

The most abundant elements found in the sedimentary pollen assemblages were *Pinus* and *Quercus*, which are the prevailing tree species in today's regional forests. During the spring and summer seasons, *Pinus* accounted for approximately 50–65% of the pollen, while *Quercus* made up ~25%. In contrast, during the fall and winter, *Pinus* dropped to less than 30%, and *Quercus* fell below 20% (see Fig. 3.5). In both situations, pollen continued to be deposited in the sediment traps throughout the

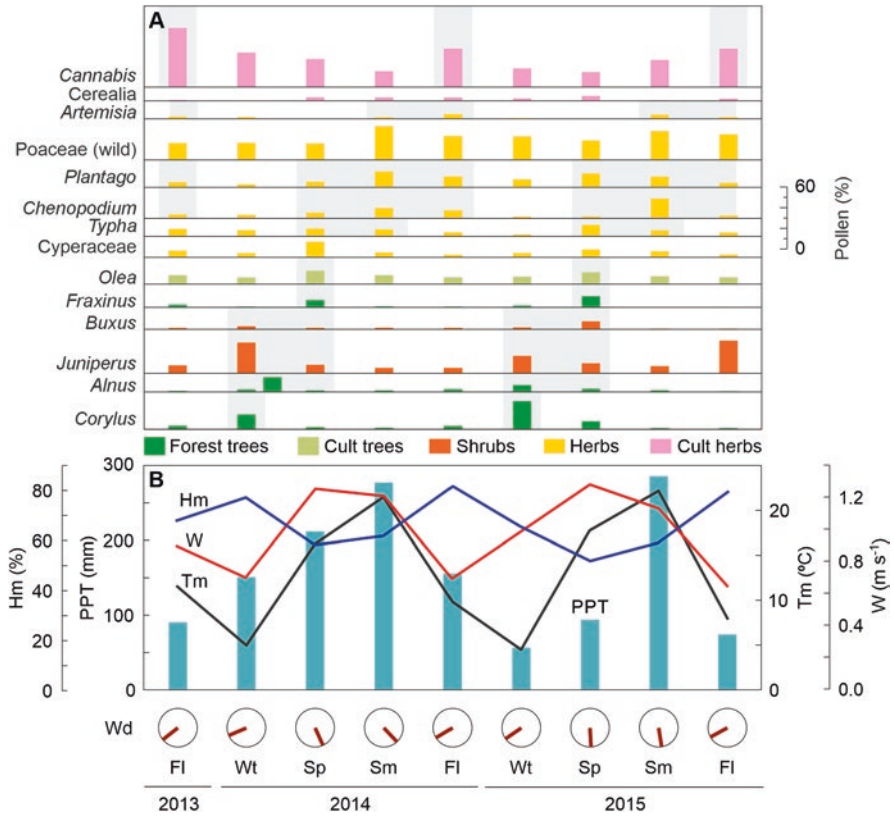


Fig. 3.6 Pollen percentages of the less abundant pollen types (a) compared with the most relevant meteorological parameters used in this study (b). Pollen percentages were calculated excluding *Pinus* and *Quercus* from the pollen sum to facilitate visualization. Taxa are ordered by their respective flowering seasons (gray bands) from bottom to top and from left to right (flowering seasons according to Bolòs et al. 2000). The flowering season of all species of the different genera present in the Montcortès region has been considered (Mercadé et al. 2013). Cultivated plants, such as *Cerealia*, *Cannabis*, and families including many genera (Poaceae, Cyperaceae), are located based on their pollen patterns due to the difficulty of establishing a definite flowering season. Meteorological parameters: Tm, average temperature (black line); Hm, relative humidity (blue line); W, wind velocity (red line); PPT, total precipitation (green bars). The wind direction is shown as circles. Sp: spring, Sm: summer, FI: fall, Wt: winter. Modified from Rull et al. (2017)

year, even when the parent plants were no longer in bloom. This phenomenon is known as pollen sedimentation lag (PSL) and can be better assessed by examining influx values, which demonstrated an exponential-like decline from spring to winter (refer to Fig. 3.5). The other pollen types were far less abundant and were represented in percentages excluding *Pinus* and *Quercus* from the pollen sum to facilitate visibility (Fig. 3.6). These pollen taxa also showed higher abundances during their corresponding flowering seasons and PSL of variable magnitude, which

demonstrates that this phenomenon is a general sedimentation feature rather than a property of the dominant pollen types.

Several mechanisms related to water dynamics, sediment resuspension, and/or catchment retention have been invoked to explain the PSL. Internal lake dynamics could be an important factor (Punning et al. 2003), as most taxa bloom during spring/summer, when the lake begins to be stratified (Fig. 1.15). This could cause the retention of part of the pollen in the thermocline, which represents a density barrier (pycnocline) delaying pollen sedimentation. The possibility of sediment resuspension cannot be disregarded because the lake is fed by groundwater that could physically disturb the sediments. This possibility could be tested by the installation of sediment traps at different water depths, along with aerobiological samplers at the surface of the lake (Bloesch 1994; Mieszczankin and Noryskiewicz 2000; Giesecke and Fontana 2008). It is also possible that the pollen deposited on catchment soils during the flowering season can be continuously washed into the lake during the year, thus contributing to the apparent PSL (St Jacques et al. 2008). This possibility could be tested by installing aerobiological samplers distributed across the catchment soils, in addition to the abovementioned combination of lake samplers and traps.

Cluster analysis yielded two groups of samples with distinct pollen assemblages corresponding to spring/summer and fall/winter. The spring/summer assemblage was characterized by *Plantago*, *Chenopodium*, *Typha*, Cyperaceae, *Fraxinus*, and *Juniperus*, whereas the fall/summer assemblage was dominated by *Cannabis* and *Corylus*. Wild Poaceae, which may include numerous species of this family, showed significant but similar abundances in both seasonal groups, thus not contributing to seasonal differentiation (Table 3.2). Interestingly, the seasonal patterns of pollen

Table 3.2 Composition of the pollen assemblages obtained by cluster analysis using the average percentages of the relevant pollen types, excluding *Pinus* and *Quercus* from the pollen sum

Pollen taxa	Spring/summer (%)	Fall/winter (%)
<i>Cannabis</i>	16.02	27.95
Cerealia	2.36	1.05
<i>Artemisia</i>	1.06	1.19
Poaceae (wild)	18.39	15.53
<i>Plantago</i>	8.66	3.92
<i>Chenopodium</i>	7.08	2.31
<i>Typha</i>	6.03	3.64
Cyperaceae	6.48	3.38
<i>Olea</i>	7.67	5.58
<i>Fraxinus</i>	3.57	0.95
<i>Buxus</i>	2.14	1.27
<i>Juniperus</i>	5.83	1.65
<i>Alnus</i>	1.44	2.00
<i>Corylus</i>	2.39	8.82

The percentages of taxa with more seasonal differentiation power are highlighted in bold. After Rull et al. (2017)

sedimentation (spring/summer vs. fall/winter) differed from those observed in varve formation, as recorded in the same trap survey, where light calcite laminations were formed mostly during summer/fall and darker organic layer developed during winter/spring (Trapote et al. 2018a). See also Chap. 1 (Sect. 5). Therefore, pollen and varve seasonality occurred with an offset of approximately one season.

3.2.2.3 Particular Pollen Types

Some specific types of pollen displayed interesting sedimentary patterns that warrant further investigation. An example of this is the remarkable observation of similar sedimentation patterns for *Pinus* and *Quercus* pollen. This is particularly noteworthy because these two genera exhibit significant differences in their morphological characteristics. *Pinus* pollen, for instance, lacks apertures and features two sizable, empty, buoyant sacci, whereas *Quercus* pollen is tricolporate/tricolporoidate and lacks distinctive morphological traits or ornamentation. Surprisingly, when these distinct pollen types found their way into the waters of Lake Montcortès, their sedimentation behaved quite similarly, even during the summer when thermal stratification remained stable. This fact suggests that internal lake dynamics might not play a crucial role in pollen sedimentation as resuspension or the influence of catchment runoff.

The *Cannabis* (hemp) pollen also provided valuable insights that require further investigation. This pollen was most prevalent during the autumn season, even though the original plant has not been recorded in either the comprehensive plant survey of the lake area (Mercadé et al. 2013) or in regional vegetation studies (Carreras et al. 2005–2006). *Cannabis* is a cultivated plant, and its pollen has been consistently present and abundant in Lake Montcortès for approximately 1400 years (Rull et al. 2021b). However, determining the exact source of this pollen has proven to be a challenging task (Rull and Vegas-Vilarrúbia 2015). Historical records indicate that this plant was cultivated in nearby lowlands such as Gerri de la Sal, La Pobla de Segur, and La Pobleta de Bellveí during the nineteenth century (Madoz 1845–1850). Additionally, it is believed that Lake Montcortès played a significant role in hemp retting, particularly between the sixteenth and nineteenth centuries, although there is a lack of historical documents to substantiate this assessment.

Olea, a plant species typically found in lowland areas, is not commonly seen in the vicinity of Montcortès, which lies on the border between lowland and mountainous ecosystems (Rull et al. in 2011 and Mercadé et al. in 2013). Consequently, it might be surprising to observe significant amounts of *Olea* pollen in the sediments of Lake Montcortès (Table 3.2 and Fig. 3.6). Nevertheless, in a prior investigation focusing on the deposition of modern pollen across an elevation gradient in the central Pyrenees, Cañellas-Boltà et al. (2009) consistently detected *Olea* pollen from the lowlands all the way up to the alpine region above 2500 m in elevation and attributed this to the influence of upward winds.

3.2.2.4 Relationships with Meteorological Variables

The influx of pollen from major tree types, specifically *Pinus* and *Quercus*, closely followed the seasonal patterns of temperature and precipitation (Figs. 3.5 and 3.6).

Table 3.3 Spearman-rank correlation coefficients between the most relevant pollen taxa and meteorological variables

Pollen taxa	T_m	H_m	P_m	PPT	W	W_d
<i>Alnus</i>	-0.200	-0.167	-0.217	-0.100	0.250	0.117
<i>Artemisia</i>	-0.008	0.661	0.025	0.226	-0.661	0.368
<i>Buxus</i>	-0.150	-0.383	-0.417	-0.100	0.500	-0.033
<i>Cannabis</i>	-0.383	0.750	0.150	-0.200	-0.767*	0.533
Cerealia	0.300	-0.500	0.000	0.067	0.617	-0.533
<i>Chenopodium</i>	0.683*	-0.033	-0.417	0.900**	0.083	-0.500
<i>Corylus</i>	-0.533	-0.033	-0.167	-0.467	0.117	0.317
Cyperaceae	0.537	-0.883**	-0.017	0.233	0.850**	-0.717*
<i>Fraxinus</i>	0.117	-0.577	0.017	-0.176	0.678*	-0.427
<i>Juniperus</i>	-0.667*	0.150	0.267	-0.700*	-0.300	0.650
<i>Olea</i>	0.650	-0.850*	0.050	0.267	0.867**	-0.867**
<i>Pinus</i>	0.667*	-0.750*	-0.200	0.517	0.800**	-0.800**
<i>Plantago</i>	0.617	-0.433	-0.050	0.433	0.567	0.650
Poaceae (wild)	0.317	0.150	0.133	0.300	-0.150	-0.150
<i>Quercus</i>	0.600	-0.700*	-0.367	0.533	0.817**	-0.767*
<i>Typha</i>	0.567	-0.650	-0.183	0.333	0.700*	-0.533

T_m , average temperature; H_m , average relative humidity; P_m , average pressure; PPT, average precipitation; W , average wind velocity; W_d , average wind direction. Significant correlations are highlighted in bold (* $\alpha < 0.05$; ** $\alpha < 0.01$). After Rull et al. (2017)

The peak pollen levels occurred during the spring when these tree species were flowering, which was one season ahead of the peak temperatures and precipitation levels during the summer. There was an inverse relationship between pollen and relative humidity. Additionally, the highest pollen influx coincided with moderate wind speeds, primarily coming from the SSE ($\sim 150^\circ$), while pollen levels were at their lowest during slower winds from the WSW ($\sim 250^\circ$). Furthermore, several individual pollen types demonstrated significant correlations with various meteorological factors (Table 3.3). Among these factors, wind velocity (W), wind direction (W_d), and relative humidity (H_m) exhibited the most notable significant correlations. However, pressure (P_m) did not display any significant correlation. Notably, *Olea*, *Pinus*, *Quercus*, and Cyperaceae pollen showed negative associations with both H_m and W_d , but were positively correlated with W . On the other hand, *Chenopodium* and *Juniperus* pollen displayed both positive and negative correlations with temperature (T_m) and precipitation (PPT). Finally, *Cannabis* pollen was only negatively correlated with wind velocity (W).

Further elaboration is warranted on these particular correlations, particularly when considering relative humidity, wind direction, and wind speed, as these factors notably influence *Olea*, *Pinus*, and *Quercus*. Cyperaceae will not be discussed here due to its diversity in terms of flowering times and pollen distribution characteristics across multiple species. As previously mentioned, *Olea* primarily grows in low-lying areas, yet its pollen can be carried upward by the wind, as supported by Cañellas-Boltà et al. (2009). Our findings from Montcortès reinforce this, indicating

that dry and windy conditions promote the deposition of *Olea* pollen in lake sediments. Moreover, the significant inverse correlation with wind direction in degrees suggests that the primary pollen source is from the SW ($\sim 225^\circ$). The same applies to the pollen from *Pinus* and *Quercus* forests, which are more prominently represented in the southern portion of the studied area (see Fig. 1.12).

Canonical correspondence analysis (CCA) was used to integrate the entire dataset. In Fig. 3.7, the scatter plot displays the first two axes, which collectively accounted for 70.74% of the overall variance. Axis 1, responsible for the most significant variation at 56.80%, exhibited a strong correlation with relative humidity and pressure when its values were positive and with wind velocity when the values were negative. Samples were arranged along this axis, following a seasonal pattern from left (spring) to right (winter), with summer and fall situated in between. In terms of pollen taxa, *Pinus*, *Quercus*, and *Fraxinus* were positioned close to the spring samples, while *Juniperus*, *Corylus*, *Cannabis*, and *Artemisia* clustered with the fall/winter group. Other taxa fell in intermediate positions. The spring group exhibited a strong correlation with temperature, precipitation, and wind velocity, whereas the fall group was notably associated with wind direction, particularly from the WSW direction during that season. This contrasts with the SSE winds prevalent in the spring/summer months. *Juniperus* and *Cannabis*, which are typically associated with the fall/winter period, were the taxa most closely linked to WSW winds.

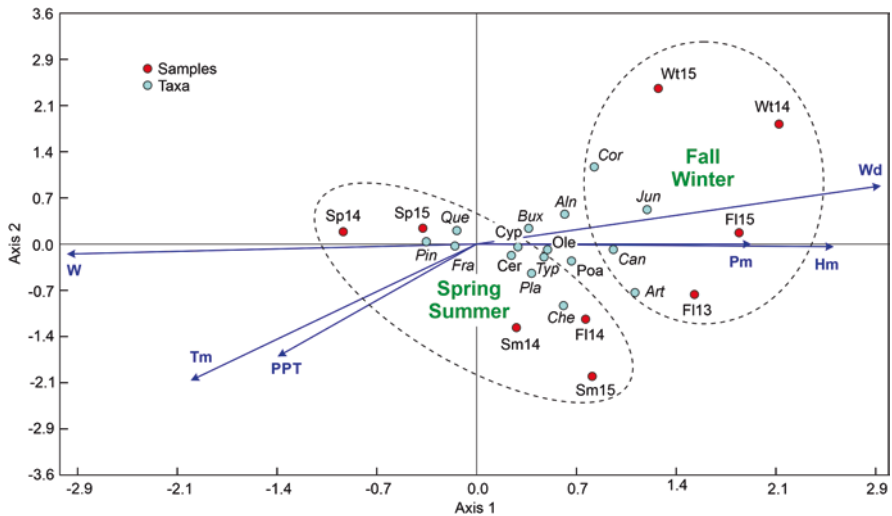


Fig. 3.7 CCA biplot using the scores of the first two axes (70.74% of the total variance). Samples are identified seasonally as follows: Sp, Spring; Sm, Summer; Fl, Fall; Wt, Winter. Meteorological parameters: T_m , average temperature; H_m , average relative humidity; P_m , average pressure; W , average wind velocity; PPT, average precipitation; W_d , average wind direction. Pollen types: *Aln*, *Alnus*; *Art*, *Artemisia*; *Bux*, *Buxus*; *Can*, *Cannabis*; *Cer*, *Cerealia*; *Che*, *Chenopodium*; *Cor*, *Corylus*; *Cyp*, *Cyperaceae*; *Fra*, *Fraxinus*; *Jun*, *Juniperus*; *Ole*, *Olea*; *Poa*, *Wild Poaceae*; *Pin*, *Pinus*; *Pla*, *Plantago*; *Que*, *Quercus*; *Typ*, *Typha*. Redrawn and modified from Rull et al. (2017)

The CCA plot confirmed the groupings identified in the cluster analysis, reinforcing the distinct seasonal patterns in pollen distribution throughout the year. It also highlighted a clear division between the spring/summer and fall/winter pollen assemblages. Additionally, this analysis identified the key meteorological factors closely related to the seasonal deposition of pollen. The primary environmental gradient was influenced by the windy, rainy, and warmer conditions of the spring/summer seasons, characterized by SSE winds, as well as the high-pressure systems and high relative humidity of the fall/winter seasons, associated with WSW winds. This gradient was strongly correlated with the prevalence of specific pollen types that typify each seasonal assemblage.

The seasonal pollen influx patterns are consistent with the anemophilous nature of dominant species, as warm temperatures, low humidity, and moderate winds promote the passive drying of flowers, facilitating the release of pollen from the anthers (Helbig et al. 2004). Nonetheless, this does not fully explain why there was a disparity in the intensity of spring pollen peaks between 2014 and 2015 (see Fig. 3.5). Although temperature and wind speed exhibited nearly identical patterns in both years, the same cannot be said for precipitation and relative humidity. Specifically, 2014 saw significantly higher precipitation levels prior to spring compared to 2015, while relative humidity was lower during the spring of 2015. These variations may have influenced pollen release, but it remains a speculative hypothesis until further localized aerobiological studies are carried out. Additionally, we cannot rule out slight differences in the sources of pollen due to a minor shift in the predominant wind direction between the spring seasons of 2014 and 2015.

3.2.2.5 Paleocological Applications

From a paleocological perspective, the differences observed in the pollen composition within varve layers can be attributed to variations in weather conditions. This suggests that pollen can serve as a valuable indicator of past environmental conditions in this particular lake. Furthermore, by analyzing the pollen found in sediment cores, it is possible to not only identify seasonal patterns throughout the year but also to date the sediments. This is particularly useful in situations where the varve record is incomplete or disturbed, as discussed in Sect. 1.2. The seasonal pollen model developed in this study, based on modern analogs, can be applied to at least the past 3000 years, as the various pollen types have consistently been present in similar proportions (Rull et al. 2021b). The established seasonal patterns described here are reliable for conducting paleoenvironmental studies of Lake Montcortès. To account for potential interannual variations, it is recommended to continue the analysis of sediment traps.

An important parameter for comparison with paleocological results is the total percentage of each pollen type across the whole modern sampling period, as down-core pollen assemblages are aggregates representing one to several years of sedimentation (Rull and Vegas-Vilarrúbia 2022). To facilitate this task, the total abundances of the most significant pollen types are provided (Table 3.4) to be compared with past pollen assemblages for a more substantiated interpretation in terms of vegetation change. Notably, the pollen of *Pinus* and *Quercus* represents almost

Table 3.4 Total percentages of the most important pollen types across the whole sampling period (fall 2013 to fall 2015), including and excluding *Pinus* and *Quercus* (P/Q)

Pollen	Plant type	Including P/Q (%)	Excluding P/Q (%)	Excluding <i>Cannabis</i> (%)
<i>Pinus</i>	Forest tree	44.98	144.17	48.44
<i>Quercus</i> (evergreen)	Forest tree	16.00	51.28	17.23
<i>Quercus</i> (deciduous)	Forest tree	7.83	25.09	8.43
<i>Cannabis</i>	Cultivated herb	7.16	22.93	7.71
Poaceae (wild)	Herb	5.66	18.13	6.09
<i>Juniperus</i>	Shrub	3.37	10.82	3.63
<i>Plantago</i>	Herb	2.19	7.01	2.36
<i>Olea</i>	Cultivated tree	2.14	6.86	2.31
<i>Chenopodium</i>	Herb	1.58	5.06	1.70
<i>Corylus</i>	Forest tree	1.37	4.41	1.48
<i>Fraxinus</i>	Forest tree	0.78	2.50	0.84
Cerealia	Cultivated herb	0.59	1.90	0.64
<i>Alnus</i>	Forest tree	0.56	1.80	0.61
<i>Buxus</i>	Shrub	0.56	1.80	0.61
<i>Artemisia</i>	Herb	0.45	1.45	0.49
<i>Rumex</i>	Herb	0.45	1.45	0.49
<i>Castanea</i>	Cultivated tree	0.31	1.00	0.34
<i>Prunus</i> -type	Cultivated tree	0.27	0.85	0.29
<i>Fagus</i>	Forest tree	0.19	0.60	0.20
<i>Juglans</i>	Cultivated tree	0.17	0.55	0.19
<i>Abies</i>	Forest tree	0.14	0.45	0.15
<i>Urtica</i>	Herb	0.14	0.45	0.15
<i>Hedysarum</i>	Cultivated herb	0.11	0.35	0.12
<i>Mentha</i> -type	Herb	0.11	0.35	0.12
<i>Helianthemum</i>	Cultivated herb	0.09	0.30	0.10
<i>Ulmus</i>	Forest tree	0.09	0.30	0.10
<i>Erica</i>	Shrub	0.06	0.20	0.07
<i>Salix</i>	Forest tree	0.05	0.15	0.05
<i>Typha</i> *	Aquatic/ semiaquatic	1.58	5.06	1.70
Cyperaceae*	Aquatic/ semiaquatic	1.50	4.81	1.62
<i>Cladium</i> *	Aquatic/ semiaquatic	0.05	0.15	0.05

Pollen types that are important in the cores analyzed have also been included for comparison. Values excluding *Cannabis* are also shown, as downcore percentages were calculated in this way (Sect. 4.1). The percentage of excluded elements is highlighted in bold. Elements outside the pollen sum (aquatic and semiaquatic plants) are indicated by an asterisk. Raw data from Rull et al. (2017)

70% of the total assemblage, followed by *Cannabis* and wild Poaceae (5–7%) and *Juniperus*, *Plantago*, and *Olea* (2–3%). The other types are ~1% or lower. If *Pinus* and *Quercus* are removed from the pollen sum, *Cannabis* and wild Poaceae rise to 18–23% and *Juniperus*, *Plantago*, and *Olea* increase to 6–10%, whereas the less abundant types range from <1 to ~5%. Comparisons of this aggregate modern pollen assemblage with past assemblages are performed quantitatively using the squared Euclidean distance (Spencer 2013) or SED (see Chaps. 4, 5, 6).

3.3 Comparison with External Drivers of Ecological Change

An important part of the paleoecological study presented in this book is the comparison of the inferred vegetation and landscape shifts with paleoclimatic trends and past human activities—considered to be external factors with respect to the vegetation, which is the response unit—along with their eventual feedbacks and synergies, aimed at establishing potential causal relationships. In this type of study, paleoclimatic and paleoanthropogenic records should be based on proxies independent from those used for vegetation reconstruction to avoid circularity. For example, some studies developed near the Lake Montcortès region in the National Park of Aigüestortes i Estany de Sant Maurici (Fig. 1.3) have attempted to establish calibration sets to estimate paleotemperature trends from pollen records (Catalan et al. 2013; Pla and Catalan 2005). In addition to the utility of these relationships to reconstruct paleoclimatic tendencies per se, these records cannot be used to unravel the effects of climatic changes on regional vegetation, as pollen proxies cannot be used to reconstruct an external forcing factor and to analyze the vegetation response to the same forcing factor (Rull and Vegas-Vilarrúbia 2022). Ideally, pollen-independent paleoclimatic reconstructions should be based on proxies from tree-ring and speleothem records, as well as biological proxies other than pollen and spores, such as diatoms, chironomids, or molecular biomarkers (e.g. GDGTs, alkenones, δD isotopes from leaf waxes and algal lipids), among others (Castañeda and Schouten 2011; Birks et al. 2012).

In the central Pyrenees, independent high-resolution paleoclimatic reconstructions of this type have been lacking for the last 3000 years, and the longest paleotemperature records are based on tree-ring chronologies and are restricted to the last ~800 years (Dorado-Liñán et al. 2012; Büntgen et al. 2017). There is also a paleoprecipitation reconstruction of the last ~500 years based on the physical properties of Lake Montcortès sedimentary varves (Vegas-Vilarrúbia et al. 2022). In this book, the general reference for paleotemperature trends is a high-resolution reconstruction of the last 4000 years based on $\delta^{13}C$ variations in a speleothem record, which is considered to be representative of the northern Iberian Peninsula (Martín-Chivelet et al. 2011) (Fig. 3.8). The age boundaries of the corresponding climatic phases are given in Table 3.5. The other shorter paleoclimatic records are used in the part corresponding to the Modern Age and Contemporary times and will be explained in more detail in Chap. 6.

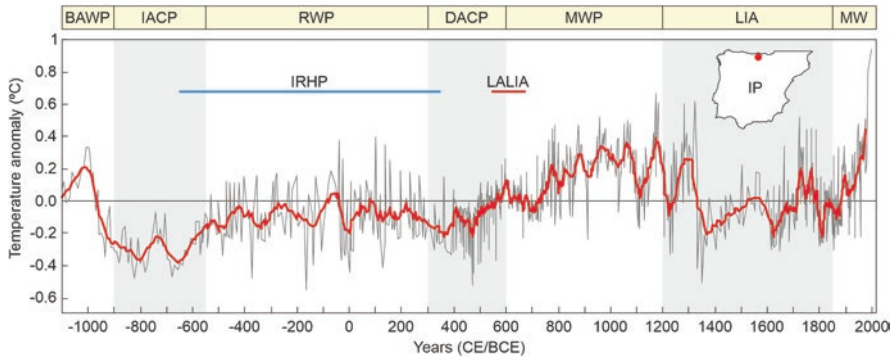


Fig. 3.8 High-resolution paleotemperature record of the last 3000 years based on $\delta^{13}\text{C}$ variations in a speleothem from the northern Iberian Peninsula (Martín-Chivelet et al. 2011). The locations of caves in which the speleothems were obtained are represented as a red dot in the contour map of the Iberian Peninsula (IP). Paleotemperature estimations are given as anomalies with respect to the last 125 years, which is the calibration interval. The thin gray line represents the raw data, and the thicker red line represents the 10-yr moving average. Raw data have been downloaded from the NOAA World Data Center for Paleoclimatology (<https://www.ncdc.noaa.gov/products/paleoclimatology>; accessed on 6 April 2022). The colder phases are highlighted by gray bands. BAWP, Bronze Age Warm Period; IACP, Ice Age Cold Period; DACP, Dark Ages Cold Period; LIA, Little Ice Age; MW, Modern Warming; MWP, Medieval Warm Period; RWP, Roman Warm Period. The Iberian-Roman Humid Period (IRHP) and the Late Antique Little Ice Age (LALIA) are based on Martín-Puertas et al. (2009) and Büntgen et al. (2016), respectively

Table 3.5 Boundaries of climatic phases according to the paleotemperature reconstruction for the northern Iberian Peninsula by Martín-Chivelet et al. (2011) (Fig. 3.8)

Climatic phase	Acronym	Age (BCE/CE)	Age (Cal yr BP)
Modern Warming	MW	1850 to present	100–0
Little Ice Age	LIA	1200–1850 CE	750–100
Medieval Warm Period/Medieval Climate Anomaly	MWP/ MCA	600–1200 CE	1350–750
Dark Ages Cold Period	DACP	300–600 CE	1650–1350
Roman Warm Period	RWP	500 BCE– 300 CE	2500–1650
Iron Age Cold Period	IACP	900–550 BCE	2850–2500
Bronze Age Warm Period	BAWP	2000–1050 BCE	3950–3000 BCE

References

- Anderson RS, Homola RL, Davis RB, Jacobson GL (1984) Fossil remains of the mycorrhizal fungal *Glomus fasciculatum* complex in postglacial lake sediments from Maine. *Can J Bot* 62:2325–2328
- Anderson PM, Bartlein JP, Brubaker LB, Gajewski K, Ritchie JC (1989) Modern analogues of late-Quaternary pollen spectra from the western interior of North America. *J Biogeogr* 16:573–596
- Bennett KD (1996) Determination of the number of zones in a biostratigraphical sequence. *New Phytol* 132:155–170

- Bennett KD, Willis KJ (2001) Pollen analysis. In: Smol JP, HJB B, Last WM (eds) Tracking environmental change using lake sediments. Vol 3: Terrestrial, algal, and siliceous indicators. Kluwer, Dordrecht, pp 5–32
- Birks HJB (1998) Numrical tools in Paleolimnology – progress, potentialities, and problems. *J Paleolimnol* 20:407–332
- Birks HJB, Birks HH (1980) Quaternary palaeoecology. E. Arnold, London
- Birks HJB, Lotter AF, Juggins S, Smol JP (2012) Tracking environmental change using lake sediments. Vol 5: Data handling and numerical techniques. Springer, Dordrecht
- Bloesch J, Burns NM (1980) A critical review of sedimentation trap technique. *Schweiz Z Hydrol* 42:15–55
- Bloesch J (1994) A review of methods used to measure sediment resuspension. *Hydrobiologia* 284:13–18
- Bolòs O, Vigo J, Masalles RM, Ninot JM (2000) Flora Manual dels Països Catalans. Pòrtic Natura, Barcelona
- Büntgen U, Myglan VS, Ljungqvist FC, McCormick M, Di Cosmo N, Sigl M et al (2016) Cooling and societal change during the Late Antique Little Ice Age from 536 to around 669 AD. *Nat Geosci* 9:231–236
- Büntgen U, Krusic PJ, Verstege A, Sangüesa-Barreda G, Wagner S, Camarero JJ et al (2017) New tree-ring evidence from the Pyrenees reveals western Mediterranean climate variability since Medieval times. *J Clim* 30:5295–5318
- Cañellas-Boltà N, Rull V, Vigo J, Mercadé A (2009) Modern pollen-vegetation relationships along an altitudinal transect in the central Pyrenees (southwestern Europe). *The Holocene* 19:1185–1200
- Carreras J, Vigo J, Ferré A (2005–2006) Manual dels hàbitats de Catalunya, vols I–VIII. Departament de Medi Ambient i Habitatge, Generalitat de Catalunya, Barcelona
- Castañeda IS, Schouten S (2011) A review of molecular organic proxies for examining modern and ancient lacustrine environments. *Quat Sci Rev* 30:2851–2891
- Catalan J, Pèlachs A, Gassiot E, Antolín F, Ballesteros A, Batalla M et al (2013) Interacción entre clima y ocupación humana en la configuración del paisaje vegetal del Parque Nacional de Aigüestortes i Estany de Sant Maurici a lo largo de los últimos 15.000 años. *Proyectos de Investigación en Parques Nacionales: 2009–2012*. Org Aut Parques Nacionales, Madrid, pp 71–92
- Clarke RC, Merlin MD (2016) *Cannabis* domestication, breeding history, present-day genetic diversity, and future prospects. *CRC Crit Rev Plant Sci* 35:293–327
- Corella JP, Amran A, Sigró J, Morellón M, Rico E, Valero-Garcés B (2011a) Recent evolution of Lake Arreo, northern Spain: influences of land use change and climate. *J Paleolimnol* 46:469–485
- Corella JP, Moreno A, Morellón M, Rull V, Giral S, Rico MT et al (2011b) Climate and human impact on a meromictic lake during the last 6,000 years (Montcortès Lake, Central Pyrenees, Spain). *J Paleolimnol* 46:351–367
- Corella JP, Brauer A, Mangili C, Rull V, Vegas-Vilarrúbia T, Morellón M et al (2012) The 1.5-ka varved record of Lake Montcortès (southern Pyrenees, NE Spain). *Quat Res* 78:323–332
- Corella JP, Benito C, Rodríguez-Lloveras X, Brauer A, Valero-Garcés BL (2014) Annually-resolved lake record of extreme hydro-meteorological events since AD 1347 in NE Iberian Peninsula. *Quat Sci Rev* 93:77–90
- Corella JP, Valero-Garcés B, Vicente-Serrano SM, Brauer A, Benito C (2016) Three millennia of heavy rainfalls in Western Mediterranean: frequency, seasonality and atmospheric drivers. *Sci Rep* 6:38206
- Court-Picon M, Buttler A, De Beaulieu J-L (2006) Modern pollen/vegetation/land use relationships in mountain environments: an example from the Champsaur valley (French Alps). *Veg Hist Archaeobotany* 15:151–168
- Dorado-Liñán I, Büntgen U, González-Rouco F, Zorita E, Montávez JP, Gómez-Navarro JJ et al (2012) Estimating 750 years of temperature variations and uncertainties in the Pyrenees by tree-ring reconstructions and climate simulations. *Clim Past* 8:919–933

- Ejarque A, Miras Y, Riera S (2011) Pollen and non-pollen palynomorph indicators of vegetation and highland grazing activities obtained from modern surface and dung datasets in the Eastern Pyrenees. *Rev Palaeobot Palynol* 167:123–139
- Faegri K, Kaland PE, Krzywinski K (1989) Textbook of pollen analysis. Wiley, Chichester
- Fleming MP, Clarke RC (1998) Physical evidence for the antiquity of *Cannabis sativa* L. *J Int Hemp Assoc* 5:80–92
- van Geel B, Buurman J, Brinkkemper O, Schelvis J, Aptroot A, van Reenen G et al (2003) Environmental reconstruction of a Roman Period settlement site in Uitgeest (The Netherlands), with especial reference to coprophilous fungi. *J Archaeol Sci* 30:873–883
- Giesecke T, Fontana SL (2008) Revisiting pollen accumulation rates from Swedish lake sediments. *The Holocene* 18:293–305
- Glew JR, Smol JP, Last WM (2001) Sediment core collection and extrusion. In: Last WM, Smol JP (eds) *Tracking environmental change using lake sediments. Vol 1: Basin analysis, coring, and chronological techniques*. Kluwer, Dordrecht, pp 73–105
- Hammer Ø, Harper DAT (2006) *Paleontological data analysis*. Blackwell, London
- Hammer Ø, Harper DAT, Ryan PD (2001) *Paleontologic statistics software for education and data analysis*. *Palaeont Electr* 4:9
- Helbig N, Vogel B, Vogel H, Fiedler F (2004) Numerical modelling of pollen dispersion on the regional scale. *Aerobiologia* 20:3–19
- Herbert AV, Harrison SP (2016) Evaluation of modern-analogue methodology for reconstructing Australian paleoclimate from pollen. *Rev Palaeobot Palynol* 226:65–77
- Huguet C, Fietz S, Moraleda N, Litt T, Heumann G, Stockhecke M, Anselmetti FS, Stur M (2012) A seasonal cycle of terrestrial inputs in Lake Van, Turkey. *Environ Sci Pollut Res* 19:3628–3635
- Jacobson GL, Bradshaw RH (1981) The selection of sites for paleovegetation studies. *Quat Res* 16:80–96
- Jankovská V, Komárek J (2000) Indicative value of *Pediastrum* and other coccal green algae in palaeoecology. *Folia Geobot* 35:59–82
- Kovach WL (1989) Comparisons of multivariate analytical techniques for use in pre-Quaternary plant paleoecology. *Rev Palaeobot Palynol* 60:255–282
- Kovach WL (1993) Multivariate techniques for biostratigraphical correlation. *J Geol Soc* 150:697–705
- Lee CM, van Geel B, Gosling WD (2022) On the use of spores of coprophilous fungi preserved in sediments to indicate past herbivore presence. *Quaternary* 5:30
- Leroy SAG, Colman SM (2001) Coring and drilling equipment and procedures for recovery of long lacustrine sequences. In: Last WM, Smol JP (eds) *Tracking environmental change using lake sediments. Vol 1: Basin analysis, coring, and chronological techniques*. Kluwer, Dordrecht, pp 107–135
- López-Vila J, Montoya E, Cañellas-Boltà N, Rull V (2014) Modern non-pollen palynomorphs sedimentation along an elevational gradient in the south-central Pyrenees (southwestern Europe) as a tool for Holocene paleoecological reconstruction. *The Holocene* 24:1757–1770
- MacDonald GM, Ritchie JC (1986) Modern pollen spectra from the western interior of Canada and the interpretation of Late Quaternary vegetation development. *New Phytol* 103:145–268
- Markgraf V, Webb RS, Anderson KH, Anderson L (2002) Modern pollen/climate calibration for southern South America. *Palaeogeogr Palaeoclimatol Palaeoecol* 181:375–397
- Martín-Chivelet J, Muñoz-García MB, Edwards L, Turrero MJ, Ortega AI (2011) Land surface temperature changes in northern Iberia since 4000 yr BP, based on $\delta^{13}\text{C}$ of speleothems. *Glob Planet Change* 77:1–12
- Martín-Puertas C, Valero-Garcés BL, Brauer A, Mata MP, Delgado-Huertas A, Dulski P (2009) The Iberian-Roman Humid Period (2600–1600 cal yr BP) in the Zóñar Lake varved record (Andalucía, southern Spain). *Quat Res* 71:108–120
- McPartland JM, Guy GW, Hegman W (2018) *Cannabis* is indigenous to Europe and cultivation began during Copper or Bronze Age: a probabilistic synthesis of fossil pollen studies. *Veg Hist Archaeobotany* 27:635–648

- Mercadé A, Vigo J, Rull V, Vegas-Vilarrúbia T, Garcés S, Lara A et al (2013) Vegetation and landscape around Lake Montcortès (Catalan pre-Pyrenees) as a tool for palaeoecological studies of Lake sediments. *Collect Bot* 32:87–101
- Mercuri AM, Accorsi CA, Bandini M (2002) The long history of *Cannabis* and its cultivation by the Romans in central Italy, shown by pollen records from Lago Albano and lago di Nemi. *Veg Hist Archaeobotany* 11:263–176
- Mieszczankin T (1997) A spacio-temporal pattern of pollen sedimentation in a dimictic lake with laminated sediments. *Water Air Soil Pollut* 99:587–592
- Mieszczankin T, Noryskiewicz B (2000) Processes that can disturb the chronostratigraphy of laminated sediments and pollen deposition. *J Paleolimnol* 23:129–140
- Montoya E, Rull V, Vegas-Vilarrúbia T, Corella JP, Giralt S, Valero-Garcés B (2018) Grazing activities in the southern Pyrenees during the last millennium as deduced from the non-pollen palynomorphs (NPP) record of Lake Montcortès. *Rev Palaeobot Palynol* 254:8–19
- Moore PD, Webb JA, Collinson ME (1991) Pollen analysis. Blackwell, Oxford
- Overpeck JT, Webb T, Prentice IC (1985) Quantitative interpretation of fossil pollen spectra: dissimilarity coefficients and the method of modern analogs. *Quat Res* 23:87–108
- Pla S, Catalan J (2005) Chrysophyte cysts from lake sediments reveal the submillennial winter/spring climate variability in the northwestern Mediterranean region throughout the Holocene. *Clim Dyn* 24:263–278
- Prentice IC (1985) Pollen representation, source area and basin size: toward a unified theory of pollen analysis. *Quat Res* 23:76–86
- Punning J-M, Terasmaa J, Koff T, Alliksaar T (2003) Seasonal fluxes of particulate matter in a small closed lake in northern Estonia. *Water Air Soil Pollut* 149:77–92
- Räsänen S (2001) Tracing and interpreting fine-scale human impact in northern Fennoscandia with the aid of modern pollen analogues. *Veg Hist Archaeobotany* 10:211–218
- Reille M (1992–98) Pollen et Spores d'Europe et d'Afrique du Nord. Laboratoire de Botanique Historique, Université d'Aix-Marseille
- Rull V (1987) A note on pollen counting in paleoecology. *Pollen Spores* 29:471–480
- Rull V (2022) Origin, early expansion, domestication and anthropogenic diffusion of *Cannabis*, with emphasis on Europe and the Iberian Peninsula. *Persp Plant Ecol Evol Syst* 55:125670
- Rull V, Vegas-Vilarrúbia T (2014) Preliminary report on a mid-19th century Cannabis pollen peak in NE Spain: historical context and potential chronological significance. *The Holocene* 24:1378–1383
- Rull V, Vegas-Vilarrúbia T (2015) Crops and weeds from the Estany de Montcortès catchment, central Pyrenees, during the last millennium: a comparison of palynological and historical records. *Veget Hist Archaeobot* 24:699–710
- Rull V, Vegas-Vilarrúbia T (2021) Conifer forest dynamics in the Iberian Pyrenees during the Middle Ages. *Forests* 12:1685
- Rull V, Vegas-Vilarrúbia T (2022) Climatic and anthropogenic drivers of forest succession in the Iberian Pyrenees during the last 500 years: a statistical approach. *Forests* 13:622
- Rull V, González-Sampériz P, Corella JP, Morellón M, Giralt S (2011) Vegetation changes in the southern Pyrenean flank during the last millennium in relation to climate and human activities: the Montcortès lacustrine record. *J Paleolimnol* 46:387–404
- Rull V, Trapote MC, Safont E, Cañellas-Boltà N, Pérez-Zanón N, Sigró J et al (2017) Seasonal patterns of pollen sedimentation in Lake Montcortès (Central Pyrenees) and potential applications to high-resolution paleoecology: a 2-year pilot study. *J Paleolimnol* 57:95–108
- Rull V, Vegas-Vilarrúbia T, Corella JP, Valero-Garcés B (2021a) Bronze Age to Medieval vegetation dynamics and landscape anthropization in the south-central Pyrenees. *Palaeogeogr Palaeoclimatol Palaeoecol* 571:110392
- Rull V, Vegas-Vilarrúbia T, Corella JP, Trapote MC, Montoya E, Valero-Garcés B (2021b) A unique Pyrenean varved record provides a detailed reconstruction of Mediterranean vegetation and land-use dynamics over the last three millennia. *Quat Sci Rev* 268:107128
- Spencer NH (2013) Essentials of Multivariate Data Analysis. CRC Press, Boca Raton

- St Jacques J-M, Cumming BF, Smol JF (2008) A statistical method for varve verification using seasonal pollen deposition. *J Paleolimnol* 40:733–744
- Tarasov PE, Nakagawa T, Demske D, Österle H, Yaeko I, Kitagawa J et al (2011) Progress in the reconstruction of Quaternary climate dynamics in the Northwest Pacific: a new modern analogue reference database and its application to the 430-kyr pollen record from Lake Biwa. *Eart-Sci Rev* 108:64–79
- Trapote MC (2019) Modern-analog studies and high-resolution paleoenvironmental reconstruction of the last 500 years using the varved sediments of the Mediterranean Lake Montcortès (Central Pyrenees). PhD diss, University of Barcelona
- Trapote MC, Vegas-Vilarrúbia T, López P, Puche E, Gomà J, Buchaca T et al (2018a) Modern sedimentary analogues and integrated monitoring to understand varve formation in the Mediterranean Lake Montcortès (Central Pyrenees, Spain). *Palaeogeogr Palaeoclimatol Palaeoecol* 496:292–304
- Trapote MC, Rull V, Giral S, Montoya E, Corella JP, Vegas-Vilarrúbia T (2018b) High-resolution (subdecadal) pollen analysis of varved sediments from Lake Montcortès (southern Pyrenean flank): a fine-tuned record of landscape dynamics and human impact during the last 500 years. *Rev Palaeobot Palynol* 259:207–222
- Vegas-Vilarrúbia T, Corella JP, Pérez-Zanón N, Buchaca T, Trapote MC, López P et al (2018) Historical shifts in oxygenation regime as recorded in the laminated sediments of lake Montcortès (Central Pyrenees) support hypoxia as a continental-scale phenomenon. *Sci Total Environ* 612:1577–1592
- Vegas-Vilarrúbia T, Rull V, Trapote MC, Cao M, Rosell-Melé A, Buchaca T et al (2020) Modern analogue approach applied to high-resolution varved sediments – a synthesis for Lake Montcortès (Central Pyrenees). *Quaternary* 3:1
- Vegas-Vilarrúbia T, Corella JP, Sigró J, Rull V, Dorado-Liñán I, Valero-Garcés B et al (2022) Regional precipitation trends since 1500 CE reconstructed from calcite sublayers of a varved Mediterranean lake record (Central Pyrenees). *Sci Total Environ* 826:153773
- Whitlock C, Larsen C (2001) Charcoal as a fire proxy. In: Last WM, Smol JP (eds) *Tracking environmental change using lake sediments. Vol 3: Terrestrial, algal, and siliceous indicators.* Kluwer, Dordrecht, pp 75–98
- Williams JW, Shuman B (2008) Obtaining accurate and precise environmental reconstructions from the modern analog technique and North American surface pollen data set. *Quat Sci Rev* 27:669–687
- Yang S, Zheng Z, Huang K, Zong Y, Wang J, Xu Q et al (2012) Modern pollen assemblages from cultivated rice fields and rice pollen morphology: application to a study of ancient land use and agriculture in the Pearl River Delta, China. *The Holocene* 22:1393–1404
- Zanon M, Davis BAS, Marquer L, Brewer S, Kaplan JO (2018) European forest cover during the past 12,000 years: a palynological reconstruction based on modern analogs and remote sensing. *Front Plant Sci* 9:253
- Zheng Z, Wei J, Huang K, Xu Q, Lu H, Tarasov P et al (2014) East Asian pollen database: modern pollen distribution and its quantitative relationship with vegetation and climate. *J Biogeogr* 41:1819–1832
- Zolitschka B, Francus P, Ojala AEK, Schimmelmann A (2015) Varves in lake sediments – a review. *Quat Sci Rev* 117:1–41



Abstract

During the warmer Late Bronze Age, regional forests were dominated by submontane and Mediterranean *Quercus* types, and the lake was surrounded by *Alnus-Corylus* gallery forests, with negligible human impact. This is the most pristine landscape recorded during the last three millennia, with a forest cover larger than at present (tree pollen >90%). Three local short-lived anthropization pulses, characterized by slash-and-burn practices by small itinerant human groups, were recorded during the Iron Age. The first event (750–640 BCE) was mainly for grazing and irreversibly removed the surrounding gallery forests, coinciding with the Iron Age Cold Period (IACP). The second pulse (340–240 BCE) was less intense and included cereal cultivation, whereas the third event occurred at the end of the Iron Age, coinciding with the onset of the Roman Warm Period. The first regional anthropization event, characterized by a significant retreat (35% and >50% less tree pollen than modern and Late Bronze times, respectively) of the dominant *Pinus* forests, began in 260 CE and peaked toward the end of the Roman epoch. Wood extraction and land opening for cereal cultivation were the most likely causes of woodland clearing. The recovery of these forests began after the fall of the Roman Empire and the transition to the Middle Ages (Migration Period) when human impact declined.

4.1 The Pollen Diagram

4.1.1 General Description

The Lake Montcortès pre-Medieval pollen diagram (Fig. 4.1) is dominated by the same trees that dominate the present regional forests, namely, evergreen *Quercus*,

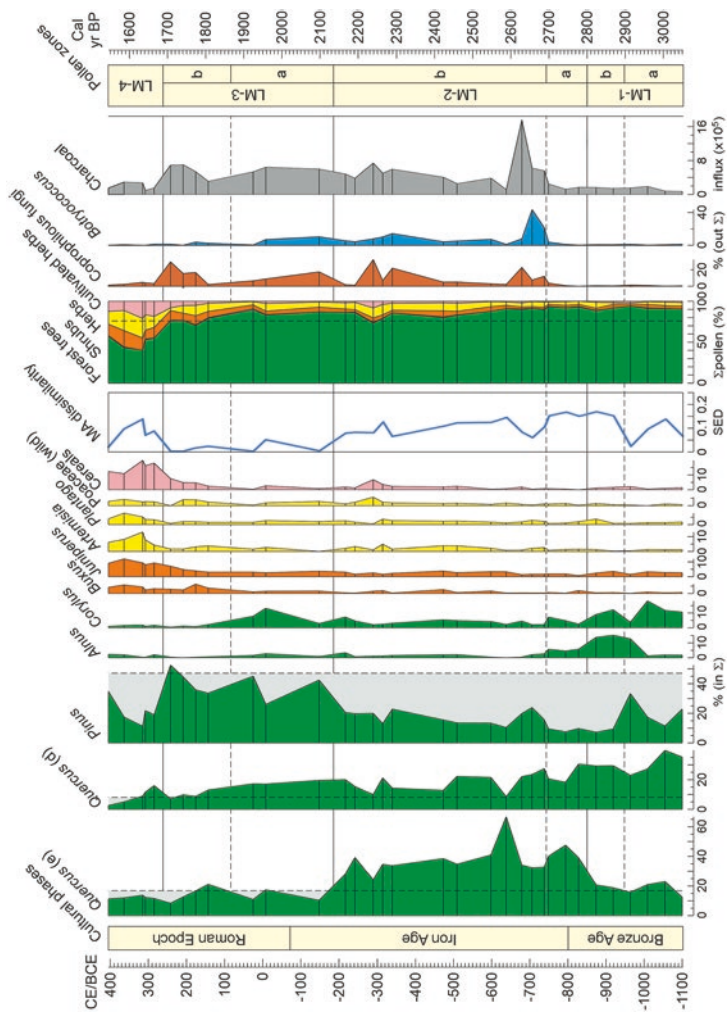


Fig. 4.1 Percentage pollen diagram of Lake Montcortès record corresponding to the pre-Medieval period, encompassing the Late Bronze Age, the Iron Age, and the Roman epoch (Σpollen, pollen sum; in Σ, outside the pollen sum). The dissimilarity between past pollen assemblages and modern analogs (MA) is represented as a blue line (SED, squared Euclidean distance). Maximum similarity between modern and past pollen assemblages is attained at SED values close to zero. Charcoal is represented in influx units (particles cm⁻² yr⁻¹). Cultural phases according to Marugan and Rapalino (2005), as explained in Chap. 2. Vertical dotted lines in the forest pollen curves and the pollen sum represent modern sedimentation percentages, excluding *Camnabitis*. In the forest pollen curves, values below these percentages are highlighted by gray bands

deciduous *Quercus*, and *Pinus* (Chap. 3; Sect. 4.2). However, these taxa show significant variations in their relative abundance. Major shifts are the change in the dominance of evergreen *Quercus* in favor of *Pinus* at the end of the Iron Age and the general decrease in all regional forest trees at the end of the Roman epoch. Other less abundant trees that show significant changes are *Alnus* and *Corylus*, which are relatively abundant only at the base of the diagram. Cultivated trees are very scarce (*Olea*, *Castanea*). Shrub and herb representatives are scarce throughout the diagram, except in the uppermost part (Late Roman epoch), where they show a general increase coinciding with the general forest decrease. The absence of *Cannabis* is also significant compared with Medieval and post-Medieval pollen diagrams (Chaps. 5 and 6). Another relevant feature is the synchronous increase in proxies for human activities, notably coprophilous fungi and charcoal in the Early Iron Age, and their conspicuous decline in the Late Roman period. The most abundant algae remain (*Botryococcus*) show a similar pattern, with the exception of the Roman epoch, when this alga almost disappears.

4.1.2 Zonation

The diagram has been subdivided into four significant pollen zones that are described in detail below (ages are between-sample interpolations).

4.1.2.1 Zone LM-1 (1100–851 BCE; 3050–2801 cal yr BP; Late Bronze)

This zone is dominated by deciduous *Quercus*, followed by evergreen *Quercus* and *Pinus*. Compared with modern pollen sedimentation, deciduous *Quercus* is much more abundant, evergreen *Quercus* shows similar values, and *Pinus* is significantly lower. Total forest-tree pollen is more abundant than at present. Also important are *Alnus* and *Corylus*, whereas other trees, shrubs, and herbs are very scarce, similar to the elements outside the pollen sum. Changes in some major elements allow subdivision into two subzones (a and b) with a boundary at 2892 cal yr BP (942 BCE). This boundary is characterized primarily by a significant decrease in *Pinus* and an increase in *Alnus*. Overall, pollen assemblages show a significant departure from modern analogs, except for some samples just below the a/b boundary, which were more similar to modern assemblages.

4.1.2.2 Zone LM-2 (851–183 BCE; 2801–2133 cal yr BP; Late Bronze-Late Iron)

A shift toward the dominance of evergreen *Quercus* (with values considerably higher than in modern samples) characterizes this pollen zone, in which deciduous *Quercus* and *Pinus* become subdominant. While deciduous *Quercus* remains at similar values throughout the pollen zone, evergreen *Quercus* experiences a gradual decrease accompanied by a progressive maintained *Pinus* increase, although the pollen of this tree remains at lower values in comparison to modern ones. Again, it is possible to split this zone into two subzones (LM2-a and LM2-b), with a boundary at 2694 cal yr BP (744 BCE), on the basis of changes in subdominant pollen types, notably *Pinus*, which experiences an increase, and the *Alnus*–*Corylus*

association, which is conspicuously reduced, especially *Alnus*. This is a zone of increasing modern-analog similarity, with a trend similar to that of evergreen *Quercus* and inverse to that of the *Pinus* curve.

The LM-2a/b boundary is also the onset of a slow minor forest-tree pollen decline that culminates at 2239 cal yr BP (289 BCE), with values similar to present, coinciding with a gentle increase in grasses, especially cereals. The most relevant difference between subzones a and b is in the elements outside the pollen sum, primarily the coprophilous fungi, *Botryococcus* and charcoal, which remain similar to pollen zone LM-1 in the LM-2a subzone but undergo a significant local increase at the beginning of subzone LM-2b, peaking at 2629 cal yr BP (679 BCE) and quickly decreasing further. From this point onward, a slow increase in coprophilous fungi and charcoal takes place with a second local peak coinciding with the already mentioned tree-pollen local minimum (2239 Cal yr BP; 289 BCE) and a further rapid decrease at the top of the zone.

4.1.2.3 Zone LM-3 (183 BCE-263 CE; 2133–1687 cal yr BP; Late Iron-Late Roman)

This zone represents a large change in the forest-tree pollen assemblages, as reflected in a meaningful dominance shift from evergreen *Quercus* to *Pinus*, with deciduous *Quercus* percentages remaining at values similar to those of zone LM-2. For the first time, *Pinus* and evergreen *Quercus* attain values similar to the present. The other elements of the pollen sum also remain at percentages similar to LM-2, except *Corylus*, which increases to values similar to LM-1 and decreases again. In this case, the definition of two subzones is based on the relative abundances of minor pollen taxa before and after 1886 cal yr BP (84 CE). The lower zone (LM-3a) is marked by the abovementioned increase in *Corylus*, whereas the upper zone (LM-3b) is characterized by the decrease in this tree and synchronous increases in shrubs and herbs, notably cereals. The total forest-tree pollen also decreases toward the top of the zone, reaching values similar to the present, which is mainly due to evergreen and deciduous *Quercus* decreasing as *Pinus* increases. Overall, the pollen assemblages of this zone are the most similar to the modern assemblage, with distances close to zero. Coprophilous fungi and charcoal increase in LM-3a and decrease near the LM-3a/b boundary to increase again and peak near the top of the zone, coinciding with the abovementioned increase in herbs/shrubs and the decline in forest trees. *Botryococcus* decreases near the a/b boundary and then almost disappears from the record.

4.1.2.4 Zone LM-4 (263–405 CE; 1687–1545 cal yr BP; Late Roman)

The decline in forest trees initiated at the top of LM-3 continues, but this time it was due to a significant *Pinus* decline to values significantly lower than at present, coeval with a maintained increase in shrubs and herbs, especially *Juniperus*, *Artemisia*, and cereals. The minimum forest-tree values occur at 1635 cal yr BP (315 CE) and are considerably lower than at present. The dissimilarity between past and modern pollen assemblages experiences a relevant increase in this zone. Coprophilous fungi do not recover from the decline experienced at the top of the former zone, and charcoal shows a minor increase in values lower than before.

4.2 Vegetation and Landscape Dynamics

Based on this pollen zonation, the dynamics of vegetation and landscape in the Lake Montcortès region can be reconstructed as follows using a cultural framework. Ages are rounded to tens, as the average resolution of the Lake Montcortès record is bidecadal (Table 3.1):

4.2.1 Late Bronze Age

Between 1100 and 850 BCE (Zone LM-1), regional vegetation was dominated by submontane *Quercus* forests, followed by Mediterranean *Quercus* forests and montane *Pinus* forests. This contrasts with modern pollen sedimentation, in which *Pinus* is always more abundant than *Quercus*, suggesting that during the Late Bronze Age, submontane and Mediterranean *Quercus* forests were more extensive than present-day coniferous forests. The Montcortès region was more forested than today, as indicated by overall regional forest percentages, which were higher than modern values (Fig. 4.1). The *Alnus–Corylus* association does not occur today in the lake catchment (Mercadé et al. 2013) or regional vegetation (Table 1.1), although the pollen of these two taxa is present in the modern pollen deposition with abundances of ~2% (*Alnus*) and ~4% (*Corylus*), excluding *Pinus* and *Quercus* pollen types (Table 3.4). If *Pinus* and *Quercus* are included and *Cannabis* is excluded, the percentages of *Alnus* and *Corylus* in modern sediments decrease to ~0.5% and ~1.5%, respectively, which is 10–15 times less than the average Late-Bronze abundance (Fig. 4.1). This strongly suggests that *Alnus* and *Corylus* parent species were much more abundant around Lake Montcortès during the Late Bronze Age than they are today.

The most likely scenario is that the lake was surrounded by *Alnus–Corylus* gallery forests, and the pollen assemblage of this association was sedimented locally from the small lake catchment (Fig. 4.2). This would be supported by present-day vegetation studies that have identified an association known as *Alnetum catalaunicum* (a variant of the *Alnetum glutinosae*), which is dominated by *Alnus jorullensis* and *Corylus avellana* and is the most common gallery forest of the central Pyrennes occurring along rivers and around lakes above 600–800 m elevation (Folch et al. 1984; Loidi 2017). Therefore, it is likely that during the Late Bronze Age, Lake Montcortès was surrounded by *Alnus–Corylus* gallery forests. The scarcity of shrub and herb representatives suggests that the lake catchment was mostly forested. The indicators of agriculture and grazing (cereals, coprophilous fungi) were negligible, and the low charcoal values indicate reduced fire incidence. The whole picture suggests a totally forested landscape with a greater forest cover than today and with very little or no human impact.

Based on archaeological findings, megalithic structures were in decline in the area, and human populations were limited to small nomadic pastoralist groups who lived either in caves or seasonal outdoor settlements (Cots 2005). Within the Montcortès catchment, there is no evidence of human settlements dating to the Late

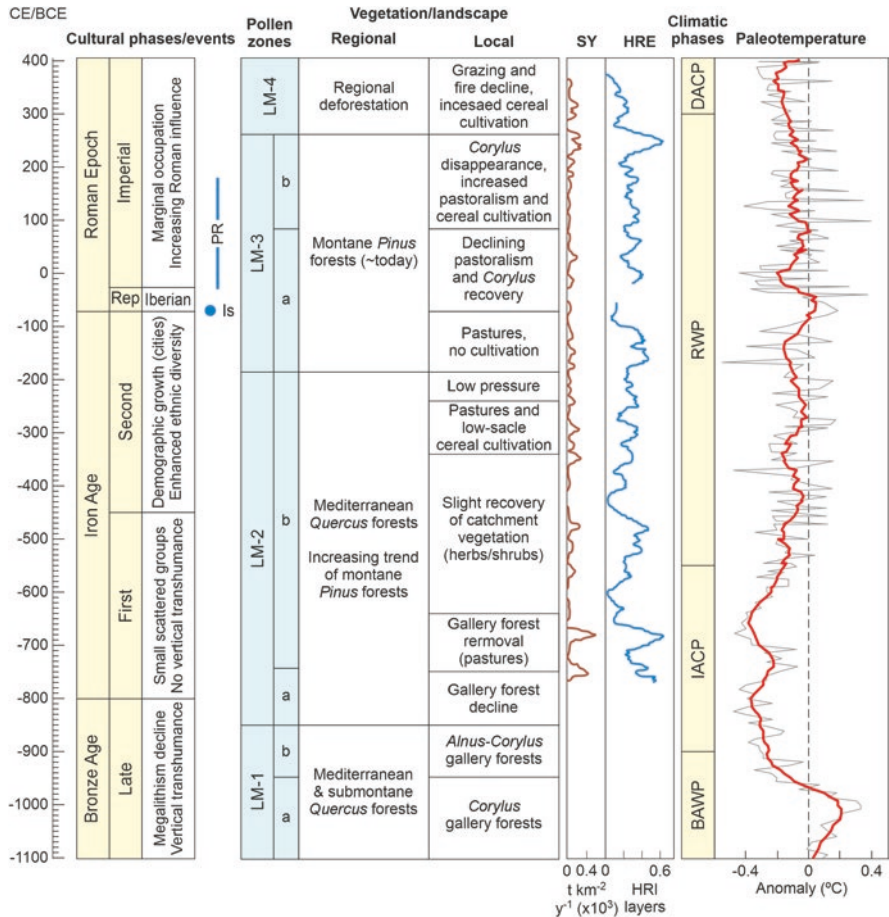


Fig. 4.2 Pollen zones (in blue) and vegetation reconstruction in relation to cultural history and climatic phases (in yellow) during the pre-Medieval interval of the Lake Montcotès record. Historical and cultural phases according to Marugan and Rapalino (2005), as explained in Chap. 2 (Rep, Republican period; PR, Pax Romana; Is, Foundation of Isona). Sediment yield (SY) in thousand tons per square km per year ($t\ km^{-2}\ yr^{-1} \times 10^3$); heavy rainfall events (HRE) in heavy rainfall-induced (HRI) layer occurrence (31-y running average) (Corella et al. 2016, 2019). Climatic phases and paleotemperature reconstruction according to Martín-Chivelet et al. (2011) for the northern Iberian Peninsula (see Fig. 3.7 for reference). The thin gray line represents the raw data, and the thicker red line represents the 10-yr moving average. DACP, Dark Ages cold period; IACP, Iron Age cold period; RWP, Roman warm period; BAWP, Bronze Age warm period

Bronze Age, which aligns with the presence of mostly undisturbed gallery forests, as previously mentioned. The Late Bronze Age lacks clear biogenic/endogenic layering and was dated by estimating sedimentation rates, making the annual nature of these layers uncertain. Nevertheless, the prevalence of organic layers and the scarcity of detrital layers suggest reduced sediment input from the watershed, which is expected in a forested landscape (Rull et al. 2021). During the Late Bronze Age, the

climate was warmer than it is today, as shown in Fig. 4.2, which may have favored the dominance of Mediterranean and submontane *Quercus* forests that typically occur at lower elevations than montane pine forests, as noted by Mercadé et al. (2013). This implies that the distribution of forested areas would have shifted slightly upward compared to the current elevational patterns.

Because there is a lack of older sediment samples in this study, it is premature to determine whether the fully forested landscape of Montcortès during the Late Bronze Age was natural or the result of a recovery from previous human disturbances. It would be particularly interesting to investigate the potential influence of the human groups responsible for constructing the Early Bronze megaliths in the Montcortès landscape (see Fig. 4.3). Additional coring efforts are necessary to explore these ideas further. Another intriguing area for research is the absence of biogenic laminations. The fact that the Late Bronze Age laminations lack the calcite layer typical of Lake Montcortès laminations (as discussed in Chap. 1, Sect. 5) suggests a nonbiogenic origin. One possible explanation is that the accumulation of organic matter may have altered the pH of deep anoxic waters, thereby preventing the preservation of the calcite layer through carbonate dissolution (Corella et al. 2011).

The *Alnus–Corylus* gallery forests were especially well developed between 3050 and 2890 cal yr BP (1100–940 BCE) (subzone LM-1b), whereas before those dates, these forests were dominated by *Corylus* alone (subzone LM-1a). The shift from local *Corylus* to *Alnus–Corylus* gallery forests coincided with a reduction in *Pinus* in regional forests and a significant increase in similarity between regional vegetation with respect to modern patterns (Fig. 4.2). *Quercus* species remained at similar values, which complicates the explanation of this event in climatic terms, although it was coeval with a general cooling that characterized the transition from the Bronze

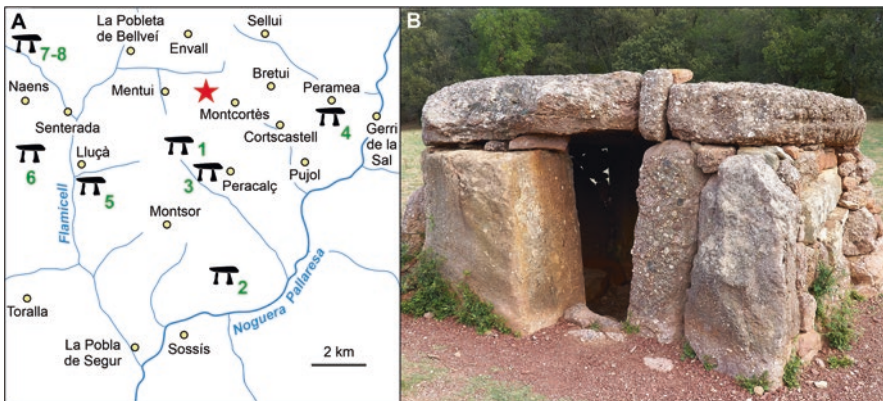


Fig. 4.3 Late Bronze dolmens (black icons, red numbers) around Lake Montcortès (red star). (a) Location sketch map (see Figs. 1.3 and 2.4 for reference). Blue lines are rivers, and yellow dots represent towns and villages. Dolmens: 1, Perauba; 2, La Llosana; 3, Castellars d'en Pey; 4, La Mosquera; 5, Moro de Reguard; 6, Moros de Cèrvoles; 7, Pinyana; 8, Mas Pallarès. After Clop and Faura (1995). (b) The dolmen of La Mosquera (4). Photo: V. Rull

Age warming period (BAWP) to the Iron Age cool period (IACP). Indicators of human activities did not experience changes that could explain the forest change, and archaeological evidence does not show any significant change that could be related to the forest change. The last 50 years of the Late Bronze Age, from 850 to 800 BCE (2800–2750 cal yr BP), corresponded to pollen zone LM-2, characterized by the dominance of Mediterranean *Quercus* forests, and will be interpreted in the next section. The transition between the Bronze Age and the Iron Age was the time of maximum dissimilarity between past and present vegetation of the entire pre-Medieval record (Fig. 4.1).

4.2.2 Iron Age

Regional forests were dominated by Mediterranean evergreen oak forests during the whole Iron Age (zone LM-2), except for the last ~100 years (2130–2020 cal yr BP; 180 BCE–70 CE), when montane pine forests initiated an increase that remained during most of the Roman epoch (zone LM-3) (Fig. 4.1). Overall, the region was still more forested than it is today. The *Alnus–Corylus* gallery forests around the lake underwent a significant reduction—coinciding with a slight increase in grazing (coprophilous fungi) and fire (charcoal) proxies—and suddenly declined when these human activities significantly increased at approximately 2700 cal yr BP (750 BCE). This date represented the anthropization of the Lake Montcortès catchment (Fig. 4.2), characterized by the removal of the *Alnus–Corylus* gallery forests (likely by fire), which was paralleled by a reduction in evergreen oak forests, probably by local deforestation of this type of forest surrounding the lake (Chap. 1; Sect. 4). During this first anthropization pulse, the regional vegetation experienced a transient increase in similarity with the present vegetation. The lake catchment was likely used mainly for grazing, as no evident signs of cultivation were recorded. The synchronous increase in freshwater algae (*Botryococcus*) could be interpreted as an increase in nutrient leaching to the lake as a consequence of local deforestation leading to an increase in catchment runoff. This possibility is supported by a conspicuous increase in sediment yield to the lake, estimated from independent proxies related to physical properties of sedimentary varves, specifically the thickness of detrital layers (Chap. 3; Sect. 5) in relation to the lake depositional area (Corella et al. 2019).

This first pulse of anthropogenic disturbance ended at 2590 cal yr BP (640 BCE) and may be interpreted as a temporary establishment of human populations that remained in the lake catchment until the vegetation cover was significantly reduced by intensive grazing. Indeed, archaeological evidence points toward the occurrence of small scattered groups living in caves or outdoor settlements, for which pastoralism was the main activity (Cots 2005). This 100-yr anthropization pulse took place during the IACP cooling, which might suggest that the Lake Montcortès watershed could have acted as a temporary refuge for small itinerant groups when climatic conditions were unsuitable to develop their usual pastoralist practices at higher elevations. This could help explain the restricted or nonexistent transhumant practices

between lowlands and highlands, which were typical of former Late-Bronze times when climates were warmer and, hence, highlands were more livable.

After the first anthropization pulse, the oak forests recovered, and the grazing, burning, and eutrophication proxies significantly decreased. However, shortly thereafter, a progressive and maintained decline in Mediterranean oak forests began, coinciding with a similar gradual increasing trend in montane pine forests. This was coeval with a slight recovery of catchment vegetation—notably shrubs and herbs, as the *Alnus–Corylus* gallery forests did not recover—and small-scale cereal cultivation, which culminated in a new century-scale phase of intensive grazing and burning practices (2290–2190 cal yr BP; 340–240 BCE), although the fire peak was lower than that in the first anthropogenic pulse. This time, however, lake waters were not eutrophicated, as indicated by the absence of algae peaks, possibly because of the increasing vegetation cover around the lake. The lack of increases in sediment yield would support this view. The gentle recovery of catchment vegetation coincided with a warming trend from the IACP to the Roman warm period (RWP), whereas the second anthropogenic pulse occurred during the stabilization of the RWP at higher temperatures, which was accompanied by similar trends in grazing and burning practices. This suggests that both climate and anthropogenic drivers contributed to the shaping of Iron Age landscapes. It is possible that warmer climates would have favored the upward migration of lowland colonizers and the development of human settlements close to the lake. After a short decline in human activities by 2200 cal yr BP (250 BCE), grazing and fire indicators increased again at the end of the Iron Age, whereas catchment herbs and local cereal cultivation almost disappeared. This occurred in the context of the dominance of maximum RWP temperatures, reinforcing the possibility of a synergistic climatic-anthropogenic forcing, as mentioned before.

It is important to bear in mind that anthropogenic pressure during the Iron Age was restricted to the small lake watershed and was likely due to the sporadic presence of pastoral nomadic groups with intermittent settlements. In this sense, it should be emphasized that the irreversible anthropization of the Lake Montcortès catchment, as manifested in the removal of the Late Bronze gallery forests, actually occurred in the Early Iron Age but the regional landscape anthropization took place later, as we will see in the following section. Therefore, in the study of spatiotemporal anthropization patterns, it is important to distinguish between local and regional contexts. From a local perspective, the direct evidence of Iron Age anthropization of the Lake Montcortès catchment reported here contrasts with previous interpretations based on indirect sedimentological evidence, which situated the onset of significant human disturbance around the lake in Medieval times (Corella et al. 2019). Similarly, Cots (2005) used archaeological findings to propose that human influence on the lake surroundings remained minimal until Roman times. On a broader scale, recent assessments of the central Pyrenees region have indicated that changes to the landscape due to human activity were predominantly observed during the Middle Ages and displayed little spatial variation (González-Sampéris et al. 2017, 2019). However, the situation in Montcortès presents a distinct scenario, which is not considered an anomaly but rather suggests the presence of spatial and temporal

gradients in Pyrenean human influence, as discussed in Chap. 5, Sect. 4.3 (Rull and Vegas-Vilarrúbia 2021).

It is also noteworthy that the anthropization of the Lake Montcortès landscape coincided chronologically with the onset of varves of biogenic/endogenic origin, characterized by the occurrence of a light calcite layer, which was absent in former laminations (Chap. 3; Sect. 1.2). It is possible that increased human-induced runoff may have led to a higher influx of carbonate and nutrients, resulting in greater productivity in the upper water layer of the lake during specific seasons when it stratifies. This, in turn, could have caused the formation of a sedimentary layer made of calcite. This phenomenon has also been observed in other karstic lakes in the Iberian region that exhibit similar patterns of annual layer deposition.

It has been suggested that the beginning of the formation of these annual layers coincided with a change in the lake water level. The lake would have transitioned from a shallower body with a carbonate platform and associated wetland environments to a deeper lake with a well-established oxygen-depleted lower layer. This idea is supported by the presence of layers rich in diatoms and organic material, indicating high primary productivity and good preservation potential in the deeper parts of the lake. In this context, the increased presence of *Botryococcus*, as recorded in our study during the early Iron Age, could be attributed to a combination of factors, including disturbances in the lake surroundings and the deepening of the lake itself.

4.2.3 Roman Epoch

Montane *Pinus* forests dominated the Lake Montcortès regional vegetation between 70 BCE and 260 CE (2020 to 1690 cal yr BP), whereas submontane and Mediterranean *Quercus* forests played a secondary role. This was the first time that forest-tree abundances were similar to today and occurred during a maintained temperature decline between the RWP maximum and the beginning of the Dark Ages Cold Period (DACP), which could have fostered a downward displacement of elevational vegetation belts at elevations similar to the present day. Not only forests but also the overall local and regional vegetation were similar to present-day patterns, as indicated by dissimilarity values close to zero during this phase (Fig. 4.2). Changes in catchment vegetation and anthropogenic pressure allowed the subdivision of this interval into two main phases.

The first phase (subzone LM-3a; 70 BCE–80 CE; 2020–1890 cal yr BP) was characterized by impoverished vegetation, an increase in *Corylus* stands and decreasing human activity, as manifested in the decline in grazing and fire practices, with respect to the ending Iron Age interval. The *Corylus* increase could be due to a slight and temporary recovery of local gallery forests, possibly favored by humans, as the fruits of this tree (hazelnuts) were well appreciated by Roman people, who actively collected them in the wild at wet sites (Peña-Chocarro et al. 2019). During this phase, a significant temperature decline took place, which might have promoted the displacement of human populations to southern lowlands, thus reducing the

anthropogenic pressure on Lake Montcortès landscapes. As mentioned in Chap. 2 (Sect. 3), historical documentation suggests a marginal occupation of the Pallars region by Romans during this phase, compared to later times. Indeed, during the Republican period of the Roman Empire, local Iberian cultures still predominated in the Pallars region, and the urban development characteristic of this historical phase was concentrated in the southern lowlands where the city of *Aeso* (now Isona; Fig. 2.4) was founded (Cots 2005).

The second phase (subzone LM-3b; 80–260 CE; 1890–1690 cal yr BP) was characterized by a significant reduction in *Corylus* stands and increasing shrubby and herbaceous vegetation cover, along with enhanced grazing and fire practices, especially toward the end of this interval. The increase in cereal cultivation was especially noteworthy, as this activity had been almost absent from the lake surroundings for ~500 years (Middle–Late Iron Age). Climatically, this phase occurred during the abovementioned maintained temperature decline characteristic of the second part of the RWP. However, temperatures were higher than in the first phase, which could have favored human occupation of the lake surroundings. Historical information also supports increasing human influence during this phase (Chap. 2; Sect. 3). The transition from the first to the second phase occurred during the interval known as *Pax Romana* (~30 BCE to 180 CE) (Parchami 2009), which was also the transition between the Republican and the Imperial period, characterized by enhanced political stability, economic prosperity, and imperial expansion—which makes the term “pax” somewhat puzzling (Goffart 1989). In the Pallars region, this transition represented an increase in both the human population and the influence of Roman culture, leading to an increase and diversification of land-use practices, which is consistent with the paleoecological trends presented here.

The dominance of regional *Pinus* forests was disrupted in 260 CE (1690 cal yr BP) by a general and significant retreat of regional forests peaking at 310 CE (1640 cal yr BP), when pollen from regional forests was significantly lower than it is today. This was the first regional deforestation event documented in the Lake Montcortès record since the Late Bronze Age and affected mainly the montane (*Pinus*) and, to a lesser extent, the submontane (deciduous *Quercus*) forests. The Mediterranean *Quercus* woodlands were not affected by this forest-clearing event. It is also noteworthy that *Pinus* forests experienced recovery after the maximum deforestation values, whereas deciduous *Quercus* maintained a decreasing trend. The general forest decline coincided with maxima in all shrubs and herbs, especially cereals, which suggests that humans were involved in the major forest retreat. The abrupt decline in grazing indicates that landscape opening was made for cereal cultivation rather than for grazing purposes. The manifest decline in fire incidence also indicates that this was not the main deforestation agent, which suggests that forests were cut down rather than burned, a common Roman practice when wood extraction was the main purpose of forest exploitation (Veal 2017). In this way, both cereals for human consumption and wood for construction purposes could have been obtained.

This first deforestation event occurred at the beginning of the DACP cooling, and temperature trends showed a striking similarity with forest trends. It is possible that

wood, or its derived charcoal, was also used as fuel for heating, whose demand would have increased following cooling trends. The general forest clearing was accompanied by small nonsignificant increases in sediment yield to the lake, probably because the lake catchment was protected from erosion by the regrowth of shrubs such as *Juniperus* and *Buxus*, which are secondary colonizers of deforested areas and abandoned terrains (Carreras et al. 2005–2006).

Pinus recovery occurred at the beginning of the European Migration Period (Chap. 2; Sect. 4) and will be discussed in more detail in the following chapter, but some preliminary estimates are already possible, which will be useful to compare this deforestation event with further episodes of the same type that occurred in the Middle Ages and the Modern Age (Chaps. 5 and 6). In this case, the intensity of Roman deforestation, as measured in terms of pollen percentage, was >45% lower than at the beginning of the Roman period, >35% lower than the present values (Fig. 4.4), and >50% lower than the Bronze Age values (Fig. 4.1) when the region was totally forested. Regarding rates, linear regression estimates of forest clearing were $-0.15\% \text{ yr}^{-1}$ ($r = -0.905$; $\alpha < 0.01$), while forest recovery proceeded at $0.18\% \text{ yr}^{-1}$ ($r = 0.969$; $\alpha < 0.01$).

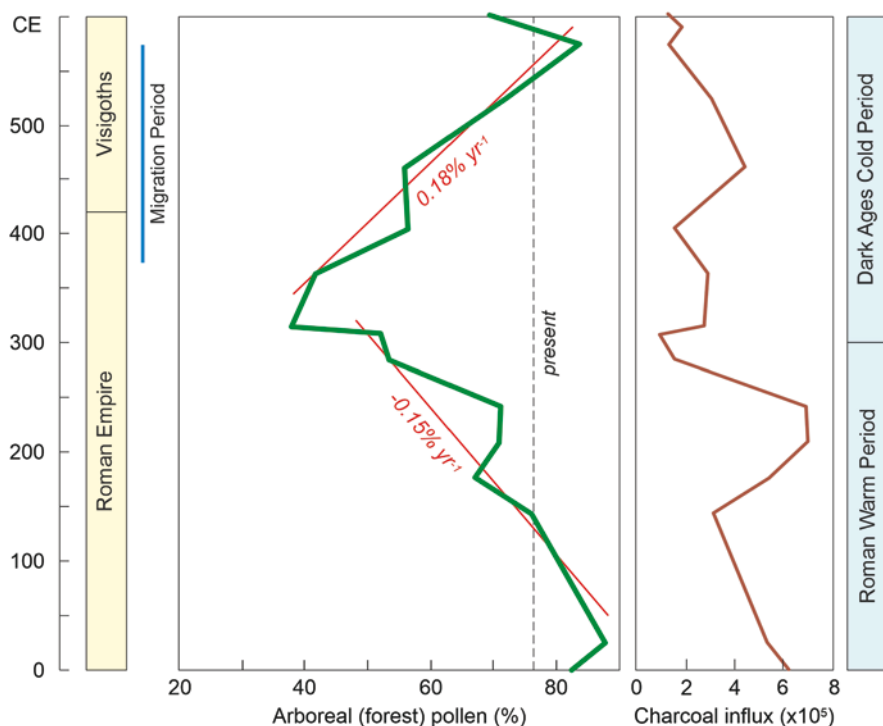


Fig. 4.4 Roman deforestation and subsequent forest recovery as expressed by the pollen curve corresponding to forest trees (green line). Rates of change are indicated by (red) regression lines and their corresponding slopes. The present values of total forest trees are indicated by a vertical dotted line

References

- Carreras J, Vigo J, Ferré A (2005–2006) Manual dels hàbitats de Catalunya, vols I–VIII. Departament de Medi Ambient i Habitatge, Generalitat de Catalunya, Barcelona
- Clop X, Faura JM (1995) La Cabana de Perauba (Peracalç, Pallars Sobirà) i el megalitisme al Pallars. *Rev Arqueol Ponent* 5:127–142
- Corella JP, Amran A, Sigró J, Morellón M, Rico E, Valero-Garcés B (2011) Recent evolution of Lake Arreo, northern Spain: influences of land use change and climate. *J Paleolimnol* 46:469–485
- Corella JP, Valero-Garcés B, Vicente-Serrano SM, Brauer A, Benito C (2016) Three millennia of heavy rainfalls in Western Mediterranean: frequency, seasonality and atmospheric drivers. *Sci Rep* 6:38206
- Corella JP, Benito G, Wilhelm B, Montoya E, Rull V, Vegas-Vilarrúbia T et al (2019) A millennium-long perspective of flood-related seasonal sediment yield in Mediterranean watersheds. *Glob Planet Change* 177:127–140
- Cots P (2005) Els pobles de la prehistòria i l'antiguitat. In: Marugan CM, Rapalino V (eds) *Història del Pallars. Dels Orígens als Nostres Dies*. Pagés Ed, Lleida, pp 13–43
- Folch R, Franquesa E, Camarasa JM (1984) *Història Natural dels Països Catalans*. Vol 7: Vegetació. Enciclopèdia Catalana, Barcelona
- Goffart W (1989) *Rome's fall and after*. Hambledon Press, London
- González-Sampéris P, Aranbarri J, Pérez-Sanz A, Gil-Romera G, Moreno A, Leunda M et al (2017) Environmental and climate change in the southern Central Pyrenees since the Last Glacial Maximum: a review from the lake records. *Catena* 149:668–688
- González-Sampéris P, Montes L, Aranbarri J, Leunda M, Domingo R, Laborda R et al (2019) Escenarios, tiempo e indicadores paleoambientales para la identificación del Antropoceno en el paisaje vegetal del Pirineo Central (NE Iberia). *Cuad Invest Geogr* 45:167–193
- Loidi J (2017) *The Vegetation of the Iberian Peninsula*. Springer, Cham
- Martín-Chivelet J, Muñoz-García MB, Edwards L, Turrero MJ, Ortega AI (2011) Land surface temperature changes in northern Iberia since 4000 yr BP, based on $\delta^{13}\text{C}$ of speleothems. *Glob Planet Change* 77:1–12
- Marugan CM, Rapalino V (2005) *Història del Pallars. Dels Orígens als Nostres Dies*. Pagés Ed, Lleida
- Mercadé A, Vigo J, Rull V, Vegas-Vilarrúbia T, Garcés S, Lara A et al (2013) Vegetation and landscape around Lake Montcortès (Catalan pre-Pyrenees) as a tool for palaeoecological studies of Lake sediments. *Collect Bot* 32:87–101
- Parchami A (2009) *Hegemonic Peace and Empire. The Pax Romana, Britannica, and Americana*. Routledge, London
- Peña-Chocarro L, Pérez-Jordà G, Alonso N, Antolín F, Teira-Brión A, Tereso JP et al (2019) Roman and medieval crops in the Iberian Peninsula: a first overview of seeds and fruits from archaeological sites. *Quant Int* 499:49–66
- Rull V, Vegas-Vilarrúbia T (2021) A spatiotemporal gradient in the anthropization of Pyrenean landscapes. Preliminary report. *Quat Sci Rev* 258:106909
- Rull V, Vegas-Vilarrúbia T, Corella JP, Trapote MC, Montoya E, Valero-Garcés B (2021) A unique Pyrenean varved record provides a detailed reconstruction of Mediterranean vegetation and land-use dynamics over the last three millennia. *Quat Sci Rev* 268:107128
- Veal R (2017) The politics and economics of ancient forests: timber and fuel as levers of Greco-Roman control. In: Derron P (ed) *Economie et Inégalité: Ressources, Échanges et Pouvoir dans l'Antiquité Classique*. Hardt Foundation, Geneva, pp 317–367



Abstract

The forest recovery of the Migration Period (376–568 CE) ended in the Visigothic epoch, when a long-term deforestation trend lasting ~4 centuries started, reaching minimum forest cover values (>50% and almost 70% less tree pollen than modern and Late Bronze values, respectively) at the beginning of Pallars independence in the tenth century. Cereal cultivation was still the main activity, but grazing and hemp cultivation for domestic purposes were increasing. The MCA (Medieval Climate Anomaly) warming could have contributed to an upward shift in vegetation belts, as manifested in the regional decrease in montane conifer forests and pastures, which may have migrated to higher elevations. Forest opening remained fairly stable (30–40% tree pollen) during most of the Pallars County phase; when wood/charcoal extraction increased, slash-and-burn practices decreased, and cultivation and grazing continued. The prolonged MCA warmer climates may have favored the decline of montane and submontane forests, which were replaced by lower-elevation Mediterranean forests. A significant expansion of lowland olive groves was recorded since 1290 CE, probably linked to the downslope migration of human populations fostered by the onset of the Little Ice Age (LIA) cold reversal. Forest recovery started by 1350 CE due to the substantial depopulation of the Pallars region as a consequence of the ending Medieval crisis.

5.1 The Pollen Diagram

5.1.1 General Description

The Medieval diagram (Fig. 5.1) shows important changes with respect to former times. Forest trees dominate the lower half of the diagram but are significantly reduced (especially *Pinus*) in the upper half, where herbs (*Artemisia*, *Plantago*, and

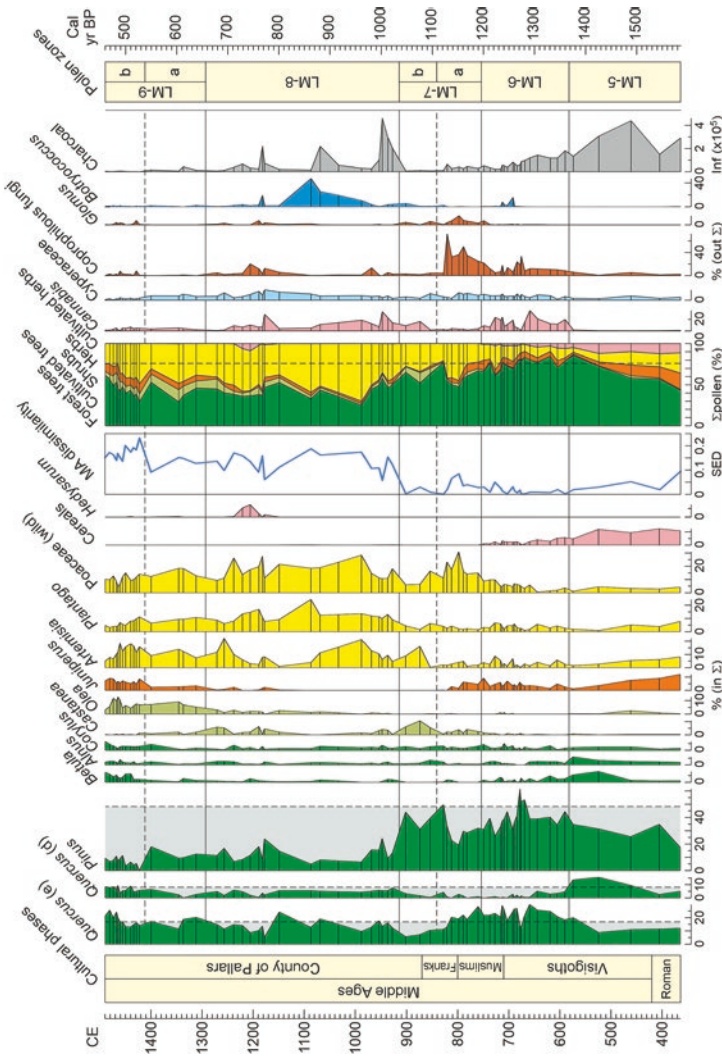


Fig. 5.1 Percentage pollen diagram of Lake Montcortès record corresponding to the Middle Ages. (Σ pollen, pollen sum; in Σ , inside the pollen sum; out Σ , outside the pollen sum). The dissimilarity between past pollen assemblages and modern analogs (MA) is represented as a blue line (SED, squared Euclidean distance). Maximum similarity between modern and past pollen assemblages is attained at SED values close to zero. Charcoal is represented in influx units (Inf; particles $\text{cm}^{-2} \text{yr}^{-1}$); note that this scale (0–40) is four times smaller than the pre-Medieval scale (0–160) (Fig. 4.1). Cultural phases according to Mangano and Rapalino (2005), as explained in Chap. 2. Vertical dotted lines in the forest pollen curves and the pollen sum represent modern sedimentation percentages, excluding *Cannabis*. In the forest pollen curves, values below these percentages are highlighted by gray bands

wild Poaceae) take the lead. The reduction in *Pinus* is sudden and drastic, reaching percentages below half of modern values. This change takes place near the beginning of the Pallars County phase and represents a sudden increase in the dissimilarity between past and modern pollen assemblages. The only important shrub in the diagram is *Juniperus*, which appears at the base and the top of the diagram and is absent in the central interval. Another novelty with respect to pre-Medieval times (Chap. 4) is the appearance of cultivated trees, especially *Olea*, which increases at the upper part of the diagram. Cultivated herbs (cereals) occur only at the base of the diagram (Early Medieval), and their disappearance coincides with the first appearance of *Cannabis* in the Montcortès record. The indicators of human activities (coprophilous fungi, charcoal) show irregular patterns that will be discussed in detail in the description of pollen zones. *Botryococcus* shows only a local peak by the middle of the Pallars County phase.

5.1.2 Zonation

In this case, the zonation of the pollen diagram is the following (boundary ages are also between-sample interpolations):

5.1.2.1 Zone LM-5 (364–582 CE; 1586–1368 cal yr BP; Early Middle Ages or Dark Ages)

This zone is dominated by *Pinus* followed by evergreen and deciduous *Quercus*, whereas other trees, such as *Betula* and *Alnus*, are also present but in lower abundances. The total abundance of forest trees shows an increase from the base, where percentages are significantly lower than in modern sedimentation, to the top, where values similar at present are attained. Shrubs (*Juniperus*) and herbs such as *Artemisia* and *Plantago* follow an inverse trend, whereas cereals are more abundant than wild herbs. The modern-analog similarity shows a gentle increase. Charcoal is also present, peaking around half of the zone, but its values are remarkably lower than in the pre-Medieval diagram, where the scale for this proxy is four times the scale of the Medieval diagram (Fig. 5.1).

5.1.2.2 Zone LM-6 (582–754 CE; 1368–1196 cal yr BP; Middle Visigoth to Muslim Phases)

A relevant change in the composition of forest assemblage is recorded in this zone due to the increase in evergreen *Quercus* and a sudden decline in deciduous *Quercus*, while *Pinus* attains values slightly below the present. *Betula* and *Alnus* also experience a small decline. As a result of these changes, the total forest pollen reaches values similar to the present. After the gentle decreasing trend of the former zone, *Juniperus*, *Artemisia*, and *Plantago* stabilize at lower values. The most important change in herbs is the increase in wild grasses coinciding with the decrease in cereals, which disappear at the end of the zone. This is also the zone where *Cannabis* appears for the first time and quickly increases to significant values. In this zone, the similarity between past and modern pollen assemblages is maximum showing a

slight decrease toward the top. For anthropogenic proxies, coprophilous fungi slightly increase, and charcoal shows a maintained decreasing trend.

5.1.2.3 Zone LM-7 (754–915 CE; 1196–1035 cal yr BP; Muslim to Frank Phases)

The *Pinus* dominance continues, but a decrease in evergreen *Quercus*, which cannot be compensated by a minor deciduous *Quercus* increase, determines a general decline of forest-tree pollen to values lower than at present. This forest decline is paralleled by an increase in wild Poaceae and the disappearance of cereals. Also relevant are the increases in coprophilous fungi and *Glomus*, as well as the low charcoal values. An important change occurs at approximately 841 CE (1109 cal yr BP), which allows subdivision into two subzones. Subzone a is characterized by a peak in wild Poaceae, the presence of *Juniperus*, and a decrease in *Cannabis* at very low values, which is accompanied by a significant increase in coprophilous fungi. In subzone b, wild Poaceae decrease, *Juniperus* disappears and *Castanea* and *Artemisia* increase, whereas *Cannabis* recovers the values of zone LM-6, and coprophilous fungi and charcoal almost disappear. The difference between the pollen assemblages of this zone and the modern assemblage continues to increase in subzone a but decreases in subzone b.

5.1.2.4 Zone LM-8 (915–1291 CE; 1035–659 cal yr BP; Late-Frank to County Phases)

This zone represents a major change, as reflected in the drastic *Pinus* reduction to values less than a quarter of modern percentages. Evergreen and deciduous *Quercus* pollen types are stable and close to modern values but slightly below. This coincides with lower values in other tree-pollen types and the consistent, but still scarce, presence of *Olea*. Shrubs (*Juniperus*) remain absent, and herbs (*Artemisia*, *Plantago*, wild Poaceae) attain their maxima, becoming dominant. Cultivated herbs are absent except for a peak of *Hedysarum* (a forage legume) at approximately 1200 cal yr BP (750 CE). *Cannabis* remains at elevated values similar to subzone LM7-b. The sudden *Pinus* decrease is accompanied by an equally abrupt increase in the modern-analog dissimilarity. Coprophilous fungi are scarce, except for a local maximum coinciding with the *Hedysarum* peak, and *Botryococcus* is scarce, except for a local peak at 1090 CE (860 cal yr BP). Charcoal is not generally abundant but shows three sharp peaks at approximately 950, 1080, and 1190 CE (1000, 870, and 760 cal yr BP, respectively).

5.1.2.5 Zone LM-9 (1291–1490 CE; 659–460 cal yr BP; Late-County Phase)

This zone does not show significant changes in major pollen types, but a general increment in forest types can be observed, which is paralleled by an inverse declining trend in wild herbs. The most important differences are a general, although modest, recovery of the less abundant trees (mainly *Betula* and *Corylus*) and shrubs (*Juniperus*), along with the consolidation of *Olea* at significant values. Outside the pollen sum, *Cannabis*, coprophilous fungi, algae, and charcoal are scarce or absent.

The upper part is different from the rest of the zone due to a conspicuous decline in *Pinus* accompanied by an increase in evergreen *Quercus*, *Betula*, and *Juniperus*, as well as a general decrease in wild herbs. This results in a general increase in trees with respect to herbs until values similar, but still lower, to present percentages. This change has been reflected in the subdivision of this zone into two subzones (a and b), with the boundary at 539 cal yr BP (1411 CE). Dissimilarity values between past and modern pollen assemblages follow the same trend as in zone LM-8 but experience a meaningful increase in the passage from subzone a to subzone b.

5.2 Vegetation and Landscape Dynamics

As in the case of pre-Medieval times (Chap. 4), the interpretation of the pollen diagram in terms of vegetation and landscape dynamics is based on the above zonation and is disclosed following the main cultural phases. As in pre-Medieval times, ages are rounded to tens owing to the general resolution of the pollen record (Chap. 4; Sect. 2).

5.2.1 Visigothic Period

This phase was characterized by two different vegetation types representing a relevant regional change in both forest composition and human practices. The first phase (Zone LM-5; 360–580 CE) coincided almost exactly with the Migration Period (Chap. 2; Sect. 4) (Fig. 5.2), and the main feature was a progressive forest recovery after the first regional deforestation that took place in late Roman times (Chap. 4; Sect. 2.3). This recovery was especially manifested in the expansion of submontane *Quercus* forests, which were more extended than at present. At the end of this phase, regional forests attained present-like patterns both in importance and composition, as indicated by the total percentages and the similarity with modern analogs (Fig. 5.1). Open vegetation significantly reduced its relevance, but cereal cultivation remained at an intensity similar to late Roman times. This, combined with the scarcity of grazing proxies, indicates that local cereal cultivation was still the main activity around the lake, while regional forests recovered. Interestingly, the expansion of these forests lasted almost three centuries (310–580 CE), whereas their reduction to minimum values had taken barely 50 years (260–310 CE; Chap. 4; Sect. 2.3). Charcoal values remained as low as in late Roman times (compare Figs. 4.1 and 5.1 considering the differences in scale), suggesting that fire was not the main deforestation agent. However, the coincidence of fire decline with forest recovery after 460 CE indicates that a certain level of forest burning should not be excluded.

The whole picture suggests that, during the Migration Period, regional forest exploitation—and therefore regional human pressure—was progressively reduced, but Roman-like local cultivation practices remained. This would be compatible with the persistence of small human groups around the lake, the cultural identity of which

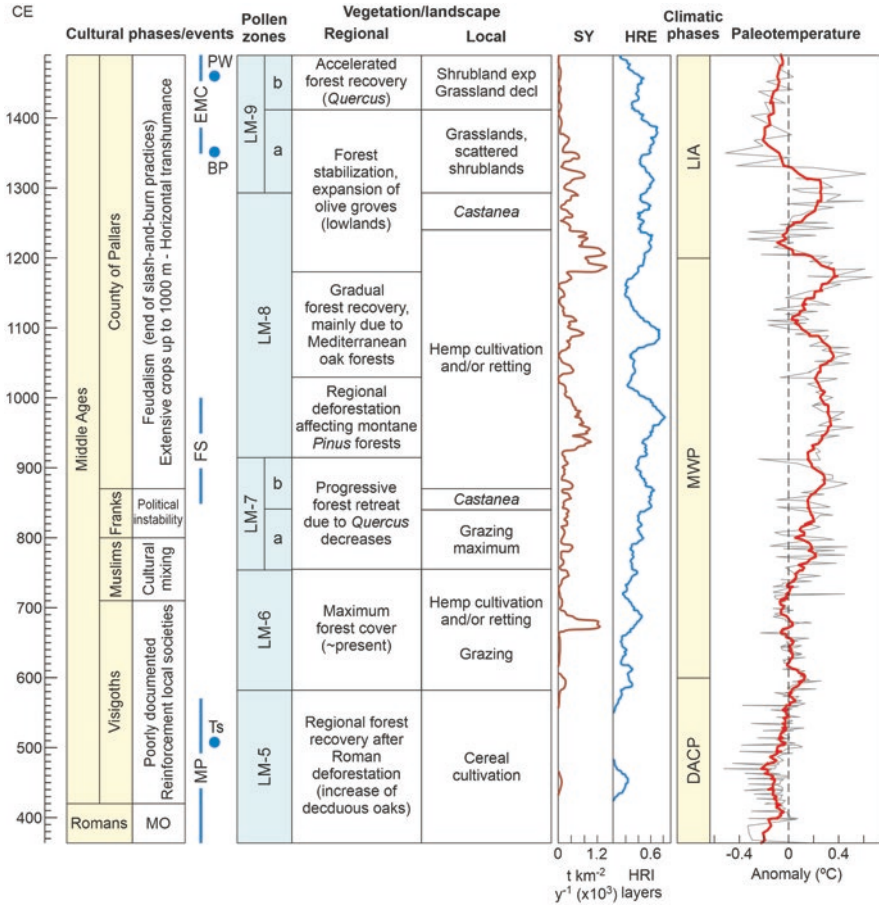


Fig. 5.2 Pollen zones (in blue) and vegetation reconstruction in relation to cultural history and climatic phases (in yellow) during the Medieval interval of the Lake Montcotès record. Historical and cultural phases according to Marugan and Rapalino (2005), as explained in Chap. 2 (MP, Migration Period (Halsall 2008); Ts, Foundation of Toulouse; FS, origin and consolidation of the feudal system; EMC, ending Medieval crisis; BP, black plague; PW, Pallars war). Sediment yield (SY) in thousand tons per square km per year ($t\ km^{-2}\ yr^{-1} \times 10^3$); heavy rainfall events (HRE) in heavy rainfall-induced (HRI) layer occurrence (31-y running average) (Corella et al. 2016, 2019). Climatic phases and paleotemperature reconstruction according to Martín-Chivelet et al. (2011) for the northern Iberian Peninsula (see Fig. 3.7 for reference). The thin gray line represents the raw data, and the thicker red line represents the 10-yr moving average. DACP, Dark Ages cold period; IACP, Iron Age cold period; RWP, Roman warm period; BAWP, Bronze Age warm period

is difficult to ascertain. As mentioned in the historical account (Chap. 2), the presence of Visigoths in the Pallars region is poorly documented, and the end of Roman domination led to the reinforcement of local autochthonous societies. Therefore, it is possible that the general landscape recovery observed in the pollen record was linked to a general relaxation of anthropogenic pressure after Roman departure,

rather than to the establishment of a new foreign culture such as the Visigothic. The paleoecological information provided above could be useful to help unravel the cultural traits of the post-Roman occupation of the Pallars region, which remains a dark prefeudal phase with little historical documentation.

The minimum sediment yield to the lake was recorded between 360 and 590 CE, coinciding with the Migration Period (Fig. 5.2). As seen above, forests—especially deciduous *Quercus* forests, which are the most abundant around the lake (Fig. 1.1)—were expanding, and this would have progressively reduced catchment erosion and transport, thus lowering sediment supply. However, climate may also have affected this reduction, as the Migration Period was coeval with a sharp decline in heavy rainfall events in the lake catchment, as estimated by the frequency of detrital layers and turbidites (Corella et al. 2016), and a phase of generally lower flood frequency in the western Mediterranean region (Benito et al. 2015). This occurred after the DACP minimum, when temperatures were rising and approached present-like values. Therefore, a combination of reduced anthropogenic pressure, changes in the precipitation regime, and rising temperatures would have shaped the regional Montcortès landscape during the Migration Period. In this case, climatic drivers would have acted directly on vegetation rather than indirectly by fostering elevational migrations of humans, as proposed in the case of the Iron Age (Chap. 4; Sect. 2.2).

Forest recovery progressed until the second phase of the Visigothic period (Zone LM-6; 580–710 CE), when the woodland extent and composition were more similar to the present with some small differences (Figs. 5.1 and 5.2). Indeed, montane *Pinus* forests dominated the landscape but were less extensive than today, whereas evergreen *Quercus* forests were subdominant but more important than at present, and submontane deciduous *Quercus* forests experienced a sudden decline. This was the time interval of maximum forest cover recorded during the Middle Ages. A differential feature with respect to former times was the onset of *Cannabis* cultivation/retting, which coincided with a noticeable decrease in cereal cultivation and an increase in grazing, along with a significant decline in fire. Therefore, a remarkable shift in land use took place, possibly linked to a cultural change from Roman-like practices (i.e., forest exploitation and cereal cultivation) to the hemp industry and grazing. It is possible that this transition represented the true end of Roman culture, although Roman domination had already been finished a couple of centuries before and its replacement by Visigothic land-use practices. It should be noted that hemp cultivation to obtain fiber for domestic uses was a common Roman practice in Italy (Mercuri et al. 2002), but this practice was not recorded in the Pallars region during Roman times (Chap. 4; Sect. 2.3). In the Montcortès record, *Cannabis* cultivation has only been documented in post-Roman times; therefore, it is suggested that this could be an indicator of a cultural shift.

With the available evidence, it is not possible to know whether *Cannabis* was cultivated locally, as this plant is anemophilous (wind-pollinated) and its pollen has a high dispersion power (Cabezudo et al. 1997; Munuera et al. 2006). Moreover, hemp retting is an additional source of *Cannabis* pollen in lake sediments, especially in lakes with hard waters such as those of Lake Montcortès (Rull and

Vegas-Vilarrúbia 2015). Therefore, although the amount of *Cannabis* pollen recorded in Lake Montcortès sediments during the Visigothic period is a reliable indicator of the onset of the hemp industry, whether this pollen was cultivated locally/regionally or originated in situ by retting remains unknown. Some studies report that in lakes used for retting purposes, the percentages of *Cannabis* pollen in sediments may reach 80–90% of the total, but values over 15% or 25% are sufficient to infer hemp retting (e.g., Peglar 1993; Mercuri et al. 2002; Lavrieux et al. 2013; Demske et al. 2016). However, studies combining pollen records with biomolecular markers such as cannabiniol or DNA are better suited to confirm this point (Lavrieux et al. 2013; Giguët-Covex et al. 2019). This topic has been reviewed by McPartland et al. (2018). As mentioned above (Chap. 3; Sect. 4.2.3), hemp pollen in modern Montcortès assemblages should proceed from long-distance dispersal, as the parent plant (*Cannabis sativa*) has not been located in local and regional vegetation studies and the lake is not presently used for retting purposes. This implies that local pollen sources are not needed to account for values up to 8% (Table 3.4), but percentages of 15–20%, as recorded in the second half of the Visigothic period, would likely need local/regional pollen sources to be attained.

A sharp major increase in sediment yield to the lake reaching unprecedented values in former times occurred at 650 CE (Fig. 5.2) and persisted during the whole Medieval period, which was linked to a substantial and maintained increase in human pressure in the lake catchment. This date coincided with a small decline in forests and hemp cultivation/retting, and a gentle increase in grazing. It is possible that forest stands around the lake, especially deciduous oak stands, were cleared for grazing purposes, which facilitated catchment erosion and sediment delivery to the lake. However, this does not seem to have been a major event comparable to the regional deforestation that occurred during Roman times, which did not produce such a marked increase in sediment yield amounts. The Middle Ages were characterized by a conspicuous and maintained increase in heavy rainfall events that could also have contributed to the Medieval increase in sediment delivery to the lake. During the second part of the Visigothic period, temperatures were similar to the present with only minor variations, which could help explain the similarity of vegetation traits with the present situation. However, the increase in Mediterranean oak forests and the decrease in montane pine forests with respect to present-day values cannot be explained solely by temperature trends.

5.2.2 Muslim Period

The period corresponding to Muslim domination in the Pallars region represented the transition between pollen zones LM-6 to LM-7, centered on 750 CE, which was characterized by a progressive forest retreat, especially in montane *Pinus* woodlands, and an expansion of grasslands, along with the onset of *Castanea* (chestnut) and the end of cereal cultivation. *Cannabis* cultivation/retting also experienced a decline and almost disappeared, whereas grazing markedly increased. In summary, a gradual vegetation opening occurred that fostered the expansion of pastures to the

detriment of woodlands and croplands. Again, little information is available in the historical documentation about this period, but it is known that the Pallars region was in an intermediate position between the Muslim Empire in the south and the Frank Empire, in the north (Fig. 2.6), which promoted the development of a high cultural diversity (Chap. 2; Sect. 4.1.2). Landscape opening and the shift from the hemp industry to pastures would help in understanding the socioeconomic traits of this period, which was characterized by rising temperatures corresponding to the first phase of the Medieval Warm Period (MWP), also known as the Medieval Climate Anomaly (MCA) (Fig. 5.2). This warming might have contributed to an upward displacement of forest belts, as expressed in the decrease in montane pine forests. However, the stability of Mediterranean *Quercus* forests does not favor this option and supports anthropogenic pine forest clearing, possibly by tree felling, as fire was at minimum values.

5.2.3 Frank Period

This was also a transitional phase, in terms of vegetation, between subzones LM-7a and LM-7b, with a boundary at 840 CE. In general, vegetation and landscape patterns were similar to those in the second half of the Muslim period, but some minor differences occurring before and after 840 CE are worth mentioning. This boundary was marked by an increase in chestnut cultivation and a decline in grasslands, along with the disappearance of *Juniperus* shrublands. Also noteworthy was the maximum grazing at 820 CE, followed by a dramatic decline in this practice, coinciding with the momentary disappearance of fire practices. Once more, historical documents on the socioeconomic features of this period are lacking (Chap. 2; Sect. 4.1.2). However, the end of fire practices, as recorded in the Montcortès paleoecological record at the end of the Frank period, coincided with the abandonment of itinerant slash-and-burn practices, as documented in historical reports during the beginning and consolidation of the feudal system (ninth to eleventh centuries) (Chap. 2; Sect. 4.3.1). Temperatures continued to increase to values higher than at present up to an MWP maximum in the second half of the Frank period, which coincided with the abandonment of grazing practices after 840 CE. It is possible that warmer MWP climates facilitated the development of grazing activities at higher elevations, and the lake catchment was no longer used for this purpose.

5.2.4 County of Pallars

During the first decades of Pallars independence (870–910 CE), the general vegetation patterns remained similar to the end of the Frank period (subzone LM-7b), but *Castanea* cultivation declined and *Cannabis* returned with values similar to the second Visigothic phase, which suggests the occurrence of local/regional hemp pollen sources in the form of either crops, retting, or both. From approximately 910 CE onward, another regional deforestation event occurred, affecting mainly pine

forests, which were abruptly reduced to roughly a quarter of their present range in only a few decades. The evergreen and deciduous oak forests slightly increased at the same time but this was insufficient to compensate for the *Pinus* decline. This represented a general landscape opening with minimum forest cover by 990 CE, followed by a gentle gradual increase and a further stabilization of forest importance until the end of pollen zone LM-8 (1290 CE). The temporary recovery was mainly due to a gradual increase in Mediterranean oak forests and montane *Pinus* forests, but the latter never returned to former values and remained below a third or less of its modern relevance. Hemp cultivation/retting continued until 1240–1250 CE, when *Cannabis* pollen was reduced to percentages similar to present-day values until the end of the Middle Ages, and hence, the occurrence of local/regional sources for this pollen was no longer warranted. The reduction in the hemp industry coincided with another phase of *Castanea* cultivation between 1250 and 1290 CE. Grazing intensity remained low along LM-8, except for a couple of small peaks, and fire incidence underwent three local peaks (950, 1080, and 1190 CE) that coincided with transient forest reductions without changing the general tendency to woodland recovery. Despite this recovery, the total forest cover remained significantly below modern values.

This part of the Pallars County period (910–1290 CE) coincided with increased sediment yield values, which showed three maxima coinciding with the abovementioned fire peaks and the corresponding reductions in forest cover (Rull et al. 2021c). This supports the observations of Corella et al. (2019) that forest burning had a large impact on sediment delivery to the lake during the Middle Ages by increasing soil erosion in the watershed. According to these authors, cultivation practices also enhanced sediment supply but to a lesser extent than burning and overgrazing. The already mentioned Medieval increase in heavy rainfall events would also have contributed to the increase in soil denudation. The Medieval regional deforestation event and further forest recovery took place during the MWP/MCA maximum, when temperatures were higher than at present. Therefore, the observed increase in Mediterranean oak forests was likely due to a climatically driven upward migration of forest belts, which would have fostered the occurrence of these lower-elevation forests (Fig. 1.10) around the lake. Similarly, higher temperatures would have favored the cultivation of hemp—which is a heliotropic (sun-loving) species that prefers warm and wet lowland climates (Small 2015; Clarke and Merlin 2016)—at Lake Montcortès elevations. This possibility is supported by historical documents that report an upward displacement of the upper boundary of lowland crops such as olive groves and vineyards to 1000 m elevation due to warmer Medieval climates (Chap. 2; Sect. 4.3.1). This is also consistent with the fact that hemp is known to have been cultivated only in the lowlands surrounding Lake Montcortès during the nineteenth century, when temperatures were similar to today (Chap. 3; Sect. 4.2.3). Therefore, in situ hemp cultivation seems to have been the source for most *Cannabis* pollen during this Medieval interval. It is also noteworthy that the three burning peaks coinciding with maxima in sediment yield occurred around the MWP warming peaks, which suggests some link between higher temperature and fire, possibly in the form of increased vegetation flammability due to higher evaporation rates.

The occurrence of these burning peaks contrasts with historical documents that report the end of slash-and-burn practices in the Pallars region during the feudal period (Chap. 2; Sect. 4.3.1). However, it should be noted that these events were isolated burning peaks within a general trend of fire decline consistent with historical observations. This point will be further discussed in the next section.

Forest stability continued during the second part of the period corresponding to Pallars County (zone LM-9; 1290–1490 CE). Chestnut cultivation receded, and olive groves expanded, coinciding with the return of shrubby vegetation (*Juniperus*) in the lake catchment, which was no longer cultivated or submitted to grazing. The expansion of *Olea* crops probably took place in the southern lowlands, as this occurred during a Little Ice Age (LIA) cooling, which seems incompatible with local cultivation of this lowland tree around the lake. The pollen of *Olea* is known to be well represented in modern sediments from mid- and high-elevation areas of the central Pyrenees situated above lowland olive groves, likely due to upward wind dispersal (Cañellas-Boltà et al. 2009). Therefore, the increase recorded in Lake Montcortès during the end of the Middle Ages could be explained by the growth of olive cultivation in the lowlands. Sediment delivery to the lake underwent a relevant decrease during this time interval, probably linked to the abandonment of local burning, cultivation, and grazing activities in the watershed. A new abrupt pine decline, yet not as intense as in the former regional deforestation event, occurred at 1410 CE, followed by an acceleration of general forest recovery due to the expansion of evergreen and deciduous *Quercus* forests. Other forest trees, such as *Betula* and *Corylus*, also increased, shrublands expanded and grasslands declined, whereas human activities (cultivation, grazing, burning) remained absent from the lake catchment, coinciding with a significant decline in sediment delivery to the lake. All these events took place during the ending Medieval crisis (1350–1487 CE), characterized by a substantial depopulation of the Pallars region and a general abandonment of crops, pastures, and forests as a consequence of wars, black plague, colder LIA climates, and the self-induced collapse of the feudal system (Chap. 2; Sect. 4.5). A large part of the Pallars population emigrated to larger lowland cities, which is consistent with the expansion of olive groves in these lowlands and the abandonment of cultivation, grazing, and forest exploitation around Lake Montcortès. This is consistent with the marked decline in sediment yield to the lake with respect to former medieval times.

5.3 A Closer Look to Medieval Deforestation

The high resolution of the paleoecological reconstruction allowed us to analyze with more detail than usual in the central Pyrenees the regional deforestation trends of the Medieval period, which has been considered a time of major anthropogenic landscape opening in this mountain range (Pèlachs et al. 2017; González-Sampérez et al. 2017, 2019; García-Ruiz et al. 2020; Rull and Vegas-Vilarrúbia 2021a, and literature therein). The period of interest, excluding the Migration Period, which was a time of forest recovery (Fig. 4.4), ranged from 600 CE to 1500 CE and was

analyzed at quasidecadal resolution (14 years per sampling interval), which almost triplicates the resolution of the first studies (Rull et al. 2011). In this way, it has been possible to record subtle shifts that remained hidden in previous surveys.

In general, the maximum regional deforestation was recorded at 990 CE, when pollen from forest trees declined to 23% (Fig. 5.3), which is 30% of modern values (77%) and 25% of Late Bronze values (91%), when the region was fully forested. This indicates that approximately three-quarters of the land was occupied by open vegetation, mainly grasslands and pastures. The forest decline began just after the Migration Period, during the Visigothic occupation, and continued during Muslim and Frank domination, attaining the abovementioned maximum at the beginning of Pallars independence, when the feudal system was already fully established. The palynological signal of this gradual forest retreat began at percentages slightly above present and occurred at average rates of $-0.12\% \text{ yr}^{-1}$ (estimated by linear

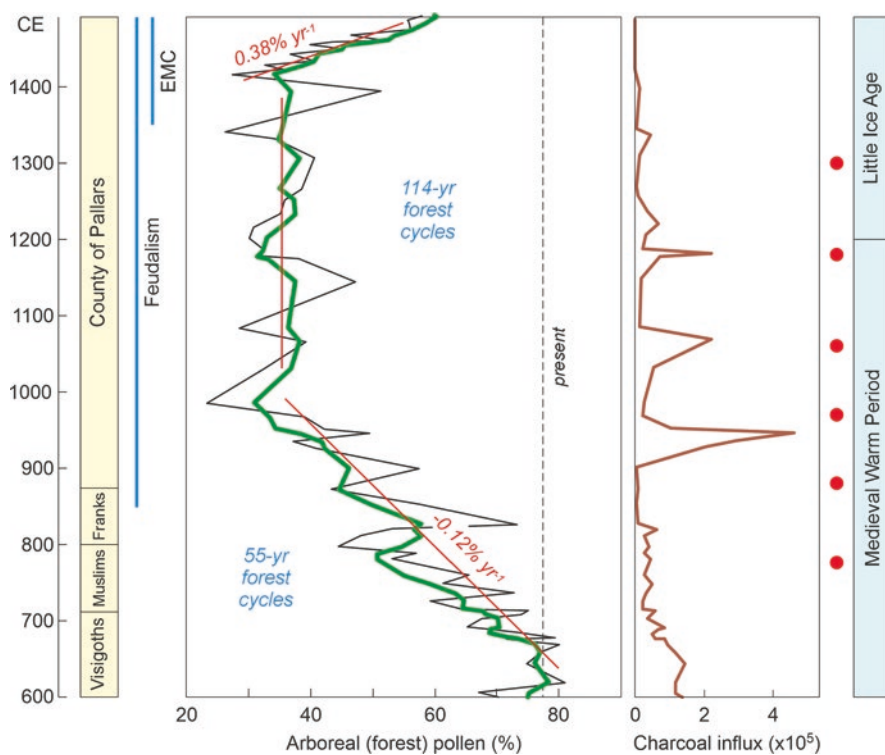


Fig. 5.3 Forest trends during the Middle Ages, as represented by the total abundance of pollen from forest trees (raw data in black, 4-point moving average in green). The present abundance is provided for reference (vertical dotted line). Regression lines used to estimate the average deforestation and recovery rates (in $\% \text{ yr}^{-1}$) are in red. Charcoal influx is expressed as particles $\text{cm}^{-2} \text{ yr}^{-1}$. Warming peaks from Fig. 5.2 are indicated by red dots. EMC, ending Medieval crisis. Modified from Rull et al. (2021c)

regression; $r = -0.887$, $\alpha < 0.01$). This decline was not monotonic but was characterized by a succession of minor retraction–expansion (turnover) cycles of 55 years on average. Two main phases can be distinguished in this general landscape opening, with a boundary near the transition between Muslim and French occupations (800 CE). This transition was characterized by an outstanding deforestation peak (<50% of arboreal pollen), culminating in a forest decline that paralleled a decrease in forest incidence. Therefore, it is possible that anthropogenic fires played a role in deforestation, although not as relevant as in pre-Medieval times (Chap. 4), owing to the significantly lower charcoal amounts recorded. The second phase began with a quick forest recovery to values similar to the present followed by a new retraction trend lasting until the Medieval forest minimum. The recovery and the first turnover cycle took place in the absence of fire (Frank period), whereas the onset of the Pallars County period witnessed a short but intense fire peak that likely precipitated the largest forest reduction recorded during the Medieval period.

After the Medieval deforestation acme (990 CE), an extended stabilization of forest cover to pollen values of approximately 35% occurred that lasted until approximately 1420 CE. Again, this general trend was spiked by several minor turnover cycles of similar intensity but twice as long (114 years) as the cycles recorded during the phase of forest decline. Two of these minor turnover cycles were linked to two minor sharp fire events (1070 CE and 1180), but others occurred in the absence of relevant fire episodes, which suggests that both burning and tree felling practices were used alone or in combination in forest exploitation. Fire incidence, however, remained at values below pre-Medieval times. In contrast with the deforestation phase, the succession of minor deforestation cycles did not precipitate a general forest decline but led to stabilization. A possible explanation is that the recurrence of minor clearing events was long enough to allow forest recovery, whereas in the deforestation phase, the higher frequency of minor forest clearing events hindered recovery and determined a cumulative effect leading to a general forest retreat (Rull et al. 2021c). A general forest recovery occurred only during the ending Medieval crisis, after 1420 CE, at pollen rates of $0.38\% \text{ yr}^{-1}$ ($r = -0.946$, $\alpha < 0.01$)—which is 3.5 times faster than the initial regional deforestation rates—in the absence of fires. This trend was also characterized by minor turnover cycles but of very low intensity, insufficient to cause a general forest retreat.

A general observation is that fire continued to be used as a deforestation agent during Medieval times, although with less frequency and intensity as in pre-Medieval times. Therefore, the historical observations that slash-and-burn practices were abolished under the feudal system to maximize control over land use (Chap. 2; Sect. 4.3.1) might be taken as a general tendency valid for the whole Pallars region. However, low-intensity burning would have remained at the local level, especially in montane areas, where these practices were common in prefeudal times. Another significant implication is that the extensive deforestation in the Montcortès region during the Middle Ages was not the result of a single sudden event that, once it ended, allowed the forests to regenerate. Instead, the contrast between deforestation and recovery patterns can be attributed to the recurring occurrence of minor deforestation pulses throughout the Medieval period. This can only be observed after

high-resolution studies, as analyses at centennial and millennial scales record only long-term/intense episodes and tend to present them as unique regional-wide events. This may not only hide other relevant trends but also distort correlations with other palynological reconstructions and with records of independent proxies for environmental drivers of vegetation change (e.g., climate and human activities).

Regarding the potential influence of climate on forest trends, three warming peaks (970 CE, 1060 CE, and 1080 CE) occurred near fire peaks and within minor deforestation events. In these particular cases, it is possible that climate–human synergies generated amplification mechanisms that exacerbated forest burning, as fire peaks were very short. Before those dates, two warming peaks coincided with local forest minima in the absence of significant burning at 780 CE and 880 CE. In these cases, tree felling would have been the main clearing agent. Another warming peak occurred at the beginning of the LIA (1300 CE), which coincided with a minor forest maximum in the absence of fire. The potential influence of climate on fire regimes has largely been debated (e.g., Bistinas et al. 2014; Andela et al. 2017; Forkel et al. 2019; Harrison et al. 2021). In the case of the Iberian Peninsula, a recent review on spatiotemporal patterns of sedimentary charcoal in relation to archaeological evidence suggests that climate would have been a major fire driver during the Holocene, even in phases of greater human impact such as the Neolithic Revolution (Sweeney et al. 2022). The forest maximum was due to the increase in Mediterranean oak forests (Fig. 5.1), which suggests a potential upward displacement of these woodlands favored by warmer climates in the absence of manifest anthropogenic pressure (see above).

5.4 Highland Forests

Medieval deforestation was a region-wide phenomenon that affected not only montane areas such as Lake Montcortès and its surroundings but also other Pyrenean landscapes, from submontane to highland environments. Based on a paleoecological review conducted by González-Sampérez et al. (2017), it was observed that early indications of human influence on the environment were detectable at certain lowland sites approximately 4000 cal yr BP during the Bronze Age. However, it was not until the Medieval period that human activities significantly impacted landscape changes, regardless of the elevation or geographic location. These researchers concluded that climate largely shaped the development of Pyrenean landscapes until the Middle Ages, when human activity became the dominant factor. By combining paleoecological and archaeological evidence, the same authors also determined that human-induced deforestation and the expansion of open vegetation in the central Pyrenees occurred in the early Medieval period, approximately 700 cal yr BP (1300 CE) (González-Sampérez et al. 2019).

Using a similar paleoecological dataset, Rull and Vegas-Vilarrúbia (2021a) argued that elevation was a meaningful variable for Pyrenean anthropization, which was a diachronous process that occurred gradually from the Bronze Age (basimontane belts) to the Medieval Ages (alpine belts), rather than a synchronous

phenomenon independent of geographical and topographical patterns, as pointed out by González-Sampérez et al. (2017). In either case, massive anthropization of subalpine/alpine areas (Fig. 1.10) would have occurred during Medieval times. The combination of historical documents, archaeological evidence, and palynological reconstructions documented the extensive Medieval deforestation of montane and subalpine landscapes (1350–2200 m elevation) in the southern central Pyrenees, mainly for herding purposes. Especially noteworthy is the case of the subalpine belt (>1600 m), where highland conifer forests were systematically removed and replaced by pastures to develop horizontal transhumance. This resulted in a general lowering of the treeline, thus expanding and connecting highland meadows and facilitating the long-distance movement of livestock (García-Ruiz et al. 2020).

In the Pallars/Val d’Aran region, the northern highlands (Figs. 2.1 and 2.2) constitute the headwaters of the Segre River, the same river basin to which Lake Montcortès belongs. Several palynological records are available in these highlands (Fig. 5.4), but only two, Lake Llebreta (1620 m) and Lake Sant Maurici (1914 m), cover a time period similar to the Montcortès record at comparable resolution

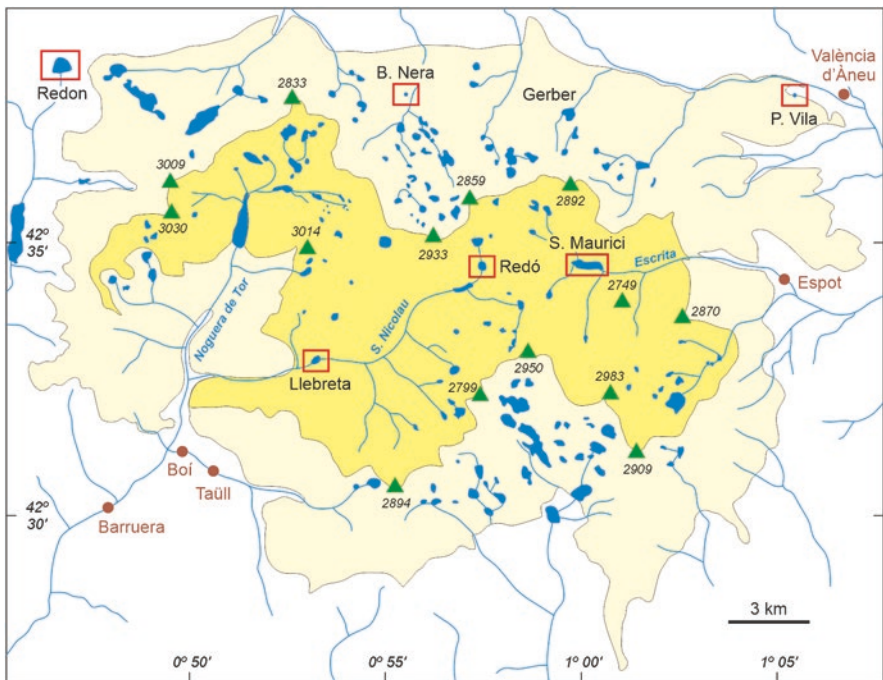


Fig. 5.4 Sketch map of the National Park of Aigüestortes i Estany de Sant Maurici (PNAESM) (Fig. 1.3) showing the location of lakes and peat bogs cored for palynological studies (red boxes). All these records correspond to highlands (subalpine/alpine belts) except Prats de Vila (P. Vila), which is in the montane belt, at 1150 m elevation. The park area is in yellow and the peripheral zone is in light yellow. Green triangles are the highest peaks with their elevations in m a.s.l. Lakes and rivers are in blue. Brown dots are the villages surrounding the park

(Catalan et al. 2013; Rull et al. 2021a). In these records—retrieved approximately 25 km north of Lake Montcortès in the National Park of “Aigüestortes i Estany de Sant Maurici” (PNAESM); Fig. 1.3)—the Middle Ages are well represented and can be compared with the Montcortès record in terms of forest development. The other highland records from the PNAESM (Redon, Redó, and Bassa Nera) encompass most of the Holocene at centennial/subcentennial resolutions (Catalan et al. 2000; Pla and Catalan 2005; Garcés-Pastor et al. 2017), which is not enough for comparison with the Medieval millennium (ca. 500–1500 CE). The Llebretra and Sant Maurici records are described below and compared with our Montcortès sequence.

5.4.1 Lake Llebretra

This pollen record encompasses the last 3600 years at bidecadal average resolution, and the data have been taken from some review papers that do not provide methodological details on site features, coring, dating, core sampling, and palynological analyses (Esteban 2003; Catalan et al. 2013). To the knowledge of the authors of this book, the original study remains unpublished.

The Llebretra record is largely dominated by *Pinus* pollen, followed by *Betula* and *Abies*, whereas other trees, such as *Corylus*, *Fagus*, and deciduous *Quercus*, are less frequent (Fig. 5.5). The total forest pollen is approximately 80% of the total. Cultivated trees occur in lower amounts, showing continuous (*Olea*) or discontinuous (*Juglans*, *Castanea*) patterns. Among herbs, wild Poaceae are the most abundant and others (*Plantago*, *Rumex*) are significantly less abundant. The only cultivated plants are cereals (including *Secale*), with very low percentages throughout the sequence. These Medieval pollen assemblages are similar to the present composition of the subalpine forests of the PNAESM, which extend from 1600 to the treeline (usually 2200–2300 m) and are dominated by *Pinus uncinata* (also known as *Pinus mugo* subsp. *uncinata*) with an ericaceous understory. In the lowermost belt of these coniferous forests, where Lake Llebretra is located, *Abies alba* may be an important component and some deciduous trees, such as *Sorbus*

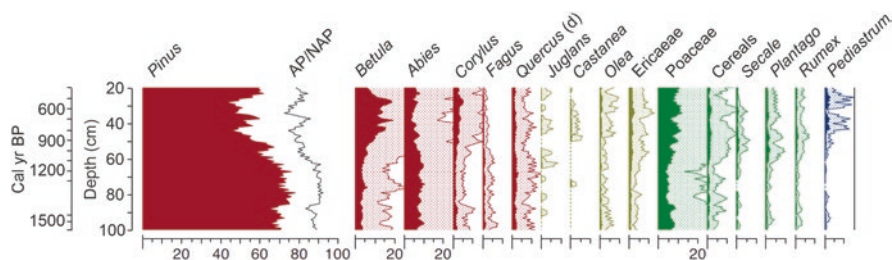


Fig. 5.5 Section of Lake Llebretra pollen diagram Lake corresponding to the Middle Ages (Catalan et al. 2013). Details on the age-depth model are not provided in the original reference. AP, arboreal pollen; NAP, nonarboreal pollen

aucuparia, *Salix capraea*, and *Betula pubescens* (birch), may occur as fast colonizers of unstable slopes or disturbed terrains, especially in areas under intense forest exploitation (Carrillo and Aniz 2013).

This record can be subdivided visually into two main phases with a boundary at approximately 1000 cal yr BP (950 CE). Between 1500 and 1000 cal yr BP (450–950 CE), *Pinus* forests were more extensive, followed by *Abies*, and *Betula* was less abundant. This situation gradually changed in the second phase (1000–400 cal yr BP; 950–1550 CE), when *Pinus* forests receded and *Betula* stands significantly increased. This shift in forest composition was accompanied by subtle increases in wild herbs and cereals, which suggests a small increase in grasslands and crops, insufficient to infer a major shift toward open landscapes. Unfortunately, no records of proxies for burning, grazing, or climate change are available for this record, but the cereal increase indicates enhanced, although not important, human pressure in the lake surroundings. This possibility could be supported by the conspicuous increase in birch observed after 1000 cal yr BP (950 CE), which could be linked to the potential of this tree as a rapid colonizer of postdisturbance forest gaps (Dubois et al. 2020). The comparatively higher expansion of *Betula* stands with respect to grasslands and crops suggests that the increasing human pressure was manifested primarily in enhanced forest exploitation, rather than in landscape opening for agricultural practices. According to these results, the landscape around Lake Llebretea was not intensively deforested during the Middle Ages.

5.4.2 Sant Maurici

More details are available for the Lake Sant Maurici record (Rull et al. 2021a). As noted in the introduction, this lake remained surprisingly uncored, despite the easy access to heavy coring equipment and the facilities available from the PNAESM administration. After a first failed attempt in 2004 (the lake was covered by an ice layer thick enough to prevent navigation but too thin to support coring devices), the lake sediments were finally retrieved in 2013.

5.4.2.1 The Lake

Lake Sant Maurici, situated at 42°34'53" N–1°00'12" E and an elevation of 1914 m (Fig. 5.4), lies in a former glacial cirque. It is now located within the *Pinus uncinata* forest belt, approximately 500 m below the treeline (Figs. 1.10 and 5.6). According to data from its own weather station, the annual average temperature is 5.4 °C and varies throughout the year, with the coldest months being January and February (–1.5 °C) and the warmest months being July and August (14 °C). Regarding precipitation, Lake Sant Maurici receives a total of 1058 mm of rainfall annually, showing two peaks in May (188 mm) and November (110 mm) and two drier months in February (63 mm) and July (65 mm). Historically, this lake was smaller and shallower than its present state. However, in 1953, the catchment was dammed, leading to the transformation of the original pond into a larger reservoir, which now spans 1100 m in length and 200 m in width, with a depth of ~25 m. This reservoir

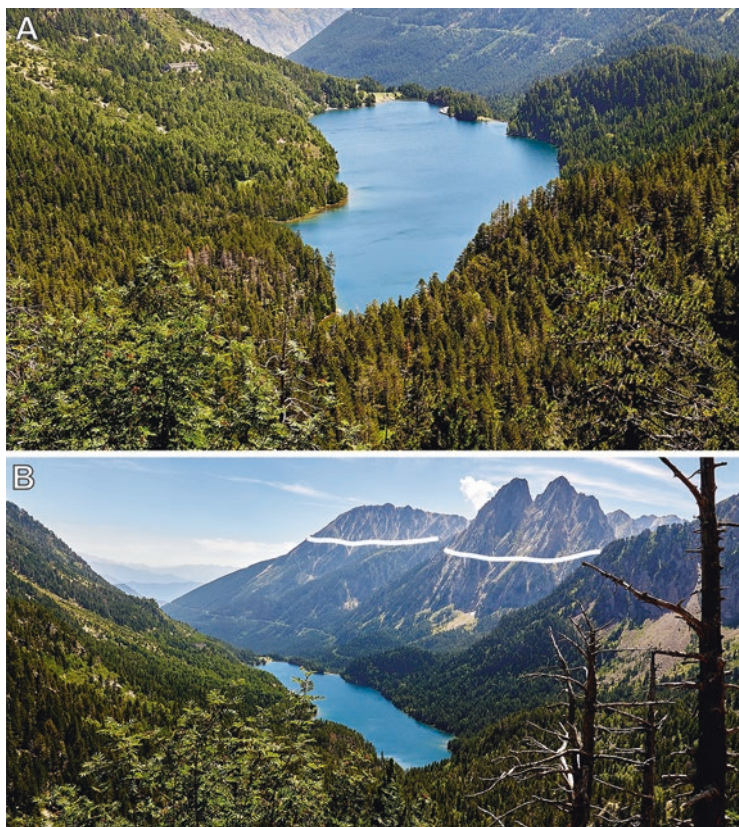


Fig. 5.6 Lake Sant Maurici and its surrounding *Pinus uncinata* forests (a), which mark the local treeline (2300–2500 m), as highlighted by white lines (b). The highest peaks around the lake attain elevations of ~2800 m. Photos: V. Rull

serves multiple purposes, including hydroelectric power generation, irrigation, and meeting the water needs of the local population.

5.4.2.2 Coring and Age-Depth Modeling

The core used for this reconstruction (SMA13-4B) was retrieved with a UWITEC piston core near the center of the lake at 18 m of water depth and consisted of 5 drives with a total depth of 860 cm. This core was stored, processed, and analyzed as Montcortès cores (Chap. 3) except for dating, which was performed by AMS ^{14}C methods. The core chronology for the upper 350 cm of the core was obtained by Bayesian modeling using BACON software (Blaauw and Christen 2011). The age-depth model (Fig. 5.7) showed that the section studied ranged from 4300 cal year BP (2350 BCE; Bronze Age) to 330 cal year BP (1620 CE; Modern Age), with a conspicuous sedimentary gap between approximately 3470 and 1500 cal year BP (1520 BCE–450 CE), which prevented the recording of the Iron Age and the Roman

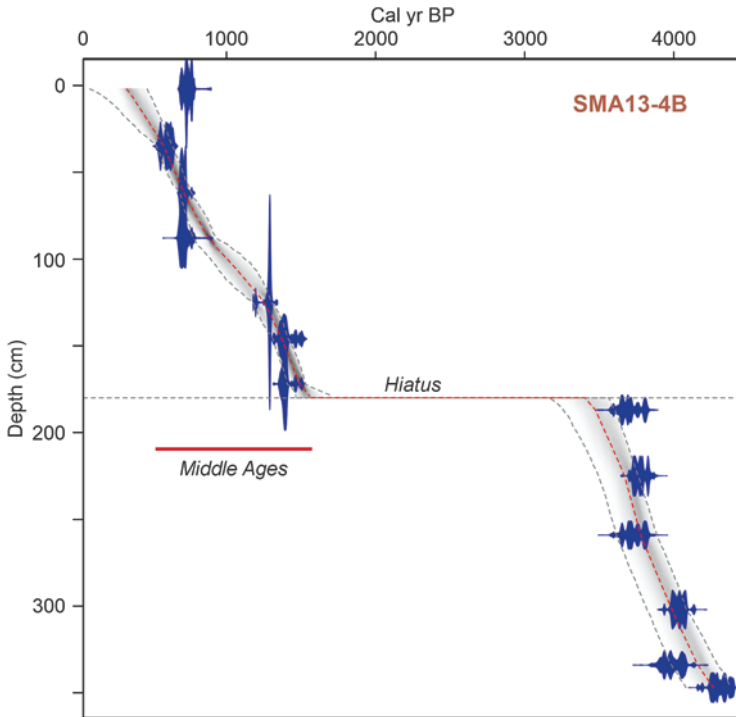


Fig. 5.7 Age-depth model for the upper part of core SMA13-4B from Lake Sant Maurici using radiocarbon dating of pollen residues (Vandergoes and Prior 2003) and BACON software (Blaauw and Christen 2011). The interval corresponding to the Middle Ages is marked by a red line. Redrawn and modified from Rull et al. (2021d)

epoch. The section above the hiatus contained the entire Medieval period, which was analyzed palynologically at bidecadal resolution (24 years per sampling interval).

5.4.2.3 Forest Dynamics

The Lake Sant Maurici pollen diagram depicted in Fig. 5.8 illustrates remarkable consistency during the Middle Ages, when the predominant landscape was characterized by *Pinus* forests, similar to the present-day environment. There was a minor disruption at the outset of this period, marked by a gradual decline in the forest and a slight increase in the presence of wild grasses and weeds during the Migration Period. This coincided with an uptick in fire occurrences, hinting at the possibility of slash-and-burn agricultural practices and, perhaps, limited cereal cultivation on a small scale. The scarcity of coprophilous fungi suggests that grazing was localized and of low intensity. These subtle alterations indicate that the subalpine forests in the Sant Maurici catchment area were not significantly impacted by human activities. This suggests that human settlements were too sparse to transform the original landscape into a highly anthropogenic landscape.

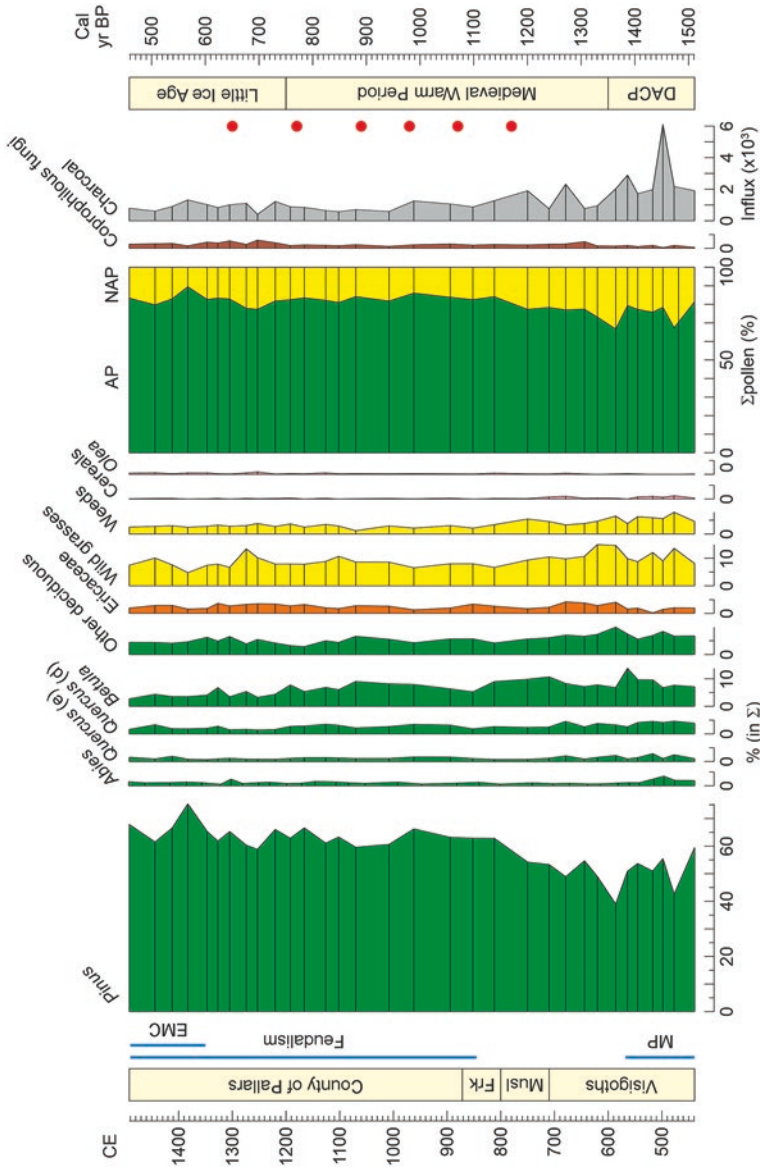


Fig. 5.8 Summary pollen diagram of the Medieval section from the Sant Maurici record (core SMA14-4B). Other deciduous trees: *Alnus*, *Corylus*, *Fagus*, *Fraxinus*, *Salix*, and *Ulmus*. Weeds: *Artemisia*, *Chenopodium*, *Plantago*, and *Rumex*. AP, arboreal pollen; NAP, nonarboreal pollen. Charcoal in influx units (particles $\text{cm}^{-2} \text{yr}^{-1}$). Red dots represent the warming peaks of Fig. 5.2. Frk, Frank Empire; Musl, Muslim Empire; EMC, ending Medieval crisis; MP, Migration Period. Redrawn and modified from Rull and Vegas-Vilarrúbia (2021b)

The most plausible interpretation is that small and sporadic, possibly seasonal, human groups existed around the lake. They likely created clearings in the forest and engaged in low-intensity agriculture. Some evidence of landscape opening is supported by a slight increase in *Betula*, a tree species known for colonizing cleared areas efficiently, and a modest expansion of wild grass and weed communities. This interpretation agrees with historical records documenting itinerant slash-and-burn agriculture in the upper montane regions (Chap. 2), where it offered various land uses in confined areas and was adapted to the pronounced seasonality of these environments.

Forest expansion commenced shortly after the Migration Period, coinciding with the initial warming of the Medieval Warm Period (MWP). The recovery continued during the Frank occupation of the Pallars region and the establishment of the feudal system. This period also marked the abandonment of slash-and-burn practices following the consolidation of the feudal system (see Chap. 2). Despite various warming and cooling episodes, no further alterations occurred thereafter, whether in the forest composition, other vegetation types, or indicators of human impact. The Ending Medieval crisis (1350–1490 CE) had a minor impact on the landscapes of Sant Maurici, leading to a slight increase in conifer forests, likely due to the significant migration of human populations to the southern lowlands. Therefore, the resilience of the San Maurici forests during the Middle Ages is evident, as they fully recovered after disturbances during the Migration Period and remained remarkably stable despite significant continental-wide climatic changes. This resilience can be traced back to the Bronze Age, as indicated by the enduring constancy of forest extent and composition (4300–3500 cal yr BP) (Rull et al. 2021a). The complete recovery of forests seems to be associated with the relatively small-scale and low-intensity/duration human impacts, but their apparent resistance to climate shifts requires further examination.

Not all elevational stages in a mountain range have the same sensitivity to record past climatic and ecological changes. The most sensitive sites are those situated close to characteristic ecotones, especially around the treeline, where temperature-driven altitudinal migrations of this ecological boundary are clearly visible in past pollen records (Kupfer and Cairns 1996; Holmeier and Broll 2005; Bruening et al. 2018). In contrast, sites situated near the middle of an ecological belt, far from its lower and upper boundaries, are less sensitive, that is, less suitable to capture the paleoecological signal of eventual elevational shifts (Rull 2005, 2015). Lake Sant Maurici (~1900 m) is located within the subalpine belt, 300 m above the lower boundary of this stage and 500 m below the upper boundary, which corresponds to the local treeline (Fig. 5.6). This means that this site would be able to record altitudinal displacements above 300–500 m that, considering the present adiabatic lapse rate of $-0.6\text{ }^{\circ}\text{C}/100\text{ m}$ elevation, correspond to temperature shifts exceeding 2–3 $^{\circ}\text{C}$, which are greater than those estimated in paleoclimatic reconstructions (Fig. 5.2). Therefore, the paleoecological sensitivity of Lake Sant Maurici is relatively low for the Middle Ages, which could partially explain the vegetation constancy recorded during this historical period in its sediments. Either way, the catchment of Lake Sant Maurici was also not deforested during the Middle Ages.

5.4.3 Subalpine Deforestation and Microrefugia

The above records show that palynological evidence for subalpine forest clearing and pasture expansion around lakes Llebreta and Sant Maurici during the Middle Ages is lacking. Rather, pine forests surrounding these lakes were likely exploited for wood and changed their composition with no major cover shifts (Llebreta) or expanded their range after a minor anthropogenic disturbance during the Migration Period (Sant Maurici). This contrasts with the idea of a general Medieval deforestation of subalpine forests for extensive grazing, as suggested by most pollen records from the central Iberian Pyrenees. Indeed, 14 of the 18 palynological studies available in this region at elevations above 1600 m showed evidence of woodland retreat and landscape opening between 700 and 1400 CE (Fig. 5.9). Exceptions are some localities that were anthropized before the Middle Ages, during the Bronze and Iron ages. Nevertheless, these comparisons should be taken with care, as records other than Llebreta and Sant Maurici are usually of subcentennial to multicentennial resolutions (Table 5.1), insufficient to resolve the events that occurred during the Middle Ages. More studies at decadal or similar resolution are needed for a sound assessment, but with the available evidence, lakes Llebreta and Sant Maurici and their catchments would have acted as microrefugia (*sensu* Rull 2009, 2010) for subalpine conifer forests in a scenario of general Medieval deforestation.

The comparatively low paleoclimatic sensitivity of Lake Sant Maurici might question this interpretation because, as estimated in the former section, eventual elevational displacements of less than 300–500 m corresponding to temperature shifts of below 2–3 °C could have remained unnoticed. This is not the case for Lake Llebreta (~1600 m), which is very close to the ecotone between the montane and subalpine belts and could therefore be sensitive to minor upward displacements of this boundary within the range of the MWP warming peaks. However, this ecotone is characterized by the boundary between *Pinus sylvestris* and *P. uncinata* (Fig. 1.10), whose pollen is morphologically indistinguishable. Therefore, in the present state of knowledge, it is not possible to discern the proportion of pollen from these two species present in the Llebreta record, which prevents us from inferring potential elevational displacements of the montane/subalpine ecotone on the basis of this record. To complicate matters further, these two species of *Pinus* are known to interbreed in their contact zone around the montane/subalpine ecotone, developing cryptic hybrids indistinguishable from the maternal species (Jasińska et al. 2010).

As a consequence, both possibilities, the existence of forest microrefugia and the occurrence of minor undetectable migrations of vegetation belts, remain open. These options, however, are far from mutually exclusive; they are fully compatible. Indeed, sites situated at elevations characterized by unresponsive forest communities due to their distance from the ecotones are, by definition, the best suited to provide stable environmental conditions for the survival of these forests in the face of climatic and/or anthropogenic changes (Fig. 5.10). Therefore, forest microrefugia, which are characterized by microenvironmental stability despite the occurrence of macroenvironmental changes, should be preferably located in these insensitive sites or in sites where temperature variations are buffered by moist conditions (Rull 2009; Ashcroft and Gollan 2013; McLaughlin et al. 2017).

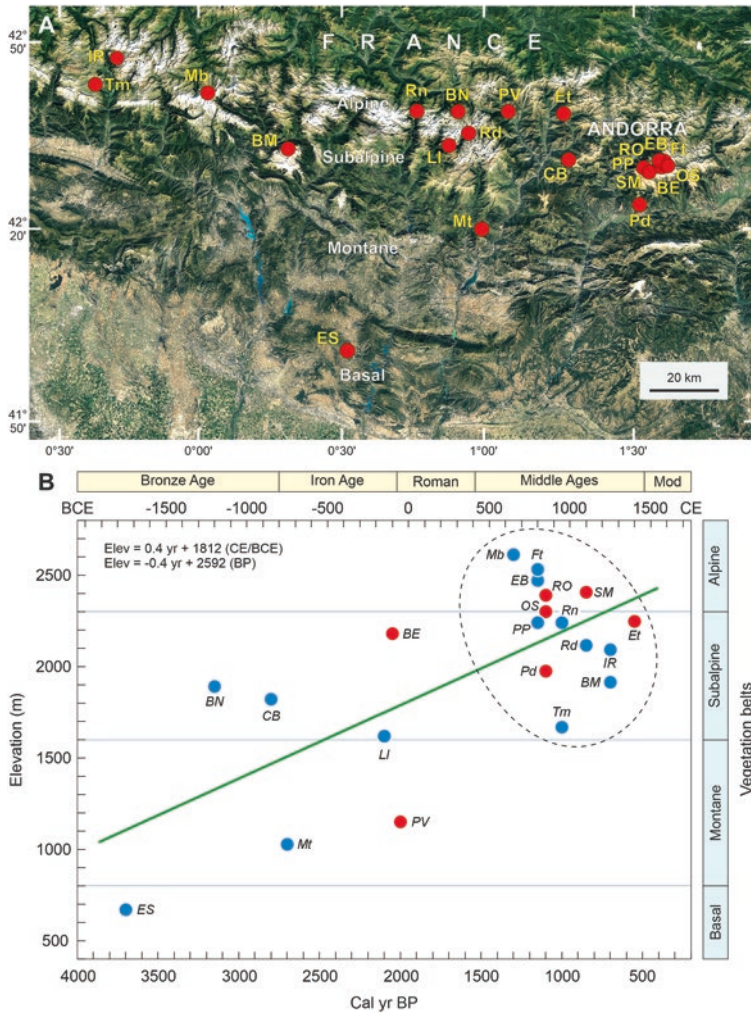


Fig. 5.9 Spatiotemporal anthropization gradient in the central Iberian Pyrenees (Rull and Vegas-Vilarrúbia 2021a). (a) Google Earth map showing the localities with palynological studies of lake and peat bog sediments recording landscape anthropization. (b) Relationships between time and landscape anthropization according to the interpretation of original references. Blue dots represent lakes, and red dots are peat bogs. The green line is the regression trend corresponding to the equation shown in the upper left ($r = 0.698$; $\alpha < 0.001$). The alpine/subalpine (>1600 m elevation) localities that were anthropized during the Middle Ages, as deduced from palynological evidence of forest clearing and landscape opening, are encircled by a dotted line. Mb, Marboré (Leunda et al. 2017); Ft, Forcat (Ejarque 2009); EB, Estany Blau (Ejarque 2009); SM, Serra Mitjana (Miras et al. 2015); RO, Riu dels Orris (Ejarque et al. 2010); OS, Orris de Setut (Ejarque et al. 2020); Et, Estanilles (Cunill et al. 2013); Rn, Redon (Pla and Catalan 2005; Catalan et al. 2014); PP, Planells de Perafita (Ejarque 2009); BE, Bosc dels Estanyons (Miras et al. 2007; Ejarque et al. 2010); Rd., Redó (Catalan et al. 2000, 2013); IR, Ibón de las Ranas (Montserrat Martí 1992); Pd, Pradell (Ejarque et al. 2009); BM, Bassa de la Mora (Pérez-Sanz et al. 2013); BN, Bassa Nera (Garcés-Pastor et al. 2016, 2017); CB, Coma de Burg (Pèlachs et al. 2007); Tm, Tramacastilla (Montserrat Martí 1992); Ll, Llebreta (Catalan et al. 2013); PV, Prats de Vila (Pèlachs et al. 2009); Mt., Montcortès (Rull et al. 2021b,c); Es, Estanya (Riera et al. 2004; González-Sampéris et al. 2017)

Table 5.1 Temporal resolution of the available vegetation reconstructions from high-elevation (subalpine/alpine) sites using pollen analysis in the central Iberian Pyrenees, excluding lakes Llebreta and Sant Maurici (Fig. 5.9)

Sites	Code	Elevation (m)	Range (yr)	Samples	yr/interval	Resolution	S/1000 yr
Marboré	Mb	2612	15,000	80	188	Bicentennial	5
Forcat	Ft	2531	9500	105	90	Centennial	11
Estany Blau*	EB	2471	1200	40	30	Multidecadal	33
Serra Mitjana	SM	2406	1500	15	100	Centennial	10
Riu dels Orris	RO	2390	8000	60	133	Centennial	8
Orris del Seut	OS	2300	3700	32	116	Centennial	9
Estanilles	Et	2247	12,000	90	133	Centennial	8
Redon	Rn	2240	10,000	130	77	Subcentennial	13
Planells de Perafita	PP	2240	10,000	50	200	Bicentennial	5
Bosc dels Estanyons	BE	2180	12,000	90	133	Centennial	8
Ibón de las Ranas	IR	2092	10,000	40	250	Bicentennial	4
Pradell*	Pd	1975	1400	37	38	Multidecadal	26
Basa de la Mora	Ma	1914	15,000	140	107	Centennial	9
Bassa Nera	BN	1891	7000	110	64	Subcentennial	16
Coma de Burg	CB	1821	10,000	70	143	Centennial	7
Tramacastilla	Tm	1668	15,000	150	100	Centennial	10

Localities with resolutions greater than centennial/subcentennial are indicated by an asterisk; these sites are outside the Noguera Pallaresa River basin, to which lakes Montcortès, Sant Maurici, and Llebreta belong (Fig. 5.9). S/1000 yr is the average number of samples per millennium, which is the approximate duration of the Middle Ages. References as in Fig. 5.9. Modified from Rull and Vegas-Vilarrúbia (2022)

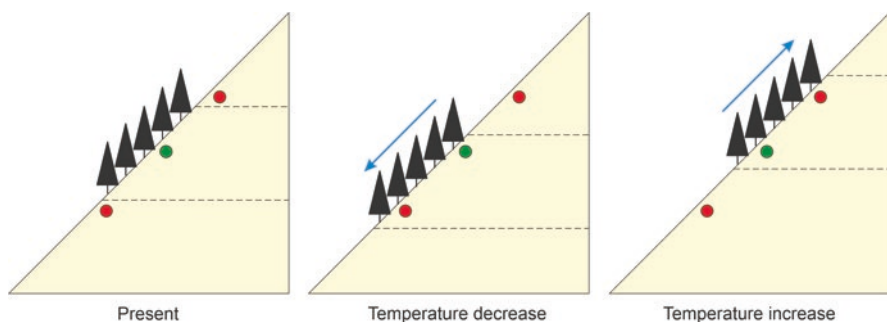


Fig. 5.10 Hypothetical example of a present forest belt (left) delimited by its altitudinal ecotones (dotted lines) and the eventual shifts experienced under cooling (center) and warming (right) trends. Sensitive sites are shown by red dots, and the insensitive site near the center of the present forest belt is represented by a green dot. When the temperature decreases, the forest belt migrates downward and covers the less sensitive site. When the temperature increases, the forest belt migrates upward, and the upper sensitive site becomes forested. The insensitive site is always within the forest belt, regardless of temperature variations, and is therefore a climatic forest microrefugium

If macroenvironmental changes are of anthropogenic origin, as is the case of large-scale deforestation of subalpine belts during the Middle Ages, forest microrefugia are areas that for some reason had not been cleared. In the case of Sant Maurici, the causes for local forest persistence in apparently natural-like conditions remain unknown. The Llebreia record may provide some clues in this respect, as it has documented a certain degree of forest exploitation since 1000 CE onward, coinciding with the consolidation of the feudal system. It is possible that some patches of subalpine forests were preserved and managed for wood and/or charcoal extraction to satisfy local needs, probably due to the existence of more permanent human settlements in the highlands, fostered by the development of extensive pastoralism practices and horizontal transhumance.

5.5 Comparison of Montcortès and Sant Maurici Medieval Forests

The observed differences in forest dynamics between the Montcortès and Sant Maurici Medieval records suggest that montane and subalpine forests from the same river basin responded differently to climatic shifts and anthropogenic pressure. In addition to the already mentioned stability in the extent and composition of Sant Maurici subalpine forests, in comparison with the intensive clearing of Montcortès montane woodlands, other differences are worth emphasizing.

Differences in taxonomic composition with elevation are evident and follow patterns similar to the present pattern. Medieval forests were dominated by *Pinus* and evergreen *Quercus* in the Montcortès record, whereas in the Sant Maurici sequence, *Pinus* was the most abundant by far (Fig. 5.11). It is assumed that the dominant *Pinus* species were *P. sylvestris* in Montcortès and *P. uncinata* in Sant Maurici, as occurs today (Fig. 1.10). Regarding anthropogenic pressure, forests around Lake Montcortès were much more disturbed by human activities during the Middle Ages, especially during the Pallars County phase, when montane pine forests were heavily exploited using fire and/or logging, depending on the time interval considered. Cereal cultivation was important during the Migration Period and was replaced by grazing, which was especially intensive during the Muslim and Frank periods, at the expense of deciduous oak forest stands surrounding the lake, which were almost totally removed. In contrast, anthropogenic disturbance in the catchment of Lake Sant Maurici was restricted to the Migration Period and consisted of local, scattered, and short-lived agricultural practices followed by rapid forest regeneration. The more intense and varied human pressure around Lake Montcortès was likely due to the proximity of lowland urban nuclei in the south. Lowland crops such as olive groves or vineyards did not reach Lake Montcortès elevations, except in some warmer MWP phases. Human occupation of the highlands around Sant Maurici was less important and probably seasonal, which could help explain the lower anthropogenic impact. Therefore, contrasting responses of montane and subalpine forests to anthropogenic drivers were largely due to differences in the type and intensity of human disturbance.

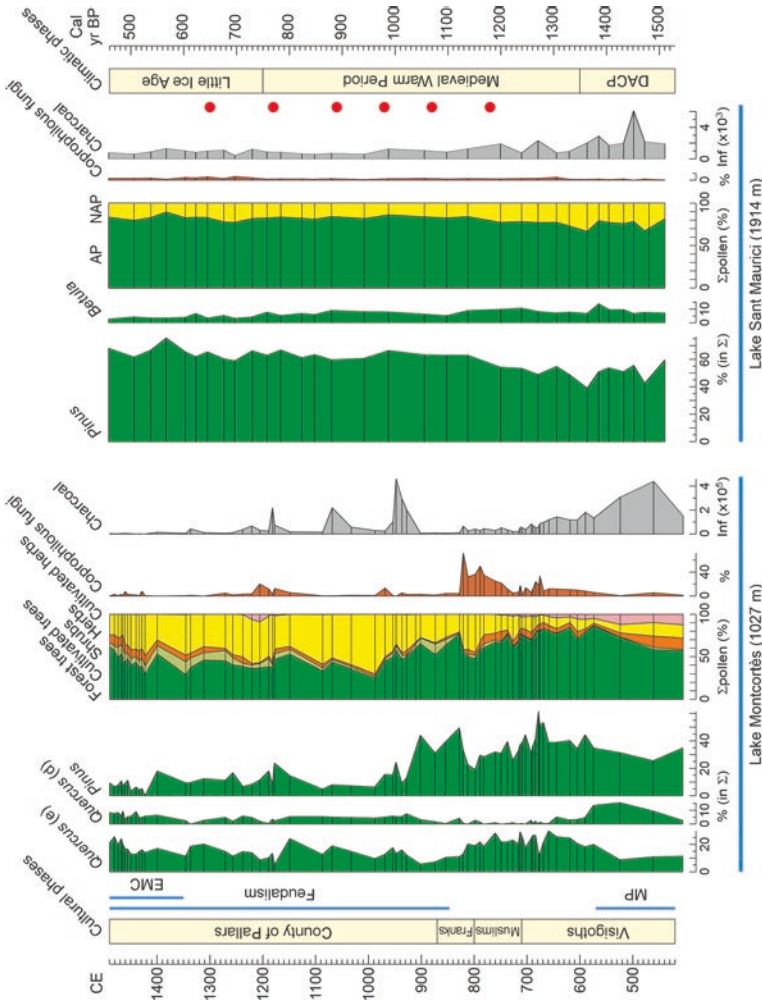


Fig. 5.11 Pollen diagram of the main components of Montcortès and Sant Maurici Medieval forests, reproduced from Figs. 5.1 and 5.8. AP, arboreal pollen; NAP, nonarboreal pollen. Charcoal in influx units (particles $\text{cm}^{-2} \text{yr}^{-1}$); note that the scale of Montcortès is two orders of magnitude (10^2) greater than that of Sant Maurici. Red dots represent the warming peaks of Fig. 5.2. DACP, Dark Ages Cold Period; EMC, ending Medieval crisis; MP, Migration Period

For climate, relevant shifts in continental extent, such as the DACP, the MWP, or the LIA, were the same for Montcortès and Sant Maurici, but the responses of the corresponding forests were different. Indeed, in Montcortès, climatic shifts seem to have been relevant drivers of forest change, either directly or indirectly, by regulating human migrations and/or favoring fire incidence. This was not the case for Sant Maurici, where no evidence of forest response to Medieval climate change was recorded. This high forest resilience in the face of environmental shifts could have been due to specific ecological features of the Sant Maurici forests or, as discussed above, to the position of the lake with respect to elevational ecotones (site insensitivity). Therefore, differences in the responses of plant communities with different taxonomic compositions, such as montane and subalpine forests, to the same climatic shifts may have been determined by idiosyncratic traits (environmental tolerance, response lags, migration speed, etc.) of the involved taxa. The eventual microrefugial character of the Lake Sant Maurici catchment prevents consideration of the differences between this site and Lake Montcortès as a general montane-subalpine elevational pattern. To find such a pattern, if it exists, new pollen records are needed at decadal or similar resolution.

References

- Andela N, Morton DC, Giglio L, Chen Y, van der Werf GR, Kasibhatla PS et al (2017) A human-driven decline in global burned area. *Science* 356:1356–1362
- Ashcroft MB, Gollan JR (2013) Moisture, thermal inertia, and the spatial distributions of near-surface soil and air temperatures: understanding factors that promote microrefugia. *Agric Forest Meteorol* 176:77–89
- Benito G, Macklin MG, Zielhofer C, Jones AF, Machado MJ (2015) Holocene flooding and climate change in the Mediterranean. *Catena* 130:13–33
- Bistinas I, Harrison SP, Prentice IC, Pereira JMC (2014) Causal relationships versus emergent patterns in the global controls of fire frequency. *Biogeosciences* 11:5087–5101
- Blaauw M and Christen JA (2011) Flexible paleoclimate age-depth models using an autoregressive gamma process. *Bayesian Analysis* 6: 457–474
- Bruening JM, Bunn AG, Salzer MW (2018) A climate-driven tree line position model in the White Mountains of California over the past six millennia. *J Biogeogr* 45:1067–1076
- Cabezudo B, Recio M, Sánchez-Laulhé JM, Trigo MM, Toro FJ et al (1997) Atmospheric transportation of marijuana pollen from north Africa to the Southwest of Europe. *Atmos Environ* 31:3323–3328
- Cañellas-Boltà N, Rull V, Vigo J, Mercadé A (2009) Modern pollen-vegetation relationships along an altitudinal transect in the central Pyrenees (southwestern Europe). *The Holocene* 19:1185–1200
- Carrillo E, Aniz M (2013) Guía del Parque Nacional de Aigüestortes i Estany de Sant Maurici. Org Aut Parques Nacionales, Madrid
- Catalan J, Pérez-Obiol R, Pla S (2000) Canvis Climàtics a Aigüestortes durant els darrers 15.000 anys. V Jornades Sobre Recerca al Parc Nacional d'Aigüestortes i Estany de Sant Maurici, Espot, pp 45–52
- Catalan J, Pèlach A, Gassiot E, Antolín F, Ballesteros A, Batalla M et al (2013) Interacción entre clima y ocupación humana en la configuración del paisaje vegetal del Parque Nacional de Aigüestortes i Estany de Sant Maurici a lo largo de los últimos 15.000 años. *Proyectos*

- de Investigación en Parques Nacionales: 2009–2012. Org Aut Parques Nacionales, Madrid, pp 71–92
- Catalan J, Pla-Rabes S, García J, Camarero L (2014) Air temperatures-driven CO₂ consumption by rock weathering at short timescales: evidence from a Holocene lake sediment record. *Geochim Cosmochim Acta* 136:67–79
- Clarke RC, Merlin MD (2016) *Cannabis* domestication, breeding history, present-day genetic diversity, and future prospects. *CRC Crit Rev Plant Sci* 35:293–327
- Corella JP, Valero-Garcés B, Vicente-Serrano SM, Brauer A, Benito C (2016) Three millennia of heavy rainfalls in Western Mediterranean: frequency, seasonality and atmospheric drivers. *Sci Rep* 6:38206
- Corella JP, Benito G, Wilhelm B, Montoya E, Rull V, Vegas-Vilarrúbia T et al (2019) A millennium-long perspective of flood-related seasonal sediment yield in Mediterranean watersheds. *Glob Planet Change* 177:127–140
- Cunill R, Soriano JM, Bal MC, Pèlachs A, Rodríguez JM, Pérez-Obiol R (2013) Holocene high-altitude vegetation dynamics in the Pyrenees: a pedoanthracology contribution to an interdisciplinary approach. *Quat Int* 289:60–70
- Demske D, Tarasov PE, Leippe C, Kotliya BS, Joshi LM, Long TW (2016) Record of vegetation, climate change, human impact and retting of hemp in Garhwal Himalaya (India) during the past 4600 years. *The Holocene* 26:1661–1675
- Dubois H, Verkasalo E, Claessens H (2020) Potential of birch (*Betula pendula* Roth and *B. pubescens* Ehrh.) for forestry and forest-based industry sector within the changing climatic and socio-economic sector context of Western Europe. *Forests* 11:336
- Ejarque A (2009) Génesis y Configuración Microregional de un Paisaje Cultural Pirenaico de Alta Montaña Durante el Holoceno: Estudio Polínico y de Otros Indicadores Paleoambientales en el Valle del Madriu-Perafita-Claror (Andorra). Universitat Rovira i Virgili, Tarragona. PhD dissertation
- Ejarque A, Julià R, Riera S, Palet JM, Orengo HA, Miras Y et al (2009) Tracing the history of high-land human management in the eastern pre-Pyrenees: an interdisciplinary palaeoenvironmental study at the Pradell fen, Spain. *The Holocene* 19:1241–1255
- Ejarque A, Miras Y, Riera S, Palet JM, Orengo HA (2010) Testing micro-regional variability in the Holocene shaping of high mountain cultural landscapes: a palaeoenvironmental case-study in the eastern Pyrenees. *J Archaeol Sci* 37:1468–1479
- Esteban A (2003) La Humanización de las Altas Cuencas de la Garona y las Nogueras (4500 a.C.–1995 d.C.). Org Aut Parques Nacionales, Madrid
- Forkel M, Andela N, Harrison SP, Lasslop G, van Marle M, Chuvieco E et al (2019) Emergent relationships with respect to burned area in global satellite observations and fire-enabled vegetation models. *Biogeosciences* 16:57–76
- Garcés-Pastor S, Cañellas-Boltà N, Clavaguera A, Calero MA, Vegas-Vilarrúbia T (2016) Vegetation shifts, human impact and peat bog development in Bassa Nera pond (Central Pyrenees) during the last millennium. *The Holocene* 27:553–565
- Garcés-Pastor S, Cañellas-Boltà N, Pèlachs A, Soriano JM, Pérez-Obiol R, Pérez-Haase A et al (2017) Environmental history and vegetation dynamics in response to climate variations and human pressure during the Holocene in Bassa Nera, Central Pyrenees. *Palaeogeogr Palaeoclimatol Palaeoecol* 479:48–60
- García-Ruiz JM, Tomás-Faci G, Diarte-Blasco P, Montes L, Domingo R, Sebastián M et al (2020) Transhumance and long-term deforestation in the subalpine belt of the central Spanish Pyrenees: an interdisciplinary approach. *Catena* 195:104744
- Giguet-Covex C, Ficetola GF, Walsh K, Poulenard J, Bajard M, Fouinat L et al (2019) New insights on lake sediment DNA from the catchment: importance of taphonomic and analytical issues on the record quality. *Sci Rep* 9:14676
- González-Sampérez P, Aranbarri J, Pérez-Sanz A, Gil-Romera G, Moreno A, Leunda M et al (2017) Environmental and climate change in the southern Central Pyrenees since the Last Glacial Maximum: a review from the lake records. *Catena* 149:668–688

- González-Sampéris P, Montes L, Aranbarri J, Leunda M, Domingo R, Laborda R et al (2019) Escenarios, tiempo e indicadores paleoambientales para la identificación del Antropoceno en el paisaje vegetal del Pirineo Central (NE Iberia). *Cuad Invest Geogr* 45:167–193
- Halsall G (2008) *Barbarian Migrations and the Roman West (376–568)*. Cambridge University Press, Cambridge
- Harrison SP, Prentice IC, Bloomfield K, Dong N, Forkel M, Forrest M et al (2021) Understanding and modelling wildfire regimes: an ecological perspective. *Environ Res Lett* 16:125008
- Holmeier FK and Broll G (2005) Sensitivity and response of northern hemisphere altitudinal and polar treelines to environmental change at landscape and local scales. *Global Ecology and Biogeography* 14: 395–419
- Jasińska AK, Wachowiak W, Muchewicz E, Boratyńska K, Montserrat JM, Boratyński A (2010) Cryptic hybrids between *Pinus uncinata* and *P. sylvestris*. *Bot J Linn Soc* 163:473–485
- Kupfer JA, Cairns DM (1996) The suitability of montane ecotones as indicators of global climatic change. *Progr Phys Geogr* 20:53–272
- Lavrieux M, Jacob J, Disnar J-R, Bréheret J-G, Le Milbeau C, Miras Y et al (2013) Sedimentary cannabitol tracks the history of hemp retting. *Geology* 41:751–754
- Leunda M, González-Sampéris P, Gil-Romera G, Aranbarri J, Moreno A, Oliva-Urcia B et al (2017) The Late-Glacial and Holocene Marbor_e Lake sequence (2612 m a.s.l., Central Pyrenees, Spain): testing high altitude sites sensitivity to millennial scale vegetation and climate variability. *Glob Planet Change* 15:214–231
- Martín-Chivelet J, Muñoz-García MB, Edwards L, Turrero MJ, Ortega AI (2011) Land surface temperature changes in northern Iberia since 4000 yr BP, based on $\delta^{13}\text{C}$ of speleothems. *Glob Planet Change* 77:1–12
- Marugan CM, Rapalino V (2005) *Història del Pallars. Dels Orígens als Nostres Dies*. Pagés Ed, Lleida
- McLaughlin BC, Ackerly DD, Klos PZ, Natali J, Dawson TE, Thompson SE (2017) Hydrologic refugia, plants, and climate change. *Glob Ecol Biogeogr* 23:2941–2961
- McPartland JM, Guy GW, Hegman W (2018) *Cannabis* is indigenous to Europe and cultivation began during Copper or Bronze Age: a probabilistic synthesis of fossil pollen studies. *Veg Hist Archaeobotany* 27:635–648
- Mercuri AM, Accorsi CA, Bandini M (2002) The long history of *Cannabis* and its cultivation by the Romans in central Italy, shown by pollen records from Lago Albano and lago di Nemi. *Veg Hist Archaeobotany* 11:263–176
- Miras Y, Ejarque A, Riera S, Palet JM, Orengo H, Euba I (2007) Dynamique holocène de la végétation et occupation des Pyrénées andorranes depuis le Néolithique ancien, d'après l'analyse pollinique de la tourbière de Bosc dels Estanyons (2180 m, Vall de Madriu, Andorre). *C R Palevol* 6:291–300
- Miras Y, Ejarque A, Riera S, Orengo H, Palet JM (2015) Andorran high Pyrenees (perafita valley, Andorra): Serra Mitjana fen. *Grana* 54:313–316
- Montserrat Martí JM (1992) Evolución Glaciar y Postglaciar del Clima y la Vegetación en la Vertiente Sur del Pirineo: Estudio Palinológico. *Monogr Inst Pirenaico Ecol (CSIC)* 6:1–147
- Munuera M, Carrión JS, Navarro C (2006) Seasonal fluctuations of the airborne pollen spectrum in Murcia (SE Spain). *Aerobiologia* 18:141–151
- Peglar SM (1993) The development of the cultural landscape around Diss Mere, Norfolk, UK., during the past 7000 years. *Rev Palaeobot Palynol* 76:1–47
- Pèlachs A, Soriano JM, Nadal J, Esteban A (2007) Holocene environmental history and human impact in the Pyrenees. *Contrib Sci* 3:421–429
- Pèlachs A, Pérez-Obiol R, Ninyerola M, Nadal J (2009) Landscape dynamics of *Abies* and *Fagus* in the southern Pyrenees during the last 2200 years as a result of anthropogenic impacts. *Rev Palaeobot Palynol* 156:337–349
- Pèlachs A, Pérez-Obiol R, Soriano JM, Cunill R, Bal M-C, García-Cordón JC (2017) The role of environmental geohistory in high-mountain landscape conservation. In: Catalan J, Ninot JM, Aniz MM (eds) *High-mountain conservation in a changing world*. Springer, Cham, pp 107–129

- Pérez-Sanz A, González-Sampéris P, Moreno A, Valero-Garcés B, Gil-Romera G, Rieradevall M et al (2013) Holocene climate variability, vegetation dynamics and fire regime in the central Pyrenees: the Basa de la Mora sequence (NE Spain). *Quat Sci Rev* 73:149–169
- Pla S, Catalan J (2005) Chrysophyte cysts from lake sediments reveal the submillennial winter/spring climate variability in the northwestern Mediterranean region throughout the Holocene. *Clim Dyn* 24:263–278
- Riera S, Wansard G, Julià R (2004) 2000-year environmental history of a karstic lake in the Mediterranean Pre-Pyrenees: the Estanya lakes (Spain). *Catena* 55:293–324
- Rull V (2005) Vegetation and environmental constancy in the Neotropical Guayana Highlands during the last 6000 years? *Rev Palaeobot Palynol* 135:205–222
- Rull V (2009) Microrefugia. *J Biogeogr* 36:481–484
- Rull V (2010) On microrefugia and cryptic refugia. *J Biogeogr* 37:1623–1625
- Rull V (2015) Long-term vegetation stability and the concept of potential natural vegetation in the Neotropics. *J Veg Sci* 26:603–607
- Rull V, Vegas-Vilarrúbia T (2015) Crops and weeds from the Estany de Montcortès catchment, central Pyrenees, during the last millennium: a comparison of palynological and historical records. *Veget Hist Archaeobot* 24:699–710
- Rull V, Vegas-Vilarrúbia T (2021a) A spatiotemporal gradient in the anthropization of Pyrenean landscapes. Preliminary report. *Quat Sci Rev* 258:106909
- Rull V, Vegas-Vilarrúbia T (2021b) Conifer forest dynamics in the Iberian Pyrenees during the Middle Ages. *Forests* 12:1685
- Rull V, Vegas-Vilarrúbia T (2022) Climatic and anthropogenic drivers of forest succession in the Iberian Pyrenees during the last 500 years: a statistical approach. *Forests* 13:622
- Rull V, González-Sampéris P, Corella JP, Morellón M, Giralt S (2011) Vegetation changes in the southern Pyrenean flank during the last millennium in relation to climate and human activities: the Montcortès lacustrine record. *J Paleolimnol* 46:387–404
- Rull V, Cañellas-Boltà N, Vegas-Vilarrúbia T (2021a) Late-Holocene forest resilience in the central Pyrenean highlands as deduced from pollen analysis of Lake Sant Maurici sediments. *The Holocene* 31:1797–1803
- Rull V, Vegas-Vilarrúbia T, Corella JP, Valero-Garcés B (2021b) Bronze Age to Medieval vegetation dynamics and landscape anthropization in the south-central Pyrenees. *Palaeogeogr Palaeoclimatol Palaeoecol* 571:110392
- Rull V, Vegas-Vilarrúbia T, Corella JP, Trapote MC, Montoya E, Valero-Garcés B (2021c) A unique Pyrenean varved record provides a detailed reconstruction of Mediterranean vegetation and land-use dynamics over the last three millennia. *Quat Sci Rev* 268:107128
- Rull V, Cañellas-Boltà N, Vegas-Vilarrúbia T (2021d) Late-Holocene forest resilience in the central Pyrenean highlands as deduced from pollen analysis of Lake Sant Maurici sediments. *Holocene* 31:1797–1803
- Small E (2015) Evolution and classification of *Cannabis sativa* (marijuana, hemp) in relation to human utilization. *Bot Rev* 81:189–291
- Sweeney L, Harrison SP, Vander Linden M (2022) Assessing anthropogenic influence on fire history during the Holocene in the Iberian Peninsula. *Quat Sci Rev* 287:107562



Abstract

The forest recovery initiated with the final Medieval crisis ended soon (1500 CE), when a third large-scale deforestation began, linked to a significant regional population increase. Maximum deforestation (~50% and >60% less tree pollen than present and Late-Bronze values) occurred by the middle eighteenth century, coinciding with the maximum of iron forges, which required abundant carbon supplies. Minimum forest cover also coincided with an abrupt increase in large-scale hemp retting, which was the main activity around the lake between the sixteenth and nineteenth centuries, to provide fiber for sails and ropes to the royal navy, which was crucial for the worldwide expansion of the Spanish Empire. Forest recovery started in the transition to Contemporary times (late-eighteenth century) and continued until the present, with a minor and brief retraction during the Industrial Revolution (mid-late nineteenth century). Hemp retting was abandoned by 1850 CE, coinciding with the end of the Spanish Empire and the dismantling of the royal navy. This was also the onset of a major regional depopulation of the Pallars region due to the massive emigration to lowland industrialized cities, notably Barcelona and its surroundings. Hemp cultivation in the southern Montcortès lowlands was revived in the 1980s to provide pulp for the paper industry and declined again in the 2000s.

6.1 The Pollen Diagram

6.1.1 General Description

The Montcortès post-Medieval diagram (Fig. 6.1) is more homogeneous than its Medieval and pre-Medieval counterparts (Figs. 4.1 and 5.1). Another characteristic

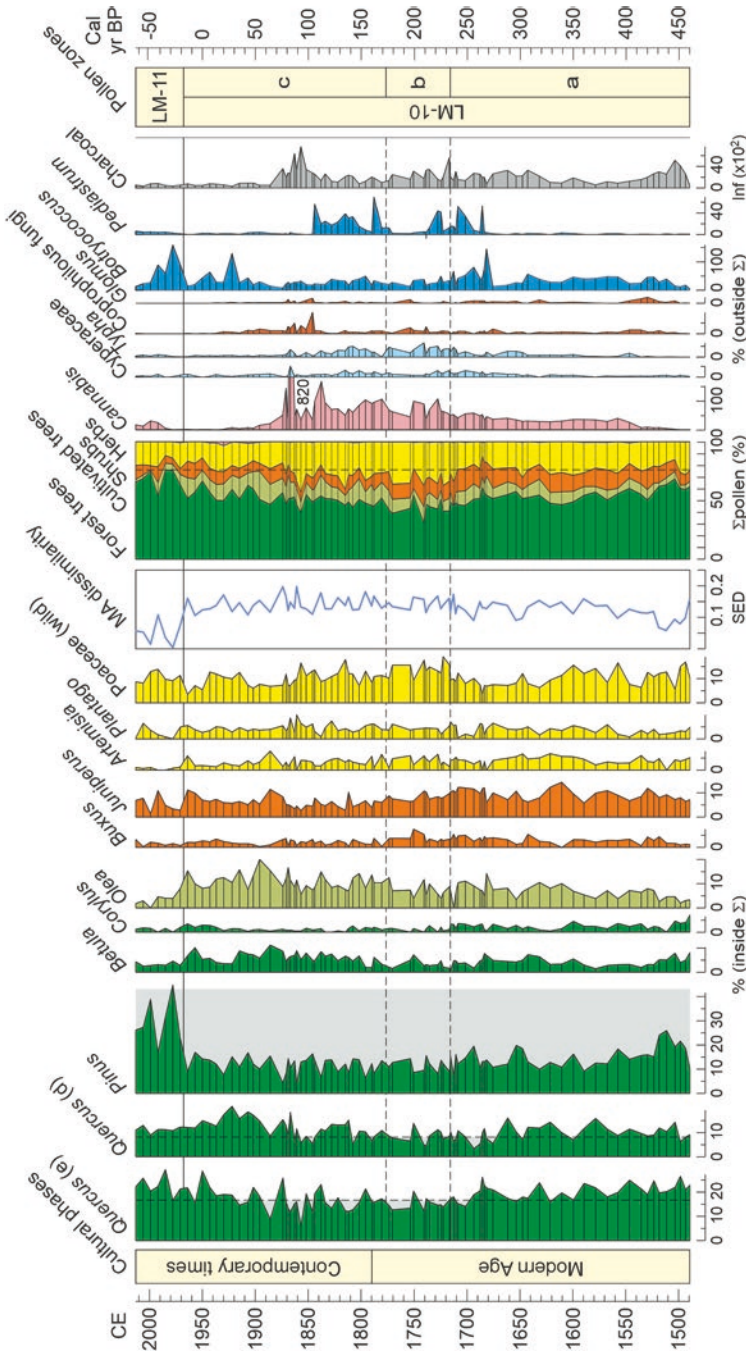


Fig. 6.1 Percentage pollen diagram of Lake Montcortès record corresponding to the Modern Age and Contemporary times. Charcoal is represented in influx units (particles $\text{cm}^{-2} \text{yr}^{-1}$). Cultural phases according to Marugan and Rapalino (2005), as explained in Chap. 2. Vertical dotted lines in the forest pollen curves and the pollen sum represent modern sedimentation percentages, excluding *Cannabids*. In the forest pollen curves, values below these percentages are highlighted by gray bands

feature of the pre-Medieval sequence is the presence of several codominant taxa instead of a few dominant pollen types. Among forest trees, evergreen *Quercus* is generally slightly above deciduous *Quercus* and *Pinus*, although *Pinus* undergoes a marked increase at the top and becomes dominant. Except for this upper section, the *Pinus* percentages are at least one-third of modern values throughout the whole diagram, whereas evergreen *Quercus* fluctuates around modern values, and deciduous *Quercus* is more abundant than in modern samples. Overall, forest trees are consistently below present-day percentages, especially in the middle part of the diagram, where they are almost half of modern values. The most abundant cultivated tree is *Olea*, with values similar to those of some forest trees, while *Juniperus* is the most abundant shrub. Among herbs, wild grasses dominate with values comparable to forest trees, taken individually. Post-Medieval pollen assemblages are markedly dissimilar to modern ones, with the exception of the uppermost part of the diagram, where the similarity significantly increases, likely due to the noticeable *Pinus* increment. The most important element outside the pollen sum is *Cannabis*, with values of 100% toward the middle of the diagram, coinciding with lower but relevant increases in aquatic plants (Cyperaceae, *Typha*) and the alga *Pediastrum*. Charcoal is present with influx values two orders of magnitude below the Medieval standards (Fig. 5.1) and three orders of magnitude below pre-Medieval times (Fig. 4.1).

6.1.2 Zonation

Owing to the outstanding homogeneity, only two significant pollen zones could be distinguished in this diagram. This zonation scheme is quite different from previous analyses in which six zones were defined by including *Cannabis* in the pollen sum (Trapote et al. 2018). As quoted in the methodological section (Chap. 3; Sect. 4.1), the awareness that the main source of *Cannabis* pollen was hemp retting, rather than local cultivation, admonished the exclusion of this type from the pollen sum, which has provided a new and simpler zonal framework that is disclosed as follows (boundaries are between-sample interpolations):

6.1.2.1 Zone LM-10 (1490–1968 CE; 460 cal yr BP to 18 cal yr Postbomb; Modern Age to the Transition to Capitalism)

This zone extends along almost the entire diagram, and therefore, the general description above applies, except for the uppermost part of the sequence, which corresponds to zone LM-11. Despite the general homogeneity of pollen assemblages, three subzones (a, b, and c) could be distinguished. Subzone a (1490–1717 CE; 460–233 cal yr BP) shows a gradual decline in forest elements, which attain minimal values in subzone b (1717–1775 CE; 233–175 cal yr BP) and progressively recover in subzone c (1775–1968 CE; 175 cal yr BP to 18 cal yr postbomb). The recession and recovery phases are not symmetrical due to some differences in the individual forest components. The main differences are in evergreen *Quercus*, which displays percentages over present-day values in subzone a and decreases to

values similar to those present in subzones b and c; and deciduous *Quercus*, with comparatively higher values in subzones a and c, and modern-like percentages in subzone b. *Olea*, *Juniperus*, and wild Poaceae also contribute to the differentiation of this subzonal pattern. Indeed, whereas junipers are more abundant in subzone a, grasses show their maximum in subzone b, and olive trees have higher values in subzone c. Overall, zone LM-10 holds maximal dissimilarity values with respect to modern pollen assemblages. Elements outside the pollen sum follow a different pattern, characterized by the occurrence of a consistent increase in *Cannabis*, aquatic macrophytes (Cyperaceae, *Typha*), and *Pediastrum* between approximately 1650–1700 CE (300–250 cal yr BP) and 1850–1880 CE (150–100 cal yr BP). An exceptional peak of *Cannabis* (>800% of the pollen sum) is recorded at 1867 CE (83 cal yr BP) followed by an abrupt decline to minimal or zero values at the top of the zone, coinciding with a similar trend in charcoal influx.

6.1.2.2 Zone LM-11 (1968–2013 CE; 18–63 cal yr Postbomb; Capitalism)

The most relevant difference of this pollen zone with respect to the former is the quick recovery of forest trees, mainly due to the spectacular recovery of *Pinus*, which attains values similar to modern samples for the first time after the abrupt mid-Medieval decline (910 CE; see Chap. 4). The similarity between the pollen assemblages of this zone and the modern analogs described in Chap. 3 is also maximized. *Betula* and *Olea* decrease to their minima and *Cannabis* reappears in the middle but with lower values as in subzone LM-10b.

6.2 Vegetation and Landscape Dynamics

As in former chapters, the interpretation of the above pollen zones in terms of vegetation and landscape change is organized by cultural and historical phases, and dates are rounded to tens to be consistent with the average resolution of the study.

6.2.1 Modern Age

This historical phase entirely falls within pollen zone LM-10, where the forest recovery following the Medieval deforestation documented in Chap. 5 continued for a short period. This recovery initiated at the onset of the ending Medieval crisis (1350 CE) (Fig. 5.1) and peaked at the beginning of the Modern Age, shortly after 1500 CE, when the gradual forest decline that characterizes subzone LM-10a began (Fig. 6.2). The declining forests were fairly different from present-day regional forests, as they were dominated by evergreen *Quercus* followed by deciduous *Quercus*, both with values slightly above the present, and *Pinus*, with abundances approximately three times smaller than at present. This composition suggests that pine forests continued to be exploited, likely by logging, due to the low fire incidence, compared with pre-Medieval and Medieval times (Sect. 1.3 of this chapter). The

Pallars population was increasing after the ending Medieval crisis, in part by the intense migration from the French side of the Pyrenees (Chap. 3; Sect. 5.2). Historical records document increased forest exploitation in the Pallars and surrounding Pyrenean regions, mainly to obtain charcoal not only for domestic uses but also to fuel the growing iron industry, as manifested in the expansion and modernization of forge devices (Pèlachs et al. 2009; Ejarque et al. 2009; Ferrer Àlòs

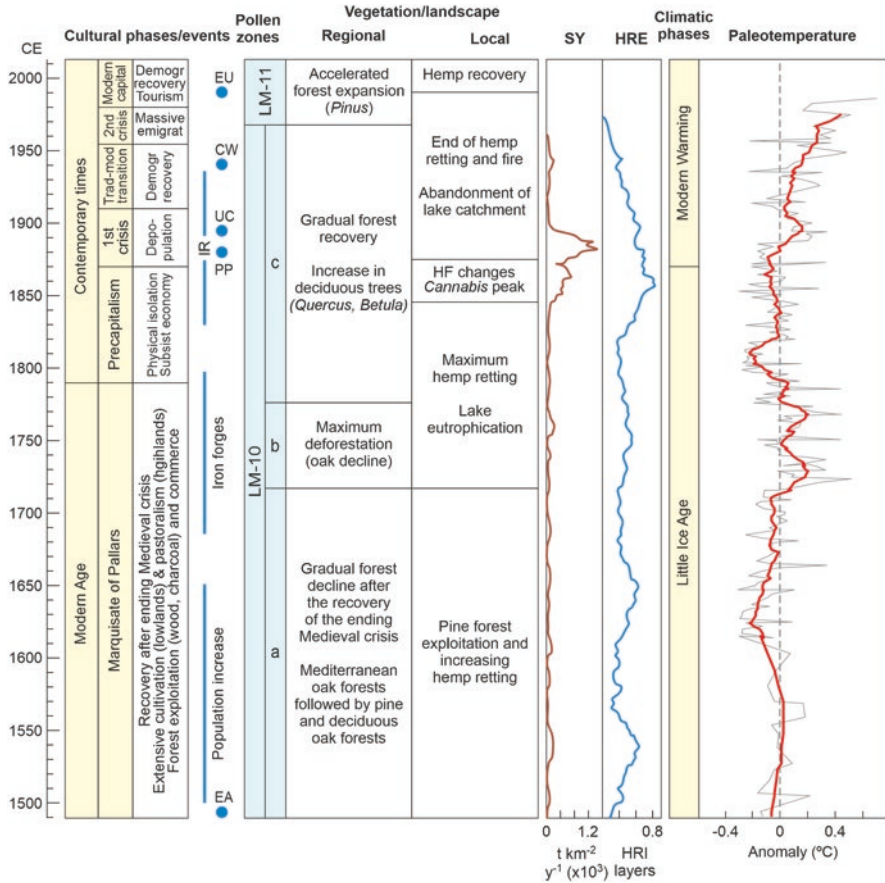


Fig. 6.2 Pollen zones (in blue) and vegetation reconstruction in relation to cultural history and climatic phases (in yellow) during the post-Medieval interval of the Lake Montcotès record. Historical and cultural phases according to Marugan and Rapalino (2005), as explained in Chap. 2; EU, European Union subsidies to hemp cultivation; IR, Industrial Revolution in Catalonia; EA, European discovery of America; PP, phylloxera plague; UC, unfavorable climates and poor harvests; CV, Spanish Civil War. Sediment yield (SY) in thousand tons per square km per year ($t\ km^{-2}\ yr^{-1} \times 10^5$); heavy rainfall events (HRE) in heavy rainfall-induced (HRI) layer occurrence (31-y running average) (Corella et al. 2016, 2019). Climatic phases and paleotemperature reconstruction according to Martín-Chivelet et al. (2011) for the northern Iberian Peninsula (see Fig. 3.7 for reference). The thin gray line represents the raw data, and the thicker red line represents the 10-yr moving average. HF, high-frequency

2017) (Fig. 6.3). Forest clearing to expand grazing lands was also a common practice, especially in mountain areas.

The increase in *Cannabis* o values up to 50% of the pollen sum and the absence of cultivation and grazing proxies suggest that hemp retting increased and became the main activity around the lake. This occurred in a regional context of demographic recovery after the ending medieval crisis, which resulted in continued forest exploitation and increased cultivation (lowlands) and pastoralism (highlands). Lake Montcortès was in an intermediate position, and neither cultivation nor grazing seemed to have been well developed in its surroundings, which is consistent with the continued paucity of sediment delivery to the lake (Fig. 6.2). It has been suggested that the lake could have been used as a water source and rest area for livestock on the way to high-mountain areas (Trapote et al. 2018). This occurred during an extended LIA cooling phase, when temperatures were usually below present ones, which does not seem to have been a handicap for increased human pressure. The potential role of climate in vegetation and landscape change during the Modern Age will be discussed after detailed quantitative analyses in Sect. 5 of this chapter.

The Montcortès forests attained their minimal extent at the end of the Modern Age, between approximately 1720 CE and 1780 CE, which suggests a peak of forest exploitation practices. In that case, Mediterranean and submontane oak forests were more affected than montane pine forests. The conspicuous increment of hemp pollen (up to 100% of the pollen sum) indicates a remarkable increase in hemp retting in lake waters, which coincided with the expansion of littoral vegetation and rising lake productivity, as indicated by significant increases in aquatic macrophytes, especially *Typha*, and freshwater algae. Retting induces changes in water quality, notably eutrophication and oxygen depletion, which can lead to important changes in aquatic communities (Anderson 1995; Tahir et al. 2011; Clarke and Merlin 2013). The ability of *Typha* and some aquatic Cyperaceae to quickly grow in



Fig. 6.3 Catalan forge (*farga*) of the XVII century from the Ethnographic Museum of Ripoll (<https://www.museuderipoll.org/>). Downloaded and reproduced with permission

nutrient-enriched waters is well known (Newman et al. 1996; Miao and Sklar 1998). Increases in *Pediastrum* and other algae, such as *Tetraedron*, have also been recorded in Lake Estanya in the Pyrenean piedmont (Fig. 5.9), as a result of retting-related eutrophication during the Middle Ages (Riera et al. 2006). In Lake Montcortès, isolated but exceptionally high values of *Tetraedron* have been found coinciding with some *Cannabis maxima* (Trapote et al. 2018). The whole picture points toward eventual lake eutrophication as a result of increased nutrient inputs from decomposing hemp plants during the retting process.

The phase of maximum deforestation coincided with a maximum of the iron industry by a significant increase in forge construction and, as a consequence, in charcoal demand (Chap. 3; Sect. 5.4.5). This occurred during a warming phase, reaching temperatures higher than present ones, within the general LIA cooling (Fig. 6.2). This warming may have promoted the upward migration of Mediterranean oak forests at elevations higher than today and boosted their exploitation around the lake, thus contributing to the local forest decline and the associated landscape opening. The rise in hemp retting could also have been indirectly favored by higher temperatures, which could have facilitated human activities in the lake catchment. A small fire peak at the beginning of the maximum deforestation phase would be compatible with some degree of forest burning, but the further decrease in this agent suggests that tree felling was likely the main forest management activity and that little relationship existed between warming and fire incidence. Once more, it is possible that this warming could have facilitated upward migrations of human populations, thus contributing to an upward expansion of forest exploitation following the ascent of Mediterranean oak woodlands. Sediment delivery to the lake continued to be low, probably because of the eutrophy-driven expansion of the littoral macrophytic belt, which could have restricted the sedimentary input to the water body.

6.2.2 Precapitalism

The end of the Modern Age and the establishment of the traditional precapitalist society coincided with the onset of a sustained forest recovery that lasted until the present. The main taxa responsible for this forest recovery were deciduous trees such as *Quercus* and *Betula*, whereas evergreen *Quercus* and *Pinus* forests remained at a similar extent as in later Modern times, when forest cover was minimal. Hemp retting was maximized and lake eutrophication continued. It is possible that forest exploitation diminished in favor of the hemp industry, thus allowing woodlands to expand. A return to LIA colder climates might have also lessened forest exploitation. Historical documents report a significant increase in *Cannabis* cultivation in the lowlands, likely as a result of technical improvements and enhanced irrigation, which boosted soil productivity and allowed the procurement of more than one harvest per year (Sanz 1995; Salrach 2004). This phenomenon has been documented for the lowlands surrounding Lake Montcortès (Madoz 1845–1950), which may have become a preferred hemp-retting center due to its proximity and the suitability of its waters for the development of microorganisms responsible for the detachment

of hemp fibers from the stalk (Rull and Vegas-Vilarrúbia 2014; see also Sect. 3 of this chapter).

A phase of high variability existed between approximately 1845 CE and 1875 CE, which was characterized by short and alternating peaks of hemp, fire, and grazing, after the abrupt disappearance of *Pediastrum*. This phase also coincided with a short deforestation event affecting primarily deciduous and evergreen oaks. One of the alternating peaks was the maximum of *Cannabis* that occurred by 1867 CE at the very end of the precapitalist period. After this phase of high-frequency changes, hemp retting declined abruptly and disappeared from the lake catchment a few decades later, coinciding with the end of macrophytic and algal eutrophication indicators. The high variability of catchment uses over a short time period (barely 30 years) is difficult to explain due to the rapid (possibly annual or less) turnover. Historically, these three decades were also characterized by rapid and significant changes, including the Carlist wars for the Spanish throne (1846–1849 CE and 1873 CE), the end of the Bourbon monarchy (1868 CE), and the proclamation of the First Republic (1873 CE). Notably, the Carlist wars have an influence on the Montcortès region, especially in La Pobla de Segur (Fig. 2.4), where the church was burned (Marugan and Rapalino 2005). From an economic point of view, this phase also witnessed relevant changes, notably the decadence of the forges (1850–1875 CE).

The 1845–1875 enigmatic period also coincided with a relevant increase in sediment yield associated with frequent heavy rainfall events, which would be consistent with a phase of higher climatic variability, especially in the precipitation regime. Corella et al. (2014) recorded a phase of extreme floods in the Montcortès catchment between 1844 CE and 1894 CE, which was correlated with a phase of maximum frequency and intensity of flooding events across the whole Iberian Peninsula (Llasat et al. 2005; Barriendos and Rodrigo 2006; Benito et al. 2008). The possibility that these extreme events would have prompted some degree of sediment reworking and further mixing should not be ruled out. In such a context, the high-frequency alternation of peaks in the palynological record could be a sedimentary artifact rather than a paleoecological feature. More studies are needed for a sound interpretation of this enigmatic interval that coincided with the first phases of the Industrial Revolution and the onset of current Global Warming.

6.2.3 Demographic Crises and the Transition to Capitalism

Forest recovery continued with further increases in deciduous *Quercus* and *Betula* stands. *Olea* and *Juniperus* also underwent significant increases, suggesting enhanced olive grove cultivation in the lowlands and shrub expansion in the vicinity of the lake to the detriment of grass meadows. The most significant shift around the lake was the end of hemp retting at the beginning of this interval (1890–1900 CE), which was coeval with the cessation of fire. Indicators of anthropogenic pressure were absent for the whole phase, which suggests the abandonment of the lake catchment by humans, a situation that remained until the late twentieth century. This occurred during the crisis of the subsistence economy, when the Pallars region

underwent a serious demographic crisis and lost a third of its population (Chap. 2, Sect. 6.2). Several factors contributed to this population crash, which was the local manifestation of a generalized European crisis, including unfavorable climates, a succession of bad harvests, and the phylloxera plague, among others. The Pallars population emigrated not only to larger cities but also to other European countries and even overseas. A further population recovery (1910–1960 CE) linked to the development of hydroelectric and dairy industries did not have a reflection in the Montcortès paleoecological record. A second crisis began in 1960 CE due to the massive emigration of the Pallars population to industrialized areas. This time interval was the beginning of modern Global Warming, but in the Pallars region, the main driver of landscape change was anthropogenic, rather than climatic. In summary, despite the profound socioeconomic changes experienced during this turbulent historical phase (including the Spanish Civil War and the Franco dictatorship), the transition from a traditional society based on a subsistence economy to a modern capitalist society appears in the Lake Montcortès record as a homogeneous phase characterized by the cessation of hemp retting and fire practices and the abandonment of the lake catchment and its surroundings.

6.2.4 Capitalism

The general depopulation of the region and the further shift to a mostly tourist-based economy fostered a general forest recovery that, in the Montcortès record, was expressed in an accelerated expansion of *Pinus* woodlands leading to present-like standards. The Lake Montcortès catchment remained free from evident human impacts until approximately 1990 CE, when *Cannabis* pollen reappeared in moderate abundance. However, according to local people, the Lake Montcortès catchment has not been used for hemp cultivation or retting in recent decades, and hence, a different source of *Cannabis* pollen should be considered (see the next section for a discussion of this topic). Instrumental records confirm that Global Warming continued in the Montcortès region (Chap. 2; Sect. 3).

6.3 Hemp Industry in Lake Montcortès and Surrounding Areas

6.3.1 The Montcortès Record

Lake Montcortès was used for hemp retting during the Modern Age and the precapitalist period, which totaled more than 300 years, from the mid-sixteenth to late-nineteenth centuries. The rise and fall of hemp retting in Lake Montcortès is strongly linked to economic and sociopolitical aspects and deserves further explanation. First, it should be noted that despite the long and intensive use of the lake for retting purposes, there is a surprising lack of information on these activities in historical documents and in the oral tradition. In addition to reviewing the historical literature,

the authors visited historical archives where unpublished documents are preserved and asked local people with historical knowledge and did not find any reference to the lake as a retting place. According to these sources, the hemp industry was active in the region, but the use of Lake Montcortès as a retting place was not mentioned, which is surprising considering the length and importance of the *Cannabis* pollen record in the sediments of this lake. This also contrasts with the situation of similar karstic lakes such as Lake Estanya (Fig. 5.9), where both historical sources and local people documented the importance of retting practices since their introduction during the Middle Ages (Riera et al. 2004, 2006). A more exhaustive review of the historical documentation is needed for a more conclusive assessment.

According to Sanz (1995), during the early Modern Age (sixteenth and seventeenth centuries), hemp farming in most of the Iberian Peninsula primarily aimed to meet local demands, such as providing fiber for clothing and trade. It is likely that the overall increase in hemp cultivation during this period was driven by the rising prices of hemp fiber. In the eighteenth century, hemp production rates rose significantly to supply materials, particularly for the naval industry, such as sails and ropes. This uptick in production coincided with a period of remarkable prosperity for the Spanish royal navy, which experienced substantial growth following the Columbian discovery of America. This growth was a crucial factor in the establishment and sustenance of the Spanish Empire, which endured until approximately 1900 CE. The post-Medieval Montcortès record of *Cannabis* pollen clearly follows these trends, as it started shortly after the American conquest and experienced the first significant increase a few decades later (Fig. 6.4). The navy was useful not only to expand the empire but also for worldwide commercial purposes, and this led to the explicit mandate of cultivating hemp in every land suitable for this purpose and selling the harvests to the crown for the growth of the royal navy. During those times, Catalonia was one of the many hemp producers, and Lleida, the province where the Pallars region and Lake Montcortès are located (Fig. 2.1), was an important area for hemp production and fiber manufacturing (Ferrer Alòs 2017). The small town of La Pobleta de Bellveí, situated 6 km W of Lake Montcortès (Fig. 1.3), is mentioned in the literature due to the outstanding skills of its inhabitants for hemp combing (Violant i Simorra 1934). Hemp cultivation was also documented in other surrounding lowland localities, such as La Pobla de Segur and Gerri de la Sal (Madoz 1845–50) (Fig. 1.3). The Montcortès record shows a marked increase in the *Cannabis* pollen curve at the beginning of the eighteenth century, which is coeval with the nationwide mandate of hemp production to be sold to the crown. In contrast with the Middle Ages, when climates were warmer (MWP) and hemp cultivation around the lake could have been possible (Chap. 5, Sect. 2.4), Modern Age climates were too cold (LIA) for hemp crops, and it is assumed that the lake was used for retting due to the suitability of its waters for such purposes.

Another peak in the Montcortès record occurred toward the end of the eighteenth century (Fig. 6.4), just after a general maximum in Spanish hemp production, especially in the eastern sector (Catalunya, Aragón, and Valencia; Fig. 2.1), which produced 70% of the total national crop. During the years 1750 to 1775 CE, there was a significant period of growth in shipbuilding in Barcelona and neighboring

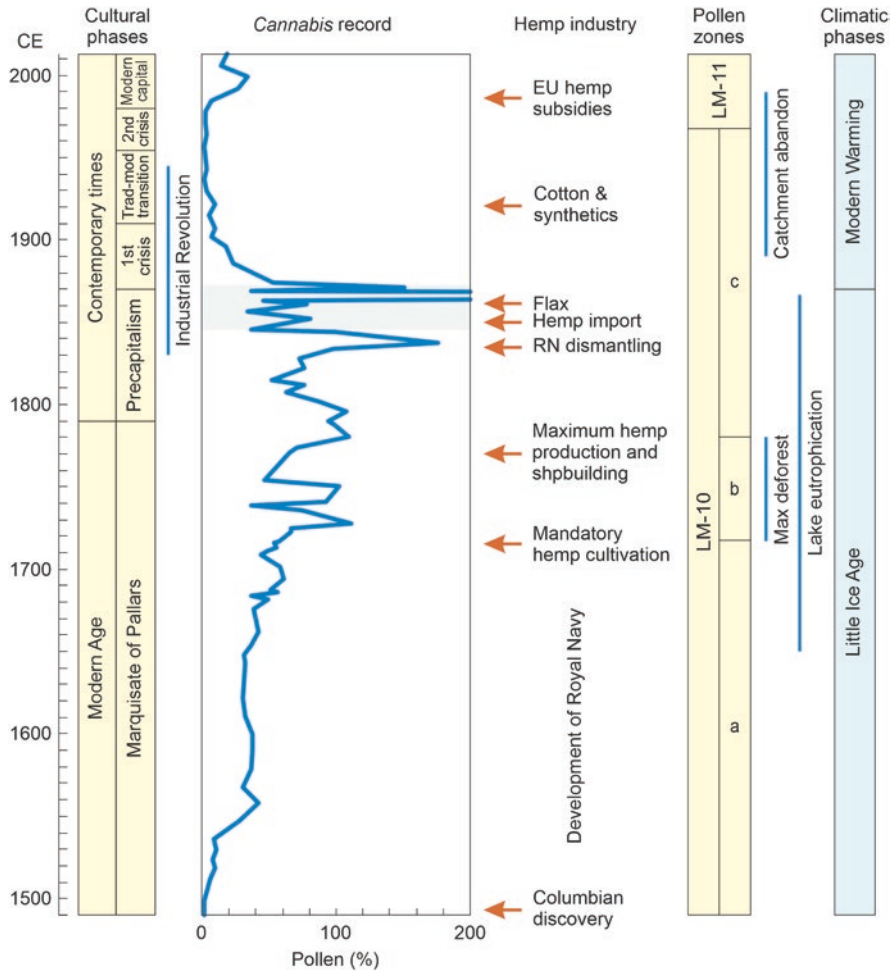


Fig. 6.4 The Montcortès *Cannabis* pollen record (red line) compared with the main events of the Spanish hemp industry during Modern and Contemporary times. Redrawn and modified from Trapote et al. (2018). The horizontal gray band represents the enigmatic 1845–1875 CE phase

shipyards. This period coincided with a broader economic boom and increased trade with America, as indicated by historical sources (Andreu 1981; Delgado 1994). However, a major transformation took place in 1834 CE when the liberal regime was established, leading to the abolishment of feudal privileges and the dismantling of the royal navy. This change was also linked to the decline of the Spanish Empire and had a profound impact on the demand for hemp fiber, causing it to sharply decline. In response to this new situation, hemp products began to be exported to other regions of the peninsula or sold at public auctions. Furthermore, the importation of hemp fiber from other countries, particularly Italy and Sardinia, and manufactured fabrics from France and the United Kingdom (beginning in 1849 CE),

played a significant role in the decline of hemp cultivation. This decline led to the replacement of hemp with other products, including alternative fiber such as flax, starting by 1860 CE (Casassas 1985). In the Montcortès record, an 1838 *Cannabis* pollen peak was followed by an abrupt drop coeval with the above-quoted sharp decline in hemp demand since 1834 (Fig. 6.4). This very characteristic and recognizable event, in both historical and paleoecological records, has been proposed as a chronological datum to be used in historical reconstructions and as a time-calibration point for high-resolution radiometric age-depth models (Rull and Vegas-Vilarrúbia 2014). Previous studies at centennial resolution using radiocarbon dating situated the *Cannabis* peak close to the abovementioned Iberian maximum of hemp production (Rull et al. 2011). However, further high-resolution analyses based on the updated age-depth varve model used in this book (Chap. 4; Sect. 1.2) confirmed that the *Cannabis* peak occurred at 1838 CE (Trapote et al. 2018) and was thus more related to the dismantling of the royal navy and the associated historical events (Fig. 6.4).

After the 1845–1875 CE enigmatic interval, hemp retting ceased in Lake Montcortès (Fig. 6.4), coinciding with the vast Pallars depopulation linked to the crisis of subsistence economy characteristic of precapitalist times. Hemp retting remained absent during the 1910–1960 CE demographic recovery and the ensuing 1960–1980 CE crisis caused by massive emigration to industrial cities. Hemp pollen reappeared in the Montcortès record in the 1980s, but neither cultivation nor retting of this plant has been documented since then in the lake surroundings, which suggests the existence of extralocal regional sources. As demonstrated in the study of modern pollen deposition (Chap. 3; Sect. 4.2), *Cannabis* is present throughout the year in significant percentages (especially in autumn, its flowering season), even in the absence of local cultivation and retting practices (Table 3.4), which has been attributed to the high dispersion power of this anemophilous pollen. Therefore, although the exact source of regional hemp pollen in modern sediments could not be located, it is assumed that it exists somewhere, and a more intensive study of regional vegetation using GIS techniques would be needed to determine its geographical origin (Rull et al. 2017). The same could be valid for the *Cannabis* pollen increase in recent decades, as recorded in the pollen diagram, which coincides with a general expansion of hemp cultivation in Catalonia and in Spain in general, favored by European Union subsidies to this activity (Karus and Kaup 2002; Gorchs and Lloveras 2003).

Hemp cultivation in Spain saw a decline in the early 1970s, but in 1972 CE, there was a resurgence of interest in this crop. Prior to the 1960s, hemp was primarily grown in irrigated semiarid regions across the eastern Iberian Peninsula, mainly for the production of thread, ropes, and fabric. However, in 1972 CE, the paper pulp industry started using hemp as a raw material instead of worn textiles. By the early 1980s, the main production center shifted from the east to the northeast, particularly Catalonia, where lowland areas at elevations of 400–900 m received higher precipitation (600–700 mm per year), eliminating the need for continuous irrigation (Gorchs and Lloveras 2003; Gorchs et al. 2017). This geographical shift coincided with a significant increase in hemp production, with output growing from less than

1000 tons in 1980 CE to over 8000 tons in 1998 CE. This growth was facilitated by the introduction of European Union subsidies for hemp cultivation, which commenced in 1985 CE at 40 euros per hectare and substantially increased to approximately 780 euros per hectare in 1996–1997 CE (see Fig. 6.5). The focus of this increased production was primarily in the southern Pyrenees region, where Lake Montcortès is situated, characterized by a wet climate. Hemp was integrated into a spring crop rotation with winter wheat, leading to significant improvements in wheat yields. This improvement was attributed to the enhancement of soil structure and the role of hemp in controlling pests, diseases, and especially weeds. Hemp's rapid early growth outcompeted most weed species, thereby reducing the weed burden for subsequent winter crops (Gorchs et al. 2017).

The increase in *Cannabis* pollen during the 1980s, as observed in Lake Montcortès, appears to be closely linked to the accelerated production of hemp during the same period, as indicated in Fig. 6.5. This suggests a likely cause-and-effect relationship. Given the ability of hemp pollen to disperse over long distances, as documented in other parts of the Iberian Peninsula (Cabezudo et al. 1997; Munuera et al. 2002; Cariñanos et al. 2004; Aboulaich et al. 2013; Aznar et al. 2022), it is plausible that hemp pollen could have easily reached Lake Montcortès from nearby pre-Pyrenean hemp cultivation areas. This hypothesis could be confirmed by modeling the dispersion of *Cannabis* pollen in the vicinity of the lake. The decline in hemp cultivation began shortly after the 1990s and was eventually abandoned in 2006 CE due to the relocation of the hemp straw processing industry (Gorchs et al. 2017). This decline in hemp cultivation corresponds with changes in pollen trends, strengthening the potential causal connection between the two. However, it is noteworthy that *Cannabis* pollen levels remained elevated compared to pre-1980 levels, persisting until at least 2015 CE, which requires further explanation. While it's possible that additional sources of hemp pollen from illegal crops may have contributed

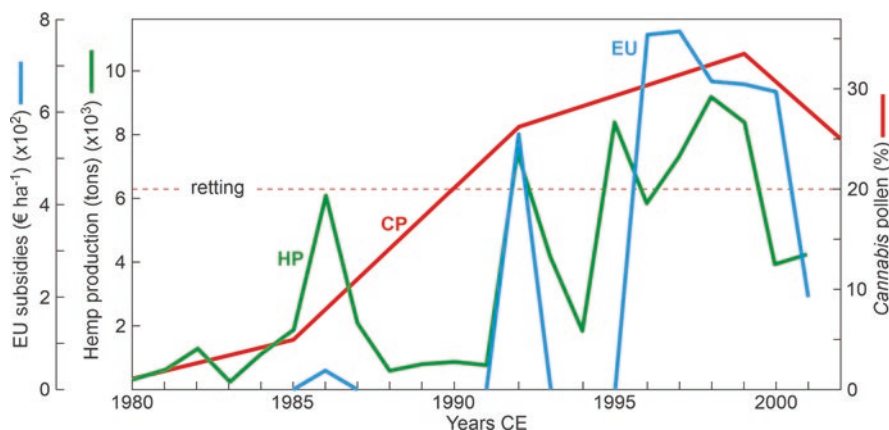


Fig. 6.5 Hemp production (HP) and European Union subsidies (EU) (raw data from Gorchs and Lloveras 2003) compared with the *Cannabis* pollen trends in Lake Montcortès sediments (Fig. 6.4). Modified from Rull and Vegas-Vilarrúbia (2023)

to this phenomenon, the supporting evidence for this is less conclusive. In recent decades, there has been a notable increase in large-scale cannabis plantations across the Iberian Peninsula, particularly along the Mediterranean coasts, as a shift away from hashish imports from northern Africa (Alvarez et al. 2016; Belackova et al. 2016). It remains to be confirmed whether this widespread trend in the peninsula has manifested in the Montcortès region, and this topic should be investigated in future studies.

6.3.2 Direct Evidence for Hemp Retting

Initially, hemp retting in Lake Montcortès was deduced from *Cannabis* pollen abundances, as explained above. However, direct evidence of this process has been obtained recently after phylogenetic identification of the bacteria that actually perform the retting process (Rull et al. 2022). Retting, also known as degumming, is a chemical method used to eliminate noncellulosic substances, typically pectins and hemicelluloses, while keeping the integrity of fibrous tissues intact, allowing the separation of individual fibers (Akin 2013). In the context of hemp, retting is carried out in anaerobic conditions by immersing the material in water to facilitate the activity of pectinolytic bacteria (Tahir et al. 2011). Initially, soluble compounds in the plant stem, such as sugars and nitrogenous substances, dissolve, creating a local bacterial community. Subsequently, water penetration facilitates the detachment of bast fibers, enabling the entry of retting bacteria that break down fiber-binding pectins. Presently, industrial retting employs specific bacterial mixtures (Akin et al. 2001). In the past, the fiber separation process occurred spontaneously when hemp stems were submerged in natural water bodies such as lakes, ponds, rivers, and artificial channels, where native bacterial communities facilitated fiber separation (Fig. 6.6). The water retting process begins with aerobic bacteria, mainly of the *Bacillus* genus, and as oxygen levels decrease, anaerobic bacteria, notably *Clostridium*, become dominant. Other significant retting bacteria belong to genera such as *Escherichia*, *Pantoea*, *Pseudomonas*, *Rhodobacter*, *Rhizobium*, and *Massilia* (Tamburini et al. 2003; Di Candilo et al. 2009; Ribeiro et al. 2015).

The submergence of male hemp plants in lakes leads to the release of pollen, which becomes incorporated into sediments, resulting in an overrepresentation of this pollen in fossil collections. However, relying solely on the abundance of pollen serves as indirect evidence for hemp retting, as highly dispersible anemophilous hemp pollen can also be found in significant quantities in lakes that were not used for hemp retting (Rull et al. 2017). Counting hemp fibers has also been used as a proxy for assessing the intensity of hemp retting, but discrepancies with pollen records and potential interference from local hemp cultivation have been observed (Iwańska et al. 2022). In recent times, the use of biomolecular methods in paleoecology has provided more reliable evidence for identifying past hemp retting in lake sediment sequences. For instance, Lavrieux et al. (2013) utilized sedimentary cannabinal, a specific compound unique to *Cannabis* and absent in pollen grains, as a dependable indicator of retting. Similarly, Giguet-Covex et al. (2019) employed



Fig. 6.6 Hemp washerwoman at Gödöllő (Hungary). Paint of Theodor von Hörmann representing the labor of hemp retting in natural waters. Freely available at Wikimedia Commons (https://commons.wikimedia.org/wiki/File:Theodor_von_Hörmann_Hanfeinlegen.jpg, downloaded 20 May 2022)

sedimentary DNA from *Cannabis sativa* to trace the history of hemp retting. In both cases, comparisons between these specific biomarkers and pollen not only helped reconstruct the retting history of the studied areas but also offered a way to reliably distinguish between *Cannabis* and *Humulus* pollen. Biomarker analysis has also been utilized to identify the microorganisms responsible for breaking down hemp fiber. For example, DNA- and RNA-based taxonomy has enabled the identification of various pectinolytic bacteria and fungi involved in the extraction of hemp fibers (Ribeiro et al. 2015). This suggests that it could theoretically be possible to document past retting processes by identifying the DNA/RNA sequences of these microorganisms in sediment samples from ancient lakes.

In the sediments of Lake Montcortès, we identified and measured the *16S rRNA* genes of bacteria known to be involved in the retting process of hemp (specifically *Bacillus/Paenibacillus*, *Clostridium*, *Escherichia*, *Pseudomonas*, *Massilia*, *Rhizobium*, *Rhodobacter*, and *Methylobacterium*). The presence of these bacteria increased from the mid-sixteenth century and remained relatively stable until the early eighteenth century. Afterward, there was a significant increase, followed by a decline in the mid-eighteenth century, another increase in the second half of the nineteenth century, and a sharp decline in the early twentieth century (Fig. 6.7). This pattern suggests that hemp retting was practiced in Lake Montcortès from the mid-sixteenth century to the early twentieth century, with the peak of activity in the first half of the eighteenth century and a less pronounced resurgence in the second half of the nineteenth century. These findings provide direct evidence that supports previous indications of hemp retting in the region, which were primarily based on indirect evidence such as pollen analysis. Furthermore, the trends in bacterial abundance align with the levels of *Cannabis* pollen, which consistently exceeded 20% throughout the retting phase and reached values between 25% and 60% during periods of more intense retting (eighteenth and nineteenth centuries). This corroborates

the use of a 15–25% threshold for hemp pollen as a reliable indicator of local retting practices, as suggested by various researchers.

The strong correlation between the activity of retting, as indicated by bacterial *16S rRNA* genes, and the abundance of hemp pollen further reinforces the previously established connections between the historical development of the hemp industry in Spain and the hemp pollen record, as shown in Fig. 6.7. For instance, the commencement of hemp retting in Lake Montcortès coincided with the Royal Navy's expansion and reached its peak shortly after hemp cultivation became mandatory throughout the country, as documented by Sanz (1995). It is also worth noting the simultaneous halt in retting activities with the significant depopulation of the Pallars region in the twentieth century. These observations suggest that Lake

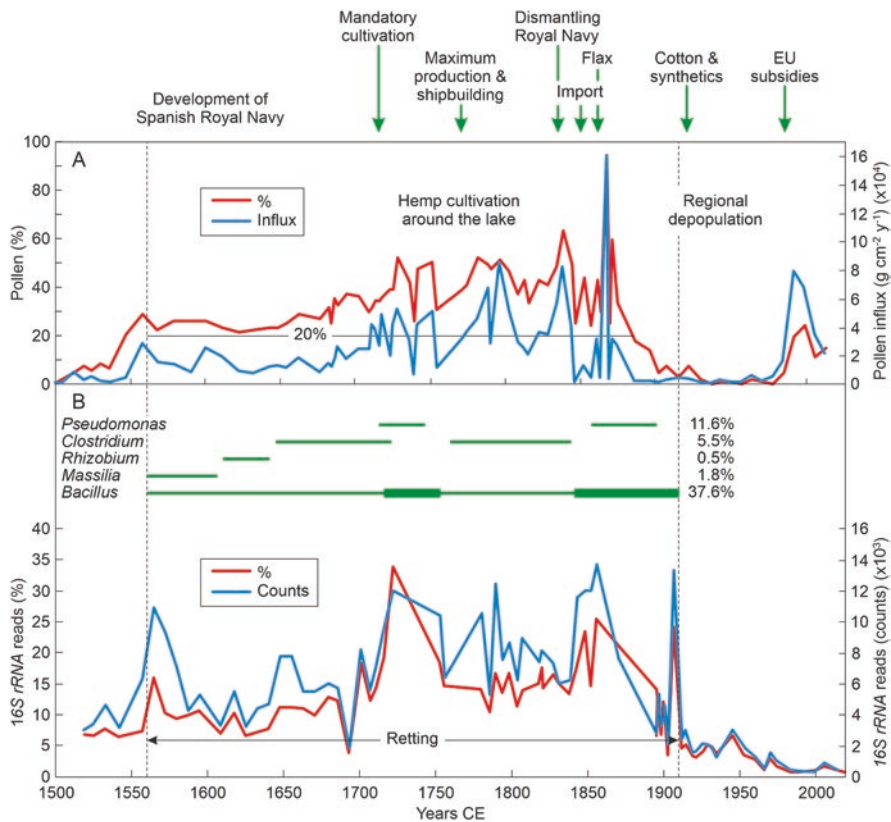


Fig. 6.7 Hemp pollen and phylogenetic bacterial trends in Lake Montcortès sediments corresponding to the last five centuries compared with the main developments of the Spanish hemp industry. (a) Percentage and influx trends from core MONT-0713-G05 (Fig. 3.1). Note the 20% threshold within the retting phase. (b) *16S rRNA* trends in core MONT-0119-11 (retrieved a few meters apart from core MONT-0713-G05) expressed as the total percentage and counts. The horizontal green lines represent the main retting taxa (maximum percentages for each taxon are given on the right side). Reproduced from Rull et al. (2022)

Montcortès may have played a pivotal role as a retting center for locally produced hemp for over four centuries, particularly during the eighteenth and nineteenth centuries. This hypothesis should be further investigated through additional studies.

There are some notable distinctions between the pollen and bacterial dynamics curves. First, the final decline in the pollen record took place several decades earlier, in the late nineteenth century, compared to the bacterial record, which saw it in the early twentieth century. This discrepancy may suggest that retting practices continued even in the absence of hemp. It is important to note that hemp cultivation dwindled significantly after the Spanish Royal Navy's dismantling by 1860 CE, and it was replaced by other fiber sources such as flax. Therefore, it is possible that flax retting replaced hemp retting toward the end of the Montcortès retting period. Further paleoecological and historical studies should explore this possibility. Another noteworthy difference is the pollen increase observed in the last few decades (1980–90 CE onward), which did not mirror the bacterial curve. This implies that this pollen likely originated from sources outside the local area and reached the lake through wind dispersal. The surge in hemp production driven by EU subsidies could play a role in this phenomenon, but the exact source of the hemp pollen in this case remains uncertain.

The changes observed in the overall retting bacteria trends were primarily driven by variations in the dominant taxon *Bacillus/Paenibacillus*, which accounted for a significant portion, up to 38%, of the entire bacterial community and remained consistently present throughout the entire retting phase. In contrast, other taxa were less abundant and exhibited intermittent presence and absence phases, indicating a distinct long-term succession pattern. The retting process initially commenced with a succession of *Massilia*, *Rhizobium*, *Clostridium*, and *Pseudomonas* until it reached its peak around the eighteenth century. Following this peak, the succession restarted, but this time, only the *Clostridium* and *Pseudomonas* stages were evident before reaching a second, less intense retting peak. This suggests that the less abundant taxa, *Massilia* and *Rhizobium*, were only present at the beginning of the retting process, and once the process was underway, these initial stages were omitted. The remaining retting taxa examined, namely, *Escherichia*, *Methylobacterium*, and *Rhodobacter*, were only sporadically present in very low proportions, without any clear presence or absence patterns.

To summarize, the examination of *16S rRNA* genes found in sedimentary samples from bacteria involved in the hemp retting process revealed that this activity took place in Lake Montcortès from the mid-sixteenth century to the early twentieth century, peaking in the first half of the eighteenth century. These findings agree with historical trends seen in hemp pollen records and are consistent with the broader patterns in the Spanish hemp industry over the past five centuries. Notably, hemp pollen levels remained consistently above 20% throughout all phases of retting, indicating that this threshold is a reliable indicator of hemp retting in the lake, consistent with the range observed in previous studies conducted in other regions (15–25%).

6.3.3 The Estanya Record

A similar palynological hemp record was found in the sediments of the nearby Lake Estanya—situated in the Mediterranean lowlands (670 m elevation) approximately 50 km SW of Lake Montcortès (Fig. 5.9)—where historical records of hemp cultivation and retting practices are available (Riera et al. 2004). The Estanya record roughly encompassed the last two millennia at multicentennial resolution (~ 300 years per sampling interval, on average) and documented the onset of the hemp industry by 600 CE (early Middle Ages), with a significant increase in the fourteenth century and a maximum in the mid-eighteenth century, followed by a sharp decline (Fig. 6.8). Due to the low resolution of this record, precise correlations with the Montcortès sequence are difficult to address, but the trends are similar and are consistent with the general development of the hemp industry in Spain. Indeed, the fourteenth-century increase was interpreted in terms of local hemp retting (Lake Estanya is also a karstic lake with hardwaters suitable for the growth of retting microorganisms), and the eighteenth-century maximum was coeval with maximum hemp production in the country to meet the needs of the royal navy. In addition, NPP analysis supported the eutrophication of lake waters, which is common under retting practices (Riera et al. 2006). The same authors attributed the

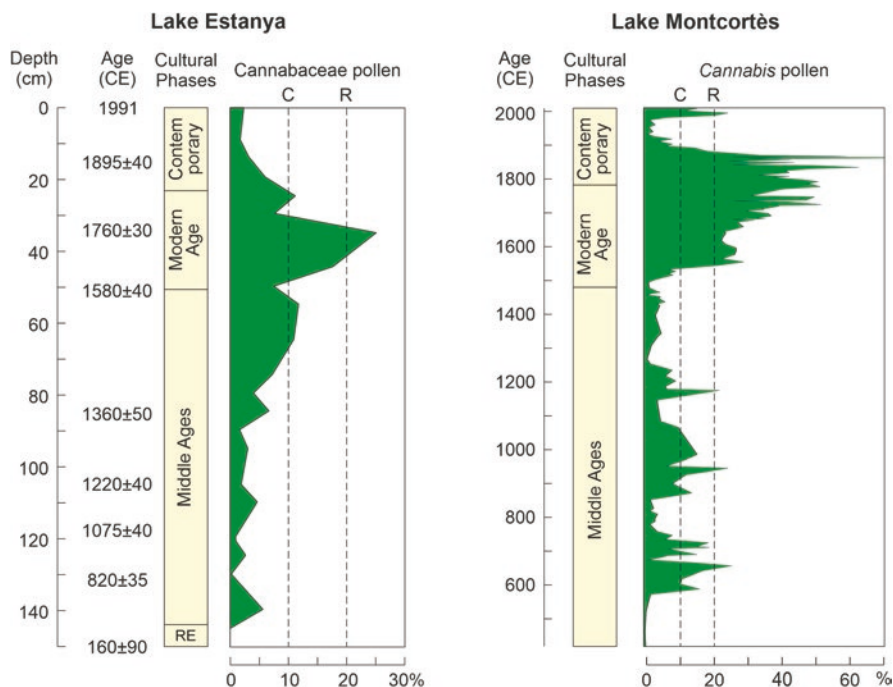


Fig. 6.8 Comparison of the Estanya and Montcortès *Cannabis* pollen records with indication of the thresholds suggested here for cultivation (C) and hemp retting (R). Reproduced from Rull et al. (2023)

post-eighteenth century abrupt decline of hemp pollen to the depopulation of the region and the end of the hemp industry, as occurred in the Montcortès region.

6.3.4 The Iberian Peninsula

The Estanya and Montcortès records are the only available for the Medieval and Modern Age development of the hemp industry and have been considered by some as the rule for the whole Iberian Peninsula (Clarke and Merlin 2013). A recent meta-analysis of continental-wide European records suggests that wild *Cannabis* could have reached the Iberian Peninsula in postglacial times, between 18.5 and 15 cal kyr BP (McPartland et al. 2018). However, this analysis included only a dozen Iberian sites. Until recently, these were the only data used to infer the spatiotemporal trends of *Cannabis* since its introduction in the Iberian Peninsula, which was obviously insufficient for a robust assessment (Rull 2022). Hence, the tempo and mode in which *Cannabis* reached and colonized the Iberian Peninsula, as well as the potential cultural and environmental influences, remain unknown. However, a recent study compiled an extensive database of nearly 60 locations in the Iberian Peninsula that contain pollen-based proof of *Cannabis* presence and examined the associated spatial and temporal trends (Rull et al. 2023). A summary of the main conclusions obtained is provided here.

The initial scattered records of hemp pollen appearing in the Middle and Upper Paleolithic period (150 to 12 cal yr BP) seem to have been introduced to the Iberian Peninsula through maritime routes from the Mediterranean or terrestrial paths from Europe, or possibly both, as depicted in Fig. 6.9. The first burst of hemp introduction, potentially in a cultivated form, probably occurred during the Neolithic, approximately 7 to 5 kyr BP, using similar routes. While it remains uncertain to what extent humans played a role in these Neolithic introductions, their involvement cannot be ruled out. There appears to have been a decline in the arrival of *Cannabis*, mainly through maritime routes, between the Chalcolithic and Roman epochs (4.5–2 kyr BP), when the innermost parts of the IP began to be colonized by this plant. A second, likely human-driven, surge in introductions occurred during the Middle Ages (1.5 kyr onward), using both maritime and overland routes. The highest levels of hemp cultivation and retting activity were documented during the Modern Ages (sixteenth to nineteenth centuries). This period coincided with a growing demand for hemp fiber to meet the needs of the Spanish royal navy, supporting imperial expansion and commerce (Fig. 6.7).

A possible connection between bursts of *Cannabis* colonization or introduction and periods of climatic warming has been observed, and this connection should be explored further in future research. Variations in regional moisture levels appear to have had less influence on these patterns. It is recommended that additional efforts be made to enhance and refine the database used in this study. These findings should be compared with archaeological and historical evidence to gain a clearer understanding of the role of human migrations and cultural changes in the historical distribution of *Cannabis* in the Iberian Peninsula.

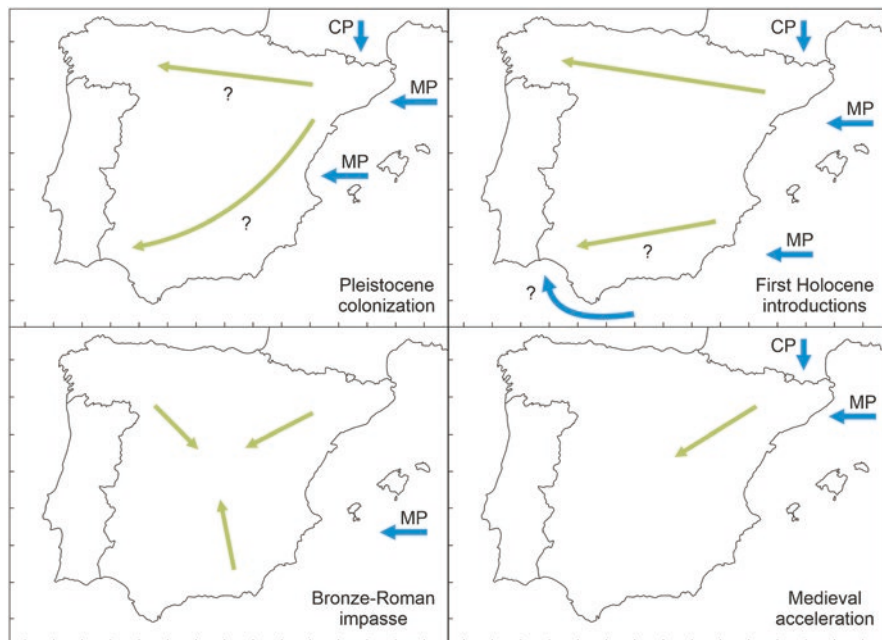


Fig. 6.9 Proposed dispersal pathways of *Cannabis* pollen into (blue arrows) and within (green arrows) the Iberian Peninsula. Reproduced from Rull et al. (2023)

6.4 Modern Age Deforestation

The resolution of the post-Medieval Montcortès record is semidecadal (6 years per sampling interval), which is more than two times the Medieval resolution (Chap. 5; Sect. 3) and enables even more detailed reconstruction of forest trends. The maximum Modern Age deforestation occurred at approximately 1740 CE, when minimal forest values of 27% were attained (Fig. 6.10), corresponding to 35% of the present values and 30% of the maximum forest cover recorded during the whole Montcortès sequence (Bronze Age). Therefore, landscape openness may be estimated to be approximately 65–70%. This occurred during the maximum development of iron forges recorded in the eighteenth century and the beginning of the maximum hemp retting, during an LIA warming reversal, and shortly after a fire peak. The deforestation trend started at 1500 CE and proceeded at relatively slow rates of $-0.07\% \text{ yr}^{-1}$ ($r = -0.889$; $\alpha < 0.01$). As in Medieval deforestation, minor clearing-recovery cycles can be recognized, this time with a recurrence of 35 years, on average. This average trend, however, is the combination of two faster deforestation phases separated by an interval of relative forest stability during the seventeenth century. This trend of forest development is paralleled by a similar tendency in fire incidence, suggesting that although forest fires were significantly less intense than in former times, burning was still an active clearing agent, which is compatible with the population increase recorded in the Pallars region after the ending

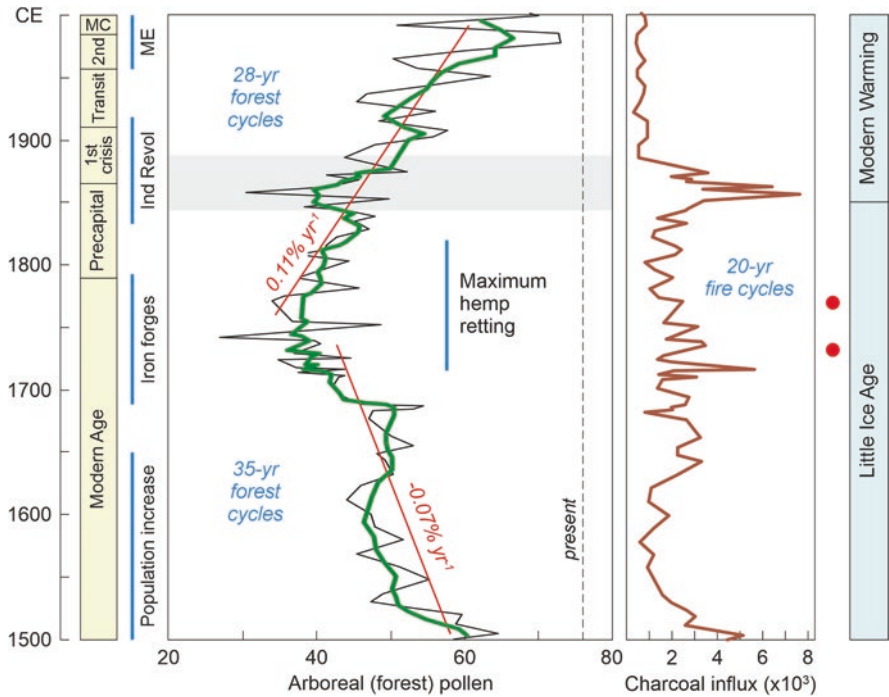


Fig. 6.10 Modern Age deforestation trends represented by the pollen from forest trees (raw data in black, 4-point moving average in green). The present abundance is provided for reference (vertical dotted line). Regression lines used to estimate the average deforestation and recovery rates (in % yr⁻¹) are in red. Charcoal influx is expressed as particles cm⁻² yr⁻¹. Warming peaks from Fig. 5.2 are indicated by red dots. ME, massive emigration of the Pallars population to industrial cities. Modified from Rull et al. (2021)

Medieval crisis (Chap. 2; Sect. 5.2). The chronological relationship with a fire peak at approximately 1630 CE and the onset of the second deforestation pulse seems evident.

Forest recovery was faster and more continuous, progressing at rates of 0.11% yr⁻¹ ($r = 0.782$; $\alpha < 0.01$) with minor cycles of 28-yr recurrence, on average. These cycles were of similar duration as those recorded during deforestation, and therefore, they cannot help explain woodland retraction and expansion patterns, as suggested in the Middle Ages. The fact that post-Medieval forest cycles are shorter than Medieval ones could also be related to the higher resolution of the Modern-Contemporary sequence, in which case cycle duration could be, in part, a sampling artifact and could not be used to infer minor forest trends. Cycles of shorter duration (20-yr on average) can also be observed for fire incidence in the interval between approximately 1600 CE and 1900 CE. These cycles are not correlated ($r = 0.174$; $\alpha > 0.1$) with forest cycles in the same interval, which prevents us from reliably inferring causal links between burning and deforestation cycles at decadal resolution. The enigmatic 1845–1875 CE event also has a manifestation in the forest curve, as

it disrupts the general recovery trend, causing an abrupt drop to values similar to maximum deforestation standards, coeval with a remarkable burning peak. Therefore, this puzzling phase in terms of land use was characterized by short but intense forest burning prior to the total catchment abandonment.

6.5 High-Resolution Statistical Analysis of Forest Succession

The higher resolution of the Montcortès record for the last five centuries, along with the availability of detailed paleoclimatic reconstructions for the same time period from nearby areas, allowed a much more detailed statistical study of the potential influence of natural climatic variability on the development of regional vegetation and landscape. The paleoclimatic reconstruction for the northern Iberian Peninsula utilized in previous analyses (Martín-Chivelet et al. 2011) provided a general framework for assessing the potential role of climate on the main paleoecological tendencies and for comparing these trends with those inferred for Medieval and pre-Medieval times. However, more recent annually resolved quantitative paleotemperature and paleoprecipitation reconstructions for the last centuries obtained in the Montcortès record and the catchment of Lake Gerber situated ~30 km north in the vicinity of PNAESM National Park (Fig. 5.4) enabled more detailed statistical comparisons. These paleoclimatic reconstructions were derived from pollen-independent proxies and, therefore, can be used to analyze the potential responses of past plant ecosystems, as deduced from palynological analysis, to paleoclimatic shifts, avoiding circularity (Chap. 3; Sect. 5).

6.5.1 Paleoenvironmental Records

The tree-ring record from the catchment of Lake Gerber encompassed the last ~830 years (1186–2014 CE) and provided a paleotemperature reconstruction for the warmest season (May–June and August–September; MJ&AS) along with a record of the intensity of Mediterranean summer (June–August; JJA) drought for the same time period (Büntgen et al. 2017) (Fig. 6.11). A reconstruction of the mean regional summer (May–September) temperature for the whole Pyrenean range based on >20 site chronologies covering the period 1260–2005 CE (Dorado-Liñán et al. 2012) is also available. However, this reconstruction has not been used in our analysis because of its regional rather than local character, and because the highly significant correlation with the Lake Gerber reconstruction ($r = 0.857$; $\alpha < 0.001$) warned about potential statistical interferences, such as collinearity, in multivariate analyses (Gareth et al. 2017). In addition to paleotemperature records, a recent study of the varve thickness of Lake Montcortès sediments provided a yearly reconstruction of autumn (September–November; SON) precipitation (Vegas-Vilarrúbia et al. 2022). A high-resolution (annual) reconstruction of extreme rainfall events for the last seven centuries is also available for the Montcortès record (Corella et al. 2014).

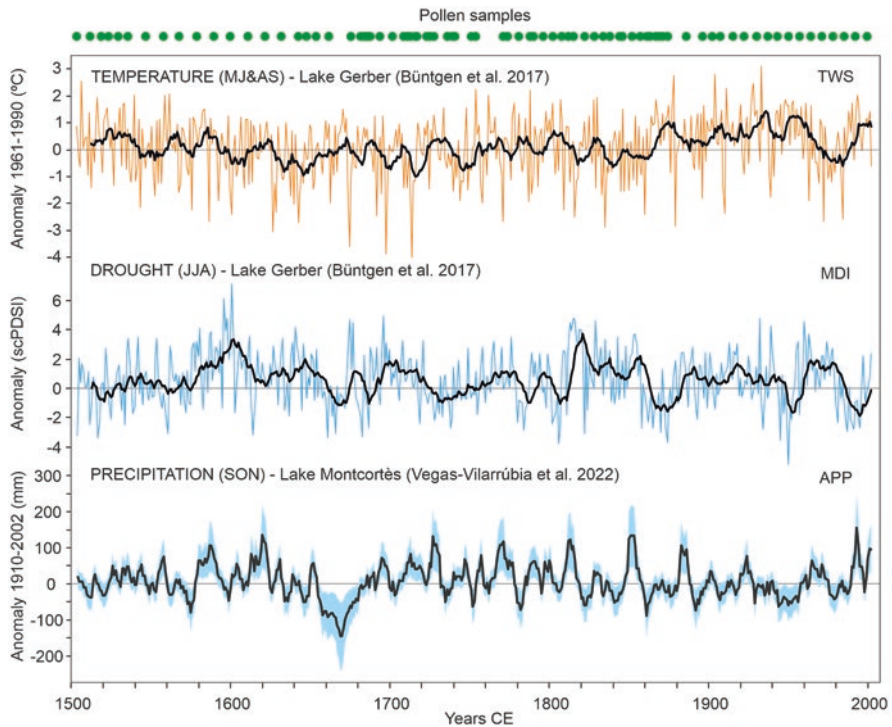


Fig. 6.11 Pollen-independent paleoclimatic reconstructions from lakes Montcortès and Gerber represented as anomalies with respect to the periods indicated. In the case of summer drought intensity, the anomalies are relative to the self-calibrated Palmer drought indices (scPDSIs) for the Mediterranean region. Samples analyzed for pollen are indicated in the upper part of the diagram. TWS, temperature of the warmest season; MDI, Mediterranean drought intensity; APP, autumn precipitation. Modified from Rull and Vegas-Vilarrúbia (2022)

However, this record is mainly based on the physical properties of detrital layers and turbiditic intervals, which are unsuitable for palynological analysis and were not considered in the pollen-based paleoecological study.

The anthropogenic influence was tested using independent proxies such as charcoal and coprophilous fungi, which were measured in influx units and percentages outside the pollen sum, respectively. As noted in the methodological section (Chap. 3; Sect. 4), charcoal is the most common proxy for fire, which is assumed to have been mostly of human origin during the recent centuries (Whitlock and Larsen 2001), whereas the spores of coprophilous fungi are reliable indicators of grazing activities (van Geel et al. 2003). In this case, emphasis has been placed on *Sporomiella*, which is especially useful as a grazing proxy because, unlike other coprophilous fungi, it is obligate for herbivory, and its spores are well preserved in the fossil record and easily distinguishable (Gill et al. 2013). Other palynological proxies for human activities, such as cultivated plants and weeds (Rull and Vegas-Vilarrúbia 2015), have not been used in the statistical analysis as proxies for human

impact because they were included in the pollen sum and, therefore, are not independent from palynological evidence for forest succession, which is the main subject of this reconstruction. In addition, cultivation and associated activities have not been as important as forest exploitation and grazing in Modern times around Lake Montcortès and the surrounding region, as shown by the scarcity of cereals and other crops in the palynological record (Fig. 6.1). The most common and abundant weeds and ruderal plants (*Artemisia*, *Plantago*, *Chenopodium*, *Rumex*) have also been avoided as anthropogenic indicators, as they may occur naturally in the region, and autochthonous representatives cannot be separated from introduced ones by pollen morphology.

As quoted above, the main targets of the statistical study that follows were regional forests and their succession over time under the influence of climatic and anthropogenic shifts. All forest trees represented in the modern assemblage and the post-Medieval pollen record were considered in this analysis (Table 3.4). Cultivated trees such as *Olea*, *Castanea*, *Juglans*, and *Prunus*-type were excluded.

6.5.2 Statistical Analyses

To compare quantitative data between paleoclimatic and palynological records, standardization was necessary because paleoclimatic records had an annual resolution, whereas palynological records had variable numbers of years in each sample. As detailed in the methodology section (Chap. 3; Sect. 1.3), we achieved the highest palynological resolution by continuously sampling core MONT-0713-G05 at 5 mm intervals, while avoiding turbidites. Consequently, the palynological samples represented varying numbers of years, ranging from 1 to 17, with an average of approximately 6 years. To facilitate statistical comparisons, we compared the results of palynological samples, which were considered averages of the years they represented, with the calculated average of paleoclimatic data for the corresponding years. For instance, the sample from 1802 CE contained 6 varves, spanning the interval from 1797 to 1802 CE, and its palynological composition was compared to the average estimated climatic parameters for those 6 years. Additionally, we homogenized the datasets chronologically due to their differing durations. The period of overlap between paleoecological and paleoclimatic data series was from 1504 to 2002 CE, encompassing 498 years and including 80 out of the 96 palynological samples available in the database.

The statistical analysis consisted of two primary stages: (i) examining how individual tree-forest taxa react to external factors and (ii) assessing the impact of these external factors on entire regional forests. Concerning the first aspect, paleoecological evidence has played a crucial role in demonstrating that species respond individually to environmental changes based on their distinct characteristics, ultimately influencing changes in forest composition over time (Davis 1984). Moreover, human activities in forests tend to be selective, with certain species being preferred for exploitation or deforestation. Consequently, understanding the specific interactions between forest tree species and external influences can provide valuable

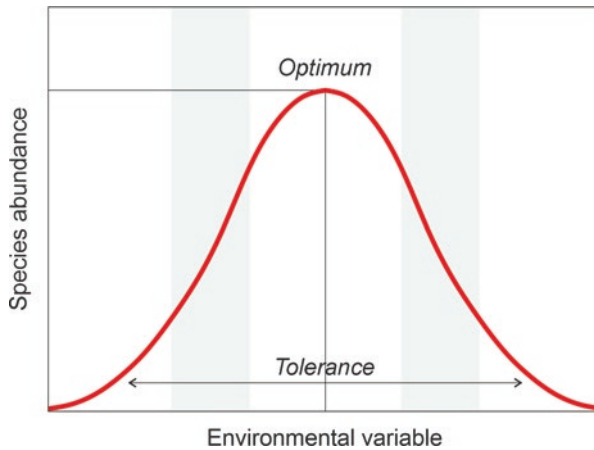


Fig. 6.12 Hypothetical Gaussian (unimodal) response of a species to an environmental variable. The intervals of quasi-linear responses are highlighted by gray bands

insights. To investigate these relationships, nonlinear Gaussian response models were employed along environmental gradients (Ter Braak and Prentice 1988; Jongman et al. 1995) (Fig. 6.12). A key aspect in understanding how different species respond to climate shifts is the time delay in their responses, which can vary among species and is especially relevant for organisms with long life cycles, such as forest trees (Rull 2020). In this study, response lags were estimated through step-wise correlation analysis, involving sequential 1-sample offsets between climatic conditions and taxon series (cross-correlation).

The second step began with the definition of forest-tree pollen assemblages using cluster analysis. The Pearson coefficient was used as the measure of similarity, and the unweighted pair group average (UPGMA) approach was the selected clustering approach (Pearson 1895; Kendall 1970). The shifts in these assemblages over time were analyzed using rate-of-change (ROC) analysis by calculating the chord distance between adjacent pairs of samples (Bennett and Humphry 1995). A useful way of representing successional trends is by defining the attraction domains of the involved plant assemblages (in this case, A1, A2, and A3) in a multidimensional space and reconstructing the successional trajectories using the chronological order of sample scores from a multivariate analysis (Rull 1992). In this case, this was addressed by redundancy analysis (RDA), a canonical version of principal component analysis (PCA), using the forest associations defined by the cluster analysis in the variable matrix and the climatic/anthropogenic factors in the environmental matrix (Legendre and Legendre 1998). RDA was preferred over canonical correspondence analysis (CCA) due to the results of individual analyses (see next section), which showed near-linear responses of major taxa to external drivers (Jongman et al. 1995).

6.5.3 Individual Responses

Figures 6.13, 6.14, 6.15 depict the outcomes of the Gaussian response analysis. Figure 6.13 reveals the forest taxa that exhibit significant responses to climatic factors, while Fig. 6.14 demonstrates the taxa that exhibit significant responses to human-related indicators. The critical significant correlation coefficient ($n = 80$; $\alpha < 0.05$) is $r = 0.217$ ($R^2 = 0.047$). Figure 6.15 presents the most striking instances of nonsignificant or misleading relationships. One noteworthy case is exemplified by *Fagus*-PPT, which displays nonsignificant relationships with flat trends ($R^2 = 0.000$). In some other instances, higher R^2 values were influenced by an abundance of zero values, which is considered a statistical artifact leading to erroneous response models (Kaul et al. 2017; Silverman et al. 2020). The prevalence of zero values was observed across nearly all minor forest components, making only the four dominant forest taxa (deciduous and evergreen *Quercus*, *Betula*, and *Pinus*) suitable for statistical response analysis.

As all the significant relationships between taxon and the environment showed either linear or exponential trends (Figs. 6.13 and 6.14), we conducted response analysis using both linear and exponential regression methods. The results revealed

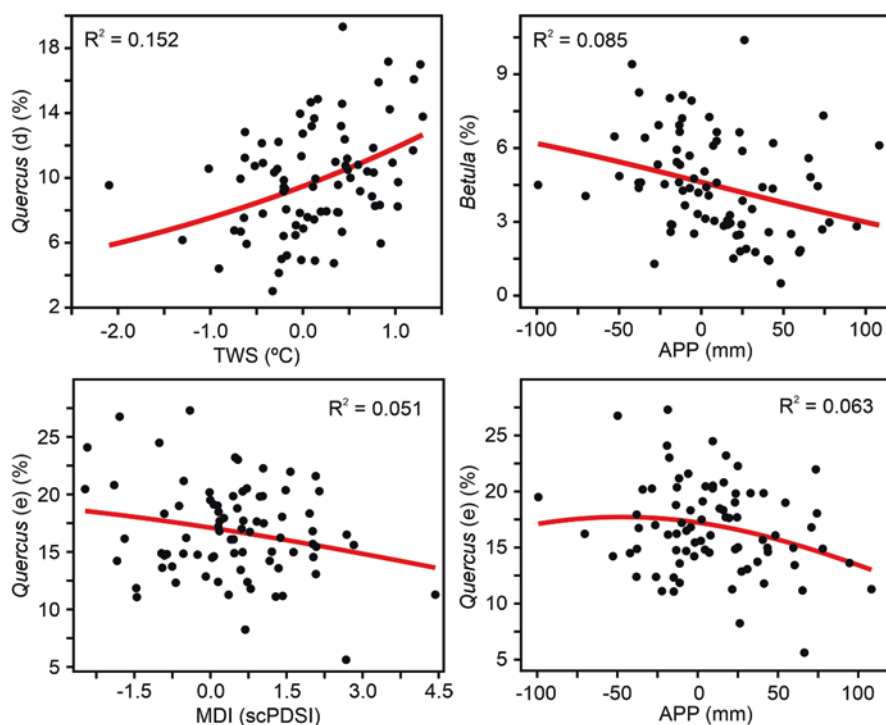


Fig. 6.13 Forest taxa with significant Gaussian responses to paleoclimatic shifts. TWS, temperature of the warmest season; APP, autumn precipitation; MDI, Mediterranean drought intensity

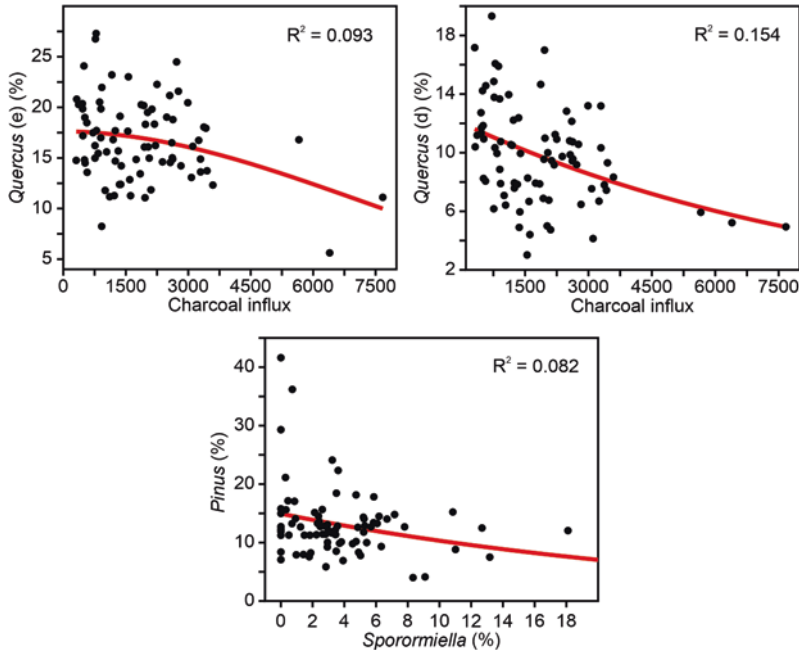


Fig. 6.14 Forest taxa with significant Gaussian responses to anthropogenic drivers. Charcoal influx in particles $\text{cm}^{-2} \text{yr}^{-1}$

that linear regression was the best fit in three cases, while exponential regression was preferable in six cases (Table 6.1). Notably, two new significant correlations were uncovered through this analysis that were not identified in the Gaussian analysis: *Quercus* (d) and *Quercus* (e) exhibited exponential and negative correlations with *Sporormiella*. In general, the differences between linear and exponential correlation values were relatively small and did not significantly impact the significance patterns. Consequently, the choice between linear or exponential models had minimal impact on the results of the individual analysis.

Table 6.1 shows that all climatic and anthropogenic drivers were linked to some major forest components. Among the climatic parameters, the highest correlation was between deciduous *Quercus* and temperature. In regard to anthropogenic variables, all significant correlations were negative. The forest elements with more significant correlations were evergreen and deciduous *Quercus*, which were positively correlated with climatic parameters and negatively correlated with anthropogenic indicators. *Pinus* did not correlate with any climatic variable, and *Betula* showed no significant correlations with anthropogenic proxies. The significant relationships obtained show a combination of linear and exponential patterns, suggesting that they may not fully represent the entire environmental range of the studied species, as shown in Fig. 6.12. This implies that the environmental parameters selected over the last 500 years have remained at suboptimal values for the dominant forest taxa, leading to limited variation in their range.

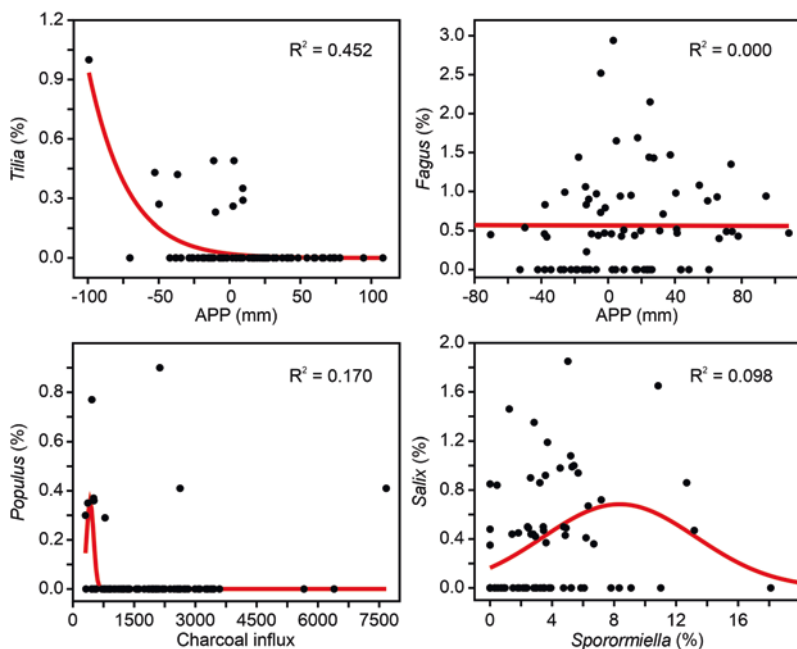


Fig. 6.15 Examples of forest taxa with nonsignificant and/or misleading responses to external factors. Charcoal influx in particles $\text{cm}^{-2} \text{yr}^{-1}$. APP, autumn precipitation; MDI, Mediterranean drought intensity

Table 6.1 Linear (normal font) and exponential (italics) correlation coefficients between the forest taxa and the external drivers that were significant in the Gaussian response analysis (Figs. 6.13 and 6.14)

	<i>Pinus</i>	<i>Quercus</i> (e)	<i>Quercus</i> (d)	<i>Betula</i>
TWS	-0.014	0.104	0.374	0.251
APP	-0.039	0.231	-0.089	-0.288
MDI	-0.032	-0.225	-0.036	-0.064
<i>Sporormiella</i>	-0.334	-0.295	-0.330	0.170
Charcoal	-0.114	-0.293	-0.402	0.064

In most significant cases, the linear and exponential models show very similar correlation coefficients, and higher values were chosen. Correlations significant at $\alpha < 0.05$ are in bold. TWS, temperature of the warmest season; APP, autumn precipitation; MDI, Mediterranean drought intensity

The previous individual analyses focused solely on examining how different forest components respond immediately (at subdecadal resolution) to external factors. This was done by comparing pollen abundance and paleoclimatic estimates during the same time intervals. The possibility of response lags between climatic shifts and forest trees has also been addressed, and the results obtained are explained in the following (Fig. 6.16). The immediate positive correlation of deciduous *Quercus* with summer temperature was maintained for lags of ~ 20 and ~ 40 years. For autumn

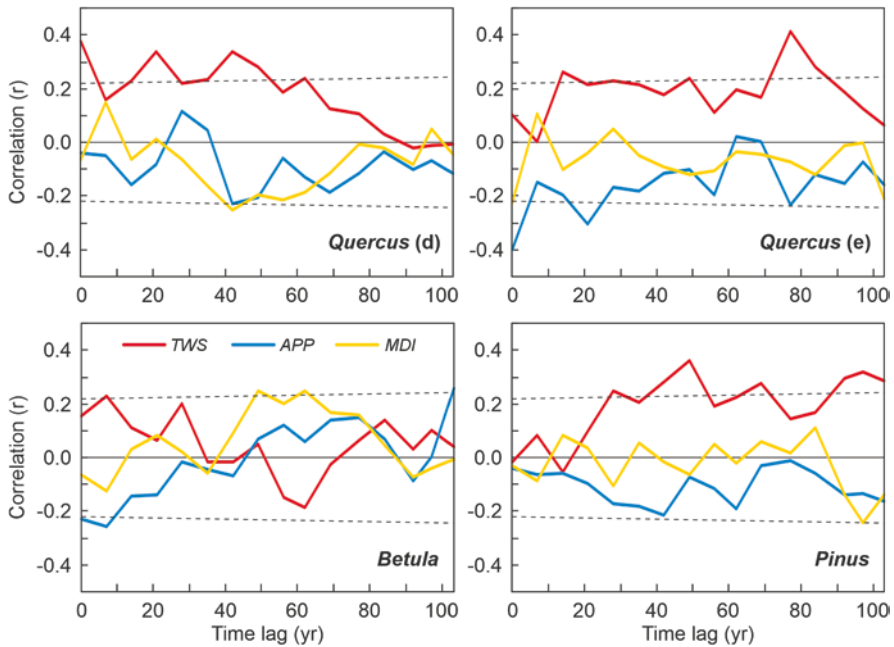


Fig. 6.16 Response lags of major forest components to the measured climatic drivers using linear models (Table 6.1). The dotted lines represent the significant correlation values at $\alpha < 0.05$. TWS, temperature of the warmest season; APP, autumn precipitation; MDI, Mediterranean drought intensity

precipitation and summer drought intensity, with nonsignificant correlations in the immediate response analyses, the relationship was significant for a 40-yr delay. Consequently, a response lag of approximately 40 years was identified for all climatic parameters, suggesting that deciduous *Quercus* has been sensitive to various climate drivers and has displayed two types of responses: one that was immediate (at a subdecadal average resolution) and another that was delayed by approximately 40 years.

Evergreen *Quercus* exhibited distinctive behavior by displaying notable delays in response, taking ~15, ~50, and ~80 years to react to changes in summer temperature. In contrast, its response to autumn precipitation and the intensity of summer drought was immediate (Table 6.1), with only a significant lag of ~20 years in response to precipitation. *Betula*, on the other hand, immediately responded to precipitation but showed response delays of ~15 years to summer temperature and autumn precipitation and a longer 50–60 year lag in response to summer drought. Similar to deciduous *Quercus*, both evergreen *Quercus* and *Betula* displayed two types of responses for the same climatic factor, autumn precipitation—immediate and delayed by ~15–20 years. Finally, *Pinus*, which did not respond immediately to any climatic drivers, displayed various response lags in relation to summer temperature (~30 yr, ~50 yr, ~70 yr, and ~100 yr), with a single significant delay of

~100 years in response to summer drought intensity. In summary, all major forest taxa responded to various climatic drivers, with characteristic response lags for each taxon.

6.5.4 Assemblage and Succession Analysis

Cluster analysis revealed three different forest assemblages: A1, dominated by *Pinus*; A2, dominated by evergreen *Quercus*; and A3, dominated by deciduous *Quercus* (Fig. 6.17). These assemblages coincided with the forest types characteristic of the Montcortès region—i.e., montane coniferous forests, Mediterranean oak forests, and deciduous submontane oak forests, respectively—which indicates that these forests have also been dominant during the last 500 yr, although they underwent variations in abundance over time. These variations were expressed as oscillations in the defined assemblages, rather than community turnover (Fig. 6.18), which indicates that regional forest succession proceeded by fluctuations in the range and abundance of these assemblages, rather than by successive replacements among them. Variations in the total forest abundance were significantly correlated ($\alpha < 0.01$) with the three assemblages, with the highest correlation being with A1 ($r = 0.666$), followed by A2 ($r = 0.621$) and A3 ($r = 0.405$). Therefore, variations in the total forest cover were more influenced by oscillations in montane and Mediterranean forests than by changes in submontane forests. ROC analysis (Fig. 6.18) showed that maximum variability occurred between approximately 1680 CE and

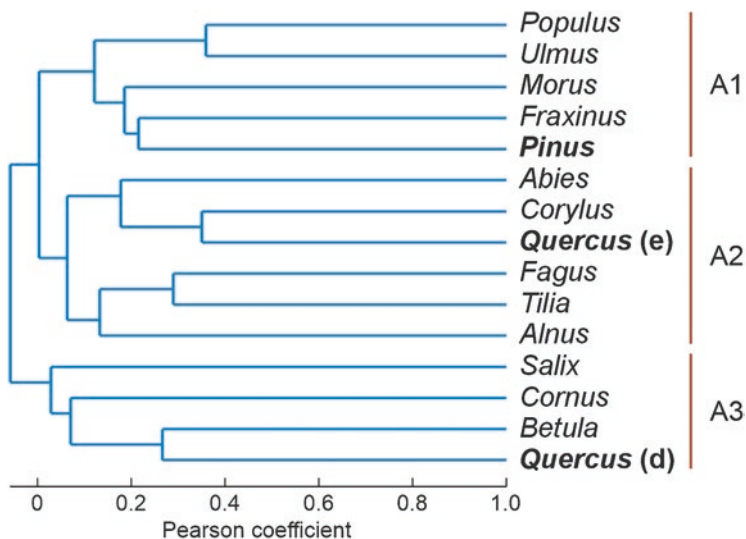


Fig. 6.17 Cluster analysis of forest-tree pollen elements. The dominant taxa of each forest assemblage are in bold. A1, assemblage 1; A2, assemblage 2; A3, assemblage 3

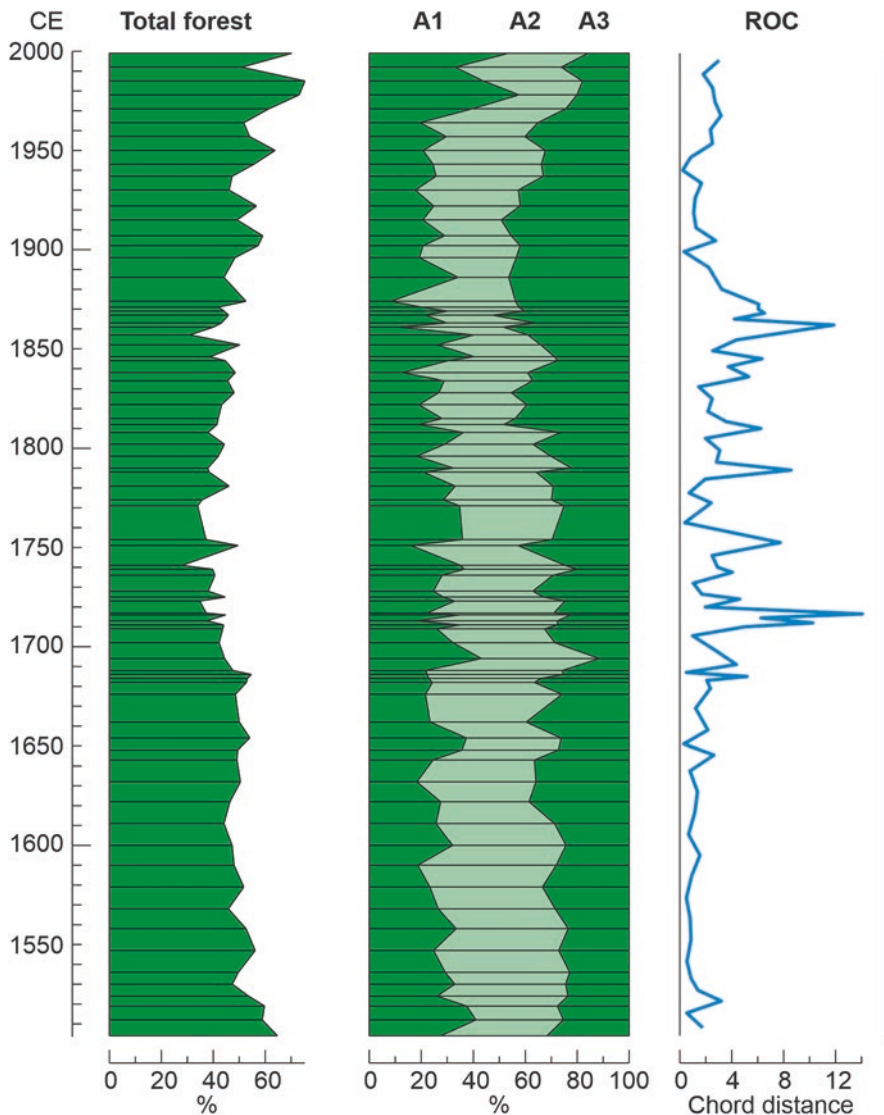


Fig. 6.18 Rate-of-change (ROC) analysis of the forest assemblages defined by cluster analysis (Fig. 6.17). Total forest percentages with respect to the pollen sum. Percentages of assemblages A1, A2, and A3 with respect to the total pollen percentages

1880 CE—which is roughly the range of maximum hemp retting (Fig. 6.4)—with two peaks at ~1710 CE and ~1860 CE, coinciding with two fire maxima (Fig. 6.10).

The results of RDA are displayed in Fig. 6.19, where attraction domains, successional trends, and external drivers are represented in the same Euclidean space. Axes 1 and 2 accounted for 11.92% (7.41% and 4.776%, respectively) of the total

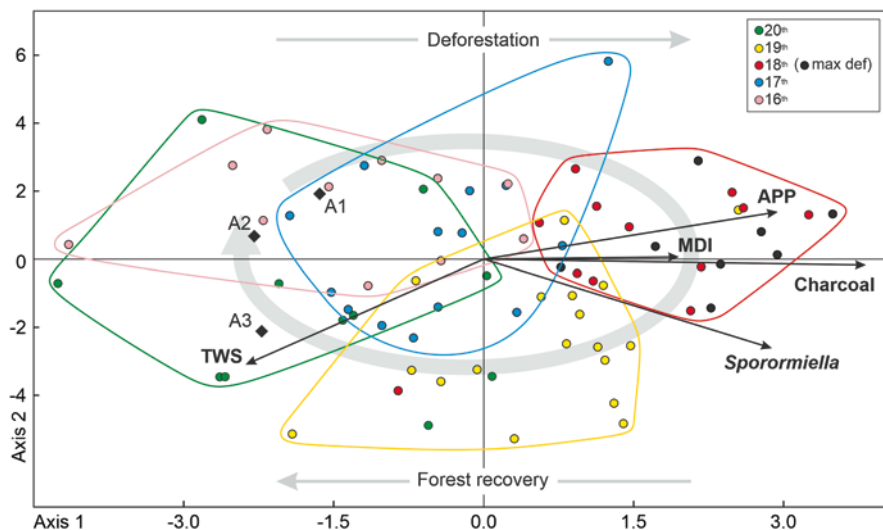


Fig. 6.19 RDA triplot representing the sample scores (colored dots; color code at the upper right) grouped by centuries, the attraction domains of forest associations (black diamonds), and the external variables (vectors). Black dots are eighteenth-century samples corresponding to the phase of maximum deforestation (max def). The general successional path is represented by a clockwise elliptical gray arrow. APP, autumn precipitation; MDI, Mediterranean drought intensity; TWS, temperature of the warmest season

variance. The taxon–environment correlations of these two axes ($r = 0.459$ and $r = 0.338$, respectively) were significant at $\alpha < 0.05$, as was the overall RDA test ($r = 0.358$). Both the variance explained and the taxon–environment correlations abruptly dropped from axis 3 (var = 0.86%; $r = 0.176$) onward, becoming nonsignificant at $\alpha < 0.05$. Therefore, only axes 1 and 2 were considered in this analysis. In the space defined by these two axes, the succession appeared as a closed path starting and ending in an intermediate A1/A2 attraction domain. The first phase (sixteenth to eighteenth centuries) ran along axis 1 toward positive values, following a deforestation trend that moved the succession away from the initial forest associations. This trend was mainly linked to fire incidence and the intensity of Mediterranean drought (MDI), which could have acted as a burning amplifier. The MDI is also well correlated with autumn precipitation (APP) ($r = 0.382$; $\alpha < 0.001$), meaning that the driest summers were followed by rainier autumns but this would have been insufficient to reverse deforestation. *Sporormiella* is also linked to maximum deforestation, likely because one of the main reasons for regional forest clearing was the expansion of pastures, which is supported by historical documents that report a significant increase in large-scale transhumance (Chap. 2; Sect. 5.4.2).

The return to former forest attraction domains (nineteenth and twentieth centuries) was linked to the decline in drought intensity and anthropogenic pressure (burning, grazing) coupled with an increase in summer temperatures (TWS), which would have favored forest recovery. The establishment of current landscapes took

place in the twentieth century, after successional sequence A3–A2–A1. In summary, human-drought feedbacks were the main contributors to forest clearing, which peaked in the eighteenth century, whereas increasing temperatures and the relaxation of anthropogenic pressure during the Industrial Revolution fostered forest recovery. The historical sociocultural trends linked to these events have already been discussed in Sects. 2 and 3. These results are consistent with the statistical relationships obtained after individual response analysis and confirm, once more, that idiosyncratic requirements of forest elements largely control the response of the communities they form to shifts in external environmental factors.

6.5.5 The Role of External Factors in Regional Forest Succession

Detailed high-resolution statistical analyses have shown that both climatic and anthropogenic drivers have affected forest dynamics over recent centuries in the shaping of the current landscapes of the Montcortès region. As discussed in several parts of this book, the influence of climatic shifts on plant species and communities could have been direct or indirect. In the first case, biological responses would have resulted from the action of environmental shifts on the niche features of the involved taxa and, as a consequence, on the composition of the communities they form, as has been seen in the individual analysis (Sect. 5.3). Indirect effects would have been mediated by humans after climatically driven human migrations and other cultural shifts. Therefore, even in post-Medieval times, when anthropogenic drivers are usually considered to be the main agents of ecological change, climate shifts should not be dismissed as potential causes and/or modulators of landscape transformations, either directly or indirectly.

Another significant implication drawn from the aforementioned statistical analyses is that changes in the environment can lead to both immediate and delayed responses due to the idiosyncratic characteristics of the species involved. In our examination of response time, we observed that some species promptly reacted to climatic shifts, typically within a few years, while others displayed delayed responses of two decades or more. Furthermore, certain species exhibited a combination of both rapid and delayed reactions to the same climate-related factor. Immediate responses often occurred because of adjustments in pollen production and release during the flowering season, which were influenced positively by temperature and sunlight and negatively by precipitation, especially in the NE Iberian Peninsula (Majeed et al. in 2018). In contrast, responses delayed by two decades or more were primarily linked to long-term population dynamics, which resulted in the expansion or contraction of the geographical ranges of the species involved and the forest communities they dominate (Wang et al. 2018; Mathys et al. 2021). For delays extending beyond a century (>100 yr), it is essential to consider the possibility of statistical artifacts, although further research is needed to make a solid assessment. These response lags can add complexity to the interpretation of statistical findings in terms of climate impacts. As of our current knowledge, we cannot disregard the potential influence of response lags as distorting factors.

Unfortunately, comparing our findings with those of other regional studies is not feasible due to the absence of similar investigations. Unlike most of the existing palynological records in the central Iberian Pyrenees (Table 5.1), our approach focuses primarily on ecological aspects rather than environmental or anthropological issues. While it is not uncommon for paleoenvironmental studies to use pollen data to reconstruct climate and human impacts, this can lead to circular reasoning. Indeed, the response of forests to external drivers cannot be assessed if both environmental and forest trends are deduced from the same palynological proxies. Another significant aspect of our analysis is that we used extensive datasets to statistically examine potential relationships between forest dynamics and external factors rather than relying solely on visual comparisons of trends. Furthermore, our analyses were carried out with a high temporal resolution (subdecadal), which is the most reliable method for reconstructing ecological forest succession. Last, we utilized high-resolution (annual) paleoclimatic data obtained from the same lake sediments or nearby sites, including a temperature reconstruction representing the entire Pyrenean range.

In summary, to conduct a robust investigation into the influence of climatic and anthropogenic factors on forest dynamics and succession, the fulfillment of these four conditions is crucial: (i) independence between forest and environmental proxies, (ii) development of high-resolution paleoecological records, (iii) use of local or regional paleoclimatic reconstructions, and (iv) application of suitable statistical methods. Neglecting these conditions can result in questionable conclusions. Predicting how forests will respond to current and future climatic and anthropogenic changes is a critical conservation challenge that demands long-term ecological observations such as those employed in this study. Approaches that do not adhere to these conditions are unlikely to provide the reliable long-term ecological data necessary to anticipate future successional trends and support predictive ecological models.

References

- Aboulaich N, Trigo MM, Bouziane H, Cabezudo B, Recio M, El Kadiri M et al (2013) Variations and origin of the atmospheric pollen of *Cannabis* detected in the province of Tetouan (NW Morocco): 2008–2010. *Sci Total Environ* 443:413–419
- Akin DE (2013) Linen most useful: perspective on structure, chemistry and enzyme for the retting flax. *ISRN Biotechnol* 2013:1–23
- Akin DE, Foulk JA, Dodd RB, McAlister DD (2001) Enzyme-retting of flax and characterization of processed fibres. *J Biotechnol* 89:193–203
- Alvarez A, Gamella JF, Parra I (2016) *Cannabis* cultivation in Spain: a profile of plantations, growers and production systems. *Int J Drug Policy* 37:70–81
- Anderson NJ (1995) Naturally eutrophic lakes: reality, myth or myopia. *Trends Ecol Evol* 10:137–138
- Andreu M (1981) La financiación de la industria naval en Barcelona (1745–1760). *Pedralbes* 1:267–294

- Aznar F, Negral L, Moreno-Grau S, Elvira-Rendueles B, Costa-Gómez I, Moreno JM (2022) *Cannabis*, an emerging aeroallergen in southeastern Spain (Region of Murcia). *Sci Total Environ* 833:155156
- Barriendos M, Rodrigo FS (2006) Study of historical flood events on Spanish rivers using documentary data. *Hydrol Sci J* 51:765–783
- Belackova V, Tomkova A, Zabransky T (2016) Qualitative research in Spanish cannabis social clubs: “The moment you enter the door, you are minimising the risks”. *Int J Drug Policy* 34:49–57
- Benito G, Thorndycraft VR, Rico M, Sánchez-Moya Y, Sopeña A (2008) Palaeoflood and floodplain records from Spain: evidence for long-term climate variability and environmental changes. *Geomorphology* 101:68–77
- Bennett KD, Humphry RV (1995) Analysis of Late-glacial and Holocene rates of vegetational change at two sites in the British Isles. *Rev Palaeobot Palynol* 85:263–287
- Büntgen U, Krusic PJ, Verstege A, Sangüesa-Barreda G, Wagner S, Camarero JJ et al (2017) New tree-ring evidence from the Pyrenees reveals western Mediterranean climate variability since Medieval times. *J Clim* 30:5295–5318
- Cabezudo B, Recio M, Sánchez-Laulhé JM, Trigo MM, Toro FJ et al (1997) Atmospheric transportation of marijuana pollen from north Africa to the Southwest of Europe. *Atmos Environ* 31:3323–3328
- Cariñanos P, Galán C, Alcázar P, Domínguez E (2004) Analysis of the particles transported with dust-clouds reaching Cordoba, Southeastern Spain. *Arch Environ Contam Toxicol* 46:141–146
- Casassas L (1985) Fibres tradicionals i emplaçaments industrials a la regió de Barcelona. *Treb Soc Cat Geogr* 4:117–128
- Clarke RC, Merlin MD (2013) *Cannabis*: evolution and ethnobotany. University California Press, Los Angeles
- Corella JP, Benito C, Rodríguez-Lloveras X, Brauer A, Valero-Garcés BL (2014) Annually-resolved lake record of extreme hydro-meteorological events since AD 1347 in NE Iberian Peninsula. *Quat Sci Rev* 93:77–90
- Corella JP, Valero-Garcés B, Vicente-Serrano SM, Brauer A, Benito C (2016) Three millennia of heavy rainfalls in Western Mediterranean: frequency, seasonality and atmospheric drivers. *Sci Rep* 6:38206
- Corella JP, Benito G, Wilhelm B, Montoya E, Rull V, Vegas-Vilarrúbia T et al (2019) A millennium-long perspective of flood-related seasonal sediment yield in Mediterranean watersheds. *Glob Planet Change* 177:127–140
- Davis MB (1984) Climatic instability, time lags, and community disequilibrium. In: Diamond J, Case TJ (eds) *Community Ecology*. Harper & Row, New York, pp 269–284
- Delgado JM (1994) La indústria de la construcció naval catalana (1750–1850). *Drassana* 2:34–39
- Di Candilo M, Bonatti PM, Guidetti C, Foche B, Grippo C, Tamburini E et al (2009) Effects of selected pectinolytic bacterial strains on water-retting of hemp and fibre properties. *J Appl Microbiol* 108:194–203
- Dorado-Liñán I, Büntgen U, González-Rouco F, Zorita E, Montávez JP, Gómez-Navarro JJ et al (2012) Estimating 750 years of temperature variations and uncertainties in the Pyrenees by tree-ring reconstructions and climate simulations. *Clim Past* 8:919–933
- Ejarque A, Julià R, Riera S, Palet JM, Orengo HA, Miras Y et al (2009) Tracing the history of highland human management in the eastern pre-Pyrenees: an interdisciplinary palaeoenvironmental study at the Pradell fen, Spain. *The Holocene* 19:1241–1255
- Ferrer Alòs L (2017) Més enllà dels gremis i de les fàbriques d’indianes. La diversitat de formes de produir a la Catalunya del segle XVIII i la primera meitat del segle XIX. *Treb Soc Cat Geogr* 83:183–211
- Gareth J, Witten D, Hastie T, Tibshirani R (2017) *An introduction to statistical learning*. Springer, New York
- van Geel B, Buurman J, Brinkkemper O, Schelvis J, Aptroot A, van Reenen G et al (2003) Environmental reconstruction of a Roman Period settlement site in Uitgeest (The Netherlands), with especial reference to coprophilous fungi. *J Archaeol Sci* 30:873–883

- Giguët-Covex C, Ficaretola GF, Walsh K, Poulenard J, Bajard M, Fouinat L et al (2019) New insights on lake sediment DNA from the catchment: importance of taphonomic and analytical issues on the record quality. *Sci Rep* 9:14676
- Gill JL, McLauchlan KK, Skibble AM, Goring S, Zirbel ZR, Williams JW (2013) Linking abundances of the dung fungus *Sporormiella* to the density of bison: implications for assessing grazing by megaherbivores in palaeorecords. *J Ecol* 101:1125–1136
- Gorchs G, Lloveras J (2003) Current status of hemp production and transformation in Spain. *J Ind Hemp* 8:45–64
- Gorchs G, Loveras J, Serrano L, Cela S (2017) Hemp yields and its rotation effects on wheat under rainfed Mediterranean climates. *Agron J* 109:1551–1560
- Iwańska O, Latoch P, Suchora M, Pidek IA, Huber M, Buback I et al (2022) Lake microbiome and trophic fluctuations of the ancient hemp rettery. *Sci Rep* 12:8846
- Jongman RHG, Ter Braak CJF, Van Tongeren OFR (1995) *Data analysis in community and landscape ecology*. Cambridge University Press, Cambridge
- Karus M, Kaup M (2002) Natural fibres in the European automotive industry. *J Ind Hemp* 7:119–131
- Kaul A, Mandal S, Davidov O, Peddada SD (2017) Analysis of microbiome data in the presence of excess zeros. *Front Microbiol* 8:2114
- Kendall MG (1970) *Rank correlation methods*. Griffin, London
- Lavrieux M, Jacob J, Disnar J-R, Bréheret J-G, Le Milbeau C, Miras Y et al (2013) Sedimentary cannabinoil tracks the history of hemp retting. *Geology* 41:751–754
- Legendre L, Legendre L (1998) *Numerical ecology*. Elsevier, New York
- Llasat MC, Barriendos M, Barrera A, Rigo T (2005) Floods in Catalonia (NE Spain) since the 14th century. Climatological and meteorological aspects from historical documentary sources and old instrumental records. *J Hydrol* 313:32–47
- Majeed HT, Periago C, Alarcón M, Belmonte J (2018) Airborne parameters and their relationship with meteorological variables in NE Iberian Peninsula. *Aerobiologia* 34:375–388
- Martín-Chivelet J, Muñoz-García MB, Edwards L, Turrero MJ, Ortega AI (2011) Land surface temperature changes in northern Iberia since 4000 yr BP, based on $\delta^{13}\text{C}$ of speleothems. *Glob Planet Change* 77:1–12
- Marugan CM, Rapalino V (2005) *Història del Pallars. Dels Orígens als Nostres Dies*. Pagés Ed, Lleida
- Mathys AS, Brang P, Stillhard J, Bugmann H, Hobi ML (2021) Long-term tree species population dynamics in Swiss forest reserves influenced by forest structure and climate. *For Ecol Manag* 481:118666
- McPartland JM, Guy GW, Hegman W (2018) *Cannabis* is indigenous to Europe and cultivation began during Copper or Bronze Age: a probabilistic synthesis of fossil pollen studies. *Veg Hist Archaeobotany* 27:635–648
- Miao SL, Sklar FH (1998) Biomass and nutrient allocation of sawgrass and cattail along a nutrient gradient in the Florida Everglades. *Wetl Ecol Manag* 5:45–263
- Munuera M, Carrión JS, Navarro C (2002) Seasonal fluctuations of the airborne pollen spectrum in Murcia (SE Spain). *Aerobiologia* 18:141–151
- Newman S, Grace J, Koebel J (1996) Effects of nutrients and hydroperiod on *Typha*, *Cladium*, and *Eleocharis*: implications for Everglades restoration. *Ecol Appl* 6:774–783
- Pearson K (1895) Notes on regression and inheritance in the case of two parents. *Proc R Soc Lond* 58:240–242
- Pèlachs A, Nadal J, Soriano JM, Molina D, Cunill R (2009) Changes in Pyrenean woodlands as a result of the intensity of human exploitation: 2,000 years of metallurgy in Vallferrera, northeast Iberian Peninsula. *Veg Hist Archaeobotany* 18:403–416
- Ribeiro A, Pochart P, Day A, Mennuni S, Bono P, Baret J-L et al (2015) Microbial diversity conserved during hemp retting. *Appl Microbiol Biotechnol* 99:4471–4484
- Riera S, Wansard G, Julià R (2004) 2000-year environmental history of a karstic lake in the Mediterranean Pre-Pyrenees: the Estanya lakes (Spain). *Catena* 55:293–324

- Riera S, López-Sáez JA, Julià R (2006) Lake responses to historical land use changes in northern Spain; the contribution of non-pollen palynomorphs in a multiproxy study. *Rev Palaeobot Palynol* 141:127–137
- Rull V (1992) Successional patterns of the Gran Sabana (southeastern Venezuela) vegetation during the last 5000 years, and its responses to climatic fluctuations and fire. *J Biogeogr* 19:329–338
- Rull V (2020) Quaternary ecology, evolution, and biogeography. Elsevier/Academic Press, London
- Rull V (2022) Origin, early expansion, domestication and anthropogenic diffusion of *Cannabis*, with emphasis on Europe and the Iberian Peninsula. *Persp Plant Ecol Evol Syst* 55:125670
- Rull V, Vegas-Vilarrúbia T (2014) Preliminary report on a mid-19th century *Cannabis* pollen peak in NE Spain: historical context and potential chronological significance. *The Holocene* 24:1378–1383
- Rull V, Vegas-Vilarrúbia T (2015) Crops and weeds from the Estany de Montcortès catchment, central Pyrenees, during the last millennium: a comparison of palynological and historical records. *Veget Hist Archaeobot* 24:699–710
- Rull V, Vegas-Vilarrúbia T (2022) Climatic and anthropogenic drivers of forest succession in the Iberian Pyrenees during the last 500 years: a statistical approach. *Forests* 13:622
- Rull V, Vegas-Vilarrúbia T (2023) A recent *Cannabis* pollen increase on the Iberian Pyrenees. *Sci Total Environ* 886:163947
- Rull V, González-Sampériz P, Corella JP, Morellón M, Giralt S (2011) Vegetation changes in the southern Pyrenean flank during the last millennium in relation to climate and human activities: the Montcortès lacustrine record. *J Paleolimnol* 46:387–404
- Rull V, Trapote MC, Safont E, Cañellas-Boltà N, Pérez-Zanón N, Sigró J et al (2017) Seasonal patterns of pollen sedimentation in Lake Montcortès (Central Pyrenees) and potential applications to high-resolution paleoecology: a 2-year pilot study. *J Paleolimnol* 57:95–108
- Rull V, Vegas-Vilarrúbia T, Corella JP, Trapote MC, Montoya E, Valero-Garcés B (2021) A unique Pyrenean varved record provides a detailed reconstruction of Mediterranean vegetation and land-use dynamics over the last three millennia. *Quat Sci Rev* 268:107128
- Rull V, Sacristán-Soriano O, Sánchez-Melsió A, Borrego CM, Vegas-Vilarrúbia T (2022) Bacterial phylogenetic markers in lake sediments provide direct evidence for historical hemp retting. *Quat Sci Rev* 295:107803
- Rull V, Burjachs F, Carrión JS, Ejarque A, Fernández S, López-Sáez JA et al (2023) Historical biogeography of *Cannabis* in the Iberian Peninsula: a probabilistic approach using palynological evidence. *Persp Plant Ecol Evol Syst* 58:125704
- Salrach JM (2004) Història Arària del Paísos Catalans. Vol 2. Edat Mitjana. Fund Catalana Recerca, Barcelona
- Sanz V (1995) D'Artesans a Proletaris: la Manufactura del Cànem a Castelló, 1732–1843. Diputació de Castelló, Castelló
- Silverman JD, Roche K, Mukherjee S, David LA (2020) Naughty all zeros in sequence count data are the same. *Comp Struct Biotech J* 18:2789–2798
- Tahir PM, Ahmed AB, SaifulAzry SOA, Ahmed Z (2011) Retting process of some bast plant fibres and its effect of fibre quality: a review. *Bioresources* 6:5260–5281
- Tamburini E, Gordillo A, Perito B, Mastromei G (2003) Characterization of bacterial pectinolytic strains involved in the water retting process. *Environ Microbiol* 5:730–736
- Ter Braak CJF, Prentice IC (1988) A theory of gradient analysis. *Adv Ecol Res* 18:271–317
- Trapote MC, Rull V, Giralt S, Montoya E, Corella JP, Vegas-Vilarrúbia T (2018) High-resolution (subdecadal) pollen analysis of varved sediments from Lake Montcortès (southern Pyrenean flank): a fine-tuned record of landscape dynamics and human impact during the last 500 years. *Rev Palaeobot Palynol* 259:207–222
- Vegas-Vilarrúbia T, Corella JP, Sigró J, Rull V, Dorado-Liñán I, Valero-Garcés B et al (2022) Regional precipitation trends since 1500 CE reconstructed from calcite sublayers of a varved Mediterranean lake record (Central Pyrenees). *Sci Total Environ* 826:153773
- Violant i Simorra R (1934) Elaboració del cànem al Pallars. *Agric Ramad* 8:150–152

- Wang WJ, Thompson FR, He HS, Fraser JS, DiJack WD, Spetich MA (2018) Population dynamics has greater effects than climate change on tree species distribution in a temperate forest region. *J Biogeogr* 45:2766–2778
- Whitlock C, Larsen C (2001) Charcoal as a fire proxy. In: Last WM, Smol JP (eds) *Tracking environmental change using lake sediments*. Vol 3: Terrestrial, algal, and siliceous indicators. Kluwer, Dordrecht, pp 75–98



Historical Deforestations and Forest Resilience

7

Abstract

The vegetation reconstruction disclosed in the former chapters allowed the definition of three major deforestation/recovery (DR) cycles during Roman, Medieval, and Modern times. Each DR cycle is assessed based on three organization levels: overall forests, types of forests, and individual forest taxa. In general, the forests under study demonstrated remarkable resilience, recovering nearly entirely after each major deforestation event (bulk resilience). The critical tipping point beyond which the forests would have irreversibly disappeared from the region was never reached, even with deforestation exceeding 60%. The identified forest types (conifer, deciduous, and sclerophyll) endured over time, displaying similar heterogeneous patterns with minor spatial adjustments (mosaic resilience). On an individual level, the primary forest taxa experienced slight variations in their relative abundances, consistently within the same attraction domains (community resilience). The high resilience observed in these Pyrenean forests is credited to the influence of metapopulation and metacommunity processes and mechanisms in a highly dynamic and patchy environment. Conservation efforts should prioritize maintaining these spatial patterns and associated ecological dynamics.

At this stage, it is interesting to compare the three major deforestation–recovery cycles documented in the Montcortès paleoecological record (Roman, Medieval, and Modern) to discuss the resilience of regional forests in the context of their conservation. Before addressing the detailed analysis of forest succession, as documented in the Montcortès record, it is necessary to briefly introduce the idea of resilience used here, along with other related terms and concepts (Rull and Vegas-Vilarrúbia 2023).

7.1 Resilience and Associated Concepts

Resilience is described as the ability of ecosystems to bounce back to their original or reference state after temporary external disruptions. This concept, originally introduced by Holling (1973), recognizes that ecosystems typically undergo changes when faced with external disturbances, but once those disturbances subside, they may return to a state with similar structure, function, and composition, thereby maintaining their identity. The intensity and duration of the disturbance are crucial factors in determining the recovery time (t), the rate of recovery (r), and the eventual state of the ecosystem following recovery (Fig. 7.1). Each ecosystem possesses its own attraction domain, which represents the range of stable states the community can adopt without losing its distinct identity (Holling 1973). The interplay between the magnitude of the disturbance and the resilience of the ecosystem determines whether the community composition remains within the same attraction domain or crosses a critical threshold, transitioning to a different attraction domain associated with a different ecosystem. This transition is referred to as a regime shift and can also be triggered by the accumulation of minor yet persistent disturbances or by amplification feedbacks that lead to nonlinear responses, meaning responses of disproportionately large magnitude compared to the intensity of the disturbance (Scheffer et al. 2001; Briggs et al. 2009).

In the context of forests, the concept of resilience has been broken down into three distinct elements: persistence, recovery, and reorganization (Falk et al. 2022). Persistence refers to a lack of noticeable change, while recovery involves returning to the initial state. Both persistence and recovery occur within the same attraction

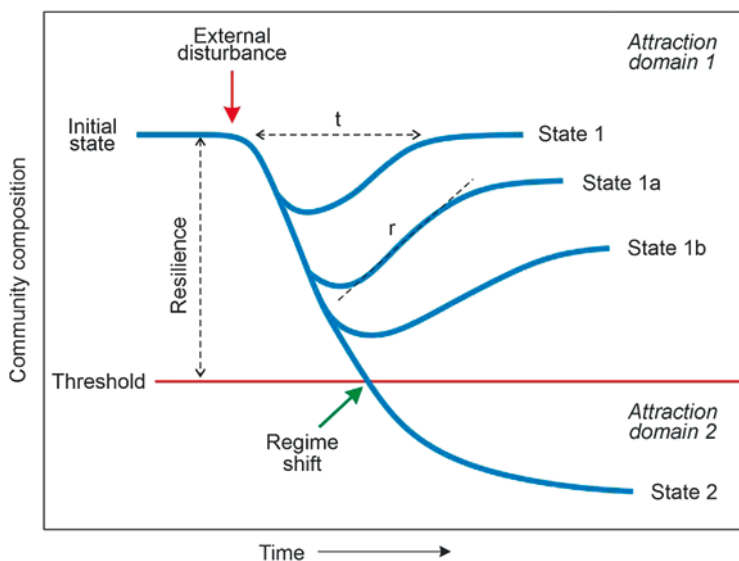


Fig. 7.1 Changes in the composition of a hypothetical community after a temporal external disturbance. t , return time; r , recovery rate. Redrawn and modified from Rull (2020)

domain. On the other hand, reorganization entails more profound compositional changes that can be either temporary (occurring within the same attraction domain) or enduring if they cross a threshold between two attraction domains, which can result in what is known as regime shifts. Changes in composition within the same attraction domain signify variations in the relative abundance of existing species or the replacement of individual species. In contrast, a regime shift entails a complete turnover of species, involving the replacement of one forest type with a different forest type or even with a nonforested community, a concept also referred to as community replacement (Rull 1990, 1992) or vegetation type conversion (Falk et al. 2022).

7.2 Resilience of Montcortès Forests

It is worth mentioning that the magnitudes of the three regional deforestation events documented in the palynological Montcortès record during the last 2000 years are very similar (Fig. 7.2). However, a more detailed statistical analysis revealed some relevant differences.

Here, the analysis was carried out at three different organizational levels: the entire forest, specific forest types, and individual taxa. This approach enabled the identification of three components that contribute to forest resilience: bulk resilience, mosaic resilience, and community resilience.

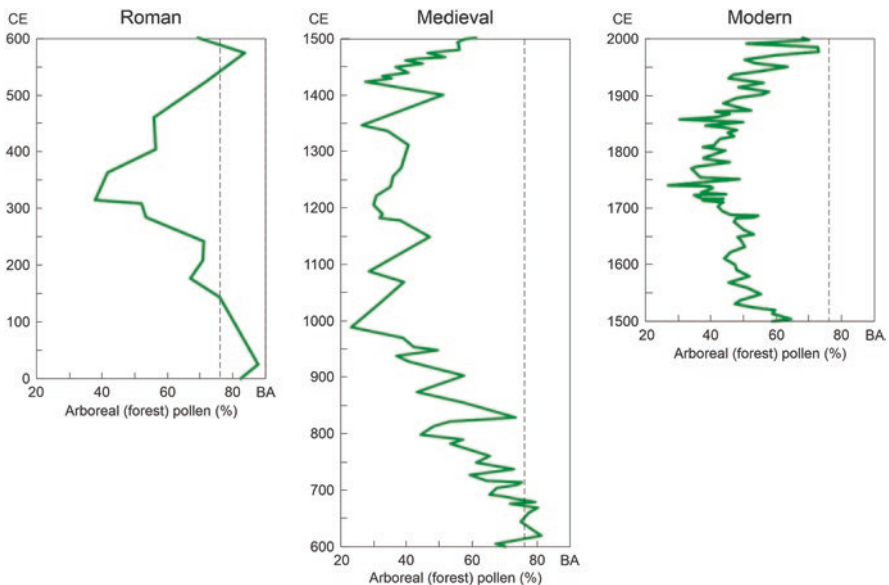


Fig. 7.2 Roman, Medieval, and Modern deforestation events, as represented by the total tree-forest pollen percentages (green curves), are plotted at the same chronological and percentage scales to facilitate comparison. Vertical dotted lines represent present-day forest percentages, and the maximum forest cover of the last 3000 years occurred during the Bronze Age (BA)

- **Bulk resilience:** This component is determined by examining the overall forest pollen, which serves as an indicator of regional forest coverage. Changes in this parameter can signal a bulk regime shift, indicating the potential replacement of forests with a different nonforested vegetation type, or it can demonstrate bulk forest resilience, where forest cover recovers after each clearing event, regardless of the specific forest type that eventually becomes established.
- **Mosaic resilience:** The Montcortès area is home to various forest types, mainly conifer forests (Cf), submontane deciduous forests (Sdf), and Mediterranean sclerophyllous forests (Msf). These forests are arranged in a characteristic mosaic pattern, characterized by the mixture of pollen from the dominant taxa of each forest type. If the pollen from one or two of these forest types disappears after deforestation, it implies a significant mosaic reorganization or the removal of the mosaic itself, resulting in the establishment of a single regional forest (regime shift). However, if the three forest types persist after deforestation with minor variations in their respective pollen percentages, it demonstrates mosaic resilience, indicating the regional persistence of the three forest types with minor reorganizations in their patch extent and arrangement.
- **Community resilience:** Assessing intracommunity resilience is challenging because it is difficult to identify specific forest patches acting as pollen sources for different pollen types. Therefore, the individual pollen components of each forest type, as represented in the pollen record, collectively define the metacommunity signal. A regime shift at the metacommunity scale is indicated by the replacement of dominant taxa in a given forest type, whereas fluctuating relative abundances within the community indicate metacommunity resilience.

In the pollen record, the most abundant forest taxa, in descending order, were *Pinus*, *Quercus* (evergreen and deciduous), *Betula*, *Corylus*, *Alnus*, *Fagus*, *Salix*, *Abies*, and *Ulmus*. Other forest elements, such as *Carpinus*, *Cornus*, *Fraxinus*, *Populus*, and *Rhamnus*, appeared infrequently as isolated or sporadic occurrences in scattered samples and were not considered in this study due to their potential to distort statistical analyses (Kaul et al. 2017; Silverman et al. 2020).

7.2.1 Bulk Resilience

The three deforestation/recovery (D/R) cycles that occurred over the past two thousand years in the Montcortès area are illustrated in Fig. 7.3 and described in Table 7.1. The longest cycle, lasting over nine centuries, was during the Medieval period (DR2), which was twice as long as the Modern cycle (DR3) and 1.6 times longer than the Roman cycle (DR1). The key distinction was that in DR2, the peak of deforestation lasted for 2.5 centuries, while in DR1 and DR3, forest recovery began immediately after reaching the lowest forest cover. The duration of deforestation during the Medieval period (over four centuries) was also longer compared to the Roman and Modern periods (2–3 centuries), whereas the time for forest recovery did not differ significantly, ranging from two centuries (Modern) to three centuries (Roman). When considering timing, forest clearing and recovery phases were

Table 7.1 Parameters used for comparisons among Roman (DR1), Medieval (DR2), and Modern (DR3) deforestation cycles in the Montcortès region (raw data: <https://data.mendeley.com/drafts/mr4h3x7x35>)

DR Cycle	Dates (CE)			Total forest pollen (%)						Time (yr)			Rates (% d ⁻¹)		
	Id	Md	Fd	Ip	Mp	Fp	Dp	Rp	Np	Dt	Rt	St	Dr	Rr	Sr
DR1	30	320	620	88	38	84	50	46	-4	290	300	1.0	1.7	1.5	0.9
DR2	620	1050–1300	1550	84	23	65	61	42	-19	430	250	0.6	1.4	1.7	1.2
DR3	1550	1780	2000	65	27	73	38	46	8	230	220	1.0	1.7	2.1	1.3

Dates (CE): Id, Initial date; Md, maximum deforestation date; Fd, final date. Total forest pollen (%): Ip, initial; Mp, minimum (maximum deforestation); Fp, final; Dp, deforestation decline (I-M); Rp, recovery increase (F-M); Np, full-cycle net gain/loss (F-I). Time (yr): Dt, deforestation phase (Md-Id); Rt, recovery phase (Fd-Mt); St, time symmetry (Rt/Dt). Rates (% of total forest pollen per decade; % d⁻¹): Dr., deforestation rates ($[Dp/Dt] \times 10$); Rr, recovery rates ($[Rp/Rt] \times 10$); Sr, rate symmetry (Rr/Dr)

quite balanced in the Roman and Modern cycles, but they were notably imbalanced during the Middle Ages. During this period, the recovery phase was 1.7 times faster than the clearing phase. In terms of the extent of deforestation, it was most severe in DR2 (61% reduction in pollen percentage), followed by DR1 (50%) and DR3 (38%). However, the intensity of recovery did not exhibit significant variations among the three DRs, ranging from 42% to 46%. The net forest losses were -19% (with 69% recovery) and -4% (with 92% recovery) during DR2 and DR1, respectively, while a net forest gain of 8% (with 121% recovery) characterized DR3. In total, over the last two millennia, there was a net forest loss of -15% (with 83% recovery). The rates of deforestation and recovery were similar and fairly balanced in the three DR cycles.

7.2.2 Mosaic Resilience

In contrast to earlier research (Rull et al. 2011), past forest types were not derived from current plant associations but were instead inferred from the pollen record using objective statistical methods. This approach aimed to maintain the possibility of discovering forest communities that differed from those existing today. However, when applying cluster analysis to individual pollen forest taxa, the results consistently matched the forest types defined for present-day vegetation, except for *Abies*, which was found to be associated with riverine forests (Rf) instead of conifer forests (Cf) (Fig. 7.4). This finding aligns with the concept of community stability over time, with only minor changes in composition, rather than a complete turnover or replacement of forest communities.

Figure 7.5 illustrates the temporal patterns of different types of forests. Cf and Msf exhibited significant correlations with the overall forest pollen trend, while Sdf and Rf did not show statistically significant associations with the broader forest trends, as indicated in Table 7.2. Cf was associated with all phases except Modern

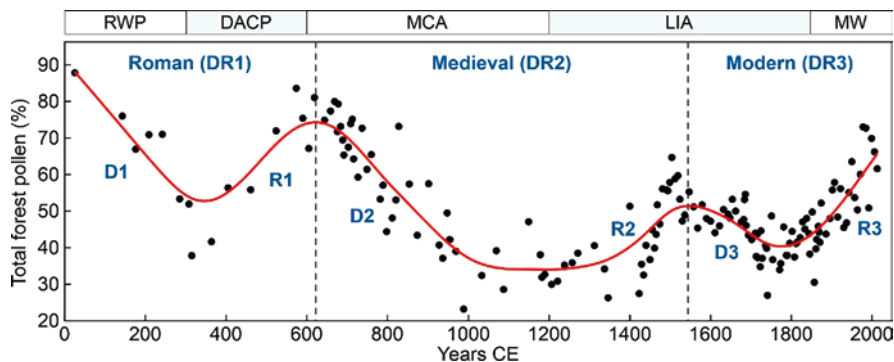


Fig. 7.3 Deforestation–recovery (DR) cycles using the total forest tree pollen. Raw data are represented as black dots and spline smoothing by a red line. Climatic phases (cold intervals in gray): RWP, Roman Warm Period; DACP, Dark Ages Cold Period; MCA, Medieval Climate Anomaly; LIA, Little Ice Age; MW, Recent Warming (Martín-Chivelet et al. 2011)

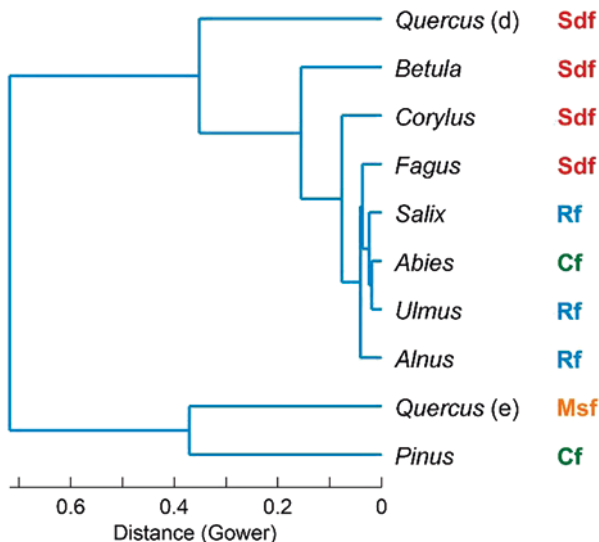


Fig. 7.4 Dendrogram using the Gower distance and the unweighted pair-group average (UPGMA) algorithm. Modern forest types are indicated on the right: Cf, conifer forest; Msf, Mediterranean sclerophyll forest; Sdf, submontane deciduous forest; Rf, riverine forest

deforestation (D3), whereas Msf displayed significant correlations with both Medieval and Modern trends. Sdf, on the other hand, was only associated with Medieval regeneration (R2) and Modern deforestation (D3). Rf did not exhibit any significant correlations in this analysis. When considering the cycles, it was observed that the Roman cycle (DR1) predominantly influenced Cf, while the Medieval cycle (DR2) impacted both Cf and Msf, with Sdf in the regeneration phase (R2). The

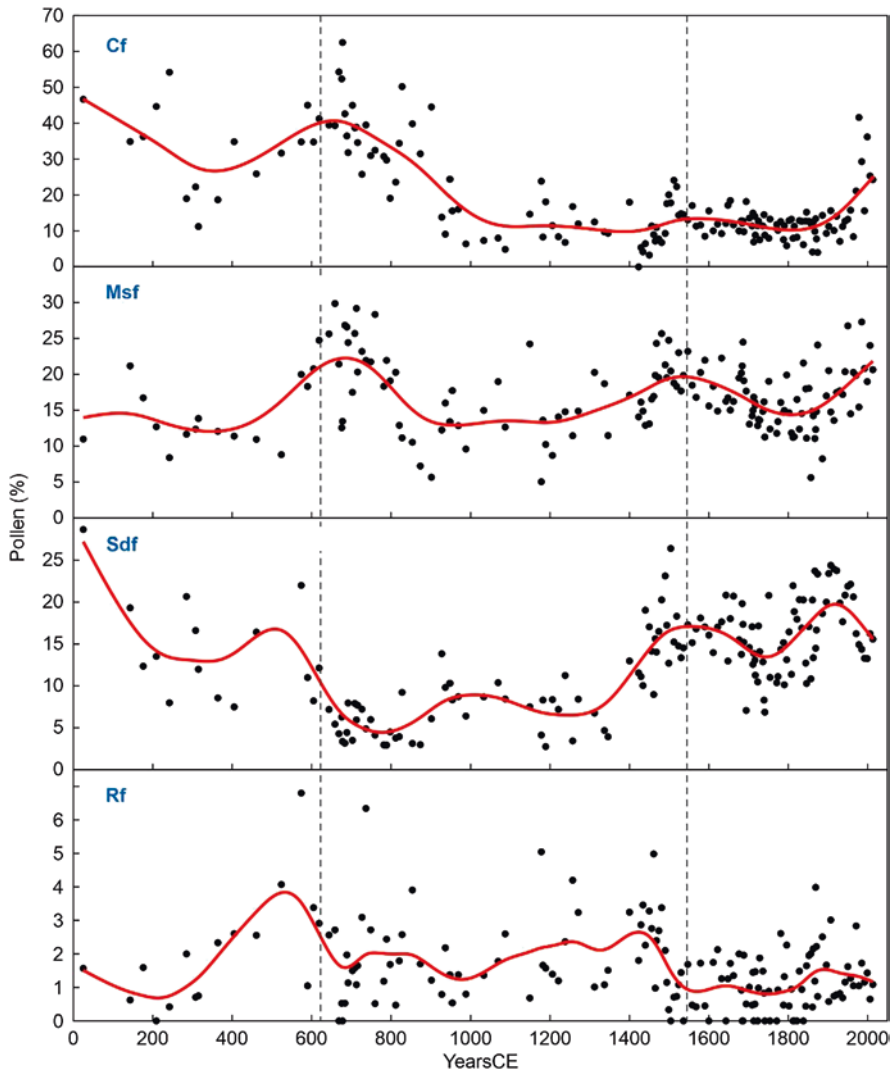


Fig. 7.5 Forest pollen groups considering the forest types defined by cluster analysis (Fig. 7.5) coincide with present-day forest associations. Conifer forest (Cf): *Pinus*; Mediterranean sclerophyll forest (Msf): evergreen *Quercus*; submontane deciduous forest (Sdf): deciduous *Quercus*, *Betula*, *Fagus*, and *Corylus*; Riverine forest: *Alnus*, *Salix*, and *Ulmus*

Modern cycle (DR3) primarily affected Msf, with Sdf in the deforestation phase (D3) and Cf in the recovery phase (R3), as shown in Fig. 7.6.

A ternary percentage diagram depicting the sample distribution in this study across the three primary forest types revealed that the greatest concentration of samples was found within the 50% range. This concentration coincided with the point where the three DR cycles intersected (Fig. 7.7). This observation suggests that the

Table 7.2 Correlations of forest types (Fig. 7.5) with total forest pollen for the total data set (overall) and for each specific deforestation and recovery phase (Fig. 7.4)

Forest type	Overall	Roman		Medieval		Modern	
		D1	R1	D2	R2	D3	R3
Cf	0.823**	0.862**	0.798**	0.890**	0.749**	0.338	0.759**
Msf	0.479**	0.056	0.651	0.540**	0.723**	0.748**	0.670**
Sdf	0.083	0.424	0.449	-0.321	0.716**	0.771**	0.218
Rf	0.101	-0.008	0.455	0.127	-0.377	0.204	0.058

Forest types: Cf, conifer forests; Msf, Mediterranean sclerophyll forests; Sdf, submontane deciduous forests; Rf, riverine forests. Correlation significance: * $p < 0.05$; ** $p < 0.01$

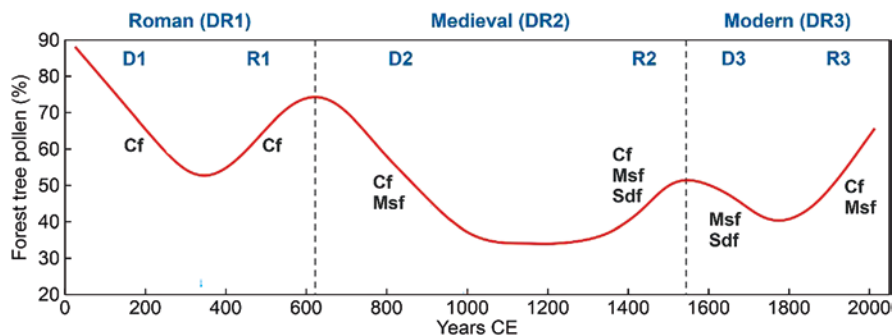


Fig. 7.6 Forest types statistically associated with the general forest trends (red line) for each particular deforestation and regeneration phase, according to the results of correlation analysis. All correlations were significant at $p < 0.01$ (Table 7.2). Cf, conifer forests; Msf, Mediterranean sclerophyll forests; Sdf, submontane deciduous forests

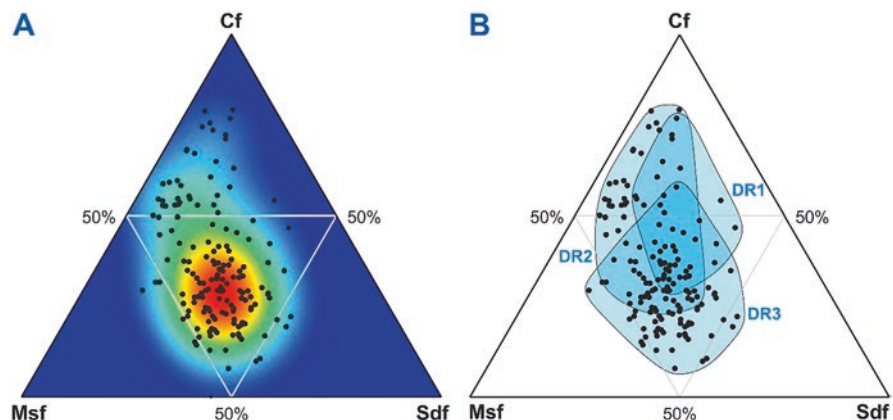


Fig. 7.7 Ternary diagram using the three main forest types (Cf, conifer forest; Msf, Mediterranean sclerophyll forest; Sdf, submontane deciduous forest). Black dots are sample values. (a) Density plot. Colors indicate the density of sample points, from higher (red) to lower (blue). (b) Sample groups according to DR cycles

forest mosaic has predominantly maintained values around this point over time. Furthermore, this finding, along with the previous evaluation of community constancy, supports the idea that changes in the forest mosaic are more likely the result of spatial reorganization of forest patches rather than abrupt regime shifts.

7.2.3 Community Resilience

Figures 7.8 and 7.9 illustrate the trends of the primary components in the forest, while their associations with the general pollen pattern are summarized in Table 7.3. The forest taxa most significantly associated with the overall forest pollen were *Pinus*, evergreen *Quercus*, *Abies*, and *Fagus* ($p \leq 0.01$). Additionally, *Corylus*, *Alnus*, and *Ulmus* exhibited lower but still significant correlations ($p \leq 0.05$). However, no significant correlations were observed for deciduous *Quercus*, *Betula*, and *Salix* ($p \geq 0.5$). Figure 7.10 shows the significant correlations during specific deforestation and recovery phases. In the case of Roman deforestation (D1), it primarily impacted *Pinus* and *Abies*, while the subsequent recovery (R1) involved only *Pinus*, with *Abies* failing to return to its pre-Roman levels (Fig. 7.8). Medieval forest clearance (D2) had substantial effects on *Pinus* and evergreen *Quercus*. Meanwhile, deciduous *Quercus* exhibited a notable increase following an early Medieval minimum (as indicated by a negative correlation (Fig. 7.9). Further recovery during the Medieval period (R2) resulted in significant increases in *Pinus*, both types of *Quercus* and *Betula*, along with a decrease in *Ulmus*, which had initially appeared during the peak of Medieval deforestation (Fig. 7.9). In contrast to previous deforestation events, Modern clearing (D3) did not influence *Pinus* and led to significant reductions in *Quercus* (both evergreen and deciduous), *Betula*, and *Corylus*. Subsequent forest recovery (R3) was marked by increases in *Pinus*, both *Quercus* types and *Ulmus*. Three forest elements (*Alnus*, *Fagus*, *Salix*) did not exhibit significant correlations with the overall forest trends throughout the various deforestation and recovery phases. These findings indicate that forest community constancy is characterized by the persistence of dominant and accompanying species over time, with some internal variations in their respective abundances. These idiosyncratic shifts within the community have resulted in continuous but minor changes within the attraction domains of the same forest types, which have endured over time.

7.3 Comparisons and Conservation Insights

The above findings suggest the following: (i) the Montcortès forests at mid-elevations demonstrated a remarkable level of resilience, recovering nearly entirely from three consecutive human-induced deforestations that occurred over the past two thousand years (bulk resilience); (ii) this resilience was also evident in the spatial arrangement of the forests, as the same types of forests observed today (Cf, Msf,

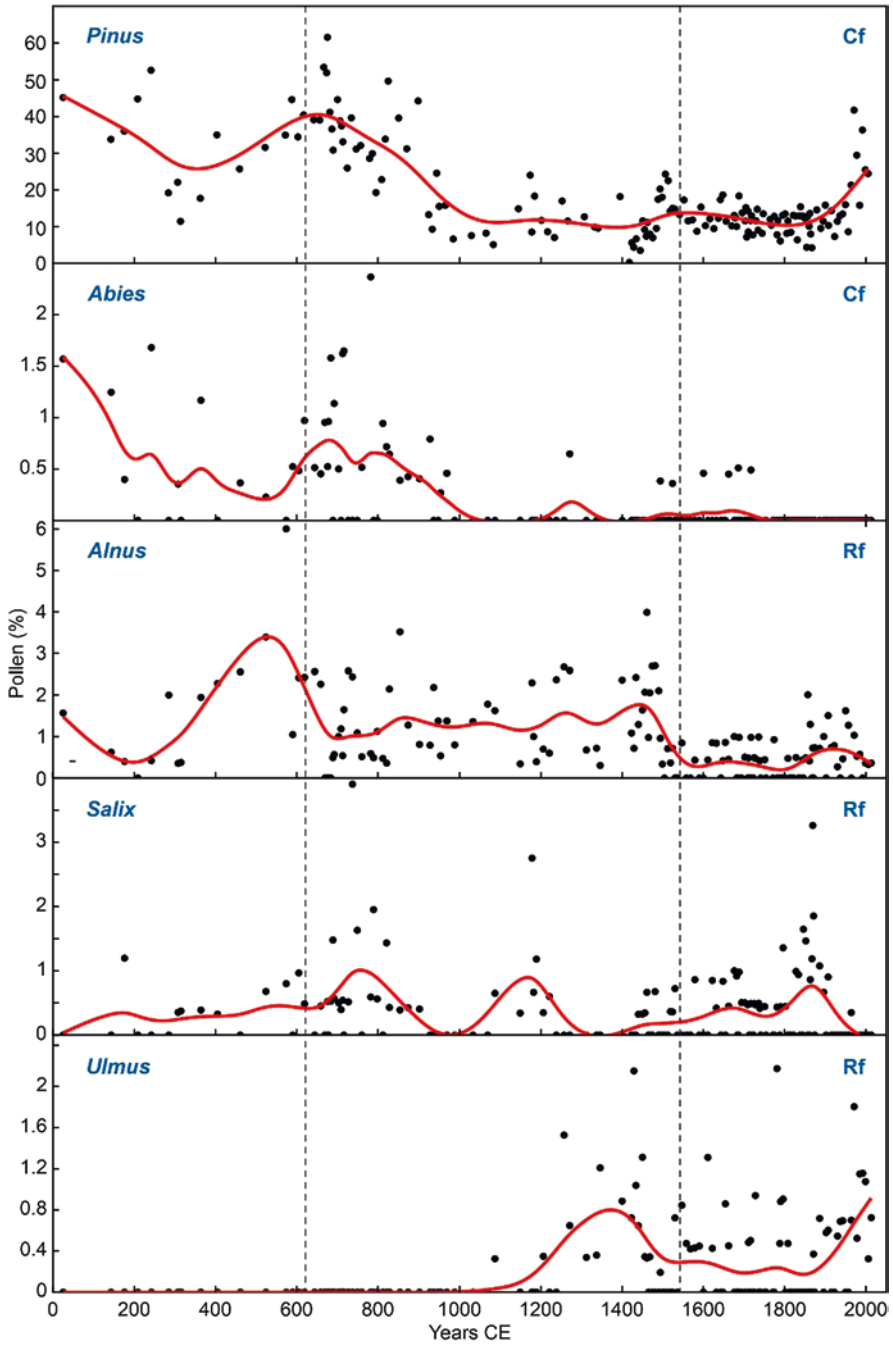


Fig. 7.8 Pollen types of coniferous forests (Cf) and riverine forests (Rf). Black dots: raw data, red line: smoothing spline

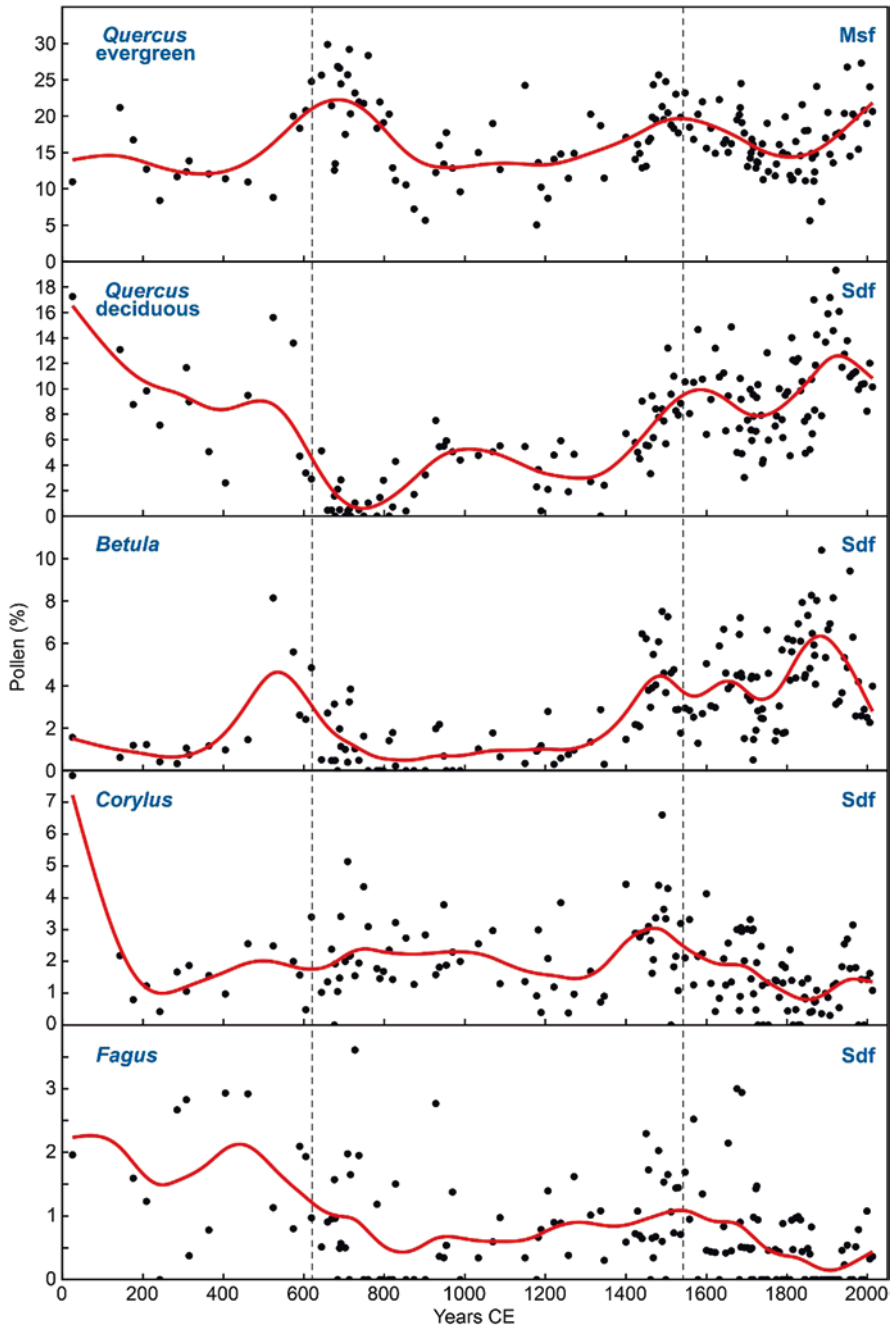


Fig. 7.9 Pollen types of Mediterranean sclerophyll forests (Msf) and submontane deciduous forests (Sdf). Black dots: raw data, red line: smoothing spline

Table 7.3 Correlations of individual forest pollen types with total forest pollen for the total data set (overall) and for each specific deforestation and recovery phase (Fig. 7.3)

Tree taxa	Overall	Roman		Medieval		Modern	
		D1	R1	D2	R2	D3	R3
<i>Pinus</i>	0.824**	0.856**	0.803*	0.889**	0.748**	0.328	0.759**
<i>Abies</i>	0.456**	0.728*	-0.306	0.292	0.223	0.178	0.000
<i>Quercus</i> (e)	0.479**	0.056	0.651	0.541**	0.723**	0.748**	0.670**
<i>Quercus</i> (d)	0.030	0.303	0.280	-0.570**	0.726**	0.500**	0.339*
<i>Betula</i>	-0.031	0.425	0.691	0.206	0.536**	0.489**	-0.211
<i>Corylus</i>	0.213**	0.528	0.360	0.033	0.304	0.392*	0.193
<i>Fagus</i>	0.211**	0.165	-0.308	0.174	0.193	0.179	0.095
<i>Alnus</i>	0.172*	0.142	0.447	-0.048	-0.133	0.050	0.179
<i>Salix</i>	0.047	-0.246	0.329	0.250	0.062	0.190	-0.288
<i>Ulmus</i>	0.170*	0.000	0.000	0.000	-0.628**	0.179	0.309*

Forest types: Cf, conifer forests; Msf, Mediterranean sclerophyll forests; Sdf, submontane deciduous forests; Rf, riverine forests. Correlation significance: * $p < 0.05$; ** $p < 0.01$

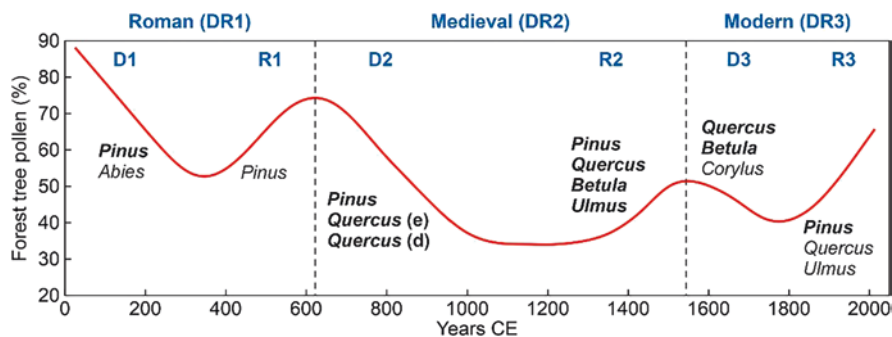


Fig. 7.10 Characterization of the different deforestation (D) and forest regeneration (R) phases in terms of the individual forest types that significantly decreased or increased, according to the results of correlation analysis. Correlations significant at $p < 0.01$ are in bold, and those significant at $p < 0.05$ are in normal font (Table 7.3). The general forest trends are represented by a red line (Fig. 7.3)

Sdf, Rf) have persisted since pre-Roman times, with only minor changes in their size and shape (mosaic resilience); and (iii) at the metacommunity level, there was a high degree of resilience, with the same tree species consistently dominating the various forest types. The composition of these communities only exhibited slight variations, always within their respective attraction domains (community resilience). In essence, these results imply that over the past two millennia, the Montcortès regional forests have not reached a critical threshold or a tipping point of no return where they would become irreversibly altered or replaced by other vegetation types, despite the significant deforestation events documented in the paleoecological record.

Reductions of 40–60% in overall forest pollen were observed, followed by recoveries of a similar scale, despite only a 15% net forest loss. The lowest point in forest cover, approximately 30% of forest pollen, was reached during the Middle Ages, indicating that a reduction of this magnitude did not lead to the complete disappearance of regional forests. Consequently, it is estimated that irreversible forest removal is likely to occur at levels below 30%. In other words, the Montcortès forests managed to bounce back and maintain their identity even after being reduced to less than a third of their original size, which can be seen as the minimum threshold for bulk resilience. All the various forest types within the Montcortès regional mosaic survived a critical point after severe reductions, even when their pollen signal disappeared in some samples. This suggests that some of these forests might have survived as smaller patches or microrefugia (Rull 2009) during periods of minimal forest cover and then expanded during recovery phases. This overall resilience of the forest mosaic largely depended on metacommunity dynamics (Holyoak et al. 2005), as well as the consistency of the community composition over time, despite minor variations. This continuity in taxonomic composition, or community resilience, likely relied on metapopulation processes and mechanisms (Hanski 1999). These mechanisms endured the phases of forest contraction and expansion in the highly dynamic microrefugial landscape. Thus, mosaic and community resilience were closely connected and largely hinged on the interplay of metapopulation and metacommunity dynamics.

In addition to the remarkable resilience observed at various levels, it is worth noting the symmetrical nature of both the clearing and recovery processes. This symmetry is evident in terms of their duration (typically spanning 2–3 centuries) and their rates (falling within the range of 1.5–2% per decade). Previous studies have pointed out that these long-term trends are made up of shorter cycles, typically lasting several decades. Shorter, higher-frequency cycles, with an average duration of approximately 50 years, were indicative of deforestation phases and hindered forest growth. On the other hand, longer, lower-frequency cycles, lasting approximately 100 years, were associated with forest development and occurred during recovery phases (Rull et al. 2021b). As discussed in former chapters, the main causes of forest clearing included opening up landscapes for croplands and grasslands, as well as wood and charcoal extraction, with varying levels of intensity depending on the historical period. Slash-and-burn practices were common before the Middle Ages but were discontinued during the feudal regime. Charcoal extraction, especially active during modern times, was driven by the growth of the iron industry. Recovery phases were facilitated by reductions in forest exploitation, and in the most recent regeneration phase (R3), intensive reforestation efforts, particularly involving pine trees. Forest recovery has been particularly noteworthy since the onset of the industrial period when the Pallars region, where Lake Montcortès is located, experienced depopulation due to migration to large cities (Chap. 2).

The simultaneous timing of deforestation phases D1 and D2 with warm periods RWP and MCA and regeneration phases R1 and R2 with cold periods DACP and

LIA (Fig. 7.3) suggest a possible influence of climate. It has been proposed that during cold periods, human societies may have migrated southward to lowland areas, thereby reducing human activity around the lake and allowing the surrounding forests to recover (Rull et al. 2021a, b). This pattern seems to have reversed in the last cycle (DR3) when deforestation (D3) occurred in the second half of the LIA cold phase, while forest regeneration (R3) coincided with the Modern Warming (MW). This shift could be attributed to the widespread extraction of charcoal throughout the region, regardless of climate conditions, leading to industrial depopulation, as previously mentioned. Individually, the contrasting behavior of evergreen and deciduous *Quercus* during the DACP-MCA interval (R1 and D2) is highlighted in Fig. 7.9. This raises the question of whether this divergence could be partly due to their different responses to climatic warming. This distinction aligns with the Mediterranean characteristics of evergreen *Quercus* species, which are better suited to warmer conditions compared to the higher-elevation submontane deciduous species. Consequently, the possibility of climate playing a role in this case cannot be dismissed, and we should also consider the potential synergies between climate and human activity.

7.3.1 Comparisons with Other Pyrenean Records

The continual recovery of mid-elevation Montcortès forests in the past stands in stark contrast to high-mountain Pyrenean regions, which were significantly deforested during historical times and still remain in that state today, with the treeline pushed well below its natural position in many areas. This extensive deforestation was most pronounced during the Medieval and Modern periods, aiming to create vast grassland landscapes conducive to extensive grazing and long-distance horizontal transhumance, as documented by various studies (González-Sampéris et al. 2017, 2019; García-Ruiz et al. 2020). Only a few small, isolated areas seemed to have been spared from deforestation and served as microrefugial zones for high-elevation conifer forests (Rull et al. 2021c). Unfortunately, most palynology studies that have examined Pyrenean deforestation offer limited temporal resolution, usually spanning centuries (Rull and Vegas-Vilarrúbia 2021a, b), making it difficult to reconstruct ecological changes and draw conclusions about forest resilience. Furthermore, many of these studies employ pollen analysis primarily to reconstruct past environments and human activities, rather than to draw ecological insights, which complicates comparisons with ecological research such as the one presented here (Rull and Vegas-Vilarrúbia 2022). The absence of truly ecological, high-resolution palynological studies tracking forest development not only hampers our understanding of the history of Pyrenean forests but also impedes our ability to inform conservation efforts.

As highlighted in previous chapters, the frequent use of pollen as a tool for studying past climates in the Pyrenees creates a problem by limiting our understanding of how past climate changes affected vegetation, specifically forests, due to circular constraints. This limitation is a significant drawback, as it hinders our ability to use

ancient ecological records for predicting how forests might respond to future climate changes. Therefore, instead of relying solely on pollen, it is preferable to use other independent proxies, such as varves, tree rings, stable isotopes, and similar methods to reconstruct past climates. In the case of Lake Montcortès, the varved nature of sediments and the availability of dendroclimatological studies in nearby areas have enabled the creation of detailed historical temperature and precipitation records (Büntgen et al. 2017; Vegas-Vilarrúbia et al. 2022). These records have been used to analyze how forests responded to climate shifts over the last five centuries, corresponding to the DR3 cycle. The most influential factors affecting forest growth and recovery have been identified as summer temperature/drought and autumn precipitation, often in combination with human activities (Rull and Vegas-Vilarrúbia 2022). Some tree species have shown delayed responses to climate shifts of two or several decades. Recent high-resolution studies have revealed that in high-mountain Pyrenean environments, climate events such as the Medieval Climate Anomaly (MCA) or the Little Ice Age (LIA) had no significant impact on forest development in the absence of human influence (Rull et al. 2021a, b, c, d). However, the absence of similar studies across the entire mountain range makes it challenging to draw broader comparisons and regional conclusions.

7.3.2 Applications to Conservation

Upon initial observation, it could be argued that the Montcortès forests, as demonstrated in this study, possess a remarkable ability to withstand adverse conditions over the past two millennia. This could lead one to believe that they do not require specific protective measures, as they seem capable of enduring significant deforestation before reaching a point of no return. However, a more nuanced and cautious examination of paleoecological evidence reveals that this perspective may be misleading for several reasons. First, it is essential to note that the recovery of these forests was not a spontaneous process but rather a response to the reduction or cessation of human impact. Without a reduction in human activity, deforestation would have continued, and the irreversible threshold would have been reached sooner or later. Therefore, alleviating anthropogenic pressure played a crucial role in halting deforestation, just as the implementation of conservation measures would. Second, the phases of forest regeneration were extended processes spanning more than two centuries, and they may not serve as suitable analogs for the near future due to the unprecedented global warming projected for the coming centuries. A potential increase in global temperatures by several degrees could disrupt the Earth's climate system, potentially leading to unpredictable consequences for the biosphere, a situation not seen in past records. Third, the fact that the precise tipping point at which the Montcortès forests would vanish remains unknown in the available paleoecological records implies that this critical threshold can only be deduced from future trends. However, once this threshold is crossed, the loss of forests would become irreversible, rendering any conservation efforts futile.

In essence, the level of uncertainty regarding the future of Montcortès forests is too great to not implement protective measures. Currently, these forests at mid-elevations lack specific protection measures, with only the lake and its immediate vicinity falling under the EU Natura 2000 network. A UNESCO Geopark has recently been established to safeguard geological heritage, including Montcortès forests, but it does not address protective measures for living systems. The primary threats to these mid-elevation forests are wildfires, both natural and human-induced, particularly during exceptionally warm, dry, and windy conditions. According to current IPCC estimates, future projections indicate a rise in temperature, aridity, and extreme events, which could worsen the occurrence of fires and forest loss in Montcortès and its neighboring mid-elevation regions. Therefore, it is imperative to implement protective measures, and the paleoecological reconstructions provided here can offer valuable insights in this context.

Instead of concentrating on the overall resilience of forests and the unpredictable identification of the tipping point for deforestation, it might be more practical and relevant to consider the concept of mosaic resilience in paleoecology. As mentioned earlier, maintaining diverse spatial patterns is crucial for the continued existence of forest ecosystems. Therefore, conservation efforts should prioritize the preservation of such a diverse landscape, especially in regard to forests, to ensure their long-term survival through metapopulation and meta-community processes and mechanisms. Within this framework, it is essential to represent every type of forest, even in small patches, such as riverine forests, to maintain the ability to recolonize disturbed areas. Additionally, creating a botanical garden and a germplasm bank that includes a wide variety of forest species could prove beneficial for safeguarding regional biodiversity and facilitating potential restoration efforts if needed.

References

- Briggs R, Carpenter SR, Brock WA (2009) Turning back from the brink: detecting and impeding regime shift in time to avert it. *Proc Natl Acad Sci USA* 106:826–831
- Büntgen U, Krusic PJ, Verstege A, Sangüesa-Barreda G, Wagner S, Camarero JJ et al (2017) New tree-ring evidence from the Pyrenees reveals western Mediterranean climate variability since Medieval times. *J Clim* 30:5295–5318
- Falk DA, van Mantgem PJ, Keeley JE, Gregg RM, Guiterman CH, Tepley AJ et al (2022) Mechanisms of forest resilience. *Forest Ecol Manag* 512:120–129
- García-Ruiz JM, Tomás-Faci G, Diarte-Blasco P, Montes L, Domingo R, Sebastián M et al (2020) Transhumance and long-term deforestation in the subalpine belt of the central Spanish Pyrenees: an interdisciplinary approach. *Catena* 195:104744
- González-Sampériz P, Aranbarri J, Pérez-Sanz A, Gil-Romera G, Moreno A, Leunda M et al (2017) Environmental and climate change in the southern Central Pyrenees since the Last Glacial Maximum: a review from the lake records. *Catena* 149:668–688
- González-Sampériz P, Montes L, Aranbarri J, Leunda M, Domingo R, Laborda R et al (2019) Escenarios, tiempo e indicadores paleoambientales para la identificación del Antropoceno en el paisaje vegetal del Pirineo Central (NE Iberia). *Cuad Invest Geogr* 45:167–193

- Hanski I (1999) *Metapopulation ecology*. Oxford University Press, New York
- Holling CS (1973) Resilience and stability of ecological systems. *Ann Rev Ecol Syst* 4:1–23
- Holyoak M, Leibold MA, Holm RD (2005) *Metacommunities: spatial dynamics and ecological communities*. Chicago University Press, Chicago
- Kaul A, Mandal S, Davidov O, Peddada SD (2017) Analysis of microbiome data in the presence of excess zeros. *Front Microbiol* 8:2114
- Martín-Chivelet J, Muñoz-García MB, Edwards L, Turrero MJ, Ortega AI (2011) Land surface temperature changes in northern Iberia since 4000 yr BP, based on $\delta^{13}\text{C}$ of speleothems. *Glob Planet Change* 77:1–12
- Rull V (1990) Quaternary palaeoecology and ecological theory. *Orsis* 5:91–111
- Rull V (1992) Successional patterns of the Gran Sabana (southeastern Venezuela) vegetation during the last 5000 years, and its responses to climatic fluctuations and fire. *J Biogeogr* 19:329–338
- Rull V (2009) Microrefugia. *J Biogeogr* 36:481–484
- Rull V (2020) *Quaternary ecology, evolution, and biogeography*. Elsevier/Academic Press, London
- Rull V, Vegas-Vilarrúbia T (2021a) A spatiotemporal gradient in the anthropization of Pyrenean landscapes. Preliminary report. *Quat Sci Rev* 258:106909
- Rull V, Vegas-Vilarrúbia T (2021b) Conifer forest dynamics in the Iberian Pyrenees during the Middle Ages. *Forests* 12:1685
- Rull V, Vegas-Vilarrúbia T (2022) Climatic and anthropogenic drivers of forest succession in the Iberian Pyrenees during the last 500 years: a statistical approach. *Forests* 13:622
- Rull V, Vegas-Vilarrúbia T (2023) Resilience of Pyrenean forests after recurrent historical deforestations. *Forests* 14:567
- Rull V, González-Sampériz P, Corella JP, Morellón M, Giralt S (2011) Vegetation changes in the southern Pyrenean flank during the last millennium in relation to climate and human activities: the Montcortès lacustrine record. *J Paleolimnol* 46:387–404
- Rull V, Cañellas-Boltà N, Vegas-Vilarrúbia T (2021a) Late-Holocene forest resilience in the central Pyrenean highlands as deduced from pollen analysis of Lake Sant Maurici sediments. *The Holocene* 31:1797–1803
- Rull V, Vegas-Vilarrúbia T, Corella JP, Valero-Garcés B (2021b) Bronze Age to Medieval vegetation dynamics and landscape anthropization in the south-central Pyrenees. *Palaeogeogr Palaeoclimatol Palaeoecol* 571:110392
- Rull V, Vegas-Vilarrúbia T, Corella JP, Trapote MC, Montoya E, Valero-Garcés B (2021c) A unique Pyrenean varved record provides a detailed reconstruction of Mediterranean vegetation and land-use dynamics over the last three millennia. *Quat Sci Rev* 268:107128
- Rull V, Cañellas-Boltà N, Vegas-Vilarrúbia T (2021d) Late-Holocene forest resilience in the central Pyrenean highlands as deduced from pollen analysis of Lake Sant Maurici sediments. *Holocene* 31:1797–1803
- Scheffer M, Carpenter S, Foley JA, Walker B (2001) Catastrophic shifts in ecosystems. *Nature* 413:591–596
- Silverman JD, Roche K, Mukherjee S, David LA (2020) Naughty all zeros in sequence count data are the same. *Comp Struct Biotech J* 18:2789–2798
- Vegas-Vilarrúbia T, Corella JP, Sigró J, Rull V, Dorado-Liñán I, Valero-Garcés B et al (2022) Regional precipitation trends since 1500 CE reconstructed from calcite sublayers of a varved Mediterranean lake record (Central Pyrenees). *Sci Total Environ* 826:153773



Synthesis, Comparisons, and Future Studies

8

Abstract

This chapter is a synthetic overview of the findings disclosed in previous chapters and is subdivided into four main parts: (i) a chronological synthesis, (ii) a statistical synthesis, (iii) a biogeographical contextualization at Peninsular (Iberian) and continental (Mediterranean) levels, and (iv) some suggestions regarding possible future research developments. The chronological synthesis situates all the evidence obtained in a single timeline and explains how the different plant taxa and vegetation types have progressed over the last three millennia, as well as the main environmental and anthropogenic drivers involved and their corresponding interactions. The statistical synthesis uses multivariate techniques to establish the most significant relationships with potential causal meaning. The two independent approaches (chronological and statistical) show remarkable coincidences and are complementary in explaining the history of local and regional vegetation trends in terms of ecological dynamics. In a peninsular context, the Montcortès record contributes to highlighting the high spatio-temporal heterogeneity in the anthropization of Iberian landscapes. In a Mediterranean context, the Montcortès record is unique in terms of temporal extent, varve continuity, absolute dating, high-resolution analyses of independent proxies, and detailed historical records, among others. The Montcortès record is proposed as a standard sequence for the western Mediterranean, which is able to provide continuous past–present ecological records at the same temporal resolution.

This chapter is a synthetic overview of previous chapters about pre-Medieval, Medieval, and post-Medieval times. Rather than merely a repetition of already presented results, this chapter provides new analyses and graphical displays considering the whole paleoecological dataset at the same time. A classical pollen diagram,

which would be simply the composition of Figs. 4.1, 5.1, and 6.1, is not provided to avoid repetitions, and the palynological results are represented instead as time series on a horizontal temporal scale to facilitate comparisons with modern ecological records in the way toward the development of long-term past–present continuous ecological time series (Rull 2009, 2014). In addition, new statistical analyses are performed aimed at synthesizing the paleoecological trends of the last 3000 years and their major drivers.

As mentioned previously, the lack of local paleoclimatic reconstructions for the whole time period covered by the Lake Montcortès record prevents the development of detailed statistical studies such as those performed for the last 500 years (Chap. 6; Sect. 5). The relationship between paleoecological and paleoclimatic trends is thus established by visual comparison with the paleotemperature curve representing northern Iberia (Martín-Chivelet et al. 2011). For the same reason, multivariate analyses do not include paleoclimatic parameters as explanatory variables. Only the major vegetation and landscape trends will be discussed here, and the reader is referred to the corresponding chapters for more details.

This chapter is subdivided into four main parts: (i) an abridged chronological synthesis, (ii) a statistical synopsis, (iii) a comparison with other Iberian and Mediterranean records, and (iv) a proposal for future research directions. The chronological part could also be viewed as a general conclusions section and could serve as a guide to locate particular points of interest that are analyzed in more detail in Chaps. 4, 5, 6. The statistical section provides new integrated multivariate analyses aimed at synthesizing the main paleoecological trends of the last three millennia in relation to the most relevant paleoenvironmental events and cultural developments. The comparison with other Iberian and Mediterranean records is aimed at placing the Montcortès record in regional and supra-regional contexts, as well as highlighting its uniqueness. The proposal for future studies is a trial to upgrade the lake and its paleoecological record to the importance they deserve for their unique potential to provide long-term past–present–future ecological time series.

8.1 Chronological Synthesis

In general, the same forest types that dominate the current landscape across the Montcortès region—i.e., pine-dominated montane conifer forests, submontane forests dominated by deciduous oaks, and Mediterranean evergreen oak forests—have also prevailed since the Late Bronze Age, although they have undergone variations in their geographical range and taxonomic composition over time. Especially noteworthy has been the occurrence of three regional deforestations during the Roman, Medieval, and Modern periods, when forest reductions of similar magnitude and rates have occurred (Fig. 8.1). The declines in forest cover have affected different forest types, depending on the epoch considered. Roman deforestation mainly affected pine forests, whereas Medieval clearing reduced all forest types, and Modern forest decline involved mainly pine and deciduous oak forests.

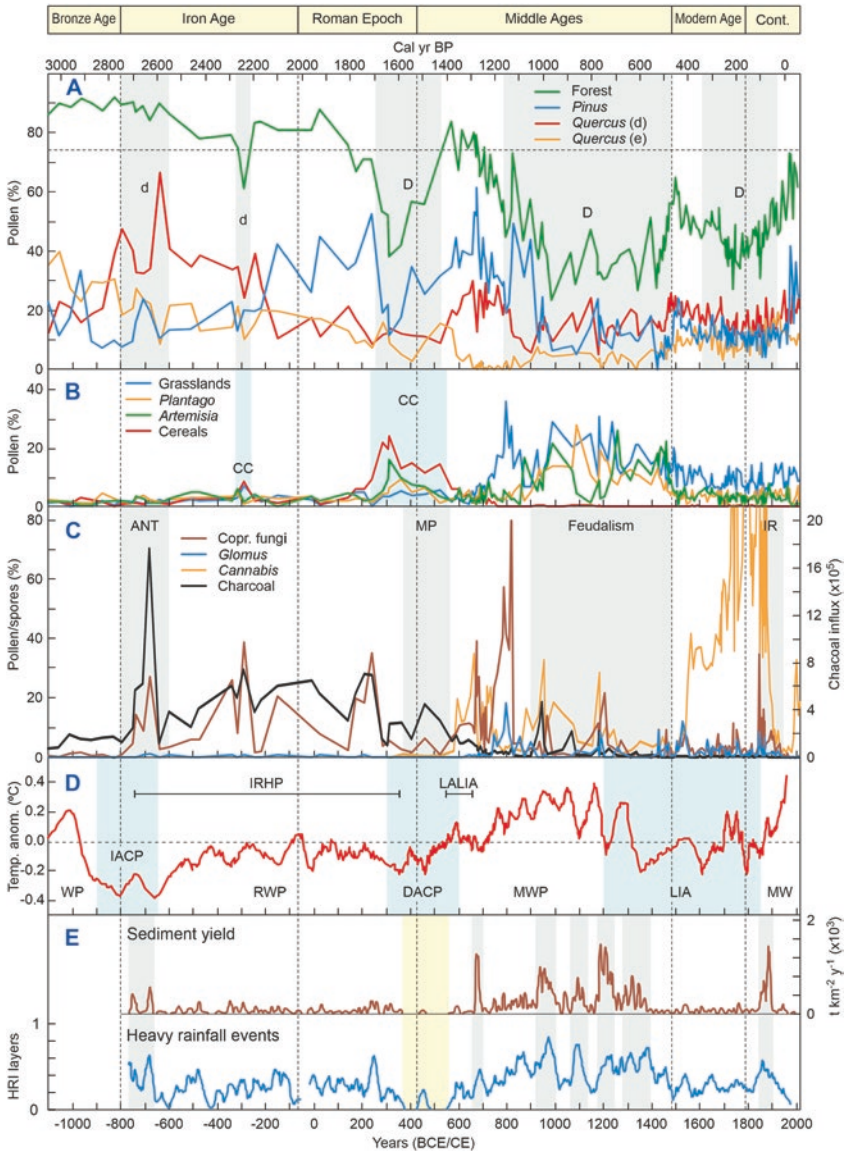


Fig. 8.1 Synthetic diagram showing the main paleoecological and paleoclimatic variables utilized in the interpretation of vegetation and landscape dynamics in the Montcortès record. (a) Forest trees (D, regional deforestations; d, local deforestations). (b) Wild and cultivated herbs (CC, cereal cultivation). (c) Proxies for human activities (ANT, anthropization; MP, Migration Period; IR, Industrial Revolution). (d) Paleotemperature trends of northern Iberia (Martín-Chivelet et al. 2011) (BWP, Bronze Age Wam Period; IACP, Iron Age Cold Period; RWP, Roman Warm Period; DACP, Dark Ages Cold Period; MWP, Medieval Warm Period; LIA, Little Ice Age; MW, Modern Warming). The blue band represents cold phases. IRHP, Iberian-Roman Warm Period (Martín-Puertas et al. 2009); LALIA, Late Antique Little Ice Age (Büntgen et al. 2016). E, sediment yield to Lake Montcortès (brown line) and frequency of heavy rainfall events (blue line), according to Corella et al. (2016, 2019). The yellow band is the Migration Period (see panel C). Gray bands emphasize the coincidence of the SY and HRE maxima

Before these large-scale woodland declines, several local and less intense forest clearances occurred during the Iron Age. The first is not manifested in the regional forest curve (only in deciduous *Quercus*) because it primarily affected local gallery forests that covered the lake surroundings. This local clearance signified the anthropization of the lake catchment, which was used for grazing after intensive forest burning, probably by itinerant human societies. The removal of local gallery forests likely facilitated catchment erosion, as indicated by an increase in sediment yield (SY) to the lake, coeval with the increased frequency of heavy rainfall events (HRE). This anthropization event occurred during the IACP when temperatures reached the minimum values of the last three millennia, which suggests that high-mountain areas would have been unsuitable for human life and pastoral activities, and montane sites such as the Lake Montcortès catchment were more appropriate for such purposes. Prior to anthropization, during the BAWP warming, regional forest cover was greater than it is today and forests were largely untouched. The second Iron Age local deforestation involved evergreen and deciduous oak forests, which were partially burned for grazing and, for the first time in the sequence, small-scale cereal cultivation. Temperatures were similar to today.

During most of the Roman epoch, the regional vegetation was dominated by *Pinus* forests, as is today, likely favored by a decreasing temperature trend and the ensuing downward displacement of vegetation belts. Human impact was low at the beginning (Republican period) and increased later (Imperial period) in the form of enhanced pastoralism and cereal cultivation. The first large-scale deforestation took place toward the end of Roman domination, as manifested in the significant reduction in regional forests dominated by *Pinus* and deciduous *Quercus*. This general human-made landscape opening was for cultivation purposes, rather than for grazing, and was carried out by burning and tree felling. The forest was exploited primarily for wood extraction, likely for construction purposes. The coincidence of maximum deforestation with minimum temperatures corresponding to the Dark Ages Cold Period (DACP) suggests that the wood was also used as fuel for heating. After the deforestation peak, *Pinus* underwent a significant recovery, but *Quercus* remained in a descending trend.

The Migration Period (MP) remains unnoticed in historical accounts of the Pallars region but has a distinct footprint in the Montcortès paleoecological record. Indeed, the transition from the Roman Empire and the Visigoth occupation was characterized by the recovery of forests, especially montane pine forests, after the first large-scale deforestation occurred during Roman times. This recovery was favored by low human pressure and coincided with increasing temperatures that characterized the DACP–MWP transition. SY and HRE were almost null, suggesting increased vegetation around the lake. The whole picture points toward the MP as a transitional phase with low human occupancy prior to the establishment of the Visigoth land-use practices. The phase corresponding to this culture was characterized by the onset of the second (Medieval) regional deforestation event, the significant increase in grazing, and the introduction of hemp, which was likely cultivated for domestic uses. Human pressure intensified, and SY and HRE experienced sharp and unprecedented increases and remained high during the whole Medieval period,

coinciding with temperatures higher than the present, corresponding to the extended MWP maximum.

Forest retreat, affecting mainly pine and deciduous oak forests, attained its maximum under the feudal system, which was established during Frank domination, after a transitional Muslim phase with little incidence on vegetation and landscape shifts, except for an abrupt decline in grazing practices. The maximum development of feudalism occurred during the political independence of the Pallars region, a phase known as the County of Pallars. Historical documents emphasize the abandonment of slash-and-burn practices and the development of extensive cultivation in the lowlands, along with large-scale horizontal transhumance in the highlands. In the Montcortès paleoecological record, fire incidence underwent a significant reduction at the end of the MP and was revitalized with feudalism in the form of short but intense peaks coinciding with equally brief and significant grazing maxima, which were coeval with similar SY peaks. Some of these fire peaks also coincided with warming maxima, suggesting the occurrence of climate-human feedback. However, fire incidence was substantially lower as in pre-Medieval times, which points toward logging, rather than fire, as the major deforestation agent. Hemp cultivation continued to be important in the region. The end of the Middle Ages was characterized by a rapid recuperation of all forest types, likely as a result of the relaxation of human pressure due to the demographic crash caused by the so-called ending Medieval crisis, which was a consequence of climatic and cultural constraints, including the self-induced collapse of the feudal system. A sharp decrease in SY occurred, likely as a consequence of a general increase in forest cover and reduced catchment erosion. Notably, major SY peaks that occurred during the Middle Ages coincided with HRE maxima, indicating that both precipitation extremes and anthropogenic deforestation would have influenced sediment delivery to the lake. However, this was not the rule in pre-Medieval times when, except for the first anthropization pulse, SY had remained low despite the occurrence of relevant HRE maxima. This finding supports that anthropogenic factors are major drivers for shifts in SY. Another interesting observation is that *Glomus*, usually considered a proxy for increased erosion rates, shows little agreement with SY trends over time, which seems to demand an alternative interpretation, at least in this record.

A comparison was made between forest dynamics in Montcortès and northern Pyrenean highlands (>1600 m elevation) during the Middle Ages using high-mountain records of similar resolution from lakes Llebreeta and Sant Maurici. In these records, evidence of regional subalpine deforestation for extensive grazing was lacking, and forests surrounding those lakes showed remarkable continuity, even a general expansion in the case of Sant Maurici, during Medieval times. This contrasts with other records from the central Pyrenees, where Medieval forest clearing was evident, although based on low-resolution records. Forest stability recorded at the Llebreeta and Sant Maurici sequences suggested the occurrence of potential microrefugia for these highland pine woodlands within a general landscape opening in subalpine environments. Also contrasting was the anthropization timing between Montcortès, which occurred in the Iron Age, and highland environments, where full landscape anthropization did not occur until the Middle Ages. A comparison of the

available records from the southern central Pyrenees suggested a statistically significant spatiotemporal anthropization gradient from the Bronze Age (southern lowlands) to the Middle Ages (northern highlands), with Montcortès (Iron Age) situated in an intermediate position, yet closer to lowland patterns.

The ending Medieval forest regeneration persisted until the beginning of the Modern Age, when the third regional deforestation began. Fire incidence was substantially reduced, and forest exploitation for wood and charcoal was considered to be the main deforestation agent. The coincidence of maximum deforestation with a phase of intense development of the coal-demanding iron industry supports this assessment. Minimum forest cover also coincided with a warming event within the general LIA cooling, compatible with a climatically triggered upward migration of Mediterranean oak forests to Montcortès elevations and the ensuing intensification of their exploitation around the lake. Forest regeneration began in Contemporary times, favored by the occurrence of two successive demographic crises caused by a combination of unfavorable environmental conditions linked to LIA cooling and the transition from traditional society, based on the subsistence economy, to modern capitalist society, characterized by the Industrial Revolution. This led to the depopulation of the Pallars region, which facilitated forest recovery and shaped present-day landscapes.

A very characteristic feature that is also not commonly mentioned in the historical records is the development of the hemp industry around Lake Montcortès, especially during Modern and precapitalist times. The waters of this lake are especially well suited for hemp retting, as their physicochemical features favor the development of the specific bacteria that produce the detachment of hemp fiber from the stalk. Hemp retting was the major, if not the only, human activity around the lake for more than three centuries (sixteenth to nineteenth), coinciding with the flourishing of the overseas Spanish Empire after the Columbian discovery of America, when hemp cultivation was mandatory to furnish fiber to the royal navy, mainly for sails and ropes. Hemp was cultivated in the surrounding Montcortès lowlands and transported to the lake for retting. The imperial decadence led to the dismantling of the navy in the mid-nineteenth century, which coincided with the end of hemp retting in Lake Montcortès and the abandonment of its catchment, coinciding with the massive emigration to industrialized cities and the resulting acceleration of forest recovery.

Another special feature of the Montcortès region for the paleoecological study of Modern and Contemporary times is the availability of nearby and in situ independent high-resolution paleoclimatic reconstructions that allowed the establishment of quantitative relationships between vegetation/landscape development and their climatic and anthropogenic (external) drivers, notably temperature, precipitation, drought, burning, and grazing. These analyses were performed individually on the main forest components and collectively, after the definition of the most relevant forest associations. Individually, the temperature of the warmest seasons (TWS) was positively associated with deciduous *Quercus*, whereas autumn precipitation (APP) was positively associated with evergreen *Quercus* and negatively associated with *Betula*. The intensity of summer drought (MDI), a characteristic Mediterranean

feature, was negatively associated with evergreen *Quercus*. For anthropogenic drivers, grazing proxies were negatively associated with all major forest components except *Betula*, whereas fire incidence was negatively associated with both deciduous and evergreen *Quercus*. The possibility of time lags in the response of these taxa to climatic variability was also analyzed. Typical and idiosyncratic response lags of one to several decades were identified, which suggests that the main forest components have immediate (at subdecadal resolution) and delayed responses to climatic shifts. Immediate responses were attributed to climatically driven changes in pollen production, whereas delayed responses were linked to long-term population dynamics.

Collectively, three main forest assemblages were defined that statistically coincided with the extant forest associations dominated by *Pinus* (montane), deciduous *Quercus-Betula* (submontane), and evergreen *Quercus* (Mediterranean) forests. Temporal changes in these forests were manifested in abundance shifts rather than taxonomic turnover, and the higher variability occurred during the eighteenth and nineteenth centuries, coinciding with the maximum hemp retting, with two main peaks coeval with minor fire events. Regional forest succession was characterized by a closed path starting and ending in an intermediate attraction domain between montane and Mediterranean forest assemblages. The major successional trends were defined by a deforestation trend (sixteenth to eighteenth centuries) associated with MDI, APP, fire incidence, and grazing, followed by a recovery trend, linked to the relaxation of human pressure and increasing TWS.

After this quantitative analysis, two main points emerge that require special attention in studies on ecological responses to environmental shifts. One is the occurrence of potential idiosyncratic response lags that can complicate the establishment of eventual relationships based solely on the comparison of instantaneous measurements, as usual in modern ecology. Another is the need for high-resolution datasets in statistical analyses of this type, as low-resolution records are unable to detect small-scale variations, which hinders the possibility not only of finding accurate relationships but also of building consistent long-term past–present ecological data series. After this study, four main conditions emerged as fundamental for the statistical analysis of climatic–ecological relationships using past records: the use of high-resolution datasets, the independence between climatic and ecological reconstructions, the comparison of paleoecological and paleoclimatid datasets from the same region, and the use of the appropriate statistical methods. In addition, not only instantaneous responses but also the possibility of delayed responses should be considered. Fulfilling these conditions is needed to properly unravel biotic responses to climatic shifts in the way toward the prediction of future ecological outputs under changing climates with a sound empirical basis. It is hoped that the results obtained in this way will be used to feed predictive models, thus increasing the reliability of their outputs.

8.2 Statistical Synthesis

The main trends of variation of the whole Montcortès dataset were resolved by principal component analysis (PCA), which yielded three significant components (Table 8.1). The first component (42% of the total variance) was positively associated with *Pinus* and negatively correlated with *Olea*, which represent montane pine forests and olive groves, respectively. Therefore, this component could be representative of the regional balance between coniferous forests and extensive lowland cultivation. The second component (24%) was associated with evergreen and deciduous *Quercus* in its positive values and with wild Poaceae in its negative values, which could be interpreted as the contrast between submontane/Mediterranean oak forests and open grasslands. The third component (11%) was positively associated with evergreen *Quercus* and wild Poaceae and negatively associated with deciduous *Quercus*, which could be indicative of the difference between parkland or

Table 8.1 Eigenvectors (variable loadings) and eigenvalues (variance explained) of the first three principal components (PC) obtained by PCA on the whole Montcortès palynological dataset using taxa above 0.5% of the pollen sum

	PC1	PC2	PC3
<i>Pinus</i>	0.930	-0.107	-0.062
<i>Abies</i>	0.019	0.022	-0.005
<i>Quercus</i> (e)	0.034	0.648	0.703
<i>Quercus</i> (d)	-0.108	0.545	-0.546
<i>Betula</i>	-0.069	0.007	-0.103
<i>Fagus</i>	0.011	0.018	0.009
<i>Alnus</i>	0.010	0.067	-0.052
<i>Corylus</i>	0.009	0.117	-0.061
<i>Salix</i>	0.005	-0.005	-0.005
<i>Ulmus</i>	-0.008	-0.006	-0.196
<i>Castanea</i>	0.015	-0.053	0.032
<i>Juglans</i>	-0.020	-0.017	-0.004
<i>Olea</i>	-0.222	-0.078	-0.196
<i>Buxus</i>	-0.028	-0.020	-0.034
<i>Erica</i>	-0.001	-0.018	0.030
<i>Juniperus</i>	-0.071	-0.017	-0.127
<i>Ephedra</i>	-0.001	-0.004	0.002
<i>Hedysarum</i>	-0.008	-0.011	-0.001
<i>Helianthemum</i>	-0.008	-0.012	0.014
<i>Artemisia</i>	-0.108	-0.183	0.106
<i>Plantago</i>	-0.097	-0.171	0.115
Poaceae (wild)	-0.181	-0.419	0.305
<i>Rumex</i>	-0.006	-0.033	0.016
Cereals	0.076	0.026	-0.100
<i>Chenopodium</i>	-0.012	-0.020	0.001
Cumulative variance (%)	42.22	66.71	77.63

The most significant loadings are highlighted in bold

oak-grassland mosaic vegetation on one side vs. submontane oak forests on the other. Overall, the variation along these three axes accounts for almost 80% of the total variance.

These relationships were displayed as Euclidean biplots for more clarity (Fig. 8.2). Sample scores were arranged chronologically in the multidimensional space defined by these three components. Indeed, the PC1–PC2 biplot clearly

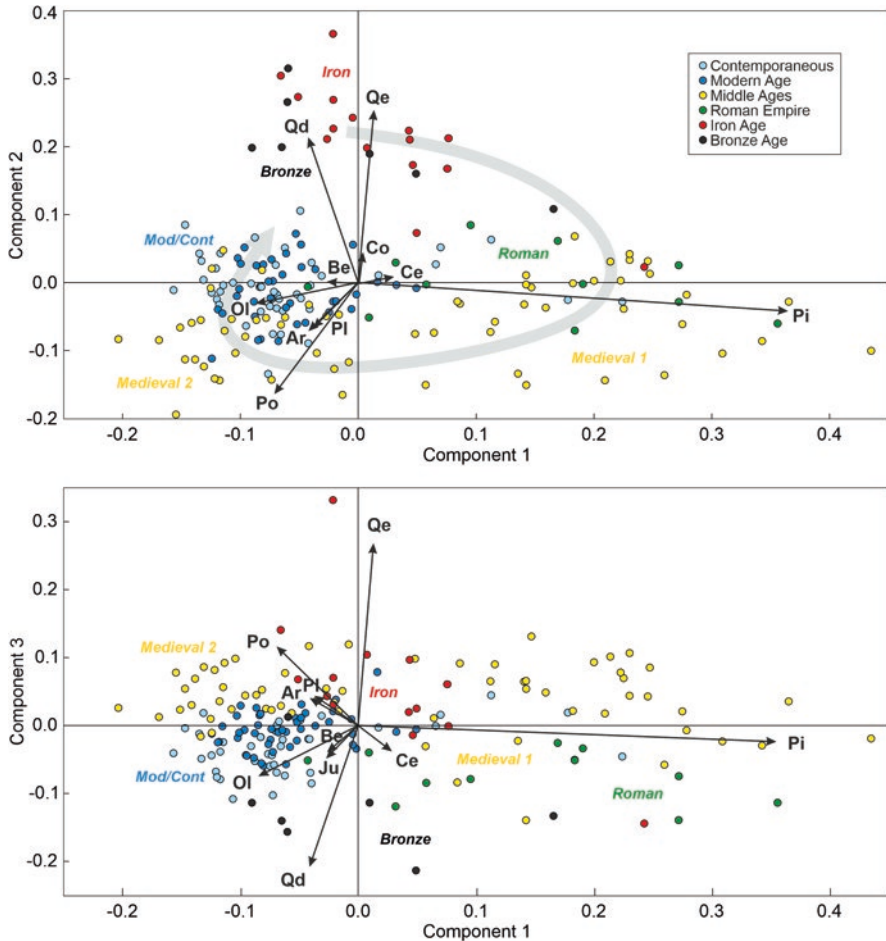


Fig. 8.2 Euclidean biplots of the sample scores within the space of the first three principal components obtained using the taxa above 0.5% of the pollen sum (see Table 8.1 for more details). Only variables with higher variable loadings are shown (Ar, *Artemisia*; Be, *Betula*; Ce, cereals; Co, *Corylus*; Ju, *Juglans*; Ol, *Olea*; Pi, *Pinus*; Pl, *Plantago*; Po, wild *Poaceae*; Qd, deciduous *Quercus*; Qe, evergreen *Quercus*). Sample scores are represented as colored dots and are sorted chronologically. The areas corresponding to the different historical phases are indicated in italics, using the same code color as in sample scores (*Medieval 1*, sixth to ninth centuries; *Medieval 2*: tenth to fifteenth centuries; *Mod/Cont*, Modern/Contemporary). Chronological trends are emphasized by a gray arrow in the background

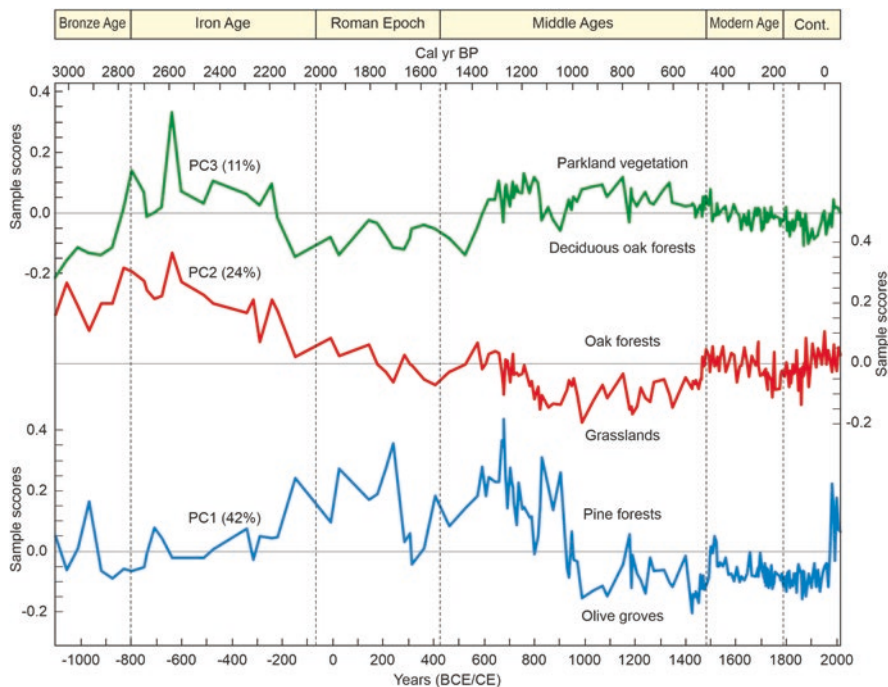


Fig. 8.3 Sample scores of the first three components from PCA plotted chronologically. See Table 8.1 and Fig. 8.2 for details on variable loadings and interpretation. The percentage of variance explained by each component is indicated

segregated Modern/Contemporary samples (positive PC2 values) and Bronze/Iron samples (negative PC1 values) from Roman (positive PC1 values) and Medieval samples, which were more widespread along PC1 and almost restricted to the negative PC2 side. Noteworthy, Medieval samples corresponding to the sixth to ninth centuries were situated on the right side of PC1, and samples corresponding to the tenth to fifteenth centuries were located on the left side of PC1, following a chronological trend consistent with the other historical periods. PC3 contributed to separating Iron and Modern/Contemporary samples (positive side) from Bronze/Medieval samples (negative side).

When sample scores were chronologically represented, the paleoecological meaning of components PC1 to PC3 became even clearer (Fig. 8.3). PC1 clearly differentiated the periods before and after ~1000 CE, when olive crops acquired importance in the lowlands situated south of Lake Montcortès. This component also recorded regional deforestations and the ensuing forest reexpansions, including the woodland recovery of recent decades, which was not expressed in other components. PC1 maxima, that is, conifer forest dominance in the absence of extensive olive groves, occurred in Roman and Medieval times, just before the first and the second regional deforestations, respectively, as well as during the last decades. PC1 minima, representing the minimum cover of pine forests and maximum

development of olive groves, coincided with the Medieval and Modern deforestation phases. PC2 also separated two distinct time periods with a transitional phase during the Roman epoch. Before those times, PC2 was at a maximum, indicating maximum cover of oak forests, in general. Minimum values of PC2, or maximum landscape opening, were recorded during Medieval and Modern woodland clearings, as a manifestation of the decline in oak forests, as occurred with pine woodlands. PC3 was more variable, with maxima (parkland/mosaic vegetation) during the Iron Age and Middle Ages, and minima (deciduous oak forests) in the Bronze Age, the Roman epoch and Contemporary times.

The statistical relationships of these PCA-defined vegetation trends with charcoal and elements outside the pollen sum (*Cannabis*, aquatic plants, fungi spores, algae) were addressed by canonical correspondence analysis (CCA), using these elements as environmental variables. The resulting eigenvalues indicated that the first two CCA axes accounted for almost three-quarters (74.81%) of the total variance and were significant at $\alpha < 0.001$. In the space of these two axes, samples were also sorted chronologically following a gradient defined by fire intensity (charcoal) on the right side and elements related to hemp retting (including eutrophy indicators such as *Typha* and *Pediastrum*) on the left side (Fig. 8.4). This gradient, corresponding to axis 1, explained almost half (49.89%) of the total variance and was therefore the main source of variability of the whole Montcortès dataset. Grazing indicators (coprophilous fungi) were more correlated with the fire vector, whereas *Glomus* and *Botryococcus* were more related to the retting vectors. Among vegetation components, cereals were more associated with the fire side and *Olea* was linked to retting vectors, the others being in intermediate positions. Along this gradient, Modern/Contemporary samples were located on the left side, associated with hemp-retting indicators, whereas Bronze, Iron, and Roman samples were well separated on the right side, along the fire vector. Medieval samples were widespread along the fire-retting gradient, with samples prior to the eleventh century situated on the fire-grazing side and samples corresponding to the twelfth to fifteenth centuries in the retting-eutrophy region. Axis 2 introduced a gradient associated with aquatic/semiaquatic plants (*Cladium* and other Cyperaceae) in negative values. Medieval samples mostly followed this gradient, which could be indicative of the relative importance of the macrophytic fringe surrounding the lake.

In summary, PCA showed that the main trends of vegetation and landscape change in the Montcortès record were defined by contrasting patterns of pinus forests-olive groves, oak forests-grasslands, and parkland/mosaic vegetation-deciduous oak forests. In addition, CCA identified the fire/grazing to hemp retting/eutrophication gradient as the main gradient explaining vegetation and landscape dynamics, followed by the importance of the aquatic/semiaquatic vegetation fringe. The projections of sample scores on the new axes provided by PCA and CCA followed a chronological order consistent with the historical phases of the last three millennia, from the Late Bronze Age to the present.

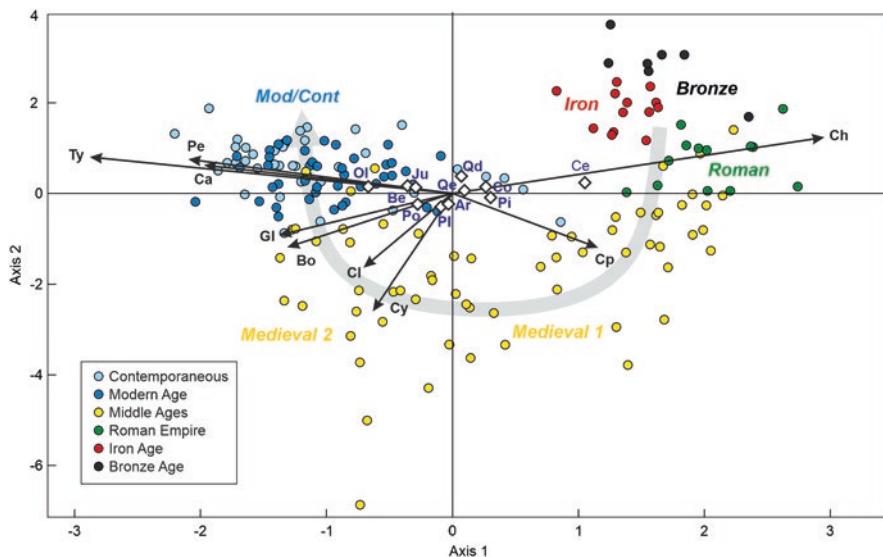


Fig. 8.4 Triplot of the CCA results using the elements inside the pollen sum as taxa variables and the elements outside the pollen sum as the environmental variables on the whole Montcortès dataset. As in the above PCA, only the most abundant taxa (open diamonds) are shown (Ar, *Artemisia*; Be, *Betula*; Ce, cereals; Co, *Corylus*; Ju, *Juglans*; Ol, *Olea*; Pi, *Pinus*; Pl, *Plantago*; Po, wild Poaceae; Qd, deciduous *Quercus*; Qe, evergreen *Quercus*). Environmental variables (vectors): Bo, *Botryococcus*; Ca, *Cannabis*; Ch, charcoal; Cl, *Cladium*; Cp, coprophilous fungi; Cy, other Cyperaceae; Pe, *Pediastrum*; Ty, *Typha*. The areas corresponding to the different historical phases are indicated in italics, using the same code color as in sample scores (Medieval 1, before the eleventh century; Medieval 2: after the eleventh century; Mod/Cont, Modern/Contemporary). Chronological trends are emphasized by a gray arrow in the background

8.3 The Iberian and Mediterranean Contexts

Comparing the Montcortès record with other Iberian and Mediterranean sequences will help understand the peculiarity and uniqueness of this paleoecological record in a wider context. The paucity of varved records available for the Iberian Peninsula hinders the establishment of high-resolution patterns at the regional level. However, it is possible to extend the comparison of the anthropization timing performed for the Pyrenees (Fig. 5.9) across the whole peninsular range in montane environments similar to Lake Montcortès. On the other hand, the availability of varved Mediterranean records longer and more continuous than Iberian records enables the establishment of supra-regional comparisons with the Montcortès record.

8.3.1 The Iberian Peninsula: Anthropization Patterns

This section is dedicated to placing the timing of human influence on Montcortès landscapes within the context of the Iberian Peninsula. To do this, we compare Lake

Montcortès with sites at similar elevations situated between the lower and higher mountain regions (~700 to 1300 meters) in Mediterranean areas outside of the Pyrenees. Of these sites, half of them (10) show evidence of human activity during the Bronze Age, with four during the Early Bronze Age, three in the Middle Bronze Age, and three in the Late Bronze Age. The other half of the sites were anthropized during different periods, including the Iron Age (3), the Roman era (3), and the Middle Ages (4) (Fig. 8.5). This analysis reveals a significant diversity in the timing of human impact, and no clear geographical patterns are evident. Notably, most of the mountain ranges we studied show a range of anthropization times from the Bronze Age to the Middle Ages, and similar anthropization timings are observed

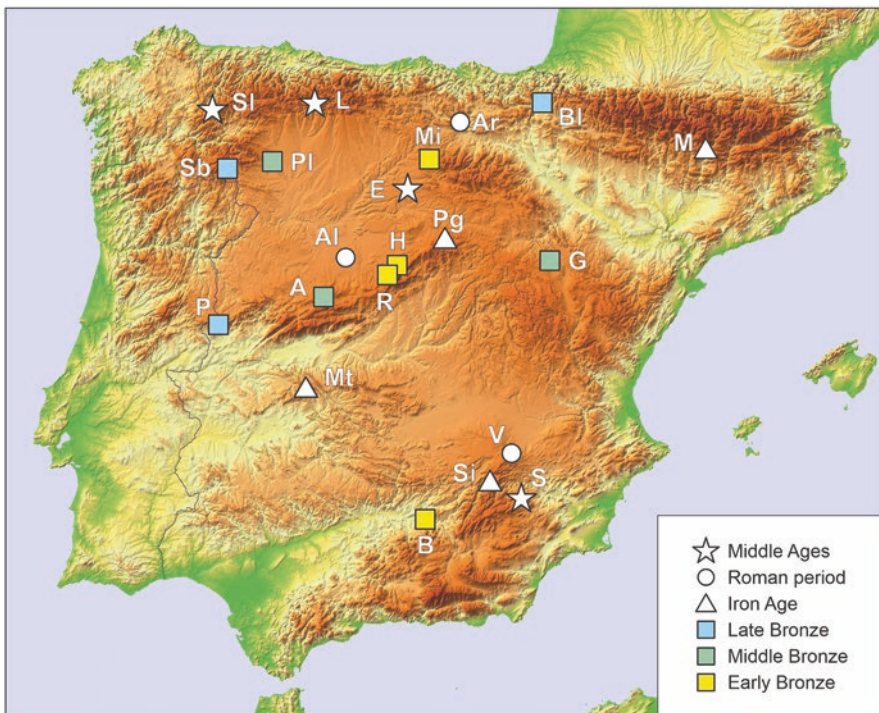


Fig. 8.5 Topographic map showing the anthropization time of montane sites (ca. 700–1300 m elevation) from the Iberian Mediterranean ranges compared to Montcortès. Raw information has been obtained from pollen analyses published by diverse authors: A = Valle Amblés (López-Sáez et al. 2009); AI = Almenara de Adaja (López-Merino et al. 2009); Ar = Arreo (Corella et al. 2013); B = Alcázar de Baeza (Fuentes et al. 2007); BI = Belate (Peñalba 1994); E = Espinosa de Cerrato (Franco-Múgica et al. 2001a); H = Calvero de la Higuera (Ruiz-Zapata et al. 2008); G = Gallocanta (Luzón et al. 2007); L = Pinar del Lillo (García-Antón et al. 1997); M = Montcortès (Rull et al. 2021a); Mi = El Mirador (Allué and Euba 2008); Mt = Garganta del Mesto (Gil-Romera et al. 2008); P = El Payo (Abel-Schaad et al. 2009); Pg = Pelagallos (Franco-Múgica et al. 2001b); PI = Pelambre (López-Sáez et al. 2009); R = Rascafría (Franco-Múgica and García-Antón 1994); S = El Sabinar (Carrión et al. 2004); Sb = Sanabria (Muñoz-Sobrinó et al. 2004); Si = Siles (Carrión et al. 2004); Sl = Suárbo (Muñoz-Sobrinó et al. 1997); V = Ojos de Villaverde (Carrión et al. 2001)

across various mountain ranges, regardless of their location. For instance, the same anthropization timing seen at Montcortès is also found in lower and higher elevation areas in the central and southern regions of Iberia, even though these regions have distinct climates and biogeographical characteristics (Loidi 2017). These findings suggest that there are diverse cultural patterns, both in terms of geography and time, which make it challenging to establish consistent spatial and temporal patterns of human influence in the transition between lower and higher mountain regions across the Iberian Peninsula. Therefore, at present, it appears that conducting localized studies focusing on specific mountain ranges is the most effective way to gain a comprehensive understanding of human impact trends in mountainous areas. However, it is important not to dismiss the possibility of a general pattern of increasing human influence with elevation for each specific mountain range, as has been observed in the Pyrenees (Rull and Vegas-Vilarrúbia 2021a, b), and further investigation in this regard is warranted.

8.3.2 The Mediterranean Region: The Uniqueness of the Montcortès Record

As advanced in the introduction, a major appealing feature of the Montcortès record is its uniqueness. The detailed study presented in the former chapters has shown that this uniqueness relies on the unusual concurrence of several particularities, such as (i) the temporal extent (3000 years) and the continuity of the absolutely dated varved record, (ii) the completeness and the comparatively high resolution (bidecadal, on average) attained in the paleoecological analysis, (iii) the availability of independent high-resolution paleoclimatic reconstructions from the same record and from nearby sites for detailed quantitative studies of ecological responses to past climatic shifts, (iv) the availability of detailed historical records for comparison with paleoecologically inferred trends in anthropogenic drivers of vegetation/landscape change, and (v) the possibility of combining past and present ecological records of similar resolution to produce true long-term ecological time series. This section is aimed at demonstrating that the uniqueness of the Montcortès record is not restricted to the Pyrenean ambit, as we have seen thus far, but can be extended to the whole Mediterranean region.

Zolitschka et al. (2015) reported ten Mediterranean lakes that contain varved records with varying characteristics in terms of thickness and extent. Figure 1 in the introduction presents these lakes, and their primary features can be found in Table 8.2. It is worth noting that only three of these lakes, namely, Nar, Montcortès, and La Cruz, are situated at elevations above 1000 meters, while the others are located in low-lying areas, with three of them, San Puoto, Butrint, and the Dead Sea, situated in or near littoral environments. The original studies indicate that only three of these lakes, specifically the Dead Sea, Montcortès, and Nar, possess extensive records spanning 1500 years or more, whereas the remaining seven have records that are approximately 650 years or less, with four of them having records of less than 70 years. Seven of these records have absolute chronologies, while three,

Table 8.2 Relevant features of varved Mediterranean lakes compiled by Zolitschka et al. (2015), with palynological studies for the last millennia

Lake	Elevation (m)	Varved record	Varve years	Varve thickness (mm)	Chronology	Palynology	Resolution	References
Nar (Turkey)	1363	300–2000 CE	1700	2.2	Absolute	300–2000 CE; 13,700 BP–present	Bidecadal to bicentennial	Jones et al. (2006); England et al. (2008); Roberts et al. (2016)
Montcortès (Spain)	1027	2699–present	2699	2.4	Absolute	~3000 BP–present	Bidecadal	Corella et al. (2016, 2019); Rull et al. (2021b)
La Cruz (Spain)	1000	1579–2002 CE	423	0.95	Absolute	~520 CE–present	Multidecadal	Burjachs (1996); Julià et al. (1998); Romero-Viana et al. (2008)
Arreo (Spain)	655	1952–1998 CE	46	1.	Floating	0–2000 CE	Multidecadal	Corella et al. (2011, 2013)
Avigliana (Italy)	353	1935–2000 CE	65	3	Absolute	1820–2000 CE	Subdecadal	Finsinger et al. (2006)
Zoñar (Spain)	300	~2530–2100 BP; ~1940–1910 BP; ~1780–1600 BP	637	~1	Floating	~3400 BP–present	Centennial	Martin-Puertas et al. (2008, 2009)
Albano (Italy)	293	1944–1990 CE	46	2.6	Absolute	14,000 BP–present	Bicentennial	Lami et al. (1994); Mercuri et al. (2002)
San Puoto (Italy)	2	1925–1995 CE	70	NA	Absolute	NA	NA	Alvisi and Dinelli (2002)
Butrint (Albania)	0	1741 CE–present	259	5	Absolute	4370 BP–2000 CE	Bicentennial	Ariztegui et al. (2010); Morellón et al. (2016)
Dead Sea (Jordanian/Israel)	–423	140 BC–1408 CE (minor gaps)	1500	0.5	Floating	2000 BCE–1516 CE; ~2500–500 BCE	Multidecadal	Migowski et al. (2004); Neumann et al. (2007); Langgut et al. (2014)

NA, not available

namely, the Dead Sea, Arreo, and Zóñar, have floating varve chronologies. Further investigations into some of these lakes have expanded these chronologies. The combination of varve counting and U/Th dating has extended the laminated record of Lake Nar to 14,000 yr BP, albeit with some discontinuities (Roberts et al. 2016). However, there have not been any new varve counting dates provided beyond the previously established date of 1700 yr BP (Jones et al. 2006). Consequently, Lake Montcortès possesses the most extensive and reliably dated varved record in the entire Mediterranean region.

Most Mediterranean varved records have been examined using palynology, but in the case of Montcortès, achieving an annual resolution has proven challenging due to the thinness of the varves, which typically range from approximately 1 to 5 mm. The level of detail in these paleoecological reconstructions varies from spanning two centuries to just a few decades. The two longest records previously mentioned, covering the eastern (Nar) and western (Montcortès) Mediterranean regions, have been analyzed at an approximately 20-year resolution on average. Figure 8.6 provides a comparison between the time intervals determined through varve counting and those studied through palynology, along with their respective resolutions, for the Mediterranean varved lakes with available information. In summary, these data indicate that the Montcortès record stands out as having the most extended pollen sequence with the highest level of detail in the entire region for the past three millennia.

In summary, Lake Montcortès stands out as a unique high-resolution record of changes in vegetation and landscapes, along with their natural and human-induced causes in the Mediterranean region over the past three millennia. This timeframe is significant, given recent research showing that the influence of hunter-gatherers, farmers, and pastoralists in reshaping the planet began approximately 3000 years ago, much earlier than what Earth scientists conventionally believed (Steffens et al. 2019). In the case of Montcortès, this is particularly noteworthy because the study demonstrates that the complete transformation of the lake's surroundings took place during the Iron Age, well before the previously accepted Middle Ages as the norm for the Pyrenees region. Another global study on sedimentation rates in lakes indicates that a substantial portion of Earth's surface started experiencing human-driven soil erosion as far back as 4000 years ago (Jenny et al. 2019). While we have not yet found sediments of this age in Lake Montcortès cores, the possibility of their existence has not been ruled out and warrants further investigation (Rull et al. 2021a).

While the Montcortès record is exceptional, it cannot accurately represent the entire Mediterranean region on its own due to the diverse nature of this region in terms of climate, biogeography, and culture (Lionello 2012; Moatti and Thiébaud 2016). To achieve a more representative approach, it would be advisable to identify at least three varved records from the western, central, and eastern Mediterranean regions, supported by absolute varve dating and high-resolution palynological studies. Lake Montcortès appears to be a suitable candidate for representing the western side, while Lakes Butrint and Nar could be chosen to represent the central and eastern regions, respectively. In Lake Nar, laminations are present up to 4000 yr BP and earlier, as reported by Roberts et al. (2016), although a complete absolute

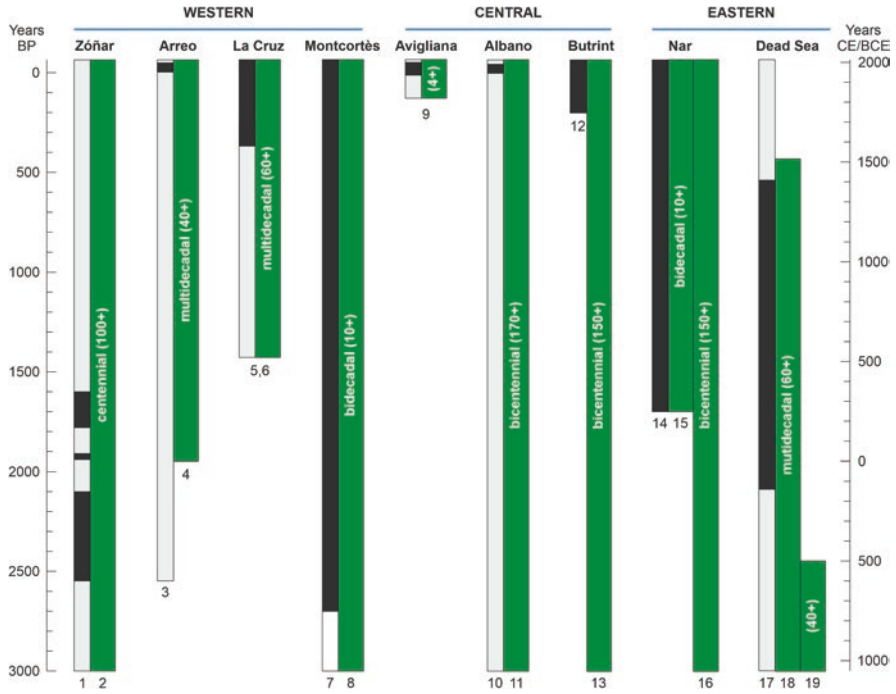


Fig. 8.6 Western, central, and eastern Mediterranean varved lakes with palynological studies (see Fig. 1 of the Introduction for location). Black intervals represent varve chronologies, and green bars are the sections with palynological studies, with an indication of their average resolution in years per sampling interval. References: Zóñar (1, Martín-Puertas et al. 2009; 2, Martín-Puertas et al. 2008); Arreo (3, Corella et al. 2013); La Cruz (5, Burjachs 1996; 3, Julià et al. 1998); Montcortès (7, Corella et al. 2019; 8, Rull et al. 2021b); Avigliana (9, Finsinger et al. 2006); Albano (10, Lami et al. 1994, 1997; 11, Mercuri et al. 2002); Butrint (12, Ariztegui et al. 2010; 13, Morellón et al. 2016); Nar (14, Jones et al. 2006; 15, England et al. 2008; 16, Roberts et al. 2016); Dead Sea (17, Migowski et al. 2004; 18, Neumann et al. 2007; 19, Langgut et al. 2014)

chronology has not yet been published. Moreover, paleoecological analyses are available with a resolution similar to that of Montcortès until 1700 years BP. Lake Butrint also exhibits laminated facies until approximately 3500 cal yr BP, as indicated by Morellón et al. (2016), which could be further investigated in terms of varve chronology. For pollen analyses, the resolution is currently insufficient (multidecadal), but it could be improved with additional sampling.

8.4 Potential Future Developments

Lake Montcortès and its catchment would be excellent candidates to establish a past–present–future ecological observatory (PPFEO) aimed at producing long-term ecological data series to infer functional ecosystem features, calibrate and validate ecological models, and to forecast potential ecological responses to future

environmental change (Rull 2014). In recent decades, the need for long-term ecological studies has been widely recognized, which has led to the creation of worldwide networks of ecological observatories, such as the LTER network (<https://lternet.edu/>), aimed at providing records of pivotal ecological parameters and processes for the near future. In this context, decadal or secular ecological time series are commonly considered to be “long-term” ecological series. However, two main handicaps emerge in this type of study. The first is that we should wait for generations to yield reliable results, and the second is that a number of relevant ecological processes—e.g., succession, community assembly, biotic responses to environmental changes, range shifts, migration, and extinction—occur at time scales larger than centuries and need longer observation periods to be fully understood. Paleoecology can provide the needed time scale for true long-term ecology (Rull and Vegas-Vilarrúbia 2011), but the handicap is the ability to merge ecological and paleoecological data into continuous and consistent data series. Long, continuous, and well-dated high-resolution studies such as those developed in the Lake Montcortès record offer an opportunity to advance toward the building of true long-term ecological data series based on the concept of time continuum.

The conceptual separation between past and present is a human construction. Time is a continuum through which species and communities flow, interact, and evolve. A biosphere of the past and a biosphere of the present do not exist separately; there is a single biosphere where ecological and evolutionary processes have occurred continuously since the origin of life on Earth. Therefore, there is no ecology of the past (paleoecology) and no ecology of the present (modern ecology, neoecology, or simply ecology) but rather a single ecology that includes both. Historically, ecology and paleoecology have been separated for psychological and methodological reasons, but not because there are any differences between them *per se* (Rull 2010, 2012). A number of paleoecologists interested in reconstructing past ecological dynamics rather than solely past environmental changes have addressed the potential usefulness of past records for ecological knowledge and nature conservation (e.g., Davis 1981; Birks 1993, 1996, 2013a, b; Jackson 2001; Flessa and Jackson 2005; Willis et al. 2010; Vegas-Vilarrúbia et al. 2011; Rull et al. 2013; Gillson and Marchant 2014; Seddon et al. 2014). Despite this, the lack of synergy between ecological and paleoecological communities is still manifest.

This is discussed in more depth by Rull (2010), but from a practical point of view, there are several reasons for many ecologists to ignore paleoecological inputs, especially the lack of sufficient temporal resolution and the poor development of quantitative methods (Huntley 1996, 2012; Rull 2012). The continuity between ecological and paleoecological data series requires the use of the same temporal resolution, which is a handicap for many paleoecological records, whose resolution is usually lower than required (Peng et al. 2011). However, paleoecological records from archives such as tree rings, varved sediments, corals, speleothems, or ice cores are able to provide annual to seasonal resolution (e.g., Hughes and Ammann 2009; Alley 2011; Pandolfi 2011; Luckman 2013; Bradley 2015; Zolitschka et al. 2015), which could be suitable for building combined ecological–paleoecological datasets. Indeed, ecological and paleoecological records overlap at seasonal to decadal

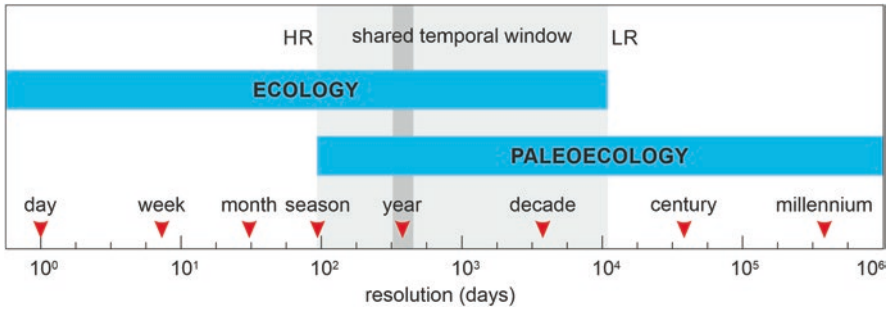


Fig. 8.7 Timescales of ecological and paleoecological studies showing the shared temporal window, ranging from seasons to decades. The higher resolution (HR) or combined ecological–paleoecological time series is attained using seasonal records, whereas the lower resolution (LR) occurs in decadal records. In paleoecology, seasonal resolution is more difficult to attain than annual resolution, which is more feasible and seems to be a suitable framework for continuous long-term ecological records. Redrawn and modified from Rull (2014)

temporal scales, with annual resolution as the most suitable window for assembling combined past–present records (Fig. 8.7).

Regarding statistical performance, paleoecological reconstructions were mostly qualitative or semiquantitative in the past, but this has notably changed in recent decades. At present, paleoecological studies are based on quantitative multivariate datasets that are analyzed with a variety of statistical techniques, including the latest developments in numerical analysis (Birks et al. 2012; Birks 2013c). In addition, regional, continental, and global datasets are available for developing meta-analyses on particular topics and selected time intervals (Fyfe et al. 2009; Peng et al. 2011; Brewer et al. 2012; Grimm et al. 2013). The idea of paleoecology as a qualitative discipline is a myth that is no longer tenable, although there is still room for improvement in the use of numerical methods and datasets for paleoecological research.

Therefore, neither temporal resolution nor data quality (i.e., quantitative approaches) seem to be serious concerns for the development of consistent ecological–paleoecological time series. The combination of past and present observations with future monitoring of the parameters of interest is already possible and could benefit from the existence of “long-term” monitoring networks, such as LTER and others, which could provide the necessary infrastructure for continuous past–present–future ecological observatories (PPFEOs). Ideally, these observatories should be placed around lakes with suitable paleoecological archives, especially varved sediments, as is the case for Lake Montcortès (Rull 2014). At present, the lake and its catchment do not even have a weather station, which is astonishing if we consider the high potential of the site for true long-term ecological monitoring. It is hoped that this book will contribute to raising awareness about this potential to pave the way toward the establishment of a pioneering PPFEO. A challenge in the Montcortès record is to attain seasonal/annual resolution in paleoecological analyses, as has been reached in other paleoenvironmental proxies. However, the varves are there, and this could only be a methodological drawback to be solved in the near

future. The uniqueness of the Montcortès record within a supra-regional Mediterranean context is an additional argument for the creation of a leading-edge observatory of this type.

References

- Abel-Schaad D, Hernández AM, López-Sáez JA, Pulido F, López L, Martínez A (2009) Evolución de la vegetación en la Sierra de Gata (Cáceres-Salamanca, España) durante el Holoceno Reciente. Implicaciones biogeográficas. *Rev Esp Micropaleontol* 41:91–105
- Alley RB (2011) Reliability of ice-core science: historical insights. *J Glaciol* 56:1095–1103
- Allué E, Euba I (2008) Los datos antracológicos de la secuencia neolítica de El Mirador (Atapuerca, Burgos): un estudio sobre el medio vegetal y la explotación de las especies vegetales leñosas. In: Hernández-Pérez MS, Soler JA, López JA (eds) *IV Cong Neolítico Peninsular 2006*. Mus Arqueol Alicante, Alicante, pp 345–352
- Alvisi F, Dinelli E (2002) Evolution of sediment composition of the coastal Lake San Puoto (Latium, Italy) in the last two centuries. *J Limnol* 61:15–26
- Ariztegui D, Anselmetti FS, Robbiani J-M, Bernasconi SM, Brati E, Gilli A et al (2010) Natural and human-induced environmental change in southern Albania for the last 300 years—Constraints from the Lake Butrint sedimentary record. *Glob Planet Change* 7:183–192
- Birks HJB (1993) Quaternary palaeoecology and vegetation science – current contributions and possible future developments. *Rev Palaeobot Palynol* 79:153–177
- Birks HJB (1996) Contributions of Quaternary palaeoecology to nature conservation. *J Veg Sci* 7:89–98
- Birks HJB (2013a) Paleoeecology. In: Elias (ed) *Encyclopedia of ecology: reference module in earth systems and environmental sciences*. Elsevier, Amsterdam. <https://doi.org/10.1016/B978-0-12-409548-9.00884-8>
- Birks HJB (2013b) Ecological palaeoecology and conservation biology: controversies, challenges and compromises. *Int J Biodiv Sci Ecosyst Serv Manage* 8:292–304
- Birks HJB (2013c) Numerical analysis methods. In: Elias SA, Mock CJ (eds) *Encyclopedia of quaternary science*. Elsevier, Amsterdam, pp 821–830
- Birks HJB, Lotter AF, Juggins S, Smol JP (2012) Tracking environmental change using lake sediments. Vol 5: Data handling and numerical techniques. Springer, Dordrecht
- Bradley RS (2015) *Paleoclimatology. Reconstructing climates of the Quaternary*. Elsevier, Amsterdam
- Brewer S, Jackson ST, Williams JW (2012) Paleoeoinformatics: applying geohistorical data to ecological questions. *Trends Ecol Evol* 27:104–112
- Büntgen U, Myglan VS, Ljungqvist FC, McCormick M, Di Cosmo N, Sigl M et al (2016) Cooling and societal change during the Late Antique Little Ice Age from 536 to around 669 AD. *Nat Geosci* 9:231–236
- Burjachs F (1996) La secuencia palinológica de La Cruz (Cuenca, España). In: Ruiz-Zapata B (ed) *Estudios Palinológicos*. Univ Alcalá, Alcalá de Henares, pp 31–36
- Carrión JS, Andrade A, Bennet KD, Navarro C (2001) Crossing forest thresholds: inertia and collapse in a Holocene sequence from south-Central Spain. *The Holocene* 11:635–653
- Carrión JS, Yll EI, Willis KJ, Sánchez P (2004) Holocene forest history of the eastern Plateaux in the Segura Mountains (Murcia, Southeastern Spain). *Rev Palaeobot Palynol* 132:219–236
- Corella JP, Amran A, Sigró J, Morellón M, Rico E, Valero-Garcés B (2011) Recent evolution of Lake Arreo, northern Spain: influences of land use change and climate. *J Paleolimnol* 46:469–485
- Corella JP, Stefanova V, El Anjoumi A, Rico E, Giralt S, Moreno A et al (2013) A 2500-year multiproxy reconstruction of climate change and human activities in northern Spain: the Lake Arreo record. *Palaeogeogr Palaeoclimatol Palaeoecol* 386:555–568

- Corella JP, Valero-Garcés B, Vicente-Serrano SM, Brauer A, Benito C (2016) Three millennia of heavy rainfalls in Western Mediterranean: frequency, seasonality and atmospheric drivers. *Sci Rep* 6:38206
- Corella JP, Benito G, Wilhelm B, Montoya E, Rull V, Vegas-Vilarrúbia T et al (2019) A millennium-long perspective of flood-related seasonal sediment yield in Mediterranean watersheds. *Glob Planet Change* 177:127–140
- Davis MB (1981) Quaternary history and the stability of forest communities. In: West DC, Shugart DB, Botkin DB (eds) *Forest succession, concepts and applications*. Springer, New York, pp 132–153
- England A, Eastwood WJ, Roberts CN, Turner R, Haldon JF (2008) Historical landscape change in Cappadocia (central Turkey): a palaeoecological investigation of annually laminated sediments from Nar Lake. *The Holocene* 18:1229–1245
- Finsinger W, Bigler C, Krähenbühl U, Lotter AF, Ammann B (2006) Human impacts and eutrophication patterns during the past 200 years at Lago Grande di Avigliana (N. Italy). *J Paleolimnol* 36:55–67
- Flessa KV, Jackson ST (2005) Forging a common agenda for ecology and paleoecology. *Bioscience* 55:1030–1031
- Franco-Múgica F, García-Antón M (1994) Análisis polínico de una turbera en Rascafría (Madrid). In: de la Serna I (ed) *Polen y Esporas: Contribución a su Conocimiento*. Serie Informes 35, pp 361–369
- Franco-Múgica F, García-Antón M, Maldonado J, Morla C, Sainz H (2001a) The Holocene history of *Pinus* forests in the Spanish Northern Meseta. *The Holocene* 11:343–358
- Franco-Múgica F, García-Antón M, Maldonado J, Morla C, Sainz H (2001b) Evolución de la vegetación en el sector septentrional del Macizo de Ayllón (Sistema Central). Análisis polínico de la turbera de Pelagallinas. *Anal Jard Bot Madrid* 59:113–124
- Fuentes N, Carrión JS, Fernández S, Nocete F, Lizcano R, Pérez C (2007) Análisis polínico de los yacimientos arqueológicos Cerro del Alcázar de Baeza y Eras del Alcázar de Úbeda (Jaén). *An Biol* 29:85–93
- Fyfe RM, de Beaulieu J-L, Binney H, Bradshaw RHW, Brewer S, Flao AL et al (2009) The European Pollen Database: past efforts and current activities. *Veg Hist Archaeobotany* 18:417–424
- García-Antón M, Franco F, Maldonado J, Morla C (1997) New data concerning the evolution of the vegetation in Lillo Pinewood (León, Spain). *J Biogeogr* 24:929–934
- Gillson L, Marchant R (2014) From myopia to clarity: sharpening the focus of ecosystem management through the lens of paleoecology. *Trends Ecol Evol* 29:317–325
- Gil-Romera G, García-Antón M, Calleja JA (2008) The late Holocene palaeoecological sequence of Serranía de las Villuercas (southern Meseta, western Spain). *Veg Hist Archaeobotany* 17:653–666
- Grimm EC, Bradshaw RHW, Brewer S, Flantua S, Giesecke T, Lézine AM et al (2013) Databases and their application. In: Elias SA (ed) *Encyclopedia of quaternary science*. Elsevier, Amsterdam, pp 831–838
- Hughes MK, Ammann CM (2009) The future of the past – an earth system framework for high-resolution paleoclimatology. *Clim Chang* 3–4:247–259
- Huntley B (1996) Quaternary palaeoecology and ecology. *Quat Sci Rev* 15:591–606
- Huntley B (2012) Reconstructing palaeoclimates from biological proxies: some often overlooked sources of uncertainty. *Quat Sci Rev* 31:1–16
- Jackson ST (2001) Integrating ecological dynamics across timescales, realtime, Q-time and deep time. *PALAIOS* 16:1–2
- Jenny J-P, Koirala S, Gregory-Eaves I, Francus P, Niemann C, Ahrens B et al (2019) Human and climate global-scale imprint on sediment transfer during the Holocene. *Proc Natl Acad Sci USA* 116:22972–22976
- Jones MD, Roberts CN, Leng MJ, Türkeç M (2006) A high-resolution late Holocene lake isotope record from Turkey and links to North Atlantic and monsoon climate. *Geology* 34:361–364
- Julià R, Burjachs F, Dasí MJ, Mezquita F, Miracle MR, Roca JR et al (1998) Meromixis, origin and recent trophic evolution in the Spanish mountain lake La Cruz. *Aquat Sci* 60:279–299

- Lami A, Niessen F, Guilizzoni P, Masaferró J, Belis CA (1994) Palaeolimnological studies of the eutrophication of volcanic Lake Albano (Central Italy). *J Paleolimnol* 10:181–197
- Lami A, Guilizzoni P, Ryves DB, Jones VJ, Marchetto A, Battarbee RW et al (1997) A Late Glacial and Holocene record of biological and environmental changes from the crater Lake Albano, central Italy: an interdisciplinary European project (PALICLAS). *Water Air Soil Pollut* 99:601–613
- Langgut D, Neumann FH, Stein M, Wagner A, Kagan EJ, Boaretto E et al (2014) Dead Sea pollen record and history of human activity in the Judean Highlands (Israel) from the Intermediate Bronze into the Iron Ages (~2500–500 BCE). *Palynology* 38:280–302
- Lionello P (2012) The climate of the mediterranean region. Elsevier, Amsterdam
- Loidi J (2017) The Vegetation of the Iberian Peninsula. Springer, Cham
- López-Merino L, López-Sáez JA, Alba F, Pérez S, Abel D, Gerra E (2009) Estudio polínico de una laguna endorreica en Almenara de Adaja (Valladolid, Meseta Norte): cambios ambientales y actividad humana durante los últimos 2800 años. *Rev Esp Micropaleontol* 41:333–348
- López-Sáez JA, Blanco A, López-Merino L, Ruiz MB, Dorado M, Valdeolmillos A et al (2009) Landscape and climatic changes during the end of the late Prehistory in the Amblés Valley (Ávila, Central Spain), from 1200 to 400 cal BC. *Quat Int* 200:90–101
- Luckman BH (2013) Dendroclimatology. In: Elias SA, Mock CJ (eds) *Encyclopedia of quaternary science*. Elsevier, Amsterdam, pp 459–470
- Luzón A, Pérez A, Mayayo MJ, Sánchez-Goñi MF (2007) Holocene environmental changes in the Gallocanta lacustrine basin, Iberian range, NE Spain. *The Holocene* 17:1–15
- Martín-Chivelet J, Muñoz-García MB, Edwards L, Turrero MJ, Ortega AI (2011) Land surface temperature changes in northern Iberia since 4000 yr BP, based on $\delta^{13}\text{C}$ of speleothems. *Glob Planet Change* 77:1–12
- Martín-Puertas C, Valero-Garcés BL, Mata MP, González-Sampériz P, Bao R, Moreno A et al (2008) Arid and humid phases in the southern Spain during the last 4000 years: the Zóñar lake record, Córdoba. *The Holocene* 18:907–921
- Martín-Puertas C, Valero-Garcés BL, Brauer A, Mata MP, Delgado-Huertas A, Dulski P (2009) The Iberian-Roman Humid Period (2600–1600 cal yr BP) in the Zóñar Lake varved record (Andalucía, southern Spain). *Quat Res* 71:108–120
- Mercuri AM, Accorsi CA, Bandini M (2002) The long history of *Cannabis* and its cultivation by the Romans in central Italy, shown by pollen records from Lago Albano and lago di Nemi. *Veg Hist Archaeobotany* 11:263–176
- Migowski C, Agnon A, Bookman R, Negendank JFW, Stein M (2004) Recurrence pattern of Holocene earthquakes along the Dead Sea transform revealed by varve-counting and radiocarbon dating of lacustrine sediments. *Earth Planet Sci Lett* 222:301–314
- Morellón M, Anselmetti FS, Ariztegui D, Brushlitt B, Sinopoli G, Wagner B et al (2016) Human-climate interactions in the central Mediterranean region during the last millennia: the laminated record of Lake Butrint (Albania). *Quat Sci Rev* 136:134–152
- Muñoz-Sobrino C, Ramil-Rego P, Rodríguez-Gutián MA (1997) Upland vegetation in the north-west Iberian peninsula after the last glaciation: forest history and deforestation dynamics. *Veg Hist Archaeobotany* 6:215–233
- Muñoz-Sobrino C, Ramil-Rego P, Gómez-Orellana L (2004) Vegetation of the Lago de Sanabria area (NW Iberia) since the end of the Pleistocene: a palaeoecological reconstruction on the basis of two new pollen sequences. *Veg Hist Archaeobotany* 13:1–22
- Neumann FH, Kagan EJ, Schwab MJ, Stein M (2007) Palynology, sedimentology and palaeoecology of the late Holocene Dead Sea. *Quat Sci Rev* 26:1476–1498
- Pandolfi JM (2011) The paleoecology of coral reefs. In: Dubinsky Z, Stambler N (eds) *Coral Reefs: an ecosystem in transition*. Springer, Dordrecht, pp 13–24
- Peñalba MC (1994) The history of the Holocene vegetation in northern Spain from pollen analysis. *J Ecol* 82:815–832
- Peng CH, Guiot J, Wu H, Jiang H, Luo Y (2011) Integrating model data in ecology and palaeoecology: advances towards a model-data fusion approach. *Ecol Lett* 14:522–536

- Roberts N, Allcock SL, Arnaud F, Dean JR, Eastwood WJ, Jones LMJ et al (2016) A tale of two lakes: a multiproxy comparison of Lateglacial and Holocene environmental change in Cappadocia, Turkey. *J Quat Sci* 31:348–362
- Romero-Viana L, Julià R, Camacho A, Vicente E, Miracle MP (2008) Climate signal in varve thickness: La Cruz (Spain), a case study. *J Paleolimnol* 40:703–714
- Ruiz-Zapata MB, Gómez C, Gil MJ, López-Sáez JA, Baquedano E, Pérez-González A, Arsuaga JL (2008) Comparación de las secuencias polínicas del Holoceno reciente del yacimiento arqueopaleontológico de El Calvero de la Higuera (Pinilla del Valle, Madrid) y de la turbera de Rascafría (Madrid). *Geotemas* 10:1484–1486
- Rull V (2009) Time's arrow: left or right? *Quat Geochronol* 4:83
- Rull V (2010) Ecology and palaeoecology: two approaches, one objective. *Open Ecol J* 3:1–5
- Rull V (2012) Community ecology: diversity and dynamics over time. *Community Ecol* 13:102–116
- Rull V (2014) Time continuum and true long-term ecology: from theory to practice. *Front Ecol Evol* 2:75
- Rull V, Vegas-Vilarrúbia T (2011) What is long term in ecology? *Trends Ecol Evol* 26:3–4
- Rull V, Vegas-Vilarrúbia T (2021a) A spatiotemporal gradient in the anthropization of Pyrenean landscapes. Preliminary report. *Quat Sci Rev* 258:106909
- Rull V, Vegas-Vilarrúbia T (2021b) Conifer forest dynamics in the Iberian Pyrenees during the Middle Ages. *Forests* 12:1685
- Rull V, Montoya E, Nogué S, Vegas-Vilarrúbia T, Safont E (2013) Ecological paleoecology in the Neotropical Gran Sabana region: long-term records of vegetation dynamics as a basis for ecological hypothesis testing. *Persp Plant Ecol Evol Syst* 15:338–359
- Rull V, Vegas-Vilarrúbia T, Corella JP, Valero-Garcés B (2021a) Bronze Age to Medieval vegetation dynamics and landscape anthropization in the south-central Pyrenees. *Palaeogeogr Palaeoclimatol Palaeoecol* 571:110392
- Rull V, Vegas-Vilarrúbia T, Corella JP, Trapote MC, Montoya E, Valero-Garcés B (2021b) A unique Pyrenean varved record provides a detailed reconstruction of Mediterranean vegetation and land-use dynamics over the last three millennia. *Quat Sci Rev* 268:107128
- Seddon AWR, Mackay AW, Baker AG, Birks HJB, Breman E, Buck CE et al (2014) Looking forward through the past: identification of 50 priority research questions in palaeoecology. *J Ecol* 102:256–267
- Steffens L, Fuller D, Boivin N, Rick T, Gauthier N, Kay A et al (2019) Archaeological assessment reveals Earth's early transformation through land use. *Science* 365:897–902
- Vegas-Vilarrúbia T, Rull V, Montoya E, Safont E (2011) Quaternary paleoecology and nature conservation with an emphasis on global warming and fire, with examples from the neotropics. *Quat Sci Rev* 30:2361–2388
- Willis KD, Bailey RM, Bhagwat S, Birks HJB (2010) Biodiversity baselines, thresholds and resilience: testing predictions and assumptions using palaeoecological data. *Trends Ecol Evol* 25:583–591
- Zolitschka B, Francus P, Ojala AEK, Schimmelmann A (2015) Varves in lake sediments – a review. *Quat Sci Rev* 117:1–41